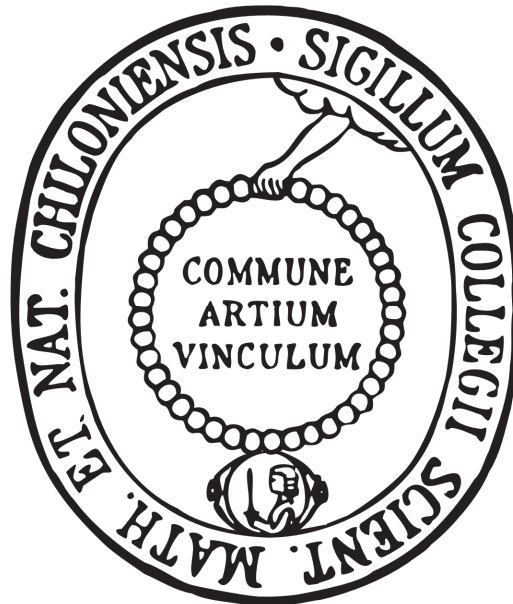# Carbohydrate Conjugates to Explore Bacterial Adhesion:

From Amadori Rearrangement to

Surface Functionalization

Dissertation

in fulfillment of the requirements for the degree "Dr. rer. nat."
of the Faculty of Mathematics and Natural Sciences
at the Christiana Albertina University of Kiel

submitted by

Tobias-Elias Gloe

from Bad Oldesloe

Kiel 2016

Statutory declaration

I hereby confirm that the work embodied in this thesis is original and, apart from advice by my supervisor, is my own work. It has not been submitted either partially or wholly, as part of a doctoral degree, to another examining body. Parts of this thesis have been published as:

Are D-*manno*-configured Amadori Products Ligands of the Bacterial Lectin FimH?
T.-E. Gloe, I. Stamer, C. Hojnik, T. M. Wrodnigg, T. K. Lindhorst, *Beilstein J. Org. Chem.* **2015**, *11*, 1096–1104.

This thesis has been prepared according to the Rules of Good Scientific Practice of the German Research Foundation.

Tobias-Elias Gloe

Abstract

Pathogenic *Escherichia coli* (*E. coli*) bacteria are responsible for a number of infectious diseases, such as neonatal meningitis, urinary tract infections, and gastroenteritis. Initiated by adhesion of bacteria to the surface of human cells, type 1 fimbriated *E. coli* utilize a mannose-specific lectin, namely FimH, at the tip of adhesive organelles, the fimbriae, for attachment to cells with high-mannose surface glycans. Therefore, the synthesis of potent inhibitors of bacterial adhesion and the development of innovative techniques for investigation of this matter are of utmost scientific as well as medicinal value and motivate the research described herein.

At first, the Amadori rearrangement was applied in the synthesis of ligands for the bacterial lectin FimH, which were further validated by performance of docking studies and biological tests. It turned out that complexation of Amadori products in the lectin binding site is compromised, which limits the activity towards inhibition of FimH-mediated bacterial adhesion. Supplementary to this work, it was interesting to utilize the Amadori rearrangement for the synthesis of colored products in order to facilitate and accelerate the purification of the highly polar Amadori products.

The preparation of a carbohydrate-centered scaffold with an AB_4-type functionalization was discussed by retrosynthetic analysis and could eventually be realized after thorough investigation. Based on this target scaffold compound, various useful glycoconjugates were synthesized, such as a tetravalent glycocluster. By testing this cluster in adhesion-inhibition assays, a multivalency effect, albeit of weak nature, was observed and conjugation with a biorepulsive OEG linker paved the way towards further studies on functional surfaces.

Furthermore, the property of cyclodextrins to undergo inclusion of hydrophobic guest molecules was utilized for developing a novel bacterial adhesion assay. Therefore, several cyclodextrin hosts and carbohydrate- as well as azobenzene-based guest molecules were synthesized and tested in different approaches in respect of the new assay. In the most successful approach, mannose cyclodextrin conjugates served as host molecules for inclusion of azobenzene units on photoresponsive PEG beads. It was demonstrated that UV light-induced isomerization of the azobenzene units resulted in a reduced bacterial adhesion to the functional beads. In this regard, the extent of this effect showed a high dependence on the molecular structure of the applied azobenzene derivative. Further development of this system gives rise to a broad spectrum of applications, such as the extraction or accumulation of pathogens from fluid samples.

Kurzfassung

Pathogene *Escherichia coli* (*E. coli*)-Bakterien sind verantwortlich für eine Reihe von Entzündungskrankheiten wie z. B. neonatale Meningitis, Harnwegsinfektionen und Gastroenteritis, welche durch Adhäsion von Bakterien an die Oberfläche menschlicher Zellen ausgelöst werden. Typ-1-fimbriierte *E. coli*-Bakterien nutzen dabei ein Mannose-spezifisches Lektin, FimH, an der Spitze adhäsiver Organellen, den Fimbrien, um an Zellen mit hochmannosidischen Oberflächensacchariden zu binden. Die Synthese von potenten Inhibitoren und die Entwicklung innovativer Techniken zur Untersuchung dieser Form der bakteriellen Adhäsion sind daher sowohl von großer wissenschaftlicher als auch medizinischer Bedeutung und motivieren die hier beschriebenen Forschungsarbeiten.

Zunächst wurden unter Anwendung der sogenannten Amadori-Umlagerung Liganden des bakteriellen Lektins FimH synthetisiert und im Anschluss durch Dockingstudien sowie biologische Tests validiert. Wie sich herausstellte, ist die Komplexierung dieser Amadori-Produkte in der Lektin-Bindungstasche beeinträchtigt und dadurch die inhibitorische Aktivität gegenüber FimH-vermittelter bakterieller Adhäsion eingeschränkt. Ergänzend zu diesen Arbeiten war es interessant, die Amadori-Umlagerung für die Synthese farbiger Produkte einzusetzen, um die chromatographische Reinigung der sehr polaren Amadori-Produkte zu vereinfachen und zu beschleunigen.

In einer Synthese-orientierten Studie wurde die Präparation eines AB_4-funktionalisierten Kohlenhydrat-Scaffoldmoleküls anhand einer retrosynthetischen Analyse diskutiert und nach sorgfältiger Untersuchung realisiert. Ausgehend von dieser Zielverbindung war es möglich, weitere nützliche Glykokonjugate zu synthetisieren wie z. B. einen tetravalenten Glykocluster. Dieser führte in Inhibitionsassays einen – wenn auch schwach ausgeprägten – Multivalenzeffekt und wurde anschließend durch Konjugation mit einem OEG-Linker für weitere Studien auf funktionalen Oberflächen vorbereitet.

Weiterhin wurde ein neuer Assay zur Untersuchung bakterieller Adhäsion entwickelt, der sich die Eigenschaft von Cyclodextrinen zu Nutze macht, hydrophobe Gastmoleküle einzulagern. Hierzu wurden verschiedene Cyclodextrin-Wirtsmoleküle sowie Kohlenhydrat- und Azobenzol-basierte Gastmoleküle hergestellt und in unterschiedlichen Ansätzen in Verbindung mit dem neuen Assay untersucht. Im erfolgreichsten Ansatz dienten Mannose-Cyclodextrinkonjugate als Wirtsmoleküle für die Einlagerung von Azobenzol-Einheiten auf photoaktiven PEG-Beads. Es konnte gezeigt werden, dass die Isomerisierung der Azobenzol-Einheiten durch UV-Licht eine Reduktion der bakteriellen Adhäsion an die funktionalen Beads zur Folge hat. Die Ausprägung dieses Effektes ist dabei stark von der molekularen Struktur der Azobenzol-Derivate abhängig. Die Weiterentwicklung dieses Systems verspricht eine Vielzahl von Anwendungsmöglichkeiten wie z. B. die Extraktion oder Anreicherung von Pathogenen aus Flüssigkeiten.

Table of Contents

How to Read This Thesis

This thesis is comprised of seven chapters with different contents, regarding the information and the research presented therein:

The general introduction (Chapter 1) of this thesis provides basic information about the field of glycobiology and bacterial adhesion. This chapter is especially important for readers that are not familiar with this kind of matter in order to fully understand the research presented herein. While Chapter 2 describes the objectives of the research embodied in this work, Chapter 3-5 comprise the actual results of the performed studies as well as their discussion. Each of these chapters includes a detailed introduction, which focuses on the respective theoretical background of the research presented in the corresponding chapter. Furthermore, Chapters 3-5 contain a published article, a submitted manuscript (and the corresponding Supporting Information), as well as unpublished results. Chapter 6 contains conclusions in form of a detailed summary of the obtained results. All experimental data as well as synthetic procedures are presented in the experimental section (Chapter 7). The appendix features UV/Vis spectra and chromatograms of selected compounds as well as abbreviations and lists of figures, schemes, and tables.

In order to prevent possible confusion, page numbers are <u>not</u> shown in sections that present published articles or manuscripts since these have their own page numbers.

1. General Introduction

1.1 Carbohydrates and Their Role in Nature

One of the most abundant classes of compounds found in nature are carbohydrates. These so-called glycans occur in various forms and have earlier been considered solely as a source of energy or as structural material. After the progress of analytical technology and research on the field of glycobiology, however, they have increasingly been recognized as part of other biomolecules, such as glycoproteins or glycolipids. Depending greatly on their molecular structure, their conformation as well as the presentation, these glycoconjugates mediate a variety of different functions that are essential to most biological systems including living organisms.

Structural Diversity of Carbohydrates

The term carbohydrate originates from the general chemical formula $C_nH_{2n}O_n$ (with $n \geq 3$) which describes their molecular composition as a combination of carbon and water. While basic monosaccharides consist of just one carbohydrate unit, oligo- and polysaccharides contain several moieties that are connected with each other through glycosidic linkages. In this regard, a large number of connection possibilities arise due to the number of hydroxyl groups available for intermolecular condensation, resulting in a high structural diversity of the oligosaccharides. Homopolysaccharides, such as cellulose, can be comprised of hundreds to thousands of D-glucose units joined through β(1→4) glycosidic bonds. While linear cellulose forms fibers, amylose has a helical shape comprised of D-glucose units, which, in contrast to cellulose, are connected through α(1→4) glycosidic linkages. Amylopectin has an even more complex structure, which is due to additional branching by α(1→6) glycosidic bonds every 24 to 30 glucose units (Scheme 1.1). Glycogen, a polysaccharide similar to amylopectin, has a much higher degree of branching and, thus, forms even bigger supramolecular structures.

Cellulose can be found in green plants as a main component of the cell wall and, therefore, is regarded as the most abundant organic compound in nature. Amylose and amylopectin occur as a mixture in starch, which is produced in plants as a form of energy storage and is a very common carbohydrate in food such as wheat, potatoes or rice. Glycogen serves the same purpose as starch but can be found exclusively in animals and fungi, where it functions as a long-term energy storage next to fats.[1]
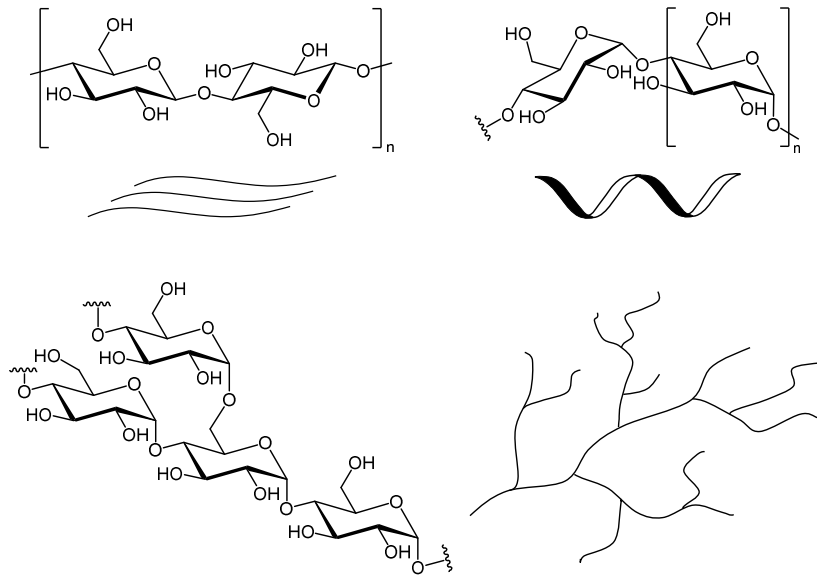
Scheme 1.1: Molecular structures of linear cellulose (top left), helical amylose (top right) and branched amylopectin (bottom). The supramolecular structure is illustrated next to the respective molecule.

Carbohydrates in Biological Systems

An intriguing fact about glycans is that they make up a large part of the membrane of all cells. In eukaryotic cells, the membrane consists of different lipids, which form a bilayer surrounding the cell, thus protecting it from external influences, such as pH changes or salts. Additionally, a variety of integral and peripheral membrane proteins are incorporated into the bilayer acting as receptors, ion channels or carrier proteins, for example (Figure 1.1A).

All proteins and lipids that are incorporated into the cellular membrane are functionalized with highly complex glycans at specific glycosylation sites, resulting in a thick layer of carbohydrates, which surrounds the whole cell. Due to its location at the outer part of the cell, this so-called glycocalyx (cf. Figure 1.1B) interacts with a broad spectrum of binding partners that induces different biological processes, which depend greatly on the particular interaction.[2] Many of these interactions have been investigated, showing that glycans as part of glycoproteins and glycolipids modulate cellular processes, such as signaling,[3] molecular recognition[4] and cell adhesion.[5]
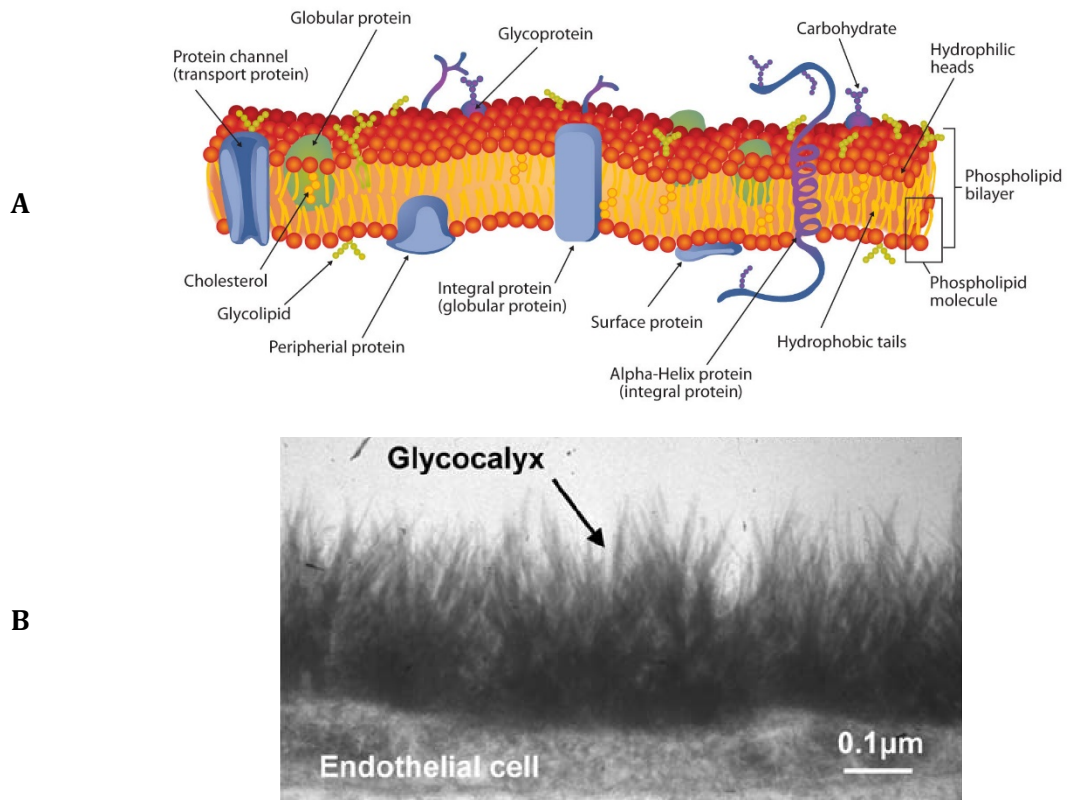
Figure 1.1: A) Schematic illustration of a cellular membrane with various incorporated proteins and lipids, which are functionalized with glycans at particular glycosylation sites.[2] B) Electron microscopic view of the glycocalyx of an endothelial cell.[6]

N-Glycans

There are two main types of glycans that are presented at protein glycosylation sites: *N*-linked and *O*-linked oligosaccharides. *N*-Glycans, being the most common kind of glycans, are bound to the amide group in the side chain of asparagine whereas the sequon (the sequence of consecutive amino acids) for *N*-glycosylation is Asn-X-Ser or Asn-X-Thr with X being any amino acid except proline. All *N*-glycans share a common core sequence of Manα1–6(Manα1–3)Manβ1–4GlcNAcβ1–4GlcNAcβ1-Asn and are subdivided into three types: high-mannose, in which exclusively mannose units are attached to the core sequence; complex, in which two to seven highly variable "antennae" are attached to *N*-acetylglucosamine (GlcNAc) units at the beginning of the core; and hybrid, in which mannose units are attached only to the Manα1–6 arm and one or two antennae to the Manα1–3 arm of the core (Figure 1.2).[7]
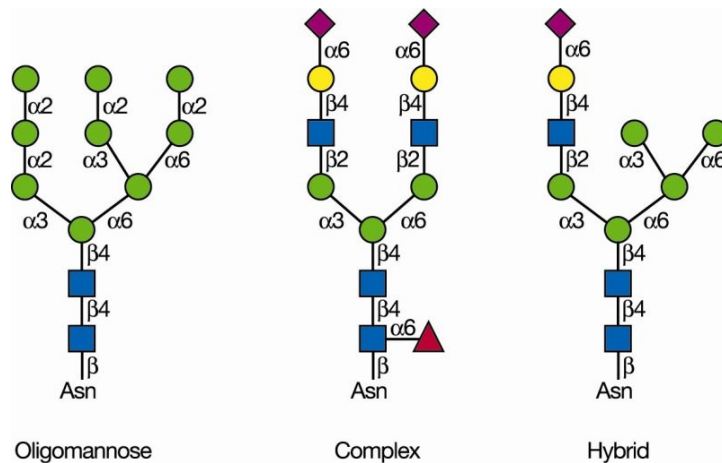
Figure 1.2: Types of *N*-glycans: high-mannose, complex and hybrid. Each *N*-glycan contains the common core Man$_3$GlcNAc$_2$Asn (blue square: GlcNAc; green circle: Man; yellow circle: Gal; purple square: Neu5Ac; purple triangle: fucose).[8]

O-Glycans

O-Glycans mainly occur in mucins, which are heavily *O*-glycosylated glycoproteins, acting as transmembrane proteins of cell surfaces, and can additionally be found in mucous secretions. In contrast to *N*-glycans, mucin *O*-glycans begin with an α-linked *N*-acetylgalactosamine (GalNAc) unit at the reducing end, which is linked to the side chain of serine or threonine. The GalNAc unit is often extended with other carbohydrates, such as *N*-acetylglucosamine (GlcNAc), galactose, fucose, or sialic acid, but most importantly not mannose, glucose, or xylose units. Mucin *O*-glycans can be branched and modified by *O*-acetylation of sialic acid and *O*-sulfation of galactose and GlcNAc.[9]

Glycolipids

Despite the sometimes heavy glycosylation of glycoproteins, the majority of carbohydrates on the cell surface are part of glycolipids. Glycans of this complex and diverse family of glycoconjugates are connected to a hydrophobic portion, which is most of the times incorporated into the cell membrane so that the carbohydrate is located in the extracellular matrix. But not all glycolipids are located at the cell surface and, for example, occur in the lumen of the endoplasmic reticulum (ER). Subfamilies of glycolipids are glycoglycerolipids, glycophosphoglycerolipids, glycosylated sterols, glycosylated prenols, lipopolysaccharides, and glycosphingolipids. The latter subfamily, including gangliosides, is one of the most frequently researched since it is involved in important cell signaling processes and occurs mainly in the nervous system. Glycosphingolipids are defined as glycolipids in which the

carbohydrate residue is connected to a ceramide backbone comprised of a sphingoid base, which is *N*-acylated with a long-chain fatty acid (Scheme 1.2).[10]
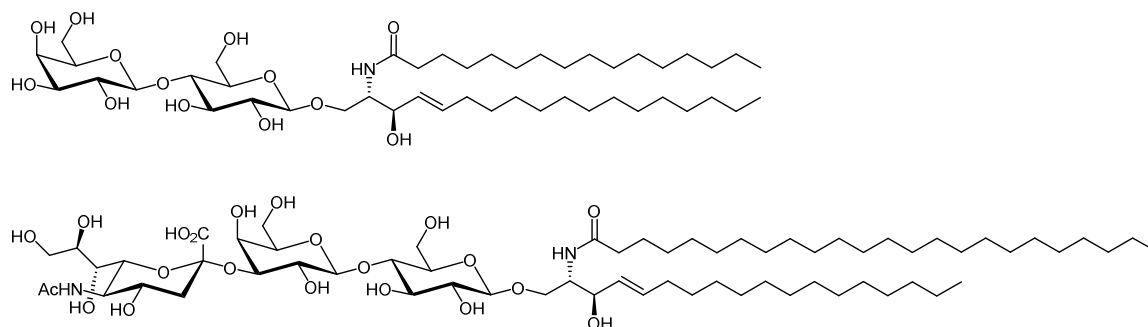
Scheme 1.2: Representative molecular structures of the glycosphingolipids lactosylceramide (top) and ganglioside GM3 (bottom).

1.2   Lectins and Their Relevance for Bacterial Adhesion

Glycans present in biological systems (whether at cell surfaces or in solution) are recognized and bound by specific carbohydrate binding proteins, which are called lectins. The specificity of the interaction with a particular carbohydrate can be as high as that between a substrate and an enzyme, or an antigen and an antibody.[11] However, the strength of a single lectin-monosaccharide interaction is relatively weak with dissociation constants in the micromolar to millimolar range.[12]

The first lectin was discovered and isolated in 1888 from the seeds of the castor oil plant by Herrmann Stillmark who described the agglutination of erythrocytes (red blood cells) by ricin.[13] At that time, this hemagglutination behavior, however, was not connected to the binding of carbohydrates by the isolated protein. This relation was drawn later by isolation of the well-known plant lectin concanavalin A (Con A) from the jack bean, being the first lectin which was identified to have a preference for binding of carbohydrates.[14] Although lectins were first discovered in plants, numerous lectins have been isolated from microorganisms and animals as well. Elucidation of the structures of various lectins from different sources has shown that their primary sequences mostly lack similarities, although they often share similarities in their tertiary structures. Further investigations, however, have revealed that the carbohydrate specificity of each lectin is caused by a conserved amino acid sequence forming the so-called carbohydrate recognition domain (CRD). Recognizing the terminal non-reducing carbohydrate moiety of glycan ligands, the CRD particularly discriminates between the α- and β-anomers, resulting in different binding affinities.[15]

Lectins in Bacteria

Like in the case of ricin, the ability to agglutinate erythrocytes has also been identified for bacteria, especially of the *Enterobacteriaceae* family. This hemagglutination activity is linked to the interaction of filamentous protein appendages on the bacterial surface, so-called fimbriae, with the glycosylated erythrocytes. Lectin subunits on the fimbriae mediate this carbohydrate-specific adhesion of the bacteria to the cell surface and, hence, the subsequent agglutination. This phenomenon of bacterial colonizing of cell surfaces by recognition and binding of the sugar decoration on cells has also been observed, for example, in the case of epithelial cells.[16]

1.3   Type 1 Fimbriae-mediated Bacterial Adhesion

Pathogenic *Escherichia coli* (*E. coli*) bacteria are responsible for a number of infectious diseases, such as neonatal meningitis, urinary tract infections, and gastroenteritis, which are triggered by adhesion of the bacteria to human cells. Adhesion occurs mainly *via* different types of fimbriae on the bacteria's surface (Figure 1.3A).[17] One important class of these adhesive organelles are type 1 fimbriae, which have been found to be responsible for specific adhesion to cells bearing glycans with a high mannose content.[18]

This special type of fimbriae is composed of the main structural pilus subunit FimA forming the pilus rod, subunits FimF, FimG, and the mannose-specific adhesin FimH, which form the distal tip fibrillum. Assembly of the fimbriae proceeds by a chaperone-usher pathway in the periplasm. Here, the fimbrial subunits (FimA, FimF, FimG, and FimH) enter in an unfolded conformation and form complexes with the chaperone FimC. Upon interaction with the usher FimD, which forms a pore in the outer membrane of the cell, the chaperone-subunit complexes again dissociate and the chaperone remains in the periplasm. The subunits then cross the outer membrane through the FimD pore and become incorporated into the growing pilus (Figure 1.3B).[19]
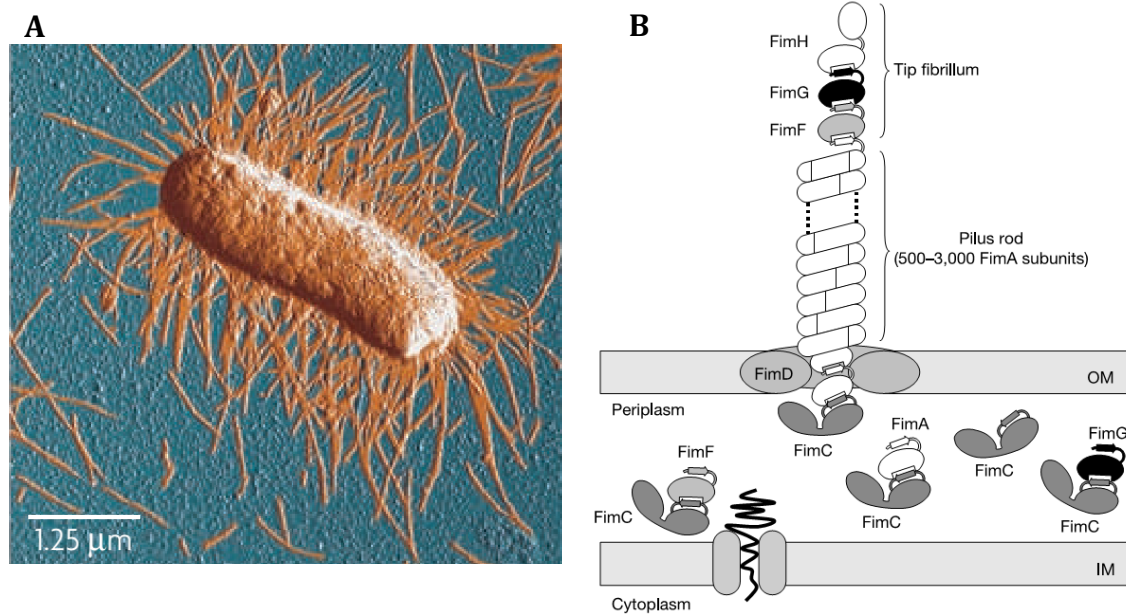
Figure 1.3: (A) TEM image of an *E. coli* cell, showing fimbriae on the cell surface.[20] (B) Assembly of type 1 fimbriae according to the chaperone-usher pathway inside the periplasm. IM: inner membrane; OM: outer membrane; FimH: fimbrial lectin; FimC: periplasmic chaperone; FimD: fimbrial usher protein; FimA, FimD, FimF, and FimG: other fimbrial subunits.[19]

The Bacterial Lectin FimH

Examination of the crystal structure of a FimH-FimC chaperone complex has revealed that the adhesin FimH actually consists of two domains, a $FimH_P$ pilus domain and a $FimH_L$ lectin domain.[21] Therein, the C-terminal $FimH_P$ domain functions as a sort of anchor, attaching the N-terminal mannose-binding $FimH_L$ domain to the pilus. At the tip of this domain, the CRD of FimH can be found, which is capable of binding a mannose moiety in its α-configuration. Later, an X-ray structure of FimH containing a mannose molecule inside the CRD was analyzed.[22] It was found that the hydroxyl groups of the mannose (excluding the anomeric hydroxyl group) interact with amino acids inside the FimH CRD through hydrogen bonds, especially with residues Phe1, Asn46, Asp47, Asp54, Gln133, Asn135, Asp140, and Phe142. Interestingly, mannosides which contain an aromatic portion, such as *p*-nitrophenyl α-D-mannoside (*p*NPMan), have been found to exhibit increased affinities for the CRD of FimH. Two distinct tyrosine residues Tyr48 and Tyr137, which form the so-called "tyrosine gate", near the entrance of the CRD (cf. Figure 1.4) undergo π-π interactions with the glycoconjugate's aromatic system, thus, improving the overall complexation within the CRD.[23]
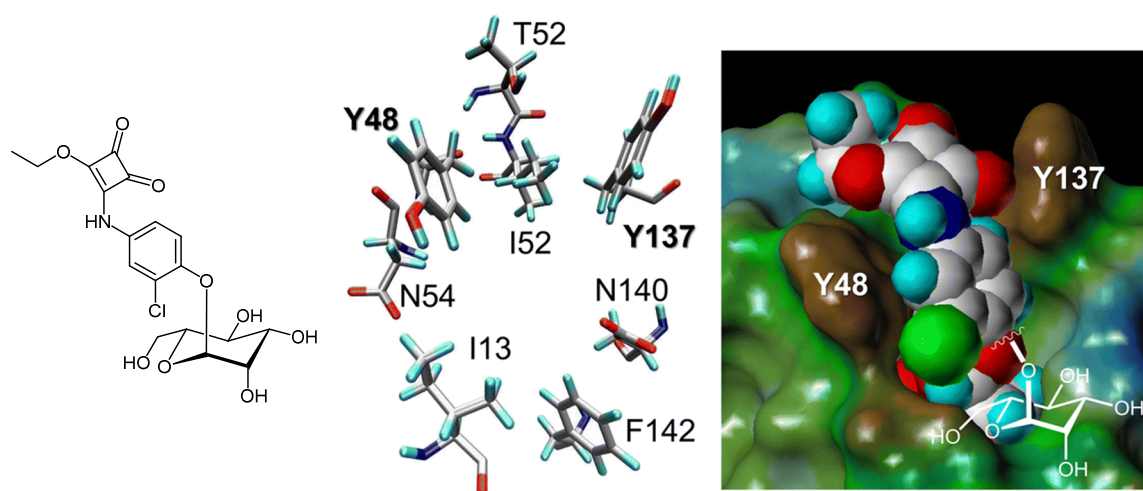
Figure 1.4: (Left) Molecular structure of an aromatic α-D-mannoside containing a squaric acid ester attached to the chloro-substituted phenyl ring in the aglycone. (Middle) Amino acid residues located at the entrance of the CRD of FimH. The "tyrosine gate" is formed at the entrance of the CRD by tyrosine residues Tyr48 and Tyr137. (Right): The CRD depicted as a Connolly surface, complexing the aromatic mannoside, which is presented as a CPK model. The aromatic system interacts with the "tyrosine gate" at the rim of the CRD.[24]

1.4   Investigation and Control of Bacterial Adhesion

Bioconjugation of Carbohydrates

For investigation of type 1 fimbriae-mediated bacterial adhesion, the synthesis of appropriate glycoconjugates by utilization of efficient chemical reactions is an unavoidable step. The field of bioconjugation is concerned with the research of selective reactions that allow for synthesis of glycoconjugates without involving protecting group manipulations, resulting in a high product yield and minor to no by-product formation. This methodology is an essential tool not only for investigation of bacterial adhesion, but also for the discovery of new drugs against diseases that are mediated through protein-carbohydrate interactions. Fields of application for bioconjugation concern the fabrication of glycoarrays on different surfaces (e. g. gold, polystyrene, glass), the preparation of oligovalent glycoconjugates, such as glycoclusters and glycodendrimers, and labeling of carbohydrates with fluorescent markers or other tags like biotin, for example.[25] Several reactions have been successfully employed in this regard, such as native chemical ligation,[26] Staudinger ligation,[27] thiol-maleimide ligation,[28] Diels-Alder reaction[29] and so-called "click chemistry".[30] Within the click chemistry concept, the copper(I)-catalyzed azide alkyne cycloaddition (CuAAC) has become the most prominent reaction.[30b, c] It is an advanced variant of the azide-alkyne Huisgen cycloaddition as first elaborated by Huisgen[31] in the 1960s.

The Cluster Effect

Since a single lectin-carbohydrate interaction is rather weak, optimization of the aglycone in order to increase the strength of interaction has been extensively performed over recent years. Another approach to improve these interactions is the investigation of multivalent glycoconjugates, which contain several mannose residues for the interaction with the lectin. It has been observed that a linear increase of ligand valency often results in a logarithmic increase of the avidity (the overall strength of all lectin-carbohydrate interactions).[32] For this phenomenon, the term "cluster effect" was coined, which is especially pronounced in lectins having multiple CRDs.[33] However, this effect has also been observed in the case of the bacterial lectin FimH, which was proven to be monomeric and having just one CRD. It was suggested that the observed cluster effect, in this case, is a result of an increased effective concentration of mannosyl residues in close proximity to the CRD of FimH. Therefore, quick rebinding of a mannose residue is statistically favored in multivalent ligands after release of a previously bound mannoside from the CRD.[16]

Control of Bacterial Adhesion by Photoresponsive Glycoconjugates

As described above, the extent of bacterial binding to glycoconjugates depends strongly on the molecular structure of the employed glycoconjugate, concerning the chemical nature of its aglycone as well as its valency. However, also the spatial arrangement of the presented carbohydrate residues, for example, on a surface has been found to be quite critical for the efficiency of bacterial adhesion. Approaches that are based on the control of the spatial arrangement of carbohydrates and, thus, the extent of bacterial adhesion, involved particular mannosides containing a photoresponsive azobenzene portion.[34]

Azobenzene[35] is a well-known photoresponsive molecule, which has been widely studied with regard to its properties towards photoisomerization.[36] When the planar and more stable E isomer is irradiated with UV light ($\lambda \approx 365$ nm), isomerization to the bent Z form is induced.[37] In case of exposure to visible light or upon thermal relaxation, back-isomerization to the E isomer takes place. The half-time ($\tau_{1/2}$) of thermal $Z{\rightarrow}E$ relaxation can vary significantly depending i. a. on the substitution of the aromatic system (Scheme 1.3).[38]
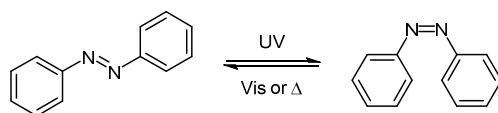
Scheme 1.3: Irradiation with UV light induces reversible *E/Z* photoisomerization of azobenzene. *Z→E* back-isomerization can be effected by exposure with visible light or thermal energy.

The first contribution which demonstrated that the photoisomerization of azobenzene glycosides and the resulting change in spatial orientation of carbohydrate moieties affects type 1 fimbriae-mediated bacterial adhesion was made by Weber *et al.* in 2014. Therein, the specific adhesion of type 1 fimbriated *E. coli* to azobenzene mannoside ligands, with a given orientation by the configuration of an azobenzene monolayer on a non-physiological surface, was investigated. Changing the orientation of the ligands by means of photoisomerization is thought to influence the recognition behavior of *E. coli* bacteria, resulting in greatly decreased adhesion. Furthermore, it was demonstrated that *Z→E* back-photoisomerization led to the original orientation of the carbohydrate moieties and thus restored bacterial adhesion (Figure 1.5).[34a]
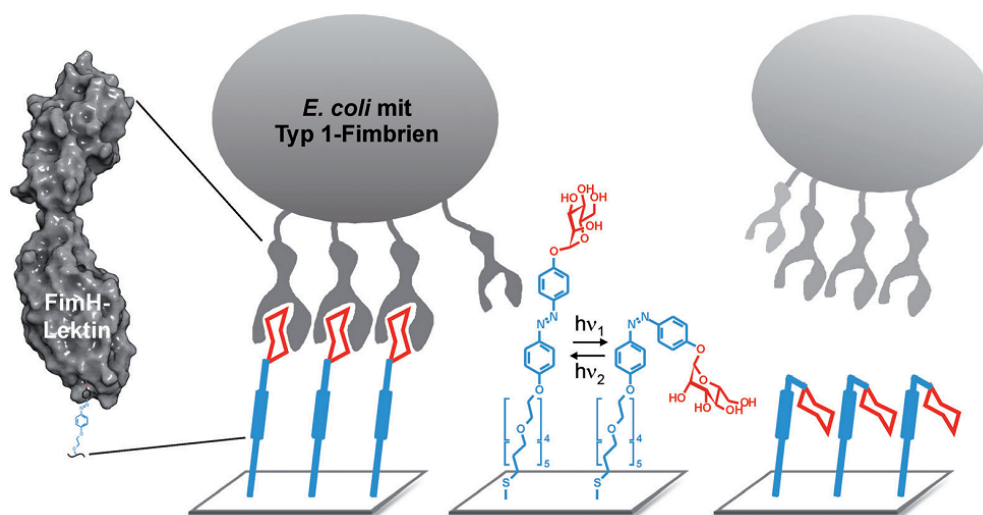
Figure 1.5: The adhesion of type 1 fimbriated *E. coli* cells is mediated by the lectin FimH at the fimbrial tip. Cellular recognition is depending on the spatial orientation of azobenzene mannosides immobilized on the surface, which can be changed by reversible *E/Z* photoisomerization with two different wavelengths.[34a]

In another approach, the methodology described above was applied to the surface of HMEC-1 human cells. Azobenzene glycosides were attached to the cell surface *via* click chemistry and the cells were subsequently irradiated with UV light. Investigation of type 1 fimbriae-mediated bacterial adhesion under static as well as flow conditions demonstrated that

adhesion to the azobenzene glycoside-modified cell surface is higher in the *E* than in the *Z*-state (Figure 1.6).[34b]
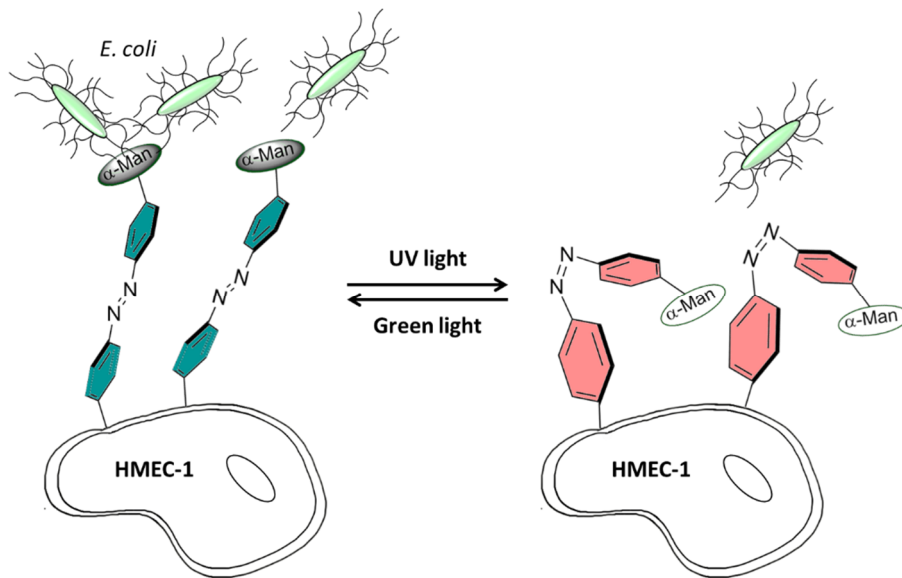
Figure 1.6: Reversible *E/Z* isomerization employing UV or visible light, respectively, allows to change the orientation of the azobenzene-conjugated sugar and to manipulate sugar-specific bacterial adhesion in parallel.[34b]

2.   Objectives

Adhesion of bacteria to human cells is a crucial step in the initiation of several infectious diseases. With the rise of bacterial strains that have become resistant to previously effective antibiotics, fighting these diseases is getting more difficult. This emphasizes the importance of research on bacterial adhesion for the further understanding of this process and the development of efficient strategies for the treatment of bacterial infections.

In the scope of this thesis, variable methodological approaches were studied in order to support and facilitate research in the field of bacterial adhesion. Since bioconjugation is an essential tool for the synthesis of glycoconjugates needed for investigation of bacterial adhesion, new ligation methods according to the bioconjugation methodology are of special interest. Chapter 3 focuses on the exploration of the Amadori rearrangement as a potential candidate for bioconjugation of carbohydrates. In this chapter, the synthesis of different Amadori products is presented as well as their examination by molecular modeling and biological testing. Furthermore, colored Amadori products are applied in order to facilitate their chromatographic purification.

Glycoclusters as well as carbohydrate scaffold compounds, which can be utilized as precursors for carbohydrate-centered glycoclusters, are valuable tools for investigation of multivalency effects in bacterial adhesion. Chapter 4 involves the synthesis of various AB_4-type carbohydrate scaffolds and a tetravalent glycocluster. Additionally, biological testing of the glycocluster is presented in respect of the investigation of multivalency effects in bacterial adhesion.

In order to enhance and facilitate research in the field of bacterial adhesion, developing new assay systems is an important step. In Chapter 5, different approaches for the development of a new assay format, which allows for "switchable" cell adhesion, are presented. Based on inclusion of azobenzene guest molecules into cyclodextrin hosts, this assay system allows for attenuation of bacterial binding to certain glycoconjugates, which are either connected to the host or the guest molecule. Switching of cell adhesion is initiated by photoisomerization of the respective azobenzene unit, disrupting the host-guest-complexes.

3. Exploration of the Amadori Rearrangement for Bioconjugation of Carbohydrates

3.1 Introduction

In general terms, the Amadori rearrangement is the acid-catalyzed reaction between α-hydroxy aldehydes and amines, leading to α-amino ketones. When applied to carbohydrates, aldoses like D-glucose (**1**) also undergo this rearrangement upon reaction with suitable amines, forming the respective *C*-glycosyl type 1-amino-1-deoxyketoses, such as **2** (Scheme 3.1).
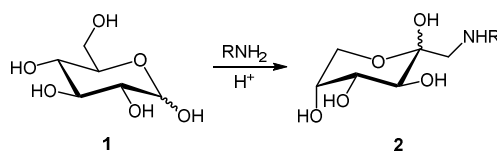
Scheme 3.1: Amadori rearrangement between an amine and D-glucose (**1**). The rearrangement product is the respective 1-amino-1-deoxyketose **2**.

The history of the Amadori rearrangement goes back to the year 1925 when the Italian chemist M. Amadori[39] claimed to have isolated two compounds by reacting D-glucose (**1**) with different aromatic amines, defining the products as a mixture of the respective glucosyl amines as well as the related Schiff bases. In the mid-1930s, Kuhn and Dansi[40] revised Amadori's experiments and concluded that the compounds he obtained were actually products of a new type of rearrangement reaction. In continuation, Kuhn and Weygand[41] described the mechanism of this reaction (Scheme 3.2), which they named the Amadori rearrangement. The initial step therein is the nucleophilic attack of an amino group at the anomeric carbon of an aldose like **1**, forming a glycosylamine **3**. Protonation induces ring opening and creates a Schiff base **4** which is in equilibrium with its enol form **5** due to enamine-imine tautomerism. Thus, tautomerization turns the enol **5** into the more stable ketone, namely 1-amino-1-deoxyketose **6**, which cyclizes to the respective hemiketal upon attack of the primary hydroxyl group at the carbonyl carbon.
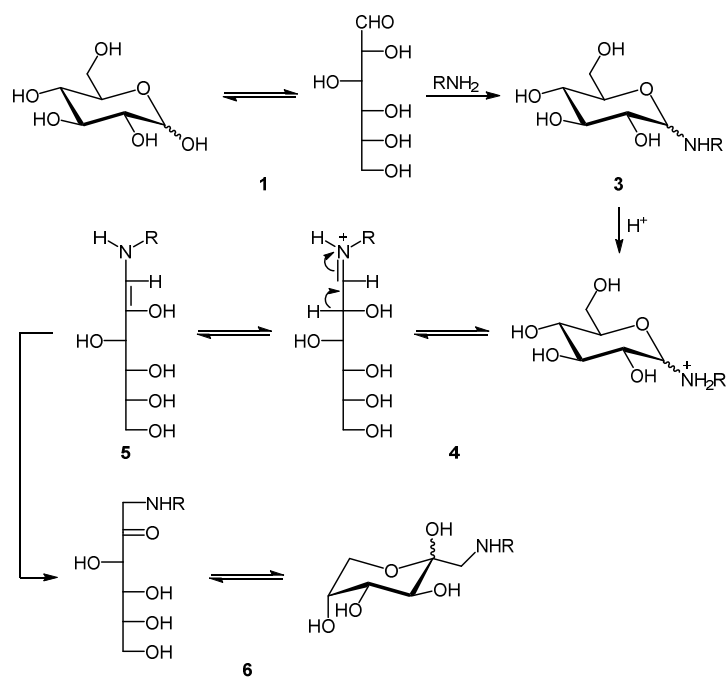
Scheme 3.2: Mechanism of the Amadori rearrangement, exemplified with D-glucose (**1**). Nucleophilic attack of an amine at the anomeric position of **1** creates a glycosylamine **3**. After protonation and ring opening, the Schiff base **4** is formed, which is in equilibrium with its enol form **5**. Keto-enol tautomerism results in 1-amino-1-deoxyketose **6**, undergoing ring closure to the corresponding hemiketal.

The Amadori rearrangement, together with the Heyns[42] rearrangement, is known as the initial step of the Maillard[43] reaction cascade, as a form of non-enzymatic browning of food. Being of great importance for flavor, taste, and color, it is a result of food processing under the influence of heat.[44] In this highly complex cascade of parallel and subsequently proceeding reactions, amino groups in amino acids, peptides, and proteins, respectively, react with reducing sugars. This affects the nutritional quality and, in some cases, also involves the formation of hazardous substances, such as the potentially cancerogenous acrylamide.[45]

Application of the Amadori Rearrangement in Organic Synthesis

Besides its occurrence in nature, the Amadori rearrangement has also found several applications in carbohydrate chemistry. In 1959, Kuhn *et al.* reported an attractive procedure for the synthesis of lactulose from lactose by employing the Amadori rearrangement as a key step.[46] This contribution is a sophisticated alternative to the previous synthesis of lactulose, which has been accomplished by application of the Lobry de Bruyn–Alberda van Ekenstein rearrangement.[47] Later, Paulsen *et al.* applied an intramolecular Amadori rearrangement in the synthesis of an iminosugar.[48] Iminosugars are carbohydrate analogs, where the endocyclic ring oxygen is substituted by a nitrogen atom. This important class of compounds has been identified as powerful glycosidase inhibitors.[49]

Despite its successful application in complex synthesis, the Amadori rearrangement suffers from a number of preparative drawbacks. The products arising from the reaction are prone to enter the Maillard cascade, leading to formation of unwanted by-products. These can act as initiators of subsequent reactions, such as dehydration, cyclization, oxidation, or fragmentation, resulting in a variety of secondary products. In addition, the products are often not very stable and may decompose during prolonged reaction times.[50]

Four main factors significantly influence the efficiency of the Amadori rearrangement: the nature of the employed amine and carbohydrate, the temperature, the reaction time, and the acid catalyst. In this regard, the Wrodnigg group was able to optimize the reaction conditions for the introduction of various amines onto the C-1 position of different carbohydrates without the requirement of any protecting group manipulations.[51] Three potent analogs of glycosidase inhibitor 2,5-dideoxy-2,5-imino-D-mannitol[52] were prepared by starting from a glucofuranose **7** (Scheme 3.3). Three different amines were then utilized for the Amadori rearrangement, giving products **8**, **9**, and **10**, respectively, in remarkably high yields. Final cyclization by means of intramolecular reductive amination gave inhibitors **11**, **12**, and **13**, respectively.
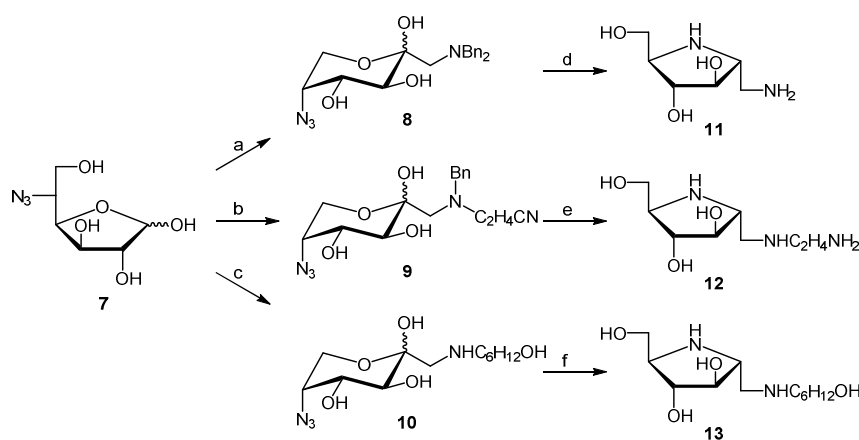
Scheme 3.3: Application of the Amadori rearrangement in the synthesis of glycosidase inhibitors **11**, **12** and **13**. a) Dibenzylamine, AcOH, EtOH, 40 °C, 1 h, 90%; b) 3-(benzylamino)propionitrile, 40 °C, 1 h, 83%; c) aminohexanol, AcOH, 40 °C, 1 h, 96%; d) H₂, Pd(OH)₂/C, MeOH, 4 d, 52%; e) H₂, Pd(OH)₂/C, MeOH, 24 h, 31%; f) H₂, Pd(OH)₂/C, MeOH, 2 h, 26%.

Each final step in the synthesis of **11**, **12**, and **13** involves the cyclization of the respective Amadori products **8**, **9**, and **10** through a sequence of successive reactions. Although a precise mechanism of this cyclization has not been published so far, a conceivable mechanism is presented by the example of Amadori product **8** (Scheme 3.4). Therein, initial hydrogenation of Amadori product **8** results in both reduction of the azide at the C-5 position as well as debenzylation of the C-1 amino group. Intramolecular attack of the C-5 amine at the anomeric

carbon of **8a** induces ring closure, forming the corresponding Schiff base **13a**, which is subsequently reduced to the glycosidase inhibitor **13**.
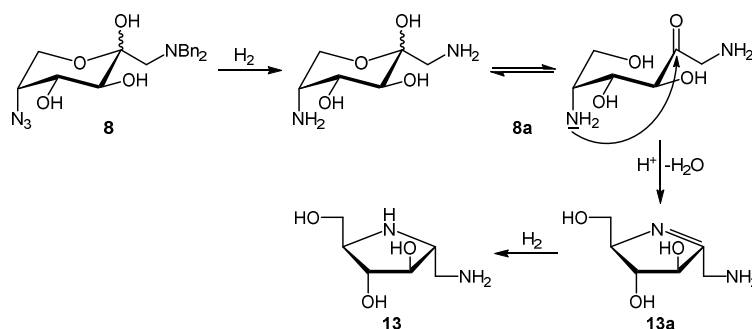
Scheme 3.4: A conceivable mechanism for the cyclization of Amadori product **8**, resulting in glycosidase inhibitor **13**.

As demonstrated by the examples described above, the Amadori rearrangement can be utilized as a powerful glycoconjugation method. However, it is important to stress that the reactants as well as the reaction conditions have to be adapted for every individual example in order to minimize side reactions and, hence, the amount of formed by-products. If these criteria are met, this glycoconjugation reaction may be suited for certain applications in the field of bioconjugation (cf. Chapter 1.4). The rearrangement products as *C*-glycosyl type glycoconjugates are of special interest for biological investigations since the glycosidic linkage of such compounds has a higher stability towards physiological hydrolysis, compared to the natural occurring *O*- as well as *N*-glycosides.[53] Even enzymatic deglycation of Amadori products does not occur in the presence of regular glycosidases, which catalyze *O*-glycoside hydrolysis. The most frequently researched deglycating enzymes are fructosyl amine oxidases, which catalyze the oxygen-mediated oxidation of Amadori compounds through cleavage at the ketoamine bond followed by release of the amine, glucosone, and H_2O_2. Although this class of enzymes mostly occurs in fungi and bacteria but not in mammals, however, only fructose-derived Amadori products are recognized and oxidized.[54]

This chapter covers the investigation of the Amadori rearrangement as a potential bioconjugation method. Research on this project was performed in collaboration with the Glycogroup at the TU Graz, owing to their enormous experience in this field, in the frame of a DFG project.[55] While the Glycogroup investigated different types of mono- but also multivalent Amadori rearrangement reactions,[56] I focused on biological testing of particular compounds in connection with the published manuscript in Chapter 3.2, which involves Amadori products as FimH ligands. Furthermore, I conducted special applications of the Amadori rearrangement in terms of chromophore-assisted purification[57] (cf. Chapter 3.3).

3.2   Are D-*manno*-configured Amadori Products Ligands of the Bacterial Lectin FimH?

* These authors contributed equally

The Lindhorst research group has outstanding experience in the investigation of type 1 fimbriae-mediated bacterial adhesion. In the course of this research, a wide range of different mono- but also multivalent glycoconjugates have been synthesized and tested as inhibitors in bacterial adhesion studies. Concerning the synthesis, the group has often made use of efficient and selective ligation reactions, such as thiourea coupling, native chemical ligation, or click chemistry in order to realize their syntheses. Therefore, the investigation of chemoselective ligation methods, particularly for the synthesis of new FimH ligands, is of high interest.

In the following article we applied the Amadori rearrangement in the synthesis of two *C*-glycosyl type D-mannoside analogues and investigated both glycoconjugates as ligands of type 1 fimbriated *E. coli* in molecular modelling studies and biological tests. It was found that both ligands have a reduced potency as inhibitors of bacterial adhesion, which was supported by molecular modelling studies, revealing that the complexation inside the carbohydrate binding site of FimH is hampered by the β-*C*-glycosidically linked aglycone.
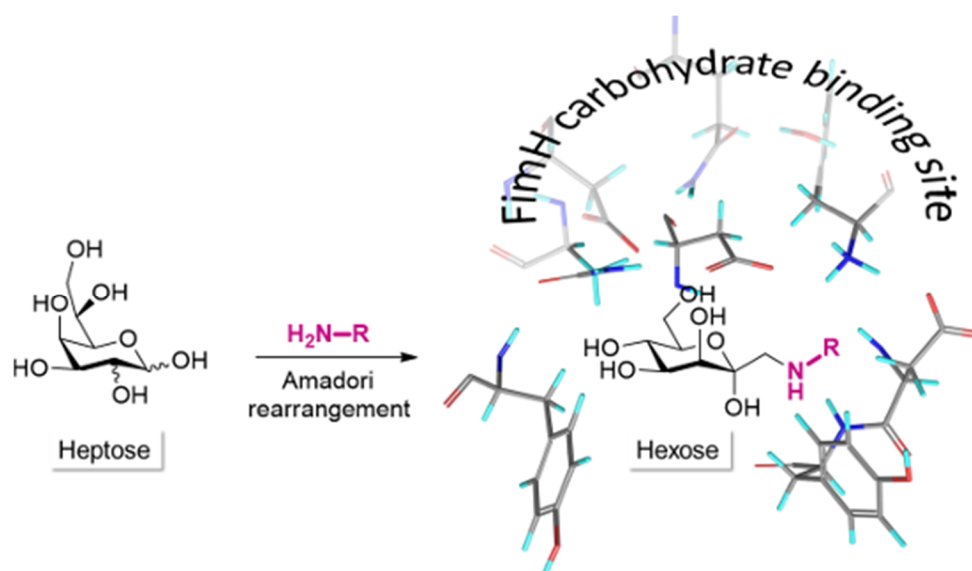
Figure 3.1: Using the Amadori rearrangement, D-*manno*-configured hexoses can be synthesized from appropriate heptoses and amines. Since the aglycone in these compounds is connected through a β-*C*-glycosidic linkage to the anomeric carbon, the complexation in the FimH carbohydrate binding site requires a different binding mode as for regular α-D-mannosides.

For this project, C. Hojnik synthesized and characterized the tested substances, I. Stamer performed and interpreted the molecular modelling studies and I conducted the biological tests and evaluated the obtained data. All authors contributed in writing the article as well as the Supporting Information (SI).

Are D-*manno*-configured Amadori products ligands of the bacterial lectin FimH?

Tobias-Elias Gloe[‡1], Insa Stamer[‡1], Cornelia Hojnik[‡2], Tanja M. Wrodnigg[*2] and Thisbe K. Lindhorst[*1]

Full Research Paper

Address:
[1]Christiana Albertina University of Kiel, Otto Diels Institute of Organic Chemistry, Otto-Hahn-Platz 3/4, D-24118 Kiel, Germany, Fax: +49 431 8807410, and [2]Glycogroup, Institute of Organic Chemistry, Technical University Graz, Stremayrgasse 9, A-8010 Graz, Austria

Email:
Tanja M. Wrodnigg[*] - t.wrodnigg@tugraz.at; Thisbe K. Lindhorst[*] - tklind@oc.uni-kiel.de

* Corresponding author   ‡ Equal contributors

Abstract

The Amadori rearrangement was employed for the synthesis of *C*-glycosyl-type D-mannoside analogues, namely 1-propargyl-amino- and 1-phenylamino-1-deoxy-α-D-*manno*-heptopyranose. They were investigated as ligands of type 1-fimbriated *E. coli* bacteria by means of molecular docking and bacterial adhesion studies. It turns out that Amadori rearrangement products have a limited activity as inhibitors of bacterial adhesion because the β-*C*-glycosidically linked aglycone considerably hampers complexation within the carbohydrate binding site of the type 1-fimbrial lectin FimH.

Introduction

The Amadori rearrangement (AR) is the reaction in which aldo-hexoses react with suitable amines under acidic catalysis to 1-amino-1-deoxyketohexoses (*C*-glycosyl-type pentose analogues) without the need of hydroxy group protection (Scheme 1). For a long time this reaction has been judged as unsuitable for preparative use as it typically leads to a complex mixture of products accompanied with a low yield of the rearrangement product itself [1]. However, we could show that the Amadori rearrangement, when applied to selected aldoses as starting materials, is a high yielding and efficient synthetic approach towards *C*-glycosyl-type glycoconjugates. For example,

when aldoheptoses are employed as starting material for the Amadori rearrangement, the respective 1-amino-1-deoxyketo-heptoses (*C*-glycosyl-type hexose analogues) can be obtained in exclusively one anomeric form as well as in excellent yields (Scheme 1) [2,3]. Thus, the Amadori rearrangement can be utilised to convert a respectively configured aldoheptose into a *C*-glycosyl-type glycoconjugate in one step and without the need of protecting group manipulations. This is intriguing in light of biorthogonal ligation methodology as Amadori products are structurally closely related to naturally occurring D-hexopyranosides. In addition, *C*-glycosyl glycoconjugates are
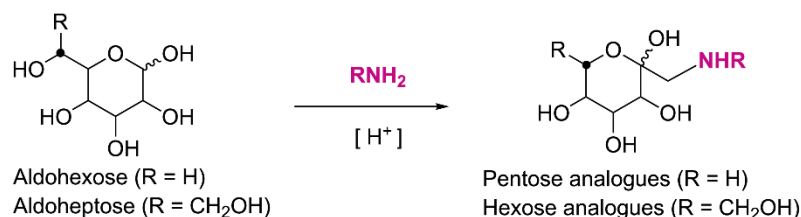
Scheme 1: The Amadori rearrangement of aldoses with amines leads to *C*-glycosyl-type glycoconjugates, namely 1-amino-1-deoxyketoses.

believed to bear great potential as therapeutics and as tools for mechanistic studies in biology. This is because they are not sensitive towards enzymatic hydrolysis such as in physiological environment, in contrast to the naturally occurring *O*- and *N*-glycosides.

With respect to our long-lasting interest in the design and investigation of ligands for the bacterial lectin FimH [4] it has been our goal to investigate the Amadori rearrangement as a method to approach new FimH ligands. These are especially relevant in the context of an anti-adhesion therapy against bacterial infections [5,6]. As FimH-mediated adhesion to the glycosylated surface of host cells is a key step in infections caused by type 1-fimbriated bacteria, FimH antagonists that inhibit bacterial adhesion can be valuable for treatment of infectious diseases [7,8]. The structure of type 1-fimbrial lectin FimH has been elucidated in X-ray analysis [9-11]. Obviously, FimH binds α-D-mannosides such as simple methyl α-D-

mannoside (MeMan, **1**) but not β-mannosides. Mannosides with an aromatic aglycone, such as *p*-nitrophenyl α-D-mannoside (*p*NPMan) and 4-methylumbelliferyl α-D-mannoside (**3**) show an improved affinity to FimH due to π–π-stacking interactions of the aromatic moiety with the so-called tyrosine gate at the entrance of the carbohydrate binding site, formed by Y48 and Y137. Additional interactions exerted by extended aglycone portions can further improve ligand affinity for FimH; for example *ortho*-chloro substitution of the phenyl ring (compounds **2** and **5**), a squaric acid partial structure (compound **4**) or heterocyclic substituents such as in indolinylphenyl mannoside **5** as recently introduced [12] (Figure 1).

With the structural requirements of the type 1-fimbrial lectin FimH for its ligands in mind, we addressed the question, if D-*manno*-configured Amadori products with their axially oriented anomeric hydroxy group can function as a new class of FimH ligands. In addition, we can assume that Amadori prod-
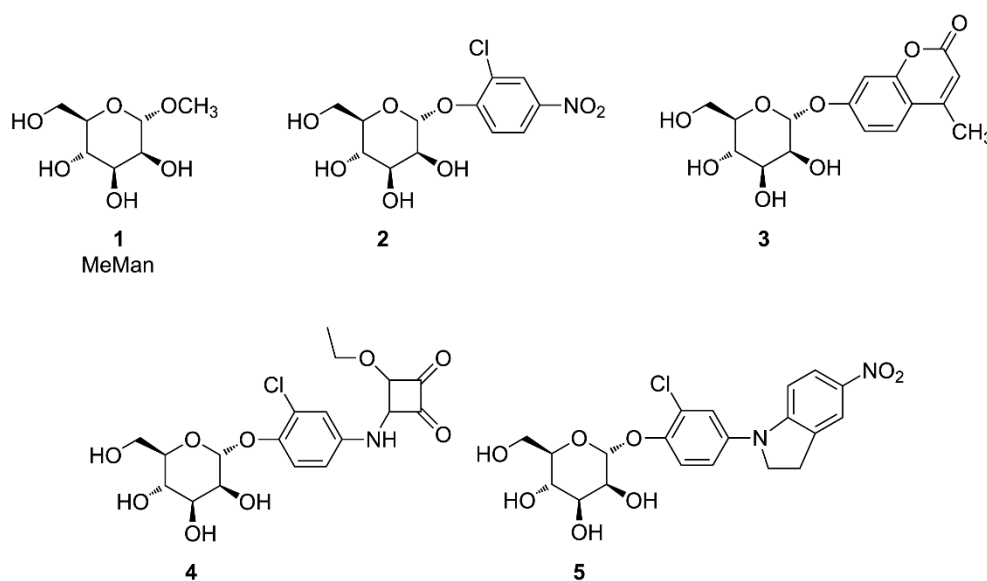
Figure 1: The bacterial lectin FimH is known to bind α-D-mannosides such as methyl α-D-mannoside **1** (MeMan) with IC$_{50}$ values in the millimolar range [4]. Based on MeMan (**1**), the affinity of the *p*NPMan derivative **2** is 717-times improved [13], that of the methylumbelliferyl mannoside **3** 116 times improved [14], that of the squaric ester monoester **4** 6900 times higher [15], and the indolinylphenyl mannoside **5** arrives at an IC$_{50}$ of 2.4 nM [8].

ucts are stable against cleavage by mannosidases, as we found earlier that D-*gluco*-configured Amadori products are no substrates for glucosidases.

Results and Discussion
Synthesis of heptopyranose 8 and Amadori products 9 and 10

To access *manno*-configured rearrangement products for the synthesis of FimH ligands, we needed to synthesise the appropriate aldoheptose starting material. Its synthesis starts with the oct-1-enitol derivative **6** which can be easily obtained by a Grignard reaction of 2,3:5,6-di-*O*-isopropylidene-D-mannose employing commercially available vinylmagnesium bromide (Scheme 2) [16,17]. This C-elongation approach leads to a mixture of C-2 diastereomers, however, during the Amadori rearrangement this centre is converted to a keto group and thus separation of the C-2 epimeric mixture prior to the Amadori rearrangement is not necessary. Simple ozonolysis of the diastereomeric mixture **6** afforded a mixture of the protected D-*glycero*-D-*galacto*- and D-*glycero*-D-*talo*-configured heptoses **7a** and **7b** in quantitative yield. After sequential

cleavage of the protecting groups, employing Zemplén conditions to remove acetyl groups [18,19] followed by acidic cleavage of the isopropylidene groups, the desired starting material for the Amadori rearrangement, a mixture of D-*glycero*-D-*galacto*/D-*talo* heptopyranoses (**8a/b**) was obtained in an overall yield of 85% from **6**. This is a synthetic route 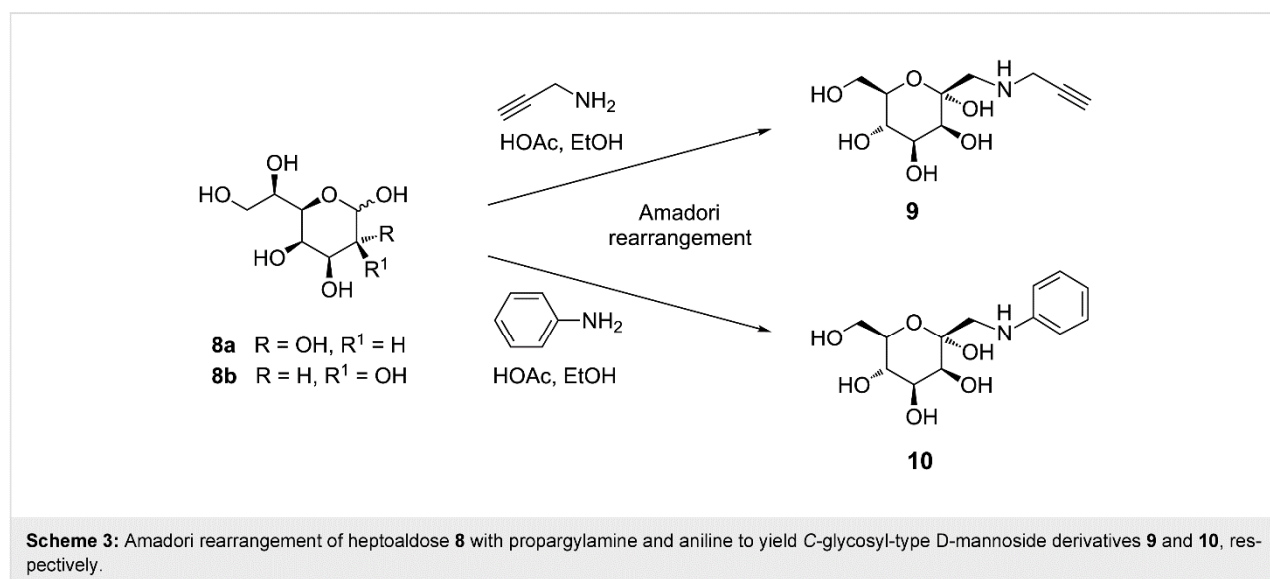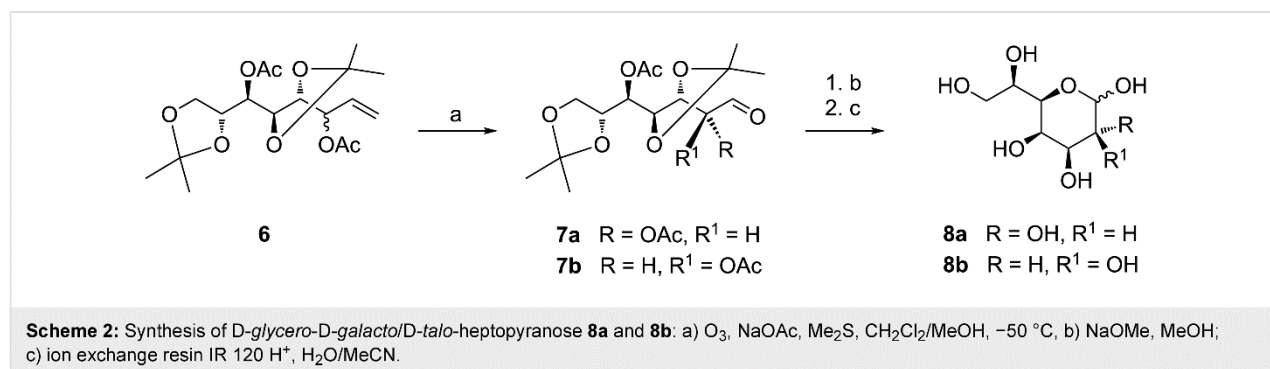to aldoheptoses **8a** and **8b** alternative to the one reported [2] with the advantage that the use of environmental hazardous as well as highly toxic HCN is not required.

Amadori rearrangement of the diasteromeric mixture **8** with an amine of choice allows an efficient and versatile approach towards D-*manno*-configured *C*-glycosyl-type glycoconjugates. In our study, we have employed two different amines in the Amadori rearrangement with **8**, propargylamine and aniline. Under typical conditions for this reaction [2] 1-progargylamino-1-deoxy-D-*manno*-heptulose **9** and 1-phenylamino-1-deoxy-D-*manno*-heptulose **10** were obtained as pure α-anomers in 77% and 24% yield, respectively (Scheme 3). The low yield of compound **10** may be explained by the low pK_a value (4.62) of aniline compared to a pK_a of 8.15 for propargylamine, the latter

Scheme 2: Synthesis of D-*glycero*-D-*galacto*/D-*talo*-heptopyranose **8a** and **8b**: a) O$_3$, NaOAc, Me$_2$S, CH$_2$Cl$_2$/MeOH, −50 °C; b) NaOMe, MeOH; c) ion exchange resin IR 120 H$^+$, H$_2$O/MeCN.

Scheme 3: Amadori rearrangement of heptoaldose **8** with propargylamine and aniline to yield *C*-glycosyl-type D-mannoside derivatives **9** and **10**, respectively.

being clearly more efficient as a nucleophile for this type of reaction. Analogous observations have been made in previous studies [20].

Rearrangement products **9** and **10** exist in their $^5C_2$ pyranoid conformation as determined by NMR analysis and can thus indeed be regarded as analogues of α-D-mannosides. The *N*-alkyl/aryl aminomethyl substituent at the anomeric position is found in the sterically favoured equatorial position located towards the β-face of the sugar ring, whereas the anomeric hydroxy group is α-positioned. Whether this particular *C*-type glycoside architecture is suited for FimH complexation had to be tested.
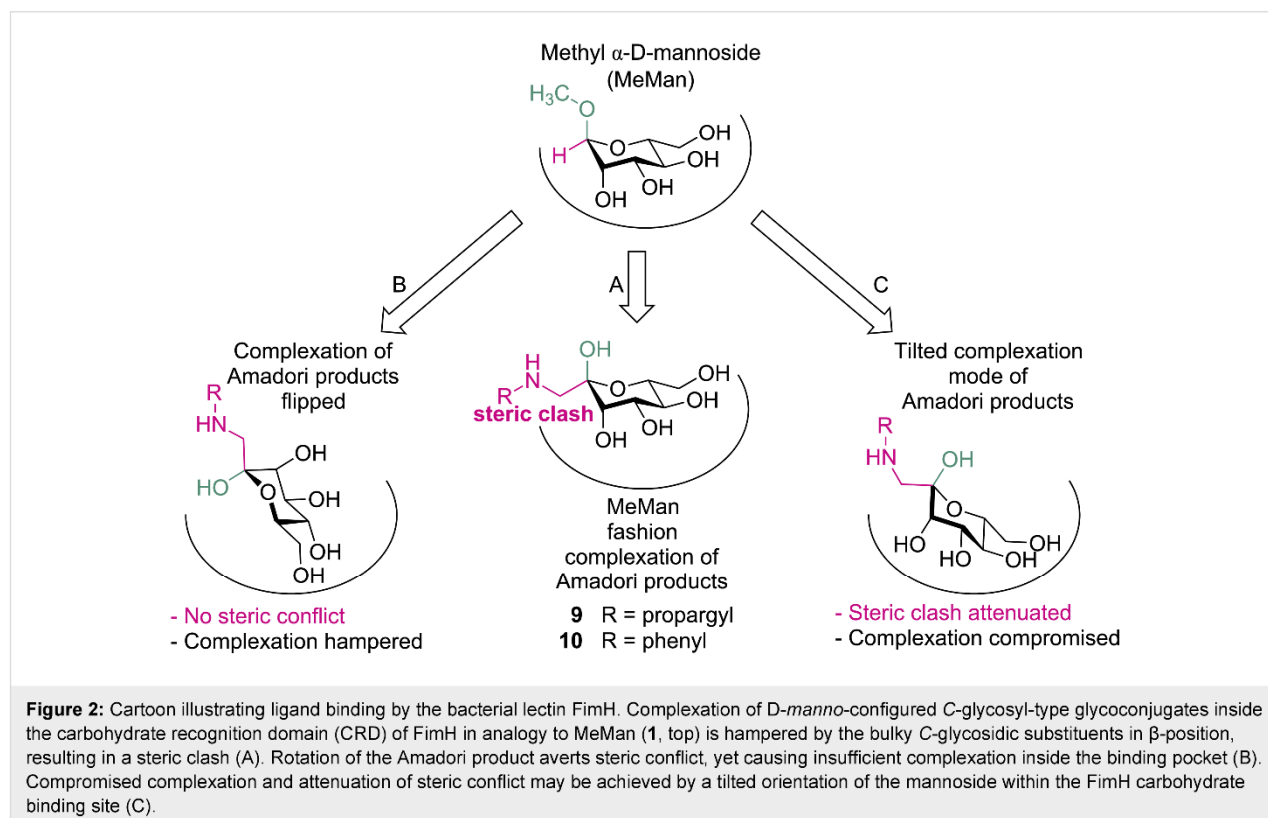
Theoretical consideration of Amadori products **9** and **10** as FimH ligands

The complexation of MeMan (**1**, cf. Figure 1) as the most simple FimH ligand in the carbohydrate binding site of FimH has been described in detail [10]. It is depicted in a simplified cartoon fashion in Figure 2. The α-configured aglycone moiety (OCH₃ in green) of the glycoside is pointing out of the binding site, whereas the axial 2-OH group as well as all other hydroxy groups of the sugar ring are complexed within the FimH carbohydrate binding site. Complexation of mannoside ligands is further supported by a conserved water molecule inside the carbohydrate binding site that is interacting mainly with the

2-OH group of the sugar ring. When the standard FimH ligand MeMan (**1**) is compared with the D-*manno*-configured *C*-glycosyl-type glycoconjugates **9** and **10**, emerging from Amadori rearrangement of the corresponding heptopyranose **8**, the axial methoxy moiety in MeMan (**1**) can be correlated with the equally axial oriented anomeric OH group of the Amadori products (Figure 2A). Then however, the equatorial anomeric (*N*-alkyl/aryl amino)methylene groups in **9** and **10** cause a steric clash in the binding pocket because of their bulkiness. To avoid this steric conflict, the Amadori products could be flipped such that the bulky aminomethyl substituent is pointing outwards of the sugar binding site (Figure 2B). But then, the anomeric hydroxy group might be sterically hindering. In addition, proper complexation of the sugar ring will be hampered due to considerable alteration of the 3D pattern of ring hydroxy groups available for hydrogen bonding. Thirdly finally, the Amadori product could be tilted such that a complexation mode results as depicted in Figure 2C. The latter binding mode suggests that binding of D-*manno*-configured Amadori rearrangement products within the FimH CRD might be possible and that Amadori products could indeed function as antagonists of natural FimH.

Docking of Amadori products **9** and **10** into the carbohydrate binding site of FimH

In order to visualise the complexation of Amadori rearrangement products **9** and **10**, respectively, inside the binding pocket

Figure 2: Cartoon illustrating ligand binding by the bacterial lectin FimH. Complexation of D-*manno*-configured *C*-glycosyl-type glycoconjugates inside the carbohydrate recognition domain (CRD) of FimH in analogy to MeMan (**1**, top) is hampered by the bulky *C*-glycosidic substituents in β-position, resulting in a steric clash (A). Rotation of the Amadori product averts steric conflict, yet causing insufficient complexation inside the binding pocket (B). Compromised complexation and attenuation of steric conflict may be achieved by a tilted orientation of the mannoside within the FimH carbohydrate binding site (C).

of FimH, flexible ligand docking studies were performed using the program Glide [21-24] as implemented in the Schrödinger program package (cf. Supporting Information File 1). For these studies we utilized the so-called open gate crystal structure of FimH [10]. Here, the tyrosine gate that is formed by the side chains of Y48 and Y137 at the entrance of the CRD, has an open conformation. Prior to docking, energies of the Amadori ligands were minimised with the program MacroModel [25] and afterwards 23 different conformers of **9** and 20 conformers of **10**, respectively, were generated with ConfGen [26,27] by using default settings. Next, these conformers were docked holding the FimH CRD fixed whereas conformational changes were allowed for the docked ligands under the influence of the force field. The resulting docking scores were calculated with the SP (single precision) scoring function and correlated with the binding affinity of the ligand for the FimH CRD. More negative scores indicate higher binding affinity than less negative values (Table 1).
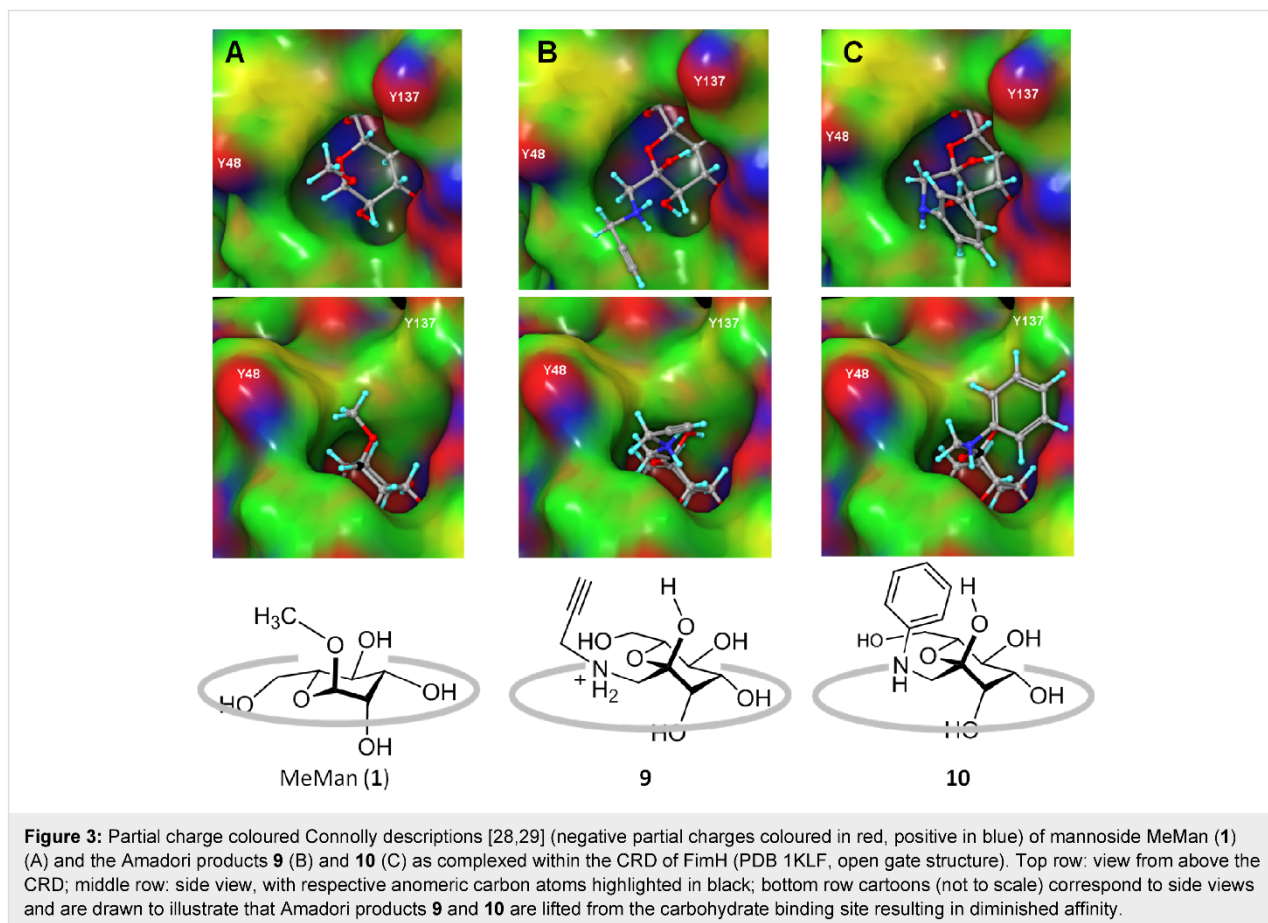
According to this docking procedure, Amadori products **9** and **10** have similar scores, which lie in the range of that for MeMan (**1**). A somewhat weaker complexation is predicted for **9** and **10** than for **1**. We had expected **10** to score clearly better than **9**,

Table 1: Docking scoring values of the most stable conformers complexed by FimH (open gate structure PDB 1KLF) of MeMan (**1**) in comparison with Amadori rearrangement products.

Compound	Scoring value
MeMan (**1**)	−6.6
9	−4.2
10	−5.7

owing to the possibility of π–π interactions between the phenyl substituent in **10** and the tyrosine gate at the entrance of the FimH CRD. However, this seems not to be the case.

We took a closer look at the docking results by comparing top scoring conformations of the different ligands (Figure 3). No difference between complexation of the Amadori products **9** and **10** and MeMan (**1**) can be seen when inspected from above the CRD. However, the side view clearly shows that the Amadori products are tilted in comparison to MeMan and somewhat lifted from the binding site (Figure 3B and C). When the respective anomeric centres are taken as a reference, **9** is lifted by 0.5 Å and **10** by 0.7 Å in comparison with complexed

Figure 3: Partial charge coloured Connolly descriptions [28,29] (negative partial charges coloured in red, positive in blue) of mannoside MeMan (**1**) (A) and the Amadori products **9** (B) and **10** (C) as complexed within the CRD of FimH (PDB 1KLF, open gate structure). Top row: view from above the CRD; middle row: side view, with respective anomeric carbon atoms highlighted in black; bottom row cartoons (not to scale) correspond to side views and are drawn to illustrate that Amadori products **9** and **10** are lifted from the carbohydrate binding site resulting in diminished affinity.
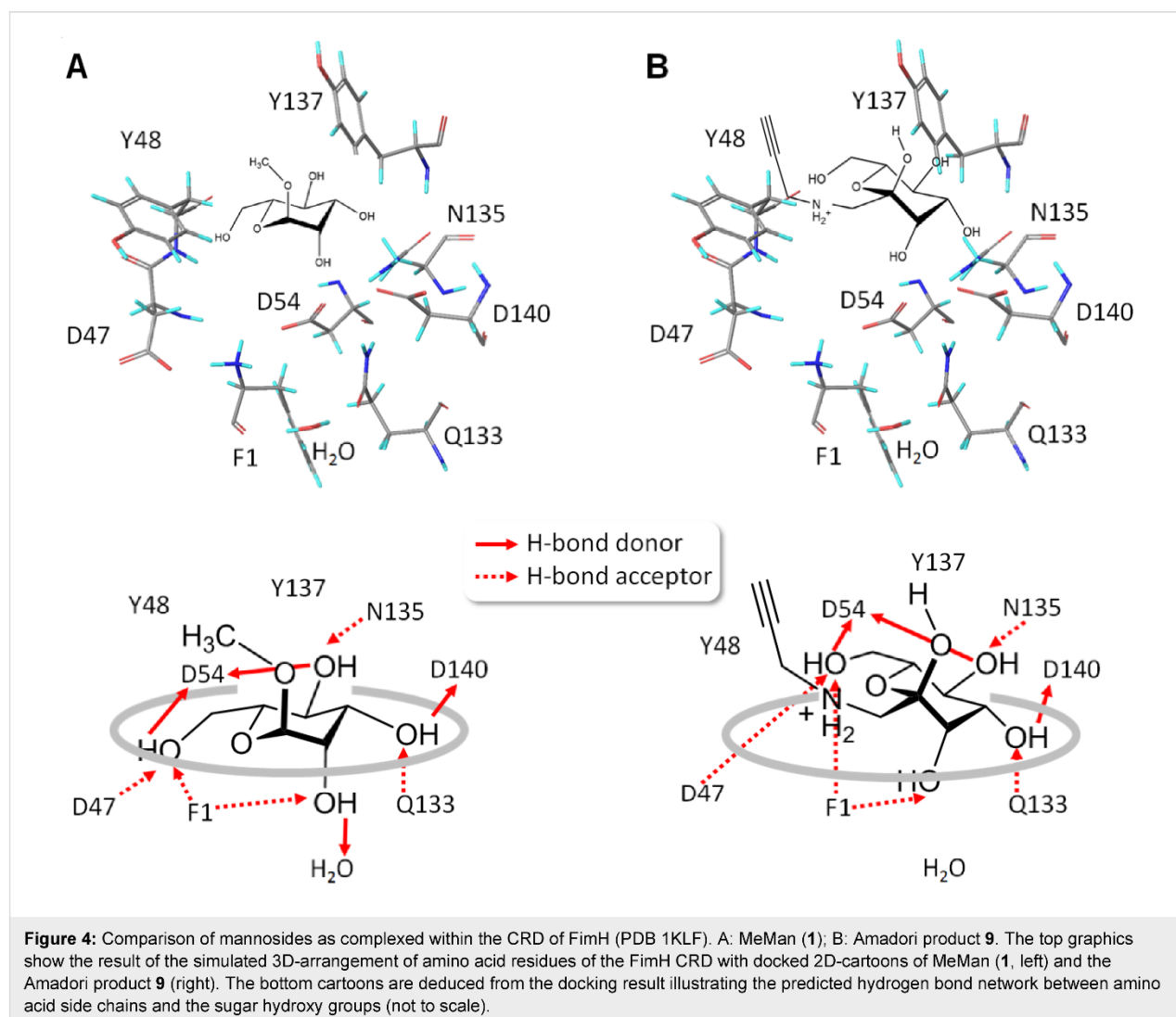
MeMan. The tilting effect apparently also prevents effective π–π interactions between the FimH tyrosine gate and Amadori product **10**.

The effect of tilting of Amadori products **9** and **10** upon FimH complexation can also be analyzed by comparison of hydrogen bonding in the complex. Close inspection of the H-bond network reveals that the average length of H-bonds established with **9** and **10**, respectively, is higher and thus the formed H-bonds are weaker than in the case of MeMan complexation. In addition, **9** and **10** cannot interact with the water molecule that is conserved in the FimH binding site (Figure 4).

Biological testing of Amadori products 9 and 10

To check the predictions made by molecular docking, inhibition–adhesion studies using type 1-fimbriated fluorescent *E. coli* were performed [30]. Accordingly, the *manno*-config-

ured glycosides **9** and **10** were used as inhibitors of FimH-mediated bacterial adhesion to mannan employing a microtiter plate format and GFP-transfected *E. coli* (pPKL1162). Serial dilutions of rearrangement products **9** and **10** in buffer were used to deliver sigmoidal inhibition curves from which IC_{50} values for both inhibitors were deduced (cf. Supporting Information File 1). The IC_{50} value of an inhibitor is the concentration at which 50% of bacterial adhesion is prevented. All assays were performed with MeMan (**1**) tested in parallel on the same plate. This allows to correlate the inhibitory potencies of **9** and **10** to that of MeMan (**1**) and report so-called relative inhibitory potencies (RIP values). This procedure allows to compare inhibitors even when they were not tested on the same plate. The results from the adhesion–inhibition assays are listed in Table 2. Both Amadori products **9** and **10** showed a lower inhibitory power than MeMan (**1**, $IC_{50} \equiv 1$). Thus, they have to be regarded as weak ligands for FimH. Unexpectedly, the propynyl derivative **9** has a slightly higher inhibitory power

Figure 4: Comparison of mannosides as complexed within the CRD of FimH (PDB 1KLF). A: MeMan (**1**); B: Amadori product **9**. The top graphics show the result of the simulated 3D-arrangement of amino acid residues of the FimH CRD with docked 2D-cartoons of MeMan (**1**, left) and the Amadori product **9** (right). The bottom cartoons are deduced from the docking result illustrating the predicted hydrogen bond network between amino acid side chains and the sugar hydroxy groups (not to scale).

than the Amadori product **10**, having a phenyl-containing agly-cone. This again shows, that the tilted complexation mode apparently compromises the possibility of favorable π–π inter-action.

Table 2: Inhibition of bacterial adhesion (*E. coli*) to a mannan-coated surface. The inhibitory potencies of Amadori rearrangement products are compared to the standard inhibitor MeMan (**1**).[a]

	9	**10**
$IC_{50} \pm SD$ (mM)	7.625 ± 1.146	10.811 ± 1.470
RIP (MeMan, **1**)	0.41	0.16

[a]SD: standard deviation (from one assay); RIP: relative inhibitory potency referenced to MeMan (**1**, tested on the same microtiter plate).

Conclusion

The Amadori rearrangement has the potential as a straight forward ligation method for conjugation of unprotected sugars and amines, when applied to suitable sugar substrates. Herein, we evaluated this synthetic method for the preparation of ligands for the α-D-mannose-specific type 1-fimbrial bacterial lectin FimH. The synthesis of heptopyranose **8** as a starting ma-terial for *manno*-configured *C*-glycosyl-type hexoses via the Amadori rearrangement was reported. We have employed propargylamine and aniline to prepare **9** and **10**, respectively. They carry an anomeric hydroxy group positioned to the α-face of the sugar ring and a rather bulky β-positioned alkyl/aryl aminomethyl group at the anomeric centre. Molecular docking of both Amadori products, **9** and **10**, into FimH suggested a rea-sonable binding mode, however in biological testing **9** and **10** showed an approx. 0.4 and 0.2 fold weaker potency as inhibi-tors of FimH-mediated bacterial adhesion than MeMan (**1**). This can be explained by the tilted fashion in which Amadori prod-ucts are complexed by FimH. They are lifted from the bottom of the CRD and this results in compromised H-bonding and weak affinity.

We learn from this interdisciplinary study that it is critical to utilize the Amadori rearrangement for the synthesis of FimH ligands because it delivers products with a limited fit for this lectin. FimH complexation of D-*manno*-configured Amadori products is challenged by the steric requirements of the *C*-glycosidic aglycone. At the same time we have characterized FimH binding of a novel ligand type that encourages further development, driven by the simple synthetic availability of this type of mannoside.

Experimental
Materials and general methods

All chemicals were purchased from Sigma-Aldrich and used without further purification. Moisture-sensitive reactions were carried out under nitrogen in dry glassware. ^{1}H and ^{13}C NMR spectra were recorded on Bruker DRX-500 and AV-600 spec-trometers at 300 K and 500.13 and 125.75 MHz, respectively. Chemical shifts are reported relative to internal tetramethyl-silane (δ = 0.00 ppm) or D_2O (δ = 4.76 ppm). Full assignment of the peaks was achieved with the aid of 2D NMR techniques (^{1}H,^{1}H-COSY and ^{1}H,^{13}C-HSQC). ESI mass spectra were recorded on an Esquire-LC instrument from Bruker Daltonics. Optical rotations were measured with a Perkin-Elmer 341 polarimeter (sodium D-line: 589 nm, length of cell: 1 dm, temp.: 20 °C) in the solvents indicated. Thin-layer chromatog-raphy was performed on precoated silica gel plates on aluminum 60 F254 (E. Merck 5554). Detection was effected by UV and/or charring with 10% sulfuric acid in EtOH and/or with ceric ammonium molybdate (100 g ammonium molybdate/8 g ceric sulfate in 1 L 10% H_2SO_4) followed by heat treatment at ≈180 °C. Flash chromatography was performed on silica gel 60 (0.035–0.070 mm, 60 A, Acros Organics 24036) using distilled solvents. For biological testing, black MaxiSorp™ plates were used from Nunc™ (Thermo Scientific™). Bacterial adhesion studies were performed according to the literature [30], using a Tecan infinite® 200 multifunction microplate reader. The band pass filters' wavelength for excitation was 485 nm and 535 nm for emission.

2,5-Di-*O*-acetyl-3,4:6,7-di-*O*-isopropylidene-D-*glycero*-D-*galacto*/D-*talo*-heptopyranose (7a, 7b): To a solution of a C-3 diastereomeric mixture of protected oct-1-enitol derivative **6** [16,17] (4.0 g, 11 mmol) in a solvent mixture of CH_2Cl_2/MeOH (80 mL, 1:1 v/v), NaOAc (2.4 g, 30 mmol, 2.8 equiv) was added. This reaction mixture was treated with ozone at −50 °C for 6 h. After TLC (Cy/EtOAc, 1:1 v/v) confirmed complete consumption of the starting material, nitrogen was bubbled through the reaction mixture for 15 min and the solution was allowed to reach room temperature, followed by addition of Me_2S (8.0 mL, 0.11 mol, 10 equiv) and stirring at rt for 45 min. The solvents were removed under reduced pressure and the obtained C-2 diastereomeric mixture of protected aldoheptoses **7a** and **7b** was used for the next step without further purifica-tion. The NMR data of the crude material confirmed signals in the expected regions.

D-*glycero*-D-*galacto*/D-*talo*-heptopyranose (8a, 8b): To a solution of a C-2-epimeric mixture of compounds **7a** and **7b** (8.55 g, containing Me_2S) in MeOH (70 mL), a solution of NaOMe (1.0 M in MeOH) was added dropwise at rt until the pH of 10 was reached and the reaction mixture was stirred at rt for 2 h until TLC (Cy/EtOAc, 1:2 v/v) showed complete consumption of the starting material. The reaction mixture was neutralized by addition of ion exchange resin (Amberlite IR 120 H^{+}, washed with MeOH). The resin was filtered off, the filtrate

was concentrated under reduced pressure and the crude product was purified by column chromatography (Cy/EtOAc, 4:1 v/v) to obtain a mixture of isopropylidene-protected D-*galacto*/D-*talo*-heptopyranose (3.08 g, 10.6 mmol) in 99% overall yield starting from compound **6**. The NMR data are in accordance with those reported [19]. To a solution of 3,4:6,7-di-*O*-isopropylidene-protected heptose (2.50 g, 8.61 mmol) in a mixture of MeCN/H$_2$O (50 mL, 1:1 v/v,), acidic ion exchange resin (Amberlite IR 120 H$^+$, washed with H$_2$O) was added until a pH of 2 was reached and the reaction mixture was stirred at 40 °C for 1 h. After TLC (CHCl$_3$/MeOH/concd. NH$_4$OH, 1/2/1 v/v/v) showed complete consumption of the starting material, the resin was filtered off and the filtrate was concentrated under reduced pressure. Column chromatography (CHCl$_3$/MeOH 10:1 v/v) gave D-*glycero*-D-*galacto*/D-*talo*-heptopyranoses **8a** and **8b** (1.55 g, 7.39 mmol) in a yield of 86%. The NMR data are in accordance with those reported [2,3].

1-(*N*-Propargyl)amino-1-deoxy-α-D-*manno*-hept-2-ulose (9): To a solution of D-*glycero*-D-*galacto*/D-*talo*-heptose **8a** and **8b** (467 mg, 2.22 mmol) in a mixture of EtOH (7 mL), 1,4-dioxane (1 mL) and water (2 drops), propargylamine (142 μL, 2.22 mmol, 1.0 equiv) and acetic acid (127 μL, 2.22 μmol, 1.0 equiv) were added and the reaction mixture was stirred at 70 °C for two days. Complete consumption of the starting material was indicated by TLC (CHCl$_3$/MeOH/NH$_4$OH, 1:2:1 v/v/v). The solvents were removed under reduced pressure and subsequent column chromatography (CHCl$_3$/MeOH, 8:1 v/v containing 1% of concd. NH$_4$OH) gave 1-propargylamino-modified ketose **9** (420 mg, 1.70 mmol) in a yield of 77%. [α]$_D$ +13.2 (*c* 2.5, MeOH); ^{1}H NMR (500 MHz, MeOH-d_4) δ 3.84 (dd, 1H, H-4), 3.82 (dd, $J_{7,6}$ = 2.2 Hz, 1H, H-7), 3.80 (d, $J_{3,4}$ = 3.3 Hz, 1H, H-3), 3.74 (dd, $J_{7,7'}$ = 11.5 Hz, $J_{7',6}$ = 5.5 Hz, 1H, H-7'), 3.72–3.69 (m, 1H, H-6), 3.62 (dd, $J_{4,5}$ = 9.4 Hz, $J_{5,6}$ = 9.5 Hz, 1H, H-5), 3.58 (d, 2H, H-8), 3.10 (d, $J_{1,1'}$ = 12.3 Hz, 1H, H-1), 2.96 (d, 1H, H-1'), 2.76 (t, 1H, H-10); ^{13}C NMR (125 MHz, MeOH-d_4) δ 97.4 (C-2), 80.3 (C-9), 74.8 (2C, C-3, C-6), 74.5 (C-10), 72.9 (C-4), 68.2 (C-5), 62.8 (C-7), 55.4 (C-1), 38.6 (C-8); ESIMS (*m/z*): calcd for [C$_{10}$H$_{17}$NO$_6$ + H]$^+$, 248.1134; found, 248.113 [M + H]$^+$.

1-(*N*-Phenyl)amino-1-deoxy-α-D-*manno*-hept-2-ulose (10): To a solution of D-*glycero*-D-*galacto*/D-*talo*-heptopyranoses **8a** and **8b** (110 mg, 523 μmol) in a mixture of EtOH (1 mL), 1,4-dioxane (0.2 mL) and water (2 drops), aniline (47.8 μL, 523 μmol, 1.0 equiv) and acetic acid (30.0 μL, 523 μmol, 1.0 equiv) were added and the reaction mixture was stirred at 70 °C for 48 h. Complete consumption of the starting material was indicated by TLC (CHCl$_3$/MeOH/NH$_4$OH, 1:2:1 v/v/v). The solvents were removed under reduced pressure and subsequent column chromatography (CHCl$_3$/MeOH,

8:1 v/v containing 1% of concd. NH$_4$OH) gave 1-phenylamino ketose **10** (35.0 mg, 123 μmol) in a yield of 24%. [α]$_D$ +21.5 (*c* 0.76, MeOH); ^{1}H NMR (500 MHz, MeOH-d_4) δ 7.11 (dd, 2H, phenyl), 6.75 (d, 2H, phenyl), 6.65 (dd, 1H, phenyl), 3.90 (dd, $J_{3,4}$ = 3.3 Hz, $J_{4,5}$ = 9.4 Hz, 1H, H-4), 3.85 (d, 1H, H-3), 3.87–3.83 (m, 1H, H-7), 3.78–3.76 (m, 1H, H-6), 3.75 (dd, $J_{6,7'}$ = 5.3 Hz, $J_{7,7'}$ = 13.7 Hz, 1H, H-7'), 3.63 (dd, $J_{5,6}$ = 9.5 Hz, 1H, H-5), 3.43 (d, $J_{1,1'}$ = 12.7 Hz, 1H, H-1), 3.27 (d,1H, H-1'); ^{13}C NMR (125 MHz, MeOH-d_4) δ 150.2, 130.0, 118.7, 114.8 (6C, phenyl), 98.9 (C-2), 74.9 (C-6), 73.3 (C-3), 72.9 (C-4), 68.7 (C-5), 63.0 (C-7), 51.4 (C-1). ESIMS (*m/z*): calcd for [C$_{13}$H$_{19}$NO$_6$ + H]$^+$, 286.1291; found, 286.129 [M + H]$^+$.

Supporting Information

Supporting Information File 1
NMR spectra, boiassays and molecular docking.
[http://www.beilstein-journals.org/bjoc/content/supplementary/1860-5397-11-123-S1.pdf]

Acknowledgements

References

1. Wrodnigg, T. M.; Eder, B. The Amadori and Heyns Rearrangements: Landmarks in the History of Carbohydrate Chemistry or Unrecognized Synthetic Opportunities?. In *Glycoscience – Epimerization, Isomerization, Rearrangement Reactions of Carbohydrates*; Stütz, A. E., Ed.; Topics in Current Chemistry, Vol. 215; Springer-Verlag: Berlin, Heidelberg, New York, 2001; pp 115–152. doi:10.1007/3-540-44422-x_6

2. Wrodnigg, T. M.; Kartusch, C.; Illaszewicz, C. *Carbohydr. Res.* **2008**, *343*, 2057–2066. doi:10.1016/j.carres.2008.02.022

3. Gallas, K.; Pototschnig, G.; Adanitsch, F.; Stütz, A. E.; Wrodnigg, T. M. *Beilstein J. Org. Chem.* **2012**, *8*, 1619–1629. doi:10.3762/bjoc.8.185

4. Hartmann, M.; Lindhorst, T. K. *Eur. J. Org. Chem.* **2011**, 3583–3609. doi:10.1002/ejoc.201100407

5. Autar, R.; Khan, A. S.; Schad, M.; Hacker, J.; Liskamp, R. M. J.; Pieters, R. J. *ChemBioChem* **2003**, *4*, 1317–1325. doi:10.1002/cbic.200300719

6. Sharon, N. *Biochim. Biophys. Acta, Gen. Subj.* **2006**, *1760*, 527–537. doi:10.1016/j.bbagen.2005.12.008

7. Ernst, B.; Magnani, J. L. *Nat. Rev. Drug Discovery* **2009**, *8*, 661–677. doi:10.1038/nrd2852

8. Jiang, X.; Abgottspon, D.; Kleeb, S.; Rabbani, S.; Scharenberg, M.; Wittwer, M.; Haug, M.; Schwardt, O.; Ernst, B. *J. Med. Chem.* **2012**, *55*, 4700–4713. doi:10.1021/jm300192x

9. Choudhury, D.; Thompson, A.; Stojanoff, V.; Langermann, S.; Pinkner, J.; Hultgren, S. J.; Knight, S. D. *Science* **1999**, *285*, 1061–1066. doi:10.1126/science.285.5430.1061

10. Hung, C.-S.; Bouckaert, J.; Hung, D.; Pinkner, J.; Widberg, C.; DeFusco, A.; Auguste, C. G.; Strouse, R.; Langermann, S.; Waksman, G.; Hultgren, S. J. *Mol. Microbiol.* **2002**, *44*, 903–915. doi:10.1046/j.1365-2958.2002.02915.x

11. Bouckaert, J.; Berglund, J.; Schembri, M.; De Genst, E.; Cools, L.; Wuhrer, M.; Hung, C.-S.; Pinkner, J.; Slättegård, R.; Zavialov, A.; Choudhury, D.; Langermann, S.; Hultgren, S. J.; Wyns, L.; Klemm, P.; Oscarson, S.; Knight, S. D.; De Greve, H. *Mol. Microbiol.* **2005**, *55*, 441–455. doi:10.1111/j.1365-2958.2004.04415.x

12. Tomašić, T.; Rabbani, S.; Gobec, M.; Mlinarič Raščan, I.; Podlipnik, Č.; Ernst, B.; Anderluh, M. *Med. Chem. Commun.* **2014**, *5*, 1247–1253. doi:10.1039/C4MD00093E

13. Firon, N.; Ashkenazi, S.; Mirelman, D.; Ofek, I.; Sharon, N. *Infect. Immun.* **1987**, *55*, 472–476.

14. Imberty, A.; Chabre, Y. M.; Roy, R. *Chem. – Eur. J.* **2008**, *14*, 7490–7499. doi:10.1002/chem.200800700

15. Sperling, O.; Fuchs, A.; Lindhorst, T. K. *Org. Biomol. Chem.* **2006**, *4*, 3913–3922. doi:10.1039/b610745a

16. Kaliappan, K. P.; Das, P.; Kumar, N. *Tetrahedron Lett.* **2005**, *46*, 3037–3040. doi:10.1016/j.tetlet.2005.03.021

17. van Boggelen, M. P.; van Dommelen, B. F. G. A.; Jiang, S.; Singh, G. *Tetrahedron* **1997**, *53*, 16897–16910. doi:10.1016/S0040-4020(97)10125-9

18. Paulsen, H.; Schüller, M.; Heitmann, A.; Nashed, M. A.; Redlich, H. *Liebigs Ann. Chem.* **1986**, 675–686. doi:10.1002/jlac.198619860409

19. Lenagh-Snow, G. M. J.; Jenkinson, S. F.; Newberry, S. J.; Kato, A.; Nakagawa, S.; Adachi, I.; Wormald, M. R.; Yoshihara, A.; Morimoto, K.; Akimitsu, K.; Izumori, K.; Fleet, G. W. J. *Org. Lett.* **2012**, *14*, 2050–2053. doi:10.1021/ol3005744

20. Wrodnigg, T. et al., unpublished results.

21. Friesner, R. A.; Banks, J. L.; Murphy, R. B.; Halgren, T. A.; Klicic, J. J.; Mainz, D. T.; Repasky, M. P.; Knoll, E. H.; Shelley, M.; Perry, J. K.; Shaw, D. E.; Francis, P.; Shenkin, P. S. *J. Med. Chem.* **2004**, *47*, 1739–1749. doi:10.1021/jm0306430

22. Halgren, T. A.; Murphy, R. B.; Friesner, R. A.; Beard, H. S.; Frye, L. L.; Pollard, W. T.; Banks, J. L. *J. Med. Chem.* **2004**, *47*, 1750–1759. doi:10.1021/jm030644s

23. Friesner, R. A.; Murphy, R. B.; Repasky, M. P.; Frye, L. L.; Greenwood, J. R.; Halgren, T. A.; Sanschagrin, P. C.; Mainz, D. T. *J. Med. Chem.* **2006**, *49*, 6177–6196. doi:10.1021/jm051256o

24. *Small-Molecule Drug Discovery Suite 2013-3: Glide,* version 6.1; Schrödinger, LLC: New York, NY, 2013.

25. *MacroModel,* version 10.2; Schrödinger, LLC: New York, NY, 2013.

26. Watts, K. S.; Dalal, P.; Murphy, R. B.; Sherman, W.; Friesner, R. A.; Shelley, J. C. *J. Chem. Inf. Model.* **2010**, *50*, 534–546. doi:10.1021/ci100015j

27. *ConfGen,* version 2.6; Schrödinger, LLC: New York, NY, 2013.

28. Connolly, M. L. *Science* **1983**, *221*, 709–713. doi:10.1126/science.6879170

29. Connolly, M. L. *J. Appl. Crystallogr.* **1983**, *16*, 548–558. doi:10.1107/S0021889883010985

30. Hartmann, M.; Horst, A. K.; Klemm, P.; Lindhorst, T. K. *Chem. Commun.* **2010**, *46*, 330–332. doi:10.1039/B922525K

Supporting Information

for

Are D-*manno*-configured Amadori products ligands of the bacterial lectin FimH?

Tobias-Elias Gloe[‡1], Insa Stamer[‡1], Cornelia Hojnik[‡2], Tanja M. Wrodnigg*[2], Thisbe K. Lindhorst*[1]

Address: [1]Christiana Albertina University of Kiel, Otto Diels Institute of Organic Chemistry, Otto-Hahn-Platz 3/4, D-24118 Kiel, Germany, Fax: +49 431 8807410, and [2]Glycogroup, Institute of Organic Chemistry, Technical University Graz, Stremayrgasse 9, A-8010 Graz, Austria

Email: Tanja M. Wrodnigg* - t.wrodnigg@tugraz.at; Thisbe K. Lindhorst - tklind@oc.uni-kiel.de

*Corresponding author

‡These authors have contributed equally.

NMR spectra, bioassays and molecular docking

Table of contents

1. ^{1}H and ^{13}C NMR spectra
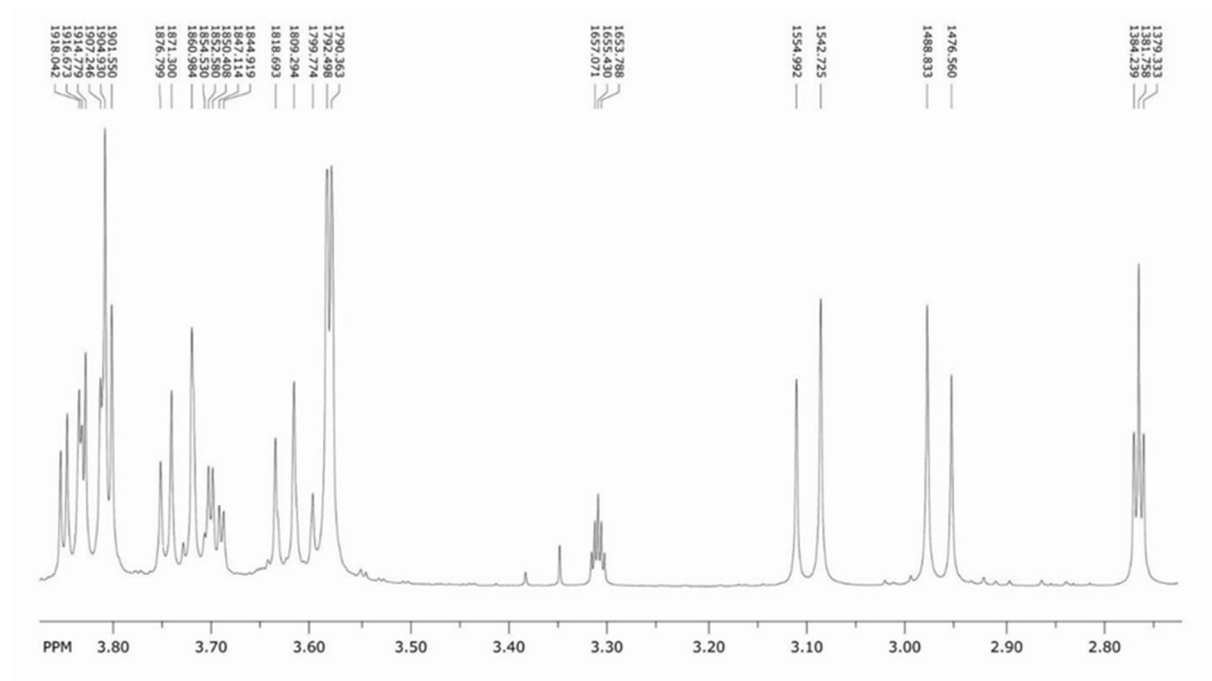
Figure S1: ^{1}H NMR spectrum of **9** in MeOD-d_4 (500 MHz).
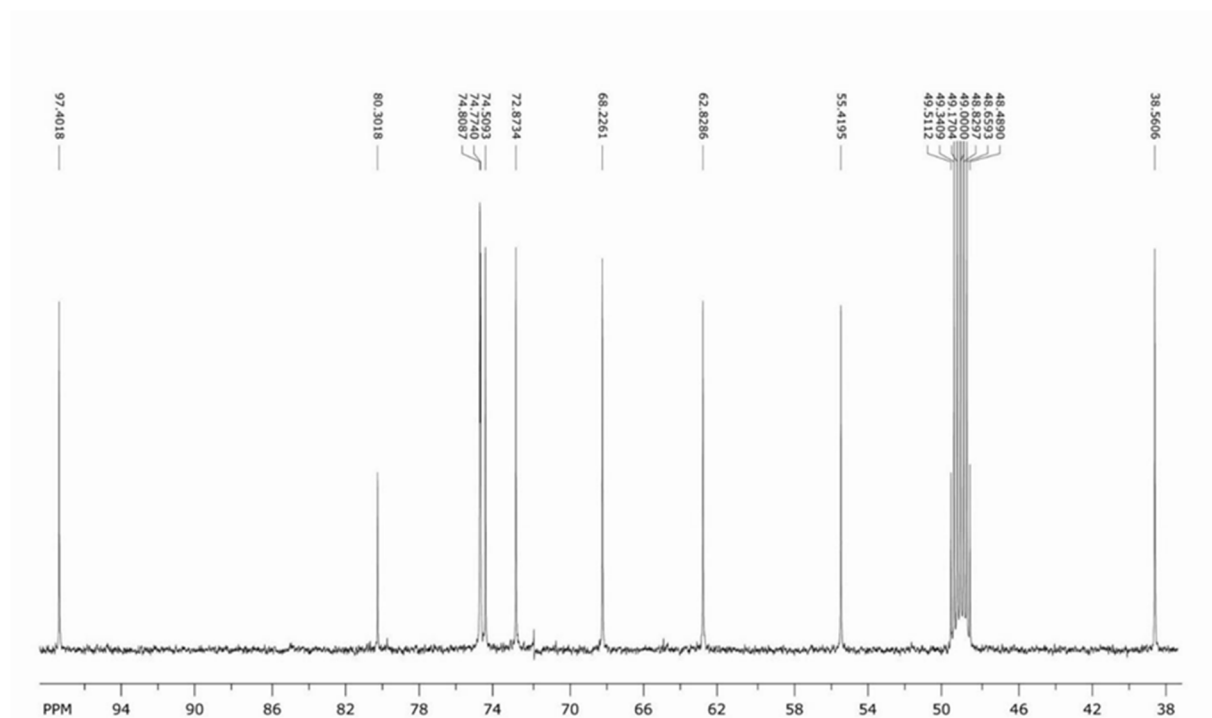
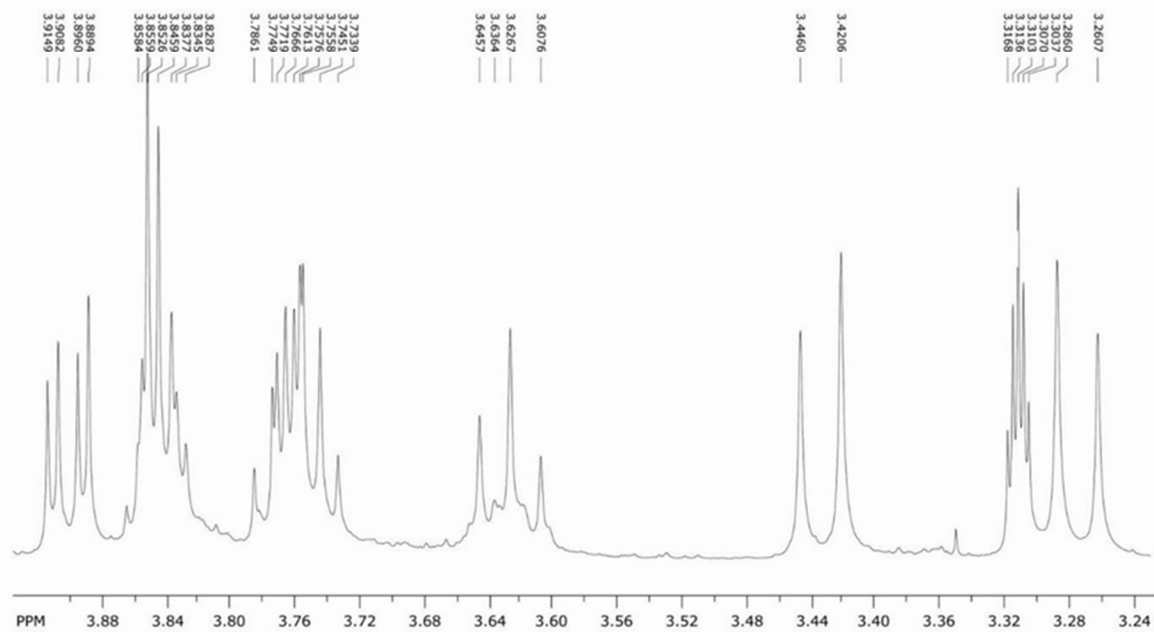**Figure S2:** ^{13}C NMR spectrum of **9** in MeOD-d_4 (125 MHz).

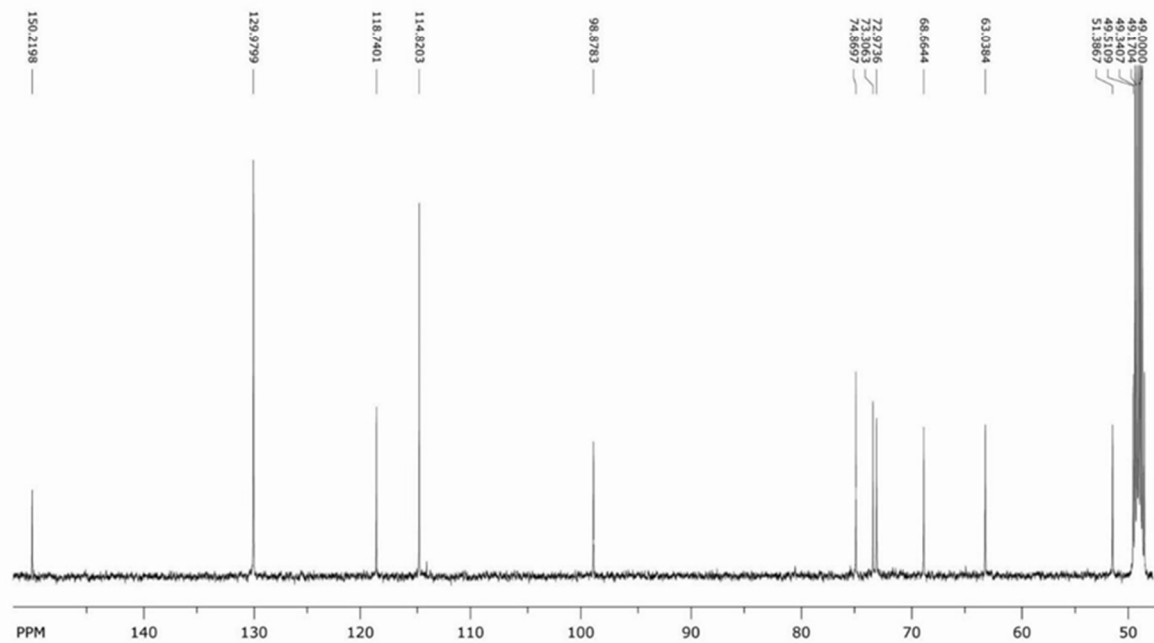**Figure S3:** ^{1}H NMR spectrum of **10** in MeOD-d_4 (500 MHz).

Figure S4: ^{13}C NMR spectrum of **10** in MeOD-d_4 (125 MHz).

2. Bioassays

Media and buffer solutions: Carbonate buffer solution (pH 9.6): sodium carbonate (1.59 g) and sodium hydrogen carbonate (2.52 g) were dissolved in distilled deionized water (1.00 L). PBS buffer solution (pH 7.2): sodium chloride (8.00 g), potassium chloride (200 mg), sodium hydrogen phosphate dihydrate (1.44 g) and potassium dihydrogen phosphate (200 mg) were dissolved in distilled deionized water (1.00 L). PBST buffer solution (pH 7.2): PBS buffer + Tween®20 (0.05% v/v). LB medium: tryptone (10.0 g), sodium chloride (10.0 g) and yeast extract (5.00 g) were dissolved in distilled deionized water (1.00 L); after autoclavation chloramphenicol (50.0 mg) and ampicillin (100 mg) were added. The buffer pH values were adjusted with aqueous 0.1 M HCl or 0.1 M NaOH solution.

Cultivation of bacteria: *E. coli* bacteria (strain pPKL1162) [1,2] were cultured from a frozen stock in LB medium and incubated overnight at 37 °C. After centrifugation and washing twice with PBS buffer (2.00 mL), the bacteria pellet was suspended in PBS buffer and the suspension was adjusted to $OD_{600} = 0.4$ (2 mg/mL) with PBS.

GFP assay: The published assay [3] was adapted and modified as follows: Black 96-well microtiter plates (Nunc, MaxiSorp) plates were treated with a solution of mannan from *Saccharomyces cerevisiae* (1.2 mg/mL in carbonate buffer, 120 µL/well) and desiccated overnight at 37 °C. After washing for three times with PBST (150 µL/well), the wells were blocked with PVA (1% in PBS, 120 µL/well) for 4 h at 4 °C. Subsequently, the plates were washed twice with PBST (150 µL/well) and once with PBS (150 µL/well). Solutions of Amadori compounds **9** and **10** as well as MeMan (**1**) were prepared (200 mM in PBS) and serial dilutions of each solution added to the mannan-coated plates (50 µl/well). Then the bacterial suspension ($OD_{600} = 0.4$, 50 µL/well) was added and the plates were incubated for 1 h at 37 °C and 100 rpm. After washing twice with PBS (150 µL), the wells were filled with PBS (100 µL/well) and the fluorescence intensity (485 nm/535 nm) was determined.
Each compound was tested at least in triplicate and in parallel with the standard inhibitor MeMan (**1**) on the same plate.
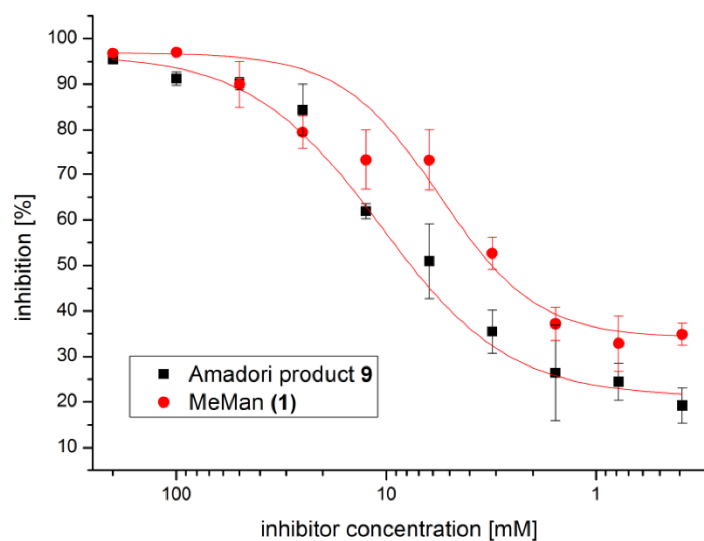
Figure S5: Inhibition curves obtained with Amadori product **9** from inhibition of type 1 fimbriae-mediated bacterial adhesion to mannan. MeMan (**1**) was tested on the same microtiter plate. The sigmoidal concentration–response curves were fitted by non-linear regression. Error bars are standard deviations from multiple (at least three) testing results on one plate.
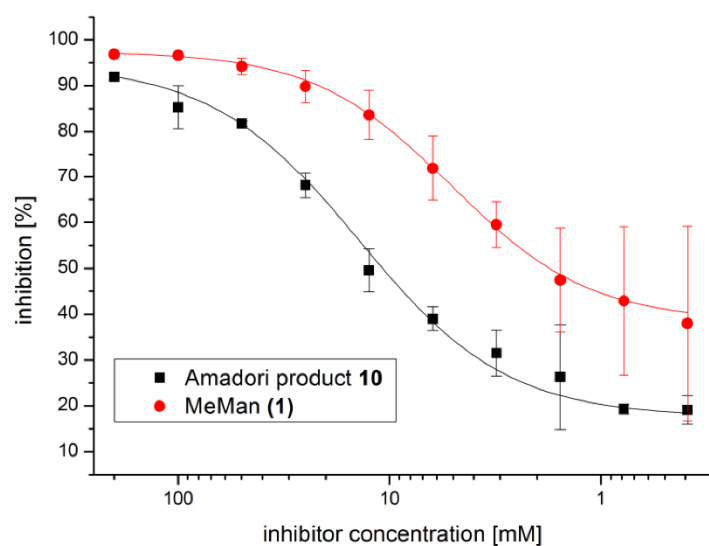

Figure S6: Inhibition curves obtained with Amadori product **10** from inhibition of type 1 fimbriae-mediated bacterial adhesion to mannan. MeMan (**1**) was tested on the same microtiter plate. The sigmoidal concentration–response curves were fitted by non-linear regression. Error bars are standard deviations from multiple (at least three) testing results on one plate.

3. Docking studies

Computer-aided docking was performed using flexible ligand docking with Glide [4-7] as implemented in the Schrödinger program package. Docking was based on the open gate crystal structure (PDB code 1KLF) of FimH [8]. The structures were minimized with the program MacroModel [9] by using default settings resulting in 23 different conformers of **9**, 20 conformers of **10** and 9 conformers of MeMan (**1**). The conformers were generated with ConfGen [10,11] and are listed in Tables S1–S3 with the respective scoring values.

Table S1: Scoring values for docking of Amadori product **9** into the open gate crystal structure of FimH.

no.	docking score	glide gscore	glide evdw	glide ecoul	glide lipo	glide hbond	glide metal	glide rewards	glide erotb	glide esite
1	-4.230	-5.423	-11.659	-30.573	-0.081	0.000	0.000	-1.716	0.992	-0.034
2	-4.229	-5.422	-11.356	-31.026	-0.096	0.000	0.000	-1.716	0.992	-0.033
3	-4.228	-5.421	-11.633	-30.576	-0.081	0.000	0.000	-1.716	0.992	-0.034
4	-4.228	-5.421	-11.626	-30.584	-0.081	0.000	0.000	-1.716	0.992	-0.034
5	-4.228	-5.421	-11.634	-30.574	-0.081	0.000	0.000	-1.716	0.992	-0.034
6	-4.210	-5.403	-11.044	-33.054	-0.096	0.000	0.000	-1.716	0.992	-0.030
7	-4.210	-5.403	-11.042	-33.066	-0.096	0.000	0.000	-1.716	0.992	-0.030
8	-4.210	-5.403	-11.038	-33.054	-0.096	0.000	0.000	-1.716	0.992	-0.030
9	-4.209	-5.402	-11.026	-33.080	-0.096	0.000	0.000	-1.716	0.992	-0.030
10	-4.209	-5.402	-11.013	-33.092	-0.096	0.000	0.000	-1.716	0.992	-0.030
11	-4.208	-5.401	-10.999	-33.094	-0.097	0.000	0.000	-1.716	0.992	-0.030
12	-4.208	-5.401	-10.994	-33.080	-0.097	0.000	0.000	-1.716	0.992	-0.030
13	-4.207	-5.400	-11.194	-30.605	-0.081	0.000	0.000	-1.716	0.992	-0.035
14	-4.207	-5.400	-11.192	-30.609	-0.081	0.000	0.000	-1.716	0.992	-0.035
15	-4.206	-5.399	-11.187	-30.614	-0.081	0.000	0.000	-1.716	0.992	-0.035
16	-4.206	-5.399	-11.183	-30.617	-0.081	0.000	0.000	-1.716	0.992	-0.035
17	-4.206	-5.399	-11.197	-30.594	-0.080	0.000	0.000	-1.716	0.992	-0.035
18	-4.187	-5.380	-10.574	-32.942	-0.097	0.000	0.000	-1.716	0.992	-0.030
19	-4.187	-5.380	-10.567	-32.944	-0.097	0.000	0.000	-1.716	0.992	-0.030
20	-4.186	-5.379	-10.546	-32.941	-0.097	0.000	0.000	-1.716	0.992	-0.030
21	-4.186	-5.379	-10.541	-32.944	-0.097	0.000	0.000	-1.716	0.992	-0.030
22	-4.167	-5.360	-10.165	-33.077	-0.095	0.000	0.000	-1.716	0.992	-0.032
23	-4.148	-5.341	-10.483	-33.017	-0.062	0.000	0.000	-1.716	0.992	-0.030

Table S2: Scoring values for docking of Amadori product **10** into the open gate crystal structure of FimH.

no.	docking score	glide gscore	glide evdw	glide ecoul	glide lipo	glide hbond	glide metal	glide rewards	glide erotb	glide esite
1	-5.693	-5.693	-15.656	-29.241	-0.041	0.000	0.000	-1.464	0.624	-0.029
2	-5.678	-5.678	-15.284	-29.690	-0.046	0.000	0.000	-1.464	0.624	-0.028
3	-5.671	-5.671	-15.162	-29.707	-0.045	0.000	0.000	-1.464	0.624	-0.028
4	-5.656	-5.656	-13.640	-31.348	-0.103	0.000	0.000	-1.464	0.624	-0.032
5	-5.653	-5.653	-14.811	-29.556	-0.045	0.000	0.000	-1.464	0.624	-0.028
6	-5.650	-5.650	-13.822	-33.156	-0.090	0.000	0.000	-1.464	0.624	-0.029
7	-5.645	-5.645	-13.374	-31.571	-0.104	0.000	0.000	-1.464	0.624	-0.032
8	-5.643	-5.643	-14.593	-30.063	-0.046	0.000	0.000	-1.464	0.624	-0.028
9	-5.625	-5.625	-13.506	-33.189	-0.089	0.000	0.000	-1.464	0.624	-0.021
10	-5.620	-5.620	-14.103	-30.763	-0.048	0.000	0.000	-1.464	0.624	-0.028
11	-5.619	-5.619	-13.139	-31.763	-0.093	0.000	0.000	-1.464	0.624	-0.029
12	-5.615	-5.615	-13.053	-31.784	-0.094	0.000	0.000	-1.464	0.624	-0.029
13	-5.615	-5.615	-13.050	-31.767	-0.094	0.000	0.000	-1.464	0.624	-0.029
14	-5.615	-5.615	-13.041	-31.787	-0.094	0.000	0.000	-1.464	0.624	-0.029
15	-5.614	-5.614	-13.035	-31.779	-0.094	0.000	0.000	-1.464	0.624	-0.029
16	-5.573	-5.573	-12.708	-32.117	-0.066	0.000	0.000	-1.464	0.624	-0.032
17	-5.573	-5.573	-12.709	-32.109	-0.066	0.000	0.000	-1.464	0.624	-0.032
18	-5.572	-5.572	-12.702	-32.123	-0.066	0.000	0.000	-1.464	0.624	-0.032
19	-5.571	-5.571	-12.682	-32.141	-0.066	0.000	0.000	-1.464	0.624	-0.032
20	-5.558	-5.558	-12.334	-32.105	-0.071	0.000	0.000	-1.464	0.624	-0.031

Table S3: Scoring values for docking of MeMan (**1**) into the open gate crystal structure of FimH.

no.	docking score	glide gscore	glide evdw	glide ecoul	glide lipo	glide hbond	glide metal	glide rewards	glide erotb	glide esite
1	-6.567	-6.567	-12.463	-28.026	-0.145	0.000	0.000	-2.085	0.300	-0.014
2	-6.564	-6.564	-12.418	-28.059	-0.144	0.000	0.000	-2.085	0.300	-0.014
3	-6.528	-6.528	-12.111	-28.445	-0.124	0.000	0.000	-2.085	0.300	-0.014
4	-6.525	-6.525	-12.059	-28.484	-0.123	0.000	0.000	-2.085	0.300	-0.014
5	-6.486	-6.486	-11.170	-29.242	-0.120	0.000	0.000	-2.085	0.300	-0.023
6	-6.484	-6.484	-11.142	-29.269	-0.119	0.000	0.000	-2.085	0.300	-0.022
7	-6.483	-6.483	-11.144	-29.281	-0.119	0.000	0.000	-2.085	0.300	-0.022
8	-6.482	-6.482	-11.125	-29.293	-0.118	0.000	0.000	-2.085	0.300	-0.022
9	-6.203	-6.203	-6.927	-33.084	-0.051	0.000	0.000	-2.085	0.300	-0.021

4. References

[1] Reisner, A.; Haagensen, J. A. J.; Schembri, M. A.; Zechner, E. L.; Molin, S., *Mol. Microbiol.* **2003**, *48*, 933-946.

[2] The GFP-tagged strain pPKL1162 was constructed in the Klemm group by introduction of the plasmid pPKL174 into strain SAR18; pPKL174 contains the fim gene cluster required for type 1 fimbriae assembly and expression. The chromosome of strain SAR18 from the Reisner group contains the GFP gene, controlled by a constitutive promoter.

[3] Hartmann, M.; Horst, A. K.; Klemm, P.; Lindhorst, T. K., *Chem. Commun.* **2010**, *46*, 330-332.

[4] Friesner, R. A.; Murphy, R. B.; Repasky, M. P.; Frye, L. L.; Greenwood, J. R.; Halgren, T. A.; Sanschagrin, P. C.; Mainz, D. T., *J. Med. Chem.* **2006**, *49*, 6177-6196.

[5] Halgren, T. A.; Murphy, R. B.; Friesner, R. A.; Beard, H. S.; Frye, L. L.; Pollard, W. T.; Banks, J. L.; *J. Med. Chem.* **2004**, *47*, 1750-1759.

[6] Friesner, R. A.; Banks, J. L.; Murphy, R. B.; Halgren, T. A.; Klicic, J. J.; Mainz, D. T.; Repasky, M. P.; Knoll, E. H.; Shelley, M.; Perry, J. K.; Shaw, D. E.; Francis, P.; Shenkin, P. S., *J. Med. Chem.* **2004**, *47*, 1739-1749.

[7] *Small-Molecule Drug Discovery Suite 2013-3: Glide*, version 6.1; Schrödinger, LLC: New York, NY, **2013**.

[8] Hung, C. S.; Bouckaert, J.; Hung, D.; Pinkner, J.; Widberg, C.; DeFusco, A.; Auguste, C. G.; Strouse, R.; Langermann, S.; Waksman, G.; Hultgren, S. J., *Mol. Microbiol.* **2002**, *44*, 903-15.

[9] *Schrödinger Release 2013-3: MacroModel*, version 10.2; Schrödinger, LLC: New York, NY, **2013**.

[10] Watts, K. S.; Dalal, P.; Murphy, R. B.; Sherman, W.; Friesner, R. A.; Shelley, J. C., *J. Chem. Inf. Model.* **2010**, *50*, 534-546.

[11] *Schrödinger Release 2013-3: ConfGen*, version 2.6; Schrödinger, LLC: New York, NY, **2013**.

3.3   Synthesis of Colored Amadori Rearrangement Products

Whereas the Amadori rearrangement has been applied in complex carbohydrate chemistry, Amadori products are prone to undergo subsequent reactions, forming complex mixtures of unwanted by-products. Depending on the structure of the amine as well as the carbohydrate utilized for the reaction, purification of rearrangement products can be demanding and, in some cases, form the main challenge of the method.[50] Due to the high polarity of both the unprotected carbohydrate moiety and the amino group at the C-1 position of the Amadori product, purification by preparative silica gel column chromatography can be sometimes restricted as it requires highly polar solvent mixtures, risking contamination with silica by column bleeding.

A conceivable way to overcome the problem of high product polarity is acetylation of the carbohydrate since this derivatization substantially increases the hydrophobicity of the compound. Nevertheless, acetylation of an Amadori product would not only effect the hydroxyl groups of the sugar ring but also the amino group at the C-1 position. Consequently, in a final deprotection step, cleavage of the *N*-acetyl group would be necessary besides *O*-deacetylation. This, however, often requires harsh reaction conditions,[58] implying the risk of decomposition.

A different approach, which facilitates and accelerates chromatographic purification of organic compounds, is the use of chromophore-tagged reaction products. In this regard, the Lindhorst group has established a methodology that allows for visual tracking of the separation process during chromatographic purification (Figure 3.2). For this strategy, the term "chromophore-supported purification" (CSP)[57] was coined and it has been demonstrated in the parallel synthesis and purification of different carbohydrate derivatives. The color labels used in CSP are based on guaiazulene, an azulene derivative which is much cheaper compared to plain azulene but has the same intense blue color, making it ideal for visualization of organic compounds. In earlier work, tagging of alcohols as well as amines was addressed by application of different guaiazulene-derived reagents.[57, 59] In a similar approach, Timmer *et al.* have employed azulen-1-yl-dicarbonyl as a protecting group for alcohols. Using this azulene-derived reagent, the protection as well as deprotection of various carbohydrate derivatives has been demonstrated.[60]

Figure 3.2: Application of the CSP methodology allows for visual tracking of the separation process during preparative column chromatography and, additionally, the isolation of target compounds is facilitated.[61]

Employing the CSP methodology in connection with the Amadori rearrangement may be of great use in order to facilitate the chromatographic purification of Amadori products. Not only does the introduction of a guaiazulene moiety result in visualization of the Amadori product as well as the formed side products, but it also increases the hydrophobicity of the molecule so that less polar solvent mixtures can be used in chromatography. For this reason, a guaiazulene-tagged amine **18** was chosen, which is accessible from the well-known guaiazulene carbonate derivative **17**.[59]

Results and Discussion

The guaiazulene carbonate derivative **17** was prepared following a known procedure, which was first described by Aumüller *et al.*[59] Here, plain guaiazulene (**14**) was deprotonated by lithium diisopropylamide (LDA), resulting in the resonance stabilized anion **15**, which was further converted to alcohol **16** by treatment with paraformaldehyde. The targeted carbonate **17** was obtained by a reaction with *N*,*N′*-disuccinimidyl carbonate (DSC) and was subsequently treated with ethylenediamine to give the guaiazulene-tagged amine **18** in a very good yield.
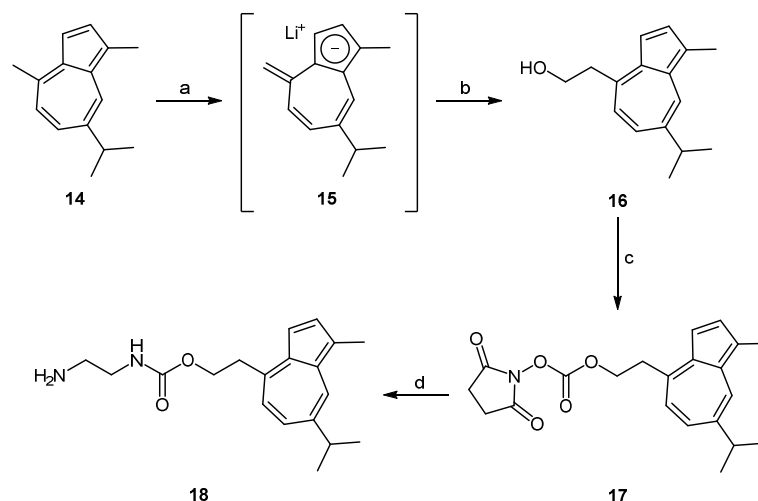
Scheme 3.5: Synthesis of guaiazulene-tagged amine **18**. a) LDA, Et$_2$O, -35 °C, 40 min; b) (CH$_2$O)$_n$, -35 °C → rt, 16 h, 54 %; c) DSC, pyridine, DMF, 40 °C, 16 h, 91%; d) ethylenediamine, 0 °C → rt, 16 h, 95%.

The guaiazulene-tagged amine **18** and aminomethylazobenzene **19** (synthesis is described in Chapter 5.3.1) were used as chromophores for CSP of Amadori products. In order to obtain D-*manno*- or D-*gluco*-configured Amadori rearrangement products, D-*glycero*-D-*talo*-heptopyranose (**20**) and D-*glycero*-D-*gulo*-heptopyranose (**21**) were needed. While **20** was obtained commercially, instead of pure heptose **21a** an epimeric mixture of D-*glycero*-D-*galacto*/D-*talo* heptopyranose (**21a/b**)[62] was provided by Cornelia Hojnik from the Glyco Group at the TU Graz. This mixture is equally suited for Amadori rearrangement reactions (compared to pure heptose **21a**) since the C-2 stereocenter is converted to a keto group during the course of the reaction.

For preparation of the *gluco*-configured Amadori products, guaiazulene-tagged amine **18** and azobenzene hydrochloride **19**, respectively, were reacted with heptopyranose **20** (Scheme 3.6) by application of optimized reaction conditions previously reported.[62a, 63] The reaction of guaiazulene-tagged amine **18** was first carried out at a temperature of 40 °C applying acetic acid as the catalyst. However, thin layer chromatography (TLC) control revealed that the reaction did not proceed at first so that the temperature was successively raised to 70 °C. This drastically accelerated the reaction but at the same time induced the formation of several side products. Nevertheless, the intense color of the guaiazulene moiety greatly facilitated the chromatographic purification so that the product **22** could be obtained in an acceptable yield of 52% (66% based on conversion, 14% starting material reisolated).

For the reaction of aminomethylazobenzene **19**, triethylamine was used instead of acetic acid since, in this case, the respective triethylammonium chloride salt acts as the acid catalyst. The reaction proceeded very slowly so that almost no conversion could be observed. Therefore, an excess of 1.5 eq of the amine and an extended reaction time was applied, which eventually

gave the desired rearrangement product **23**, however, in a low yield of 6% with slight contaminations. Here again, the formation of various side products was observed, though not to the same extent as for Amadori product **22** due to the low conversion of azobenzene derivative **19**.
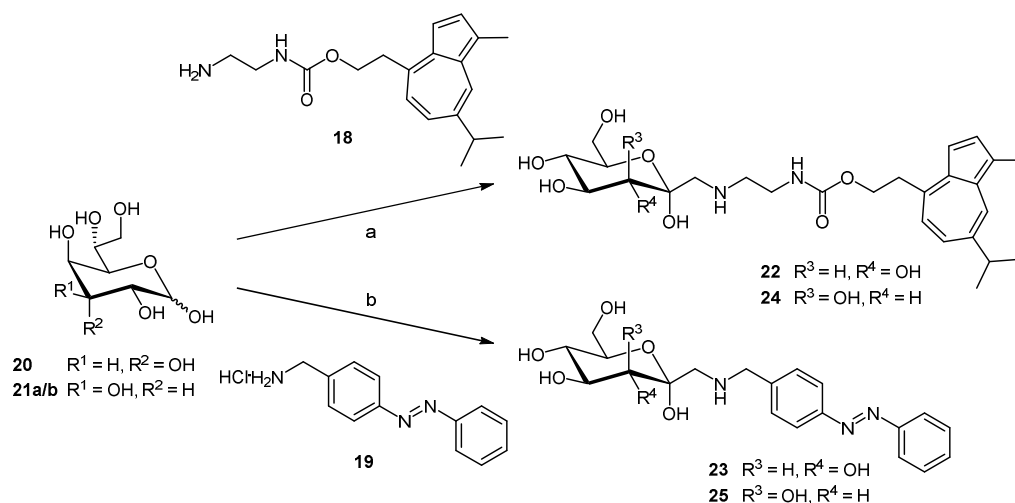
Scheme 3.6: Amadori rearrangement of heptopyranoses **20** and **21a/b** with guaiazulene-tagged amine **18** and azobenzene derivative **19**, respectively. a) For product **22**: EtOH, 1,4-dioxane, H_2O, AcOH, 70 °C, 5 h, 51%; for prouct **24**: EtOH, 1,4-dioxane, H_2O, AcOH, 70 °C, 7 h, 54%; b) for product **23**: EtOH, 1,4-dioxane, H_2O, TEA, 70 °C, 10 h, 6%; The azobenzene Amadori compound **25** was obtained contaminated with side products.

For preparation of *manno*-configured Amadori products, heptopyranoses **21a/b** were reacted with amines **18** and **19**, respectively, by applying the same reaction conditions as in the synthesis of the *gluco*-configured Amadori products (Scheme 3.6). As described above, the reaction of heptoses **21a/b** with guaiazulene-tagged amine **18** also did not proceed at first and the temperature was raised to 70 °C. The formation of side products was similar as in the case of the *gluco*-configured compound and the *manno*-configured Amadori product **24** was obtained in a similar yield of 54% (59% based on conversion, 5% starting material reisolated). The rearrangement reaction of azobenzene derivative **19** and heptoses **21a/b** proceeded very slowly so that also in this case an excess of the amine and an extended reaction time was applied. In contrast to the preparation of the respective *gluco*-configured compound, however, the desired Amadori product **25** was only obtained in heavily contaminated form together with side products, which were not further characterized.

Comparison of the Amadori rearrangement reaction in the *manno*- and *gluco*-series, respectively, demonstrates that the configuration at the C-3 carbon of the respective heptose does not have a significant influence on the result of the reaction. Rather, it was the reactivity of the employed amine that played a key role for the success of the reaction. While application

of the guaiazulene-tagged amine **18** resulted in a good conversion in both cases (*gluco* and *manno*), the preparation of azobenzene Amadori compounds **23** and **25** was considerably hampered by the amine's low reactivity.

Despite the good conversion of guaiazulene-tagged amine **18**, the formation of the observed side products undeniably influenced the yield of the reaction. It seems as if the carbamate group in the Amadori products **22** and **24** is not sufficiently stable under the conditions applied. The relatively high temperatures combined with the presence of acid may have resulted in partial cleavage of this functional group or induced other decomposition reactions. Nevertheless, the intense blue color of the guaiazulene moiety considerably facilitated the chromatographic purification of Amadori products **22** and **24** so that all impurities could be efficiently separated.

Amadori reactions carried out with azobenzene derivative **19** were critically hampered and only resulted in very low formation of the corresponding products **23** and **25**. Due to the insufficient conversion it can be speculated that the pH value resulting from the applied amine hydrochloride-triethylamine system may be unfavorable for the rearrangement reaction. In the future, the corresponding free amine may be preferably utilized for this particular reaction. As demonstrated above, the CSP method could be successfully applied in the synthesis of guaiazulene-derived Amadori products **22** and **24**. Using the azobenzene moiety as a chromophore for CSP of Amadori products **23** and **25**, however, turned out to be less efficient and resulted in pronounced tailing, which significantly affected the purity of the obtained products.

4.   Carbohydrate Scaffold-based Glycoclusters for Investigation of Bacterial Adhesion

4.1   Introduction

Various kinds of scaffold molecules have been frequently utilized for the construction of complex dendritic glycostructures and glycoclusters. The synthesis of these branched compounds is of high interest for the establishment of new methods in combinatorial chemistry. In particular, multivalent carbohydrate-containing structures can be employed for the investigation of multivalency effects in lectin or bacterial binding.[64]

A scaffold compound can be defined as a multifunctional molecule, which allows for (orthogonal) attachment of various moieties with different spatial orientations (Scheme 4.1). Benzene derivatives such as 1,3,5-tris(bromomethyl)benzene, for example, can be utilized as planar scaffolds while a tetraol allows for functionalization in a type of tetrahedral manner. More elaborate supramolecular compounds have been prepared by scaffolds derived from biomolecules, such as amino acids, peptides, and carbohydrates.[65] The fixed stereochemistry of these compounds allows a three-dimensionally directed functionalization. Furthermore, each functional group can be addressed selectively based on their different reactivities or orthogonal functionalization.
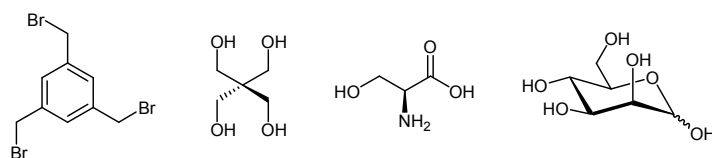
Scheme 4.1: Examples of scaffold molecules allowing for further functionalization, resulting in a different spatial orientation of the attached moieties.

The molecular rigidity and fixed stereochemistry of carbohydrates qualifies them as excellent scaffolds for the preparation of carbohydrate-centered glycomimetics. Especially their multifunctionality paves the way for interesting applications. For instance, it allows for direct introduction of five equal functional groups, which can be used to create carbohydrate-centered octopus glycosides.[66] Further branching of the introduced functionalities has also been employed in the preparation of dendrimers and larger glycoclusters.[67] Additionally, functional groups can be introduced in an orthogonal manner based on an appropriate

protection group strategy. In this way, heteroglycoclusters have been prepared, which mimic glycans as present in native biological systems more closely than common homoglycocluster. This makes them valuable tools for the investigation of multivalent protein-carbohydrate interactions, which resemble those occurring in biological systems.[68]

Uniformly derivatized glucoside scaffolds have been synthesized by alkylation of the well-known β-propargyl glucoside **26** and of α-allyl glucoside **28** with either propargyl bromide or allyl chloride, respectively. While the propargylated scaffold **27**[69] has been employed earlier for further functionalization according to the click chemistry methodology, the allylated scaffold **29**[66a, c] offers many other possibilities for further derivatization.
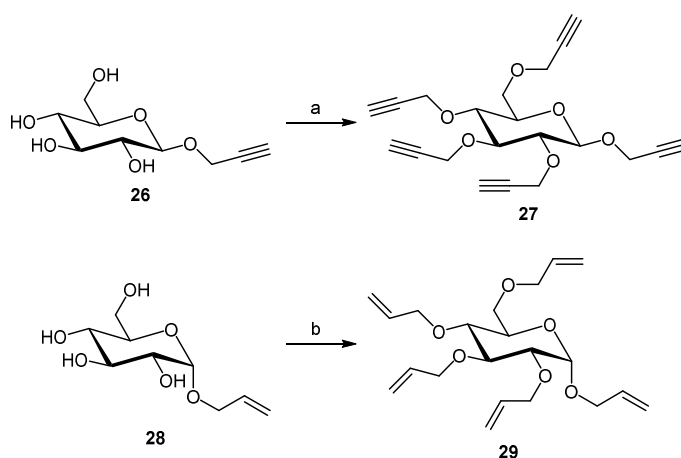
Scheme 4.2: Synthesis of uniformly functionalized glucoside scaffold molecules. a) propargyl bromide, NaH, DMF, 54%; b) allyl chloride, NaH, TBABr, DMF, 76%.

Many articles have been published involving the derivatization of allylated scaffold **29α** and **29β**, respectively, to create glycoclusters or branched dendritic molecules (Scheme 4.3). Ozonolysis of **29α**, for example, was utilized to prepare the pentaaldehyde **30**,[66a] which was further derivatized to a valuable pentaamine *via* reductive amination. Another useful transformation is the epoxidation of the pentaalkene with *m*-chloroperoxybenzoic acid (*m*-CPBA), giving pentaepoxide **31**,[70] which can be used, for example, as a starting material for ring opening reactions with nucleophiles. According to the concept of click chemistry, a photolytic thiol-ene reaction with cysteamine hydrochloride has been employed in the synthesis of pentaammonium hydrochloride **32**[66a] in excellent yield. On the other hand, the hydroboration of pentaalkene **29β** by 9-borabicyclo[3.3.1]nonane (9-BBN) was utilized to prepare pentaalcohol **33**. Subsequently, multiple glycosylation reactions were applied to create a pentavalent glycocluster from this compound.[71]
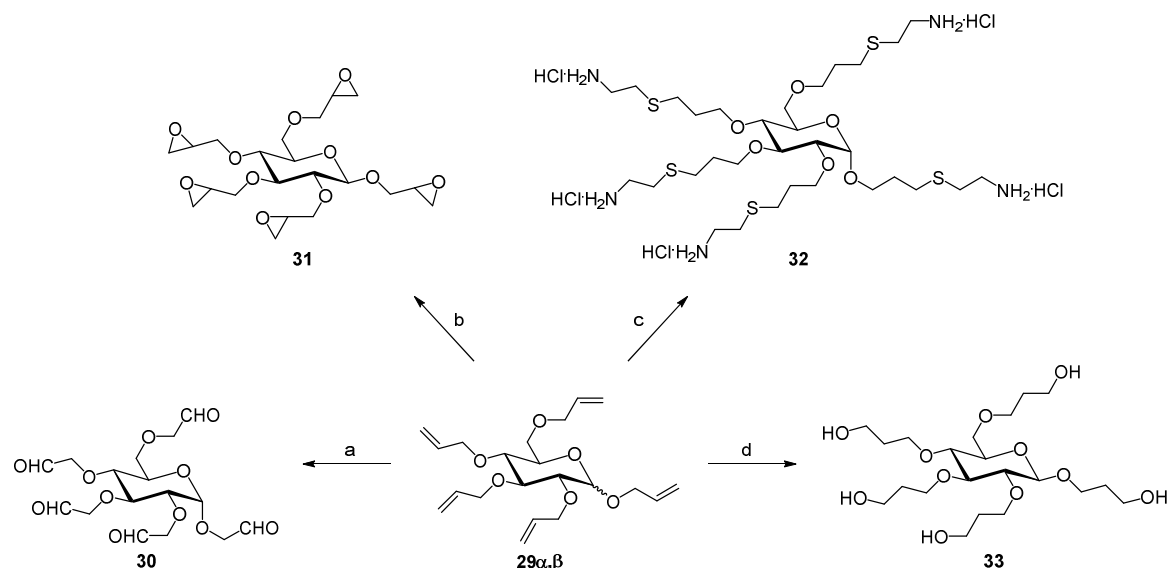
Scheme 4.3: Derivatization of pentavalent scaffold **29α/β**. a) **29α**, O_3, $NaHCO_3$, CH_2Cl_2, MeOH, then PPh_3, 75%; b) **29β**, *m*-CPBA, $CHCl_3$, 70%; c) **29α**, cysteamine hydrochloride, MeOH, h·ν (254 nm), 97%; d) 1. **29β**, 9-BBN, THF, 2. NaOH, H_2O_2, 62%.

A special class of carbohydrate scaffolds are those bearing an AB_4-type functionalization. These scaffolds are synthesized mostly by an early introduction of the 'A' functional group in the aglycone, for instance, by a glycosylation reaction while the remaining hydroxyl groups are subsequently derivatized with a second 'B' functional group in a uniform manner. In this way, highly versatile scaffolds with an orthogonal functionality become available, which give rise to tetravalent glycoclusters, for example.[64] Further applications involve labelling with tags, such as biotin, or immobilization on appropriate surfaces to form glycoarrays.[72]

A variety of this kind of carbohydrate scaffolds has been synthesized and employed in different applications (Scheme 4.4). In analogy to the pentaalkene **29** described above, a tetraalkene **34**[73] was prepared, which bears an alkyl bromide chain in the aglycone. Later the same compound was employed in the synthesis of a tetravalent glycocluster **35**.[74] A different scaffold was prepared by propargylation from galactoside **36**,[75] which, on the other hand, was obtained from the respective allyl galactoside by a thiol-ene reaction with Boc-protected cysteamine. This scaffold **37** was efficiently transformed *via* CuAAC reaction into a biotinylated tetravalent glycocluster as a carbohydrate probe for coating of magnetic beads. In analogy, scaffold **40**[76] was prepared by propargylation of glucoside **38** and subsequent ester cleavage to yield **39**. Further transformation *via* CuAAC reaction and peptide coupling yielded a potent lipopeptide vaccine.
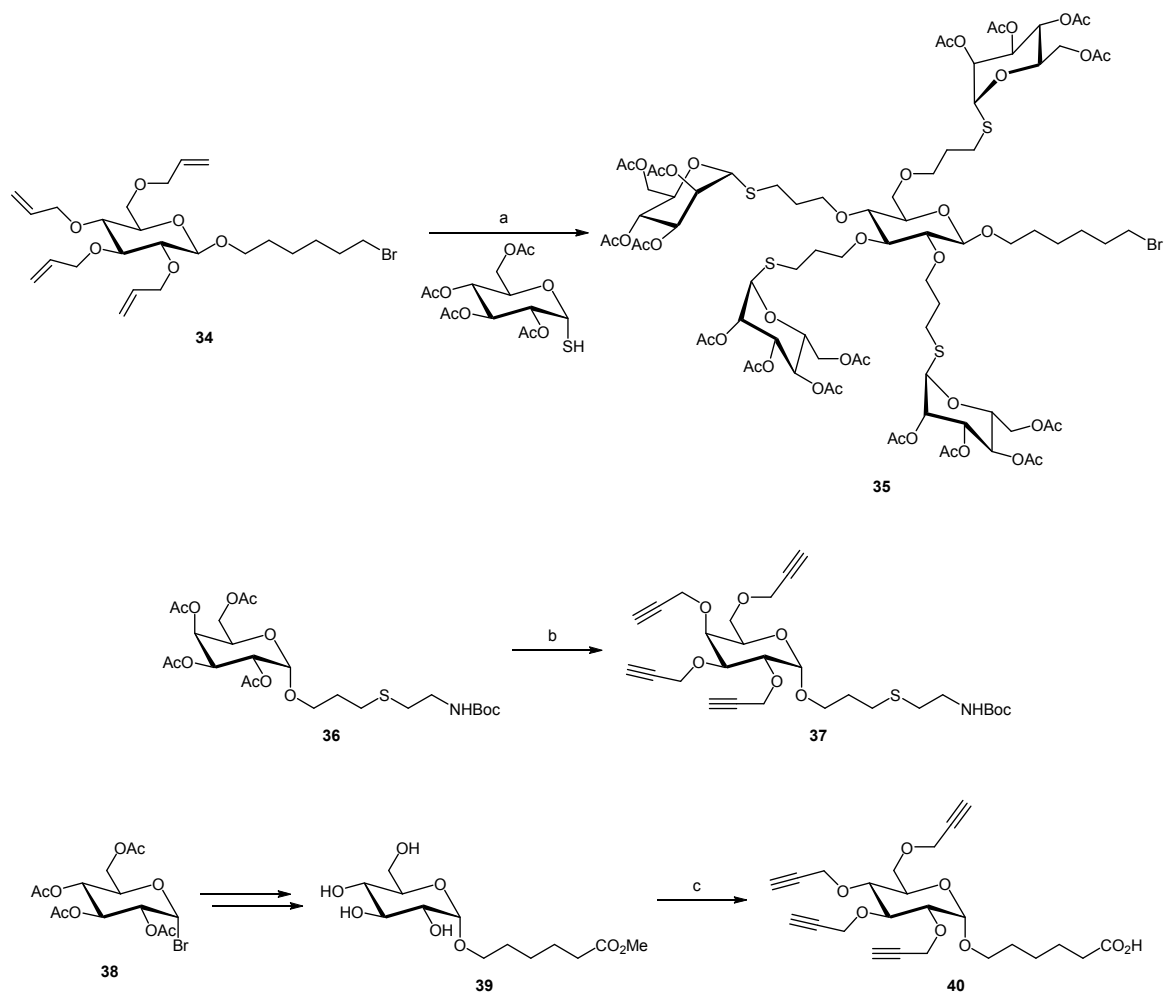
Scheme 4.4: Synthesis of different AB$_4$-type carbohydrate scaffolds and a tetravalent glycocluster. a) MeOH, h·ν (254 nm), 40%; b) 1. NaOMe, MeOH, 89%, 2. propargyl bromide, NaH, THF, 51%; c) 1. propargyl bromide, NaH, THF, 2. NaOH (2 M), 31% overall yield (starting from **38**).

This chapter covers different research topics involving the synthesis of carbohydrate-scaffold compounds and tetravalent glycoclusters as well as their biological testing towards inhibition of bacterial adhesion. While Chapter 4.2 presents a submitted manuscript, which includes the synthesis of carbohydrate-centered scaffold compounds, unpublished results from biological tests of a tetravalent glycocluster as well as the preparation of an OEG glycocluster conjugate are presented in Chapter 4.3. All syntheses in this chapter were performed by myself (unless indicated otherwise).

4.2   Synthesis of AB₄ Carbohydrate Scaffolds as Branching Units in the Glycosciences

T.-E. Gloe, A. Müller, A. Ciuk, T. M. Wrodnigg, T. K. Lindhorst, *Carbohydr. Res.* **2015**, submitted.

Carbohydrates are excellent scaffolds for the synthesis of carbohydrate-centered glycomimetics due to their molecular rigidity, fixed stereochemistry as well as their multifunctionality. Especially carbohydrate scaffolds containing functional groups that can be addressed in an orthogonal manner (such as AB₄-type scaffolds) are valuable tools for the investigation of multivalency effects in lectin binding. Their orthogonal functionalization allows for both the introduction of several carbohydrate moieties but also attachment of the resulting glycocluster (or dendrimer) to a surface, for example.

In the following manuscript, we report on the preparation of AB₄-type carbohydrate scaffolds containing various ethyl aglycone moieties, functionalized with 'A' and four functional groups 'B' at positions 2, 3, 4, and 6 of the sugar ring. Following a retrosynthetic approach, different synthetic pathways were evaluated to achieve AB₄-type derivatization. Even unsuccessful routes, nevertheless, provided valuable precursor scaffold compounds for other applications. The final sequence was demonstrated in the synthesis of the targeted azido-functionalized N₃(NHBoc)₄-type scaffold, from which an isothiocyanate scaffold compound as well as a tetravalent glycocluster were prepared. Additionally, a photoresponsive scaffold compound containing an azobenzene moiety was synthesized.
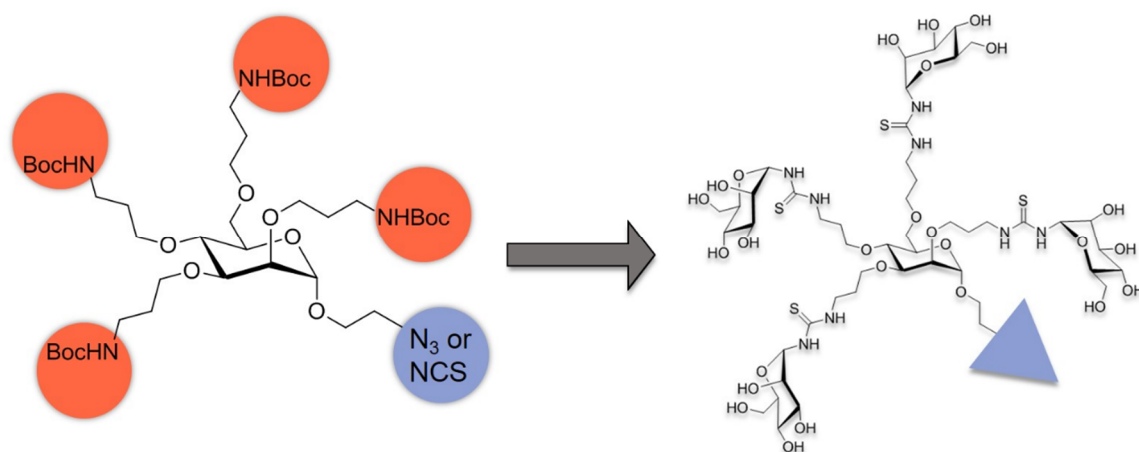
Scheme 4.5: Azide or isothiocyanate functionalized carbohydrate scaffolds can be transformed into the corresponding tetravalent glycocluster containing the 'A' portion as an orthogonal functional group for further derivatization.

For this project, A. Müller prepared a propargylated azobenzene derivative for the synthesis of a photoresponsive scaffold compound and A. Ciuk prepared an allylated scaffold as a precursor molecule. All other compounds found in this manuscript were synthesized by myself. The manuscript was written by T. M. Wrodnigg, T. K. Lindhorst and myself, I prepared the supporting information.

Synthesis of AB4-type carbohydrate scaffolds as branching units in the glycosciences

Tobias-Elias Gloe[1], Anne Müller[1], Anna Ciuk[1], Tanja M. Wrodnigg[2], Thisbe K. Lindhorst[1*]

[1] *Christiana Albertina University of Kiel, Otto Diels Institute of Organic Chemistry, Otto-Hahn-Platz 3/4, D-24118 Kiel, Germany, Fax: +49 431 8807410*
[2] *Glycogroup, Institute of Organic Chemistry, Technical University Graz, Stremayrgasse 9, A-8010 Graz, Austria*

Correspondence should be addressed to Thisbe K. Lindhorst, E-mail: tklind@oc.uni-kiel.de

Abstract

Carbohydrate scaffolds, functionalised according to an AB4-type, were prepared on the basis of α-D-mannopyranosides with various ethyl aglycone moieties, functionalised with 'A'. Four functional groups 'B' were installed at positions 2, 3, 4, and 6 of the sugar ring. In particular, we were interested in preparing $N_3(NH_2)_4$-functionalised mannosides as multifunctional branching units for further orthogonal derivatisation or immobilisation on surfaces. A detailed synthetic study was performed which revealed that an azido function 'A' had to be installed at an advanced stage of the synthesis for successful preparation of the desired AB4-type carbohydrate scaffolds. The most successful synthetic sequence involved tetra-cyanoethylation of a 2-benzyloxyethyl mannopyranoside and subsequent reduction with in situ Boc protection to achieve $(NHBoc)_4$ functionalisation. Finally, the benzyloxyethyl aglycon was converted into the corresponding azidoethyl moiety to gain access to the desired $N_3(NHBoc)_4$-functionalised carbohydrate scaffold. Its utilisation was exemplified by straightforward synthesis of a photosensitive glycoconjugate and a tetravalent glycocluster. Such compounds may be immobilised on functional surfaces to serve as tools in cell adhesion studies.

Keywords: glycoclusters; octopus glycosides; orthogonality, multivalency; protecting groups

1

1. Introduction

Monosaccharides as well as oligosaccharides have frequently been employed as core molecules of scaffolds to allow for multivalent conjugation with biomolecules, including carbohydrates[1] or peptides,[2] for various glycobiological and medicinal applications.[2,3] By this approach, all functional groups of a sugar ring can be uniformly derivatised to prepare, for example, carbohydrate-centred octopus glycosides in a multi-glycosylation reaction.[4] Alternatively, orthogonality can be introduced to a carbohydrate scaffold. Previously, glycosides with up to 5-fold orthogonal functionalities were utilised in combinatorial chemistry.[5] Highly versatile carbohydrate scaffolds can be achieved according to an AB_4-type functionalisation.[6] This type of scaffold glycoside may be synthesised from monosaccharides featuring a functional group 'A' in the aglycone part, whereas the remaining four functionalities of the sugar ring are uniformly decorated with a group 'B', which is orthogonal to 'A' (Fig. 1). Thus, AB_4-type carbohydrate scaffolds can be converted into tetravalent glycoclusters.[1] These can be labelled, or immobilised to form glycoarrays,[7] and further elaborated into complex structures via the functional group 'A' of the aglycon.

Various AB_4-type carbohydrate scaffolds have been described (cf. Fig. 1) and were employed, for example, as delivery systems.[2] Our interest in AB_4-type functionalised glycosides is directed at their utilisation in surface-based cell adhesion assays based on simple click chemistry.[8] Consequently, we planned to combine azido (A) and amino (B) functional groups in an AB_4-type carbohydrate scaffold based on α-D-mannopyranoside. The azido function is amenable to bioorthogonal click reactions as well as Staudinger(-Bertozzi) ligation,[9] whereas the amino groups can be conjugated by peptide coupling, thiourea bridging,[10] or Amadori rearrangement.[11]
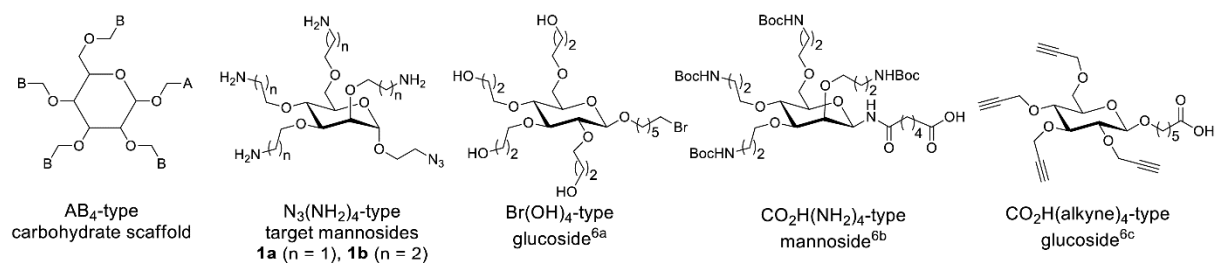
Figure 1. AB_4-type carbohydrate scaffold molecules (left) can be used to achieve, for example, tetravalent glycoclusters equipped with an orthogonal functional group 'A' for further labelling, multimerisation, or immobilisation, respectively. Here, the $N_3(NH_2)_4$-type mannosides **1a** and **1b** were targeted. For comparison, three representative known examples of AB_4-type carbohydrate scaffolds are depicted.

Following guiding references, we anticipated that the synthesis of an AB$_4$-type functionalised glycoside with A = N$_3$ and B = NH$_2$ would be rather straightforward. However, our target turned out to be more challenging than anticipated.

2.   Results and discussion

2.1.   Retrosynthetic considerations concerning target AB$_4$-type mannosides **1a** and **1b**

Regardless of whether 2,3,4,6-tetra-*O*-aminoethyl mannoside **1a** or the tetra-*O*-aminopropyl analogue **1b** is targeted, the retrosynthetic considerations may be based on the early introduction of the azido group starting from known 2-azidoethyl α-D-mannopyranoside **3**[12] as suitable starting material (Scheme 1). We expected the N$_3$ group to be compatible with the intended synthetic approaches, I – IV, which had in common that the desired four amino groups (B) would be established in the last step of the synthesis.

Following approach I (Scheme 1), the four free amino groups in **1a** could be liberated from tetra-*N*-Boc protected precursor **2**, which, in turn, should be easily available from **3** by reaction with 2-(*tert*-butyloxycarbonylamino)ethyl bromide. However, no conversion of the starting material was observed under standard reaction conditions in the presence of sodium hydride. We assume that deprotonation of the carbamate moieties competed with deprotonation of the hydroxy groups in compound **3** resulting in consumption of the base without desired alkylation. Another plausible cause for the failure of this reaction step may be the low reactivity of the leaving group. This assumption was supported by the successful reaction of **3** with allyl bromide (see below).

Approach II, addressing compound **1a** (Scheme 1), involved the tetra-aldehyde **4**. This can be derived by ozonolysis of tetra-*O*-allyl mannopyranoside **5** and subsequent reductive work-up. The following reductive amination according to published work[13] would yield target scaffold **1a**. However, ozonolysis of **5** led to a multitude of products which were not further characterised. The desired compound **4** could not be isolated from this mixture. Alternatively, tetra-aldehyde **4** may be obtained from compound **6** by controlled hydrolysis of the diethyl acetals. Starting from 2-azidoethyl α-D-mannoside **3**, the acetal functionalisation may be introduced employing bromoacetaldehyde diethyl acetal. However, acetal **6** could only be obtained in an unsatisfying yield of 13%.

Pathway III involving tetranitrile **7** was considered for the synthesis of **1b** (Scheme 1). Compound **7** may be easily available by base-catalysed cyanoethylation of starting material **3**

with acrylonitrile in a Michael-type reaction. With 1,8-diazabicyclo[5.4.0]undec-7-en (DBU),[14] potassium hydroxide,[15] or strongly basic ion exchange resin[16] as basic catalysts, only partial cyanoethylation was achieved. Gratifyingly, per-cyanoethylation was accomplished with caesium carbonate[17] yielding **7** in 57% yield (not shown, cf. section 4. Experimental). In the next step, it was necessary to reduce the rather robust nitrile substituents to amino groups in the presence of the azido group to ensure orthogonal functionalisation of the product. For this purpose moderately active hydride donors, such as diisobutylaluminium hydride (DIBAL), may be employed. However, this approach was not met with success, and the desired product could not be isolated.
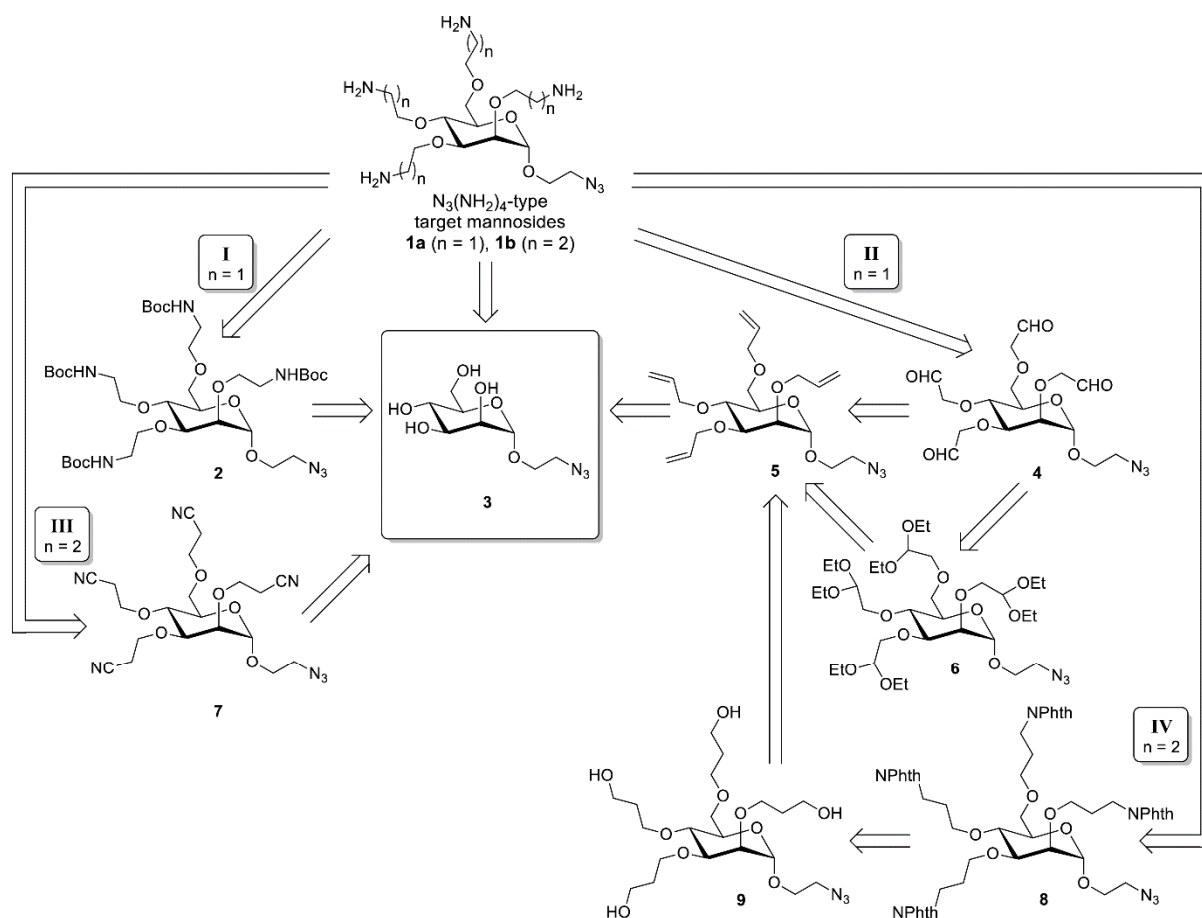
Scheme 1. Retrosynthetic considerations for the synthesis of the AB$_4$-type mannosides **1a** and **1b** according to four retrosynthetic pathways, I, II, III, and IV, based on 2-azidoethyl α-D-mannoside (**3**).

Finally, pathway IV can be envisaged to access **1b** based on a procedure earlier introduced by our group for the synthesis of trehalose-based octopus glycosides.[18] In this case, the amino functions are released from phthalimido groups (compound **8**), which in turn, may be obtained from tetra-hydroxypropyl-functionalised mannoside **9** by Appel reaction and subsequent substitution of the four bromide substituents with potassium phthalimide or, alternatively, by

direct introduction employing phthalimide as the acid component in a Mitsunobu protocol. This synthetic sequence had been employed by Toth and Simerska in order to prepare carbohydrate-based templates for drug delivery.[14] Tetraol **9** in turn, may be available from tetra-*O*-allylated glycoside **5** by hydroboration.

Indeed, synthesis of the tetra-*O*-allyl mannoside **5** from **3** proceeded smoothly in 84% yield (Scheme 2). Based on earlier work[19] we expected effective anti-Markovnikov borane addition employing 9-borabicyclo[3.3.1]nonane (9-BBN). However here, hydroboration of **5** with 9-BBN led to decomposition of the starting material. It can be speculated that hydroboration-azide alkylation occurred in this step.[20]

Alternatively, tetra-O-allyl mannoside **5** was employed in a thiol-ene radical addition reaction[21] exploiting *N*-Boc-protected cysteamine and azoisobutyronitrile (AIBN) as radical initiator furnishing compound **10** in 55% yield with concomitant reduction of the azido group (Scheme 2). Thus, with the availability of compound **10** an AB$_4$-type carbohydrate scaffold was obtained, lacking however the desired orthogonality of functional groups.
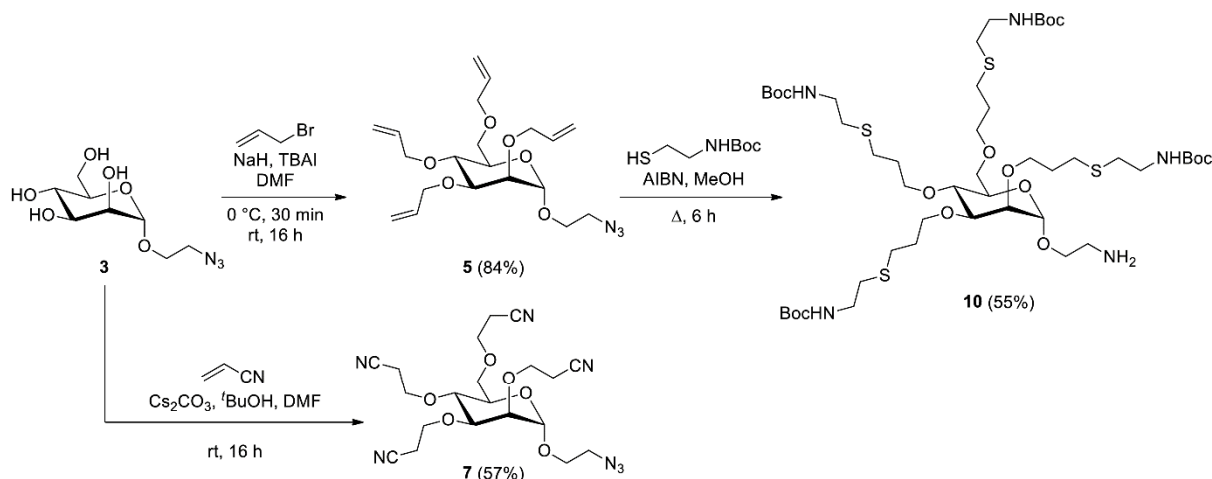
Scheme 2. Synthesis of the AB$_4$-type mannosides **5** and **7** from **3**. Thiol-ene reaction (**5** to **10**) led to reduction of the azido function in the aglycon.

Because non of the four pathways outlined in Scheme 1 led us to the synthesis of the desired N$_3$(NH$_2$)$_4$-type mannoside scaffold, we consequently changed our synthetic plan.

2.2. Synthesis of the target AB$_4$-type mannosides **22** and **23**

Preliminary experiments as outlined in Scheme 1 had revealed that the azido group in the aglycon was responsible for most of the synthetic difficulties discussed in the above. Thus, we had to change our initial strategy in favour of installing the N$_3$ moiety at an advanced stage of the synthetic protocol. We started with the reaction of per-*O*-acetylated D-mannopyranose **12**

with *N*-(2-hydroxyethyl)phthalimide furnishing mannopyranoside **13**. This, in turn, was conventionally deprotected to give free glycoside **14** in almost 50% overall yield (Scheme 3). Attempted per-*O*-allylation (compound **15**) was accompanied by decomposition and formation of various side products. Likewise, when this reaction sequence was carried out with 2-*N*-Cbz-aminoethyl α-D-mannoside[22] unsatisfactory yields were obtained.
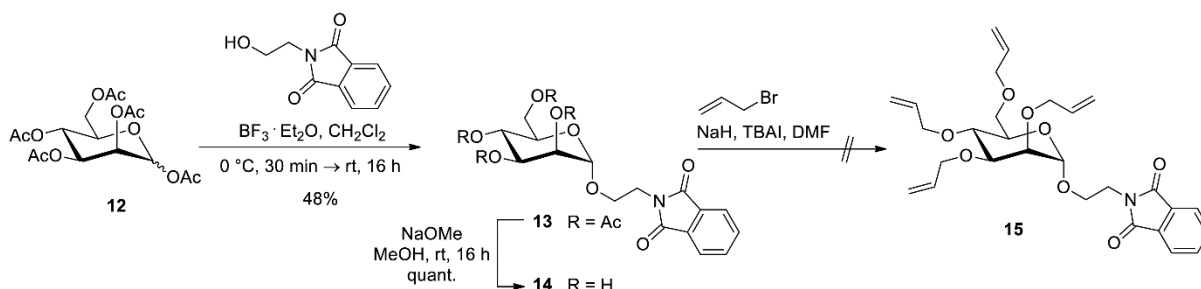
Scheme 3. Lewis acid-promoted glycosylation of mannose pentaacetate (**12**) with *N*-(2-hydroxyethyl)phthalimide and subsequent deprotection gives rise to **14**. Subsequent allylation to **15** was not successful.

Consequently, in order to achieve the desired AB$_4$-type scaffold with N$_3$/(NH$_2$)$_4$ substituents we employed *O*-benzyl-protected 2-hydroxyethyl mannoside **17**,[23] obtained in 81% yield by Lewis acid-promoted mannosylation of 2-benzyloxyethanol with glycosyl donor **16**[24] (Scheme 4). Following de-*O*-acetylation under Zemplén conditions,[25] the reaction with acrylonitrile in the presence of caesium carbonate furnished tetra-nitrile **19** in 74% yield.
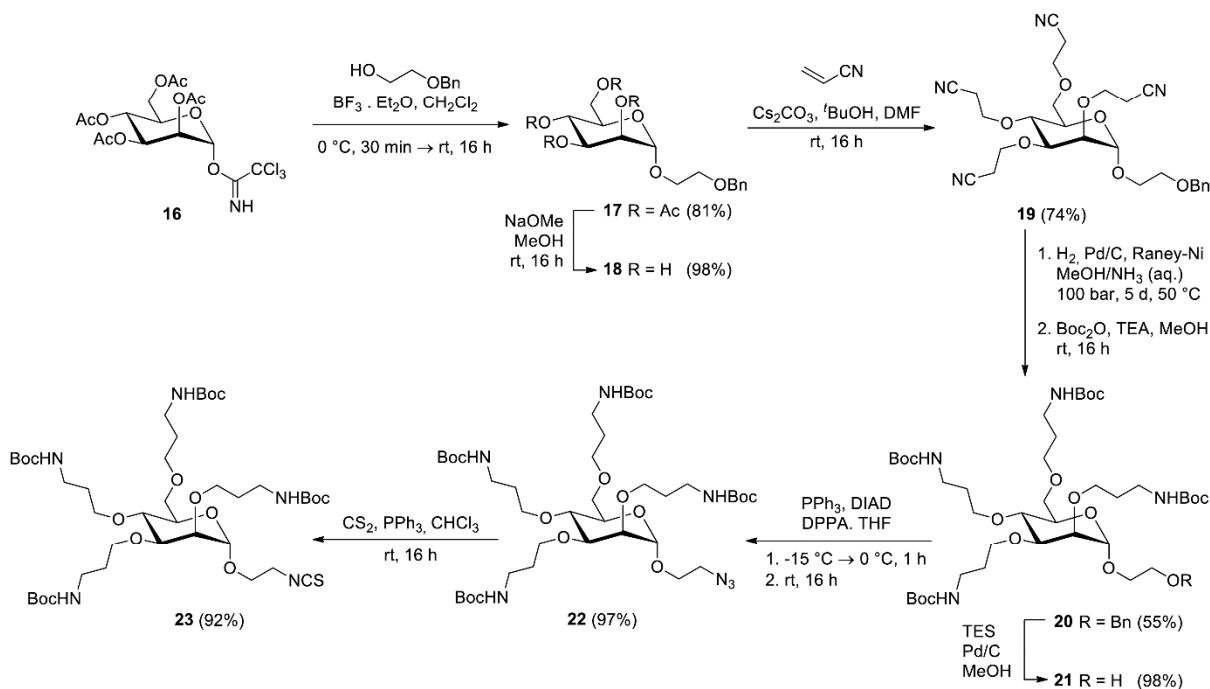
Scheme 4. Synthesis of the desired AB$_4$-type carbohydrate scaffolds **22** and **23**.

For optimisation of the reduction conditions to convert cyanoethyl groups of compound **19** into the corresponding aminopropylated mannoside, metal hydrides were tested, as used earlier by Toth and coworkers,[6d] and various conditions for catalytic hydrogenation (Table 1). Reduction of tetranitrile **19** with different metal hydrides resulted in yields around 30% with the exception of lithium aluminium hydride, which led to decomposition of the starting material **19**. Hydrogenation with Raney-Ni (and Pd-C) under strongly alkaline conditions (LiOH or NaOH) also led to decomposition, whereas under acidic or neutral reaction conditions no conversion occurred (Table 1). When Raney-Ni was employed in a mixture of methanol and aqueous ammonia, a complex mixture was obtained consisting of partially reduced products as well as by-products resulting from retro-Michael reaction. Finally, hydrogenation under the catalysis of both, Pd/C and Raney-Ni at high pressure (100 bar) resulted in pure **20** after in situ *N*-Boc protection of all amino groups along the sugar moiety in 55% yield. Interestingly, the *O*-benzyl group in compound **19** was not removed under these reaction conditions. Subsequent catalytic transfer hydrogenation using Pd/C and triethylsilane[26] provided unprotected alcohol **21** in almost quantitative yield.

Table 1. Optimisation of the reaction conditions for the synthesis of compound **20**.

Metal hydride	Solvent	T	Reaction time	Yield[#]
LiAlH$_4$	THF	0 °C → rt	16 h	decomposition
DIBAL	THF	70 °C	24 h	35%
NaBH$_4$/ NiCl$_2$ · 6 H$_2$O	MeOH	0 °C → rt	16 h	29%
DodBMS*	THF	70 °C	16 h	30%

Catalyst Acid or Base	Solvent, P (H$_2$)	T	Reaction time	Yield[#]
Raney-Ni, 10% Pd-C LiOH	1,4-dioxane, H$_2$O, atmospheric pressure	80 °C	24 h	decomposition
Raney-Ni NaOH	EtOH, THF, 1,4-dioxane, 5 bar	rt	96 h	decomposition
Pd(OH)$_2$ HCl-Et$_2$O	CHCl$_3$, EtOH, 15 bar	rt	72 h	no conversion
Raney-Ni (neutral)	MeOH, 50 bar	rt	72 h	no conversion
Raney-Ni aq. NH$_3$	MeOH, 50 bar	rt	96 h	partial reduction
Raney-Ni, 10% Pd-C aq. NH$_3$	MeOH, 100 bar	45 °C	120 h	55%

Yields refer to isolated **20** after in situ-Boc protection

* DodBMS: borane dodecyl methyl sulfide complex[28]

With **21** in hands, the desired AB$_4$-type mannoside **22**, carrying an azido function 'A' and four *N*-Boc-aminopropyl moieties 'B', could be obtained in a Mitsunobu reaction with diphenylphosphoryl azide (DPPA)[27] making azidoethyl mannoside **22** available in an overall yield of 31% over six steps from trichloroacetimidate **16**. Furthermore, NCS/(NH$_2$)$_4$-analogue **23** could be prepared from **22** in over 90% under aza-Wittig reaction conditions employing carbon disulphide (CS$_2$) as nucleophile.

2.3. Utilisation of AB$_4$-type mannosides

Of the AB$_4$-type mannosides **19**-**23** now available, **21** was utilised for the direct synthesis of alkyne-functionalised azobenzene glycoconjugate **25** in 70% yield via azobenzene derivative **24** (Scheme 5). This compound represents a valuable building block for the synthesis of multivalent photosensitive glycoconjugates as well as for the exploration of photoswitchable cell adhesion.[29]
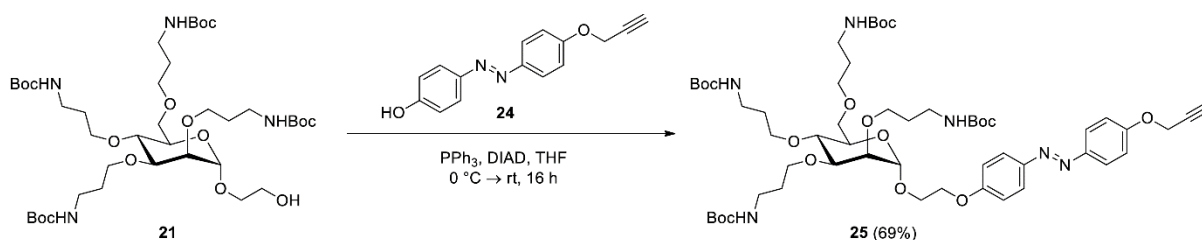
Scheme 5. Synthesis of the photoswitchable AB$_4$-type mannoside **25** from the OH(NHBoc)$_4$-functionalised scaffold **21**.

Mannoside **22** was utilised as starting material for the synthesis of tetravalent glycocluster **28** (Scheme 6). *N*-deprotection of compound **22** employing trifluoroacetic acid (TFA) yielded the corresponding tetraammonium salt in quantitative yield. Its subsequent reaction with acetyl-protected α-D-mannopyranosyl isothiocyanate **26**[30] in dichloromethane and diisopropylethylamine (DIPEA) provided thiourea-bridged glycocluster **27**, which was subjected to Zemplén deacetylation.[25] Final purification yielded tetravalent glycocluster **28** in 63% over three steps. Biological evaluation of compound **28** in bacterial adhesion assays is currently in progress.
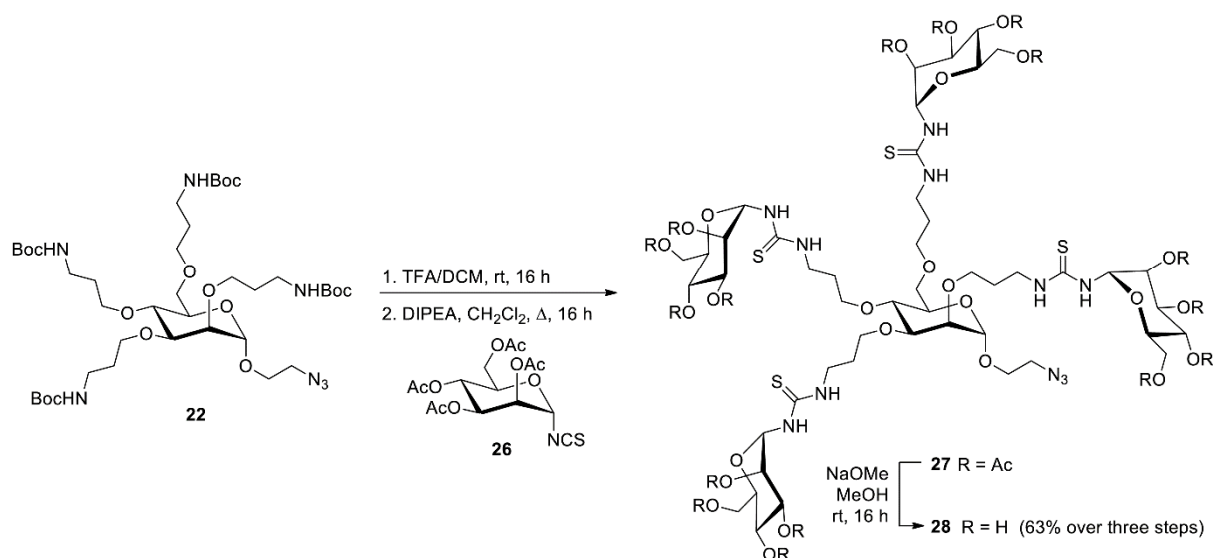
Scheme 6. Synthesis of the azido-functionalised tetravalent glycocluster **28** from the $N_3(NHBoc)_4$-functionalised mannoside **22**.

3. Conclusion

In continuation of our earlier work on octopus glycosides[6a, 6c, 13, 19] we have prepared various orthogonally functionalised AB_4-type carbohydrate scaffolds, namely **10**, **19-23**, **25**, and **28**. In particular, we have achieved the synthesis of $N_3/(NHBoc)_4$-functionalised mannoside **22** from mannosyl trichloroacetimidate **16** in 30% yield over six steps. Along this synthetic route, the desired azido group in the aglycon portion had to be established at an advanced stage. The now available AB_4-type mannosides clearly offer an interesting variety of options for further ligation, including unusual connection such as by multiple Amadori rearrangement. We have demonstrated the potential of compounds **21** and **22** by the preparation of the photoswitchable glycoconjugate **25** and the tetravalent glycocluster **28**, respectively. These are planned to be immobilised on functional surfaces by click chemistry and may serve as valuable tools for the exploration of carbohydrate-specific cell adhesion.

4. Experimental

4.1 Methods and materials

All chemicals were purchased from Sigma-Aldrich, Alfa Aesar or TCI and used without further purification. Moisture-sensitive reactions were carried out under a nitrogen atmosphere in dry reaction vessels. Thin layer chromatography (TLC) was performed on aluminium backed silica

gel plates (GF 254, Merck). Detection was achieved by UV light and/or charring with 10% sulfuric acid in EtOH or with vanillin reagent (3.0 g vanillin and 0.5 mL H_2SO_4 in 100 mL EtOH) followed by heat treatment at $\approx$180 °C. Flash chromatography was carried out on silica gel 60 (Merck, 230-400 mesh, particle size 0.040-0.063 mm) using distilled solvents. NMR spectra were recorded on Bruker DRX-500 and AV-600 spectrometers at 300 K and 500.13 MHz for [1]H- and 125.75 MHz for ^{13}C NMR spectra. Chemical shifts are referenced to the residual proton of the NMR solvent. Data are presented as follows: chemical shift, multiplicity (s = singlet, d = doublet, t = triplet, q = quartet, m = multiplet and br = broad signal), coupling constant in Hertz (Hz) and integration. Full assignment of the peaks was achieved with the aid of 2D NMR techniques (^{1}H,^{1}H-COSY and ^{1}H,^{13}C-HSQC). Optical rotations were measured with a Perkin-Elmer 241 polarimeter (sodium D-line: 589 nm, length of cell: 1 dm) in the solvents indicated. Infrared (IR) spectra were recorded on a Perkin Elmer FT-IR Paragon 1000 (ATR) spectrometer and were reported in cm^{-1}. ESI mass spectra were recorded on an Esquire-LC instrument from Bruker Daltonics. High-resolution ESI mass spectrometry was performed on an Agilent 6224 ESI-TOF instrument.

4.2   Preparative procedures

4.2.1   2-Azidoethyl 2,3,4,6-tetra-*O*-allyl-α-D-mannopyranoside (**5**)

The azidoethyl α-D-mannopyranoside **3** (1.01 g, 4.06 mmol, 1.0 eq) and TBAI (749 mg, 2.03 mmol, 0.5 eq) were dissolved in dry DMF (50 mL). Then NaH (812 mg, 20.3 mmol, 60% dispersion in mineral oil, 5.0 eq) was added to the solution in portions and the mixture was stirred for 30 min at room temperature. Allyl bromide (2.11 mL, 24.4 mmol, 6.0 eq) was slowly added to the suspension and stirring was continued for 16 h. The resulting solution was poured onto ice-cold water and was then extracted three times with CH_2Cl_2. The combined organic phases were dried over $MgSO_4$, it was filtered and the filtrate was concentrated under reduced pressure. Purification of the crude mixture by flash chromatography (cyclohexane/EtOAc, 5:1) gave product **5** (1.39 g, 3.40 mmol, 84%) as a colourless syrup: $[\alpha]_{20}^{D}$ +35.4 (*c* 1.0, MeOH); R_f = 0.66 (cyclohexane/EtOAc, 2:1); ^{1}H NMR (500 MHz, $CDCl_3$): δ 5.97-5.87 (m, 4H, 4 C$\underline{H}$=CH$_2$), 5.32 (m$_c$, 1H, CH=C$\underline{H}$′H), 5.29-5.26 (m, 2H, CH=C$\underline{H}$′H), 5.24 (ddd, $J_{OCH,=CH}$ = 1.6 Hz, $J_{CH=,=CH}$ = 3.4 Hz, $J_{=CH,=CH}$ = 9.5 Hz, 1H, CH=C$\underline{H}$′H), 5.20-5.12 (m, 4H, 4 CH=CH′$\underline{H}$), 4.87 (d, $J_{1,2}$ = 1.6 Hz, 1H, H-1), 4.35 (m$_c$, 1H, OC$\underline{H}$′HCH=CH$_2$), 4.22-4.06 (m, 6H, 3 OC$\underline{H}$′HCH=CH$_2$, 3 OCH′$\underline{H}$CH=CH$_2$), 4.01 (m$_c$, 1H, OCH′$\underline{H}$CH=CH$_2$), 3.88 (ddd, $J_{CHN_3,OCH}$ = 3.5 Hz, $J_{CH'N_3,OCH}$ = 5.8 Hz, $J_{OCH,OCH'}$ = 10.7 Hz, 1H, OC$\underline{H}$′HCH$_2$N$_3$), 3.74-3.67

(m, 6H, H-2, H-3, H-4, H-5, H-6a, H-6b), 3.60 (m$_c$, 1H, OCH′$\underline{\text{H}}$CH$_2$N$_3$), 3.40 (ddd, 1H, $J_{\text{CHN}_3,\text{OCH}}$ = 3.5 Hz, $J_{\text{CH′N}_3,\text{OCH}}$ = 7.3 Hz, $J_{\text{OCH,OCH′}}$ = 13.2 Hz, 1H, OCH$_2$CH′HN$_3$), 3.33 (ddd, 1H, $J_{\text{CHN}_3,\text{OCH}}$ = 3.5 Hz, $J_{\text{CH′N}_3,\text{OCH}}$ = 5.8 Hz, $J_{\text{OCH,OCH′}}$ = 13.3 Hz, 1H, OCH$_2$CH′HN$_3$); ^{13}C NMR (125 MHz, CDCl$_3$): δ 135.2, 135.1, 135.0, 135.0 (4 $\underline{\text{C}}$H=CH$_2$), 117.6, 117.0, 116.9, 116.7 (4 CH=$\underline{\text{C}}$H$_2$), 98.6 (C-1), 79.4 (C-3), 74.9 (C-2, C-4), 74.1, 72.5, 72.3 (3 O$\underline{\text{C}}$H$_2$CH=CH$_2$), 72.2 (C-5), 71.4 (O$\underline{\text{C}}$H$_2$CH=CH$_2$), 69.5 (C-6), 66.6 (O$\underline{\text{C}}$H$_2$CH$_2$N$_3$), 50.7 (OCH$_2$$\underline{\text{C}}H_2N_3$); IR (ATR) ṽ: 2915, 2869, 2104, 1096, 1058, 993, 921 cm^{-1}; ESI-MS (*m/z*): [M + Na]$^+$ calcd for C$_{20}$H$_{31}$N$_3$O$_6$, 432.211, found, 432.212.

4.2.2   2-Azidoethyl 2,3,4,6-tetra-*O*-(2-cyanoethyl)-α-D-mannopyranoside (**7**)

Mannoside **3** (200 mg, 798 μmol, 1.0 eq) was dissolved in DMF (1.0 mL) and the solution was diluted with ^{t}BuOH (5.0 mL). After addition of acrylonitrile (4.26 mL, 64.3 mmol, 80 eq), the solution was stirred for 5 min at room temperature, when Cs$_2$CO$_3$ (1.04 g, 3.19 mmol, 4.0 eq) was added. The resulting suspension was vigorously stirred for 2 d at room temperature and was then filtered over a pad of Celite$^®$. The filtrate was concentrated under reduced pressure and the resulting crude product was purified by column chromatography (cyclohexane/EtOAc, 1:1 to 1:5) to yield cyanoethylated mannoside **7** (211 mg, 458 μmol, 57%) as a slightly yellow syrup: [α]$_{25}$^{D} +18.7   (*c* 0.96, CH$_2$Cl$_2$); R_f = 0.31   (cyclohexane/EtOAc, 1:2); ^{1}H NMR (500 MHz, CDCl$_3$): δ 4.92 (d, $J_{1,2}$ = 1.8 Hz, 1H, H-1), 4.09-4.02 (m, 2H, 2 OC$\underline{\text{H}}$′HCH$_2$CN), 3.97 (dd, $J_{5,6a}$ = 3.8 Hz, $J_{6a,6b}$ = 11.6 Hz, 1H, H-6a), 3.93-3.81 (m, 8H, H-2, H-4, OC$\underline{\text{H}}$′HCH$_2$CN, OCH′$\underline{\text{H}}$CH$_2$CN, OC$\underline{\text{H}}$$_2CH_2CN, OC\underline{\text{H}}$$_2CH_2N_3$), 3.75-3.71 (m, 2H, H-3, OCH′$\underline{\text{H}}$CH$_2$CN), 3.69-3.61 (m, 3H, H-5, H-6b, OCH′$\underline{\text{H}}$CH$_2$CN), 3.40 (m$_c$, 2H, OCH$_2$C$\underline{\text{H}}$$_2N_3$), 2.75-2.56 (m, 8H, 4 OCH$_2$C$\underline{\text{H}}$$_2$CN); ^{13}C NMR (125 MHz, CDCl$_3$): δ 118.9, 118.5, 118.3, 118.2 (4 CN), 98.5 (C-1), 80.5 (C-3), 77.0 (C-2), 74.2 (C-4), 72.4 (C-5), 69.7 (C-6), 67.6 (O$\underline{\text{C}}$H$_2$CH$_2$CN), 67.0 (O$\underline{\text{C}}$H$_2$CH$_2$N$_3$), 66.8 (O$\underline{\text{C}}$H$_2$CH$_2$CN), 66.5 (O$\underline{\text{C}}$H$_2$CH$_2$CN), 65.6 (O$\underline{\text{C}}$H$_2$CH$_2$CN), 50.6 (OCH$_2$$\underline{\text{C}}H_2N_3$), 19.7, 19.5, 19.5, 19.3 (4 OCH$_2$$\underline{\text{C}}H_2$CN); IR (ATR) ṽ: 2935, 2885, 2251, 2104, 1412, 1367, 1287, 1224, 1106, 1062 cm^{-1}; ESI-MS (*m/z*): [M + Na]$^+$ calcd for C$_{20}$H$_{27}$N$_7$O$_6$, 484.192, found, 484.189.

4.2.3   2-Aminoethyl 2,3,4,6-tetra-*O*-{3-*S*-[2-*N*-(*tert*-butyloxycarbonyl)aminoethyl]-thiopropyl}-α-D-mannopyranoside (**10**)

A solution of the tetraalkene **5** (265 mg, 647 μmol, 1.0 eq) and 2-(Boc-amino)ethanethiol (1.49 g, 8.41 mmol, 13 eq) in dry MeOH (10 mL) was heated to 75 °C. Then, AIBN (a tip of a spatula) was added and the mixture was stirred for 6 h at this temperature. The solution was

then allowed to cool to room temperature and stirring was continued for 16 h. After concentration under reduced pressure and purification of the crude mixture by flash chromatography (CH$_2$Cl$_2$/MeOH/TEA, 98:1:1) gave product **10** (388 mg, 347 µmol, 54%) as a colourless syrup: $[\alpha]_{25}^{D}$ +13.5 (*c* 0.95, CH$_2$Cl$_2$); R_f = 0.12 (CH$_2$Cl$_2$/MeOH/TEA, 98:1:1); ^{1}H NMR (500 MHz, CDCl$_3$): δ 5.11-5.03 (m, 3H, 3 N$\underline{H}$Boc), 4.86 (d~s, 1H, H-1), 3.84-3.80 (m, 1H, OCH´$\underline{H}$CH$_2$CH$_2$S), 3.74 (m$_c$, 1H, OCH´$\underline{H}$CH$_2$CH$_2$S), 3.71-3.47 (m, 14H, 2 OC$\underline{H}$´HCH$_2$CH$_2$S, 2 OC$\underline{H}_2$CH$_2$CH$_2$S, OC$\underline{H}_2$CH$_2$NH$_2$, H-2, H-3, H-4, H-5, H-6a, H-6b), 3.29 (m$_c$, 8H, 4 SCH$_2$C$\underline{H}_2$NHBoc), 2.92 (m$_c$, 2H, OCH$_2$C$\underline{H}_2$NH$_2$), 2.67-2.57 (m, 16H, 4 OCH$_2$CH$_2$C$\underline{H}_2$S, 4 SC$\underline{H}_2$CH$_2$NHBoc), 1.90-1.75 (m, 8H, 4 OCH$_2$C$\underline{H}_2$CH$_2$S), 1.43 (br s, 36H, 4 NHC(O)OC(C$\underline{H}_3$)$_3$), 1.31-1.24 (m, 2H, NH$_2$); ^{13}C NMR (125 MHz, CDCl$_3$): δ 155.6 (C=O), 98.6 (C-1), 79.9 (C-3), 79.5 (NHC(O)O$\underline{C}$(CH$_3$)$_3$), 76.1 (C-2), 75.0 (C-4), 72.0 (C-5), 71.2, 70.2, 70.0 (3 O$\underline{C}$H$_2$CH$_2$CH$_2$S), 69.6 (C-6), 68.4 (O$\underline{C}$H$_2$CH$_2$NH$_2$), 41.2 (OCH$_2$$\underline{C}H_2NH_2$), 39.9 (SCH$_2$$\underline{C}H_2$NHBoc), 32.3 (S$\underline{C}H_2CH_2$NHBoc), 30.4, 30.2, 30.0, 29.8 (4 OCH$_2$$\underline{C}H_2CH_2$S), 28.6 (OCH$_2CH_2$$\underline{C}H_2$S, NHC(O)OC($\underline{C}H_3$)$_3$); IR (ATR) ṽ: 3348, 2974, 2924, 2868, 1690, 1511, 1364, 1245, 1163, 1109, 1042 cm^{-1}; ESI-MS (*m/z*): [M + H]$^+$ calcd for C$_{48}$H$_{93}$N$_5$O$_{14}$S$_4$, 1092.5680, found, 1092.5713.

4.2.4 2-*N*-phthalimidylethyl 2,3,4,6-tetra-*O*-acetyl-α-D-mannopyranoside (**13**)

Mannose pentaacetate (**12**) (273 mg, 700 µmol, 1.0 eq) and *N*-(2-hydroxyethyl)phthalimide (160 mg, 840 µmol, 1.2 eq) were dissolved in dry CH$_2$Cl$_2$ (5.0 mL). Then, BF$_3$·etherate (488 µL, 3.85 mmol, 5.5 eq) was added dropwise at 0 °C and the solution was stirred for 30 min at this temperature. After stirring for 16 h at room temperature, the solution was diluted with CH$_2$Cl$_2$ and the solution was poured onto ice-cold water. The aqueous phase was extracted three times with CH$_2$Cl$_2$ and the combined organic phases were washed with satd. aq. NaHCO$_3$ solution, brine and water. The organic phase was dried over MgSO$_4$, filtered and the filtrate was concentrated under reduced pressure. Purification of the crude mixture by flash chromatography (toluene/EtOAc, 3:1) gave product **13** (174 mg, 334 µmol, 48%) as a colourless sirup: R_f = 0.42 (toluene/EtOAc, 1:1); ^{1}H NMR (600 MHz, CDCl$_3$): δ 7.89-7.85 (m, 2H, Ar-H), 7.74-7.71 (m, 2H, Ar-H), 5.29-5.19 (m, 3H, H-2, H-3, H-4), 4.88 (d, $J_{1,2}$ = 1.4 Hz, 1H, H-1), 4.21 (dd, $J_{5,6a}$ = 5.5 Hz, $J_{6a,6b}$ = 12.2 Hz, 1H, H-6a), 4.04 (dd, $J_{5,6b}$ = 2.3 Hz, $J_{6a,6b}$ = 12.2 Hz, 1H, H-6b), 4.00-3.96 (m, 1H, OCH$_2$C$\underline{H}$´HN), 3.94-3.88 (m, 3H, H-5, OCH$_2$CH´$\underline{H}$N, OC$\underline{H}$´HCH$_2$N), 3.79-3.75 (OC$\underline{H}$´$\underline{H}$CH$_2$N), 2.13, 2.10, 2.00, 1.96 (each s, each 3H, 4 OAc); ^{13}C NMR (125 MHz, CDCl$_3$): δ 170.8, 170.0, 169.8, 169.8, 168.2 (5 C=O), 134.2 (Ar-C), 132.1 (Ar-C$_{quart}$), 123.6 (Ar-C), 97.2 (C-1), 69.5 (C-2), 69.0 (C-5), 69.0 (C-3), 66.2 (C-4), 64.7

(O$\underline{C}$H$_2$CH$_2$N), 62.5 (C-6), 37.1 (OCH$_2$$\underline{C}H_2$N), 21.0, 20.9, 20.8, 20.8 (4 CO$\underline{C}$H$_3$); ESI-MS (*m/z*): [M + Na]$^+$ calcd for C$_{24}$H$_{27}$NO$_{12}$, 544.143, found, 544.143.

4.2.5 2-*N*-phthalimidylethyl-α-D-mannopyranoside (14)

The acetyl-protected mannoside **13** (167 mg, 321 μmol, 1.0 eq) was dissolved in CH$_2$Cl$_2$ (2.0 mL) and the solution was diluted with MeOH (6.0 mL). A freshly prepared 1 M NaOMe solution (1 M, 482 μL, 1.5 eq) was added and the reaction was stirred for 16 h at room temperature. After neutralization with Amberlite$^®$ IR 120 ion exchange resin the solution was filtered and the filtrate was concentrated under reduced pressure to yield mannoside **14** (112 mg, 318 μmol, quant.) as a colourless sirup: R_f = 0.24 (EtOAc/MeOH, 5:1); ^{1}H NMR (500 MHz, CDCl$_3$): δ 7.82-7.78 (m, 2H, Ar-H), 7.71-7.67 (m, 2H, Ar-H), 4.84 (d~s, 1H, H-1), 3.90-3.78 (m, 6H, H-2, H-4, H-6a, OCH$_2$C$\underline{H}$$_2N, OC\underline{H}$´HCH$_2$N), 3.72-3.66 (m, 3H, H-5, H-6b, OCH´$\underline{H}$CH$_2$N), 3.42 (m$_c$, 1H, H-3); ^{13}C NMR (125 MHz, CDCl$_3$): δ 168.4 (C=O), 134.2 (Ar-C), 132.0 (Ar-C$_{quart}$), 123.5 (Ar-C), 99.7 (C-1), 72.7 (C-3), 71.5 (C-5), 70.9 (C-2), 66.3 (C-4), 64.2 (O$\underline{C}$H$_2$CH$_2$N), 61.1 (C-6), 37.4 (OCH$_2$$\underline{C}H_2$N).

4.2.6 2-Benzyloxyethyl 2,3,4,6-tetra-*O*-acetyl-α-D-mannopyranoside (17)

The trichloroacetimidate **16**[27] (13.0 g, 26.4 mmol, 1.0 eq) and 2-benzyloxyethanol (4.51 mL, 31.7 mmol, 1.2 eq) were dissolved in dry CH$_2$Cl$_2$ (180 mL). Then, BF$_3$-etherate (5.27 mL, 42.2 mmol, 1.6 eq) was added dropwise at 0 °C and the solution was stirred for 30 min at this temperature. After stirring for 16 h at room temperature, the solution was diluted with CH$_2$Cl$_2$ and the organic phase was washed with satd. aq. NaHCO$_3$ solution until no further gas formation was observed. The organic phase was dried over MgSO$_4$, filtered and the filtrate was concentrated under reduced pressure. Purification of the crude mixture by column chromatography (toluene/EtOAc, 4:1 to 3:1) gave product **17** (10.3 g, 21.3 mmol, 81%) as a colourless sirup: [α]$_{25}$^{D} +29.0 (*c* 1.0, CH$_2$Cl$_2$); R_f = 0.50 (toluene/EtOAc, 1:1); ^{1}H NMR (500 MHz, CDCl$_3$): δ 7.37-7.27 (m, 5H, Ar-H), 5.38 (dd, $J_{2,3}$ = 3.4 Hz, $J_{3,4}$ = 10.1 Hz, 1H, H-3), 5.30-5.26 (m, 2H, H-2, H-4), 4.88 (d, $J_{1,2}$ = 1.6 Hz, 1H, H-1), 4.58 (d, $J_{OCHPh,OCH´Ph}$ = 12.1 Hz, 1H, OC$\underline{H}$´HPh), 4.55 (d, $J_{OCHPh,OCH´Ph}$ = 12.1 Hz, 1H, OCH´$\underline{H}$Ph), 4.23 (dd, $J_{5,6a}$ = 5.1 Hz, $J_{6a,6b}$ = 12.4 Hz, 1H, H-6a), 4.09-4.04 (m, 2H, H-5, H-6b), 3.86-3.82 (m, 1H, OC$\underline{H}$´HCH$_2$OBn), 3.72-3.65 (m, 3H, OCH´$\underline{H}$CH$_2$OBn, OCH$_2$C$\underline{H}$$_2$OBn), 2.15, 2.08, 2.03, 2.00 (each s, each 3H, 4 OAc); ^{13}C NMR (125 MHz, CDCl$_3$): δ 170.8, 170.2, 170.0, 169.9 (4 C=O), 138.2 (Ar-C$_{quart}$), 128.6, 127.9, 127.8 (3 Ar-C), 97.8 (C-1), 73.4 (O$\underline{C}$H$_2$Ph), 69.7 (C-2), 69.3 (C-3), 69.0 (OCH$_2$$\underline{C}H_2$OBn), 68.5 (C-5), 67.5 (O$\underline{C}$H$_2$CH$_2$OBn), 66.3 (C-4), 62.5 (C-6), 21.0,

20.9, 20.8 (4 CO$\underline{C}$H$_3$); IR (ATR) ṽ: 3373, 3250, 2930, 2866, 1745, 1738, 1694, 1369, 1244, 1214, 1044, 976, 745 cm^{-1}; ESI-MS (*m/z*): [M + Na]$^+$ calcd for C$_{23}$H$_{30}$O$_{11}$, 505.168, found, 505.171.

4.2.7 2-Benzyloxyethyl-α-D-mannopyranoside (18)

The acetyl-protected mannoside **17** (10.2 g, 21.1 mmol, 1.0 eq) was dissolved in CH$_2$Cl$_2$ (40 mL) and the solution was diluted with MeOH (120 mL). A freshly prepared NaOMe solution (1 M, 31.7 mL, 1.5 eq) was added and the reaction was stirred for 16 h at room temperature. After neutralization with Amberlite® IR 120 ion exchange resin the solution was filtered and the filtrate was concentrated under reduced pressure to yield mannoside **18** (6.51 g, 20.7 mmol, 98%) as a colourless syrup: [α]$_{25}^D$ +35.1 (*c* 0.77, MeOH); R_f = 0.33 (EtOAc/MeOH, 5:1); ^{1}H NMR (500 MHz, MeOH-*d$_4$*): δ 7.36-7.25 (m, 5H, Ar-H), 4.80 (d, $J_{1,2}$ = 1.7 Hz, 1H, H-1), 4.56 (m$_c$, 2H, OC$\underline{H}_2$Ph), 3.88-3.85 (m, 1H, OC$\underline{H}$ˊHCH$_2$OBn), 3.83-3.80 (m, 2H, H-2, H-6a), 3.73-3.68 (m, 2H, H-3, H-6b), 3.68-3.56 (m, 5H, H-4, H-5, OCHˊ$\underline{H}$CH$_2$OBn, OCH$_2$C$\underline{H}_2$OBn); ^{13}C NMR (125 MHz, CDCl$_3$): δ 139.6 (Ar-C$_{quart}$), 129.4, 128.9, 128.7 (3 Ar-C), 101.8 (C-1), 74.6 (C-5), 74.1 (O$\underline{C}$H$_2$Ph), 72.6 (C-3), 72.1 (C-2), 70.4 (OCH$_2$$\underline{C}H_2$OBn), 68.6 (C-4), 67.8 (O$\underline{C}$H$_2$CH$_2$OBn), 62.9 (C-6); IR (ATR) ṽ: 3350, 2923, 1702, 1453, 1360, 1245, 1133, 1093, 1053, 1025, 975, 727 cm^{-1}; ESI-MS (*m/z*): [M + Na]$^+$ calcd for C$_{15}$H$_{22}$O$_7$, 337.126, found, 337.124.

4.2.8 2-Benzyloxyethyl 2,3,4,6-tetra-*O*-(2-cyanoethyl)-α-D-mannopyranoside (19)

The synthesis was performed by using mannoside **18** (3.30 g, 10.5 mmol, 1.0 eq), acrylonitrile (55.7 mL, 840 mmol, 80 eq), caesium carbonate (13.7 g, 42.0 mmol, 4.0 eq), DMF (10 mL) and *tert*-butanol (50 mL) by following the procedure described for the preparation of **9**, giving rise to the cyanoethylated mannoside **19** (4.08 g, 7.75 mmol, 74%) after column chromatography (cyclohexane/EtOAc, 1:1 to 1:5) as a slightly yellow syrup: [α]$_{25}^D$ +19.5 (*c* 1.1, CH$_2$Cl$_2$); R_f = 0.33 (cyclohexane/EtOAc, 1:2); ^{1}H NMR (500 MHz, CDCl$_3$): δ 7.38-7.28 (m, 5H, Ar-H), 4.91 (d, $J_{1,2}$ = 1.8 Hz, 1H, H-1), 4.56 (d, $J_{OCHPh,OCHˊPh}$ = 12.1 Hz, 1H, OC$\underline{H}$HPh), 4.54 (d, $J_{OCHPh,OCHˊPh}$ = 12.1 Hz, 1H, OCHˊ$\underline{H}$Ph), 4.06 (ddd, $J_{OCH,CHCN}$ = 4.3 Hz, $J_{OCH,CHˊCN}$ = 6.6 Hz, $J_{OCH,OCHˊ}$ = 9.7 Hz, 1H, OC$\underline{H}$ˊHCH$_2$CN), 3.97-3.83 (m, 7H, OCHˊ$\underline{H}$CH$_2$CN, 2 OC$\underline{H}_2$CH$_2$CN, H-4, H-6a), 3.81-3.77 (m, 3H, OC$\underline{H}_2$CH$_2$OBn, H-2), 3.74-3.62 (m, 6H, OC$\underline{H}_2$CH$_2$CN, OCH$_2$C$\underline{H}_2$OBn, H-3, H-5), 3.58 (dd, $J_{5,6b}$ = 1.6 Hz, $J_{6a,6b}$ = 11.6 Hz, 1H, H-6b), 2.75-2.55 (m, 8H, 4 OCH$_2$C$\underline{H}_2$CN); ^{13}C NMR (125 MHz, CDCl$_3$): δ 138.1 (Ar-C$_{quart}$), 128.6, 128.0, 127.9 (3 Ar-C), 118.9, 118.5, 118.3, 118.2 (4 CN), 98.2 (C-1), 80.5 (C-3), 77.0 (C-2), 74.3 (C-4), 73.4

(O$\underline{C}$H$_2$Ph), 71.8 (C-5), 69.7 (C-6), 69.2 (OCH$_2\underline{C}$H$_2$OBn), 67.5 (O$\underline{C}$H$_2$CH$_2$CN), 67.0 (O$\underline{C}$H$_2$CH$_2$OBn), 66.6, 66.5, 65.5 (4 O$\underline{C}$H$_2$CH$_2$CN), 19.6, 19.6, 19.5, 19.2 (4 OCH$_2\underline{C}$H$_2$CN); IR (ATR) $\tilde{\upsilon}$: 2883, 2251, 1454, 1412, 1365, 1328, 1289, 1221, 1105, 1062, 739, 700 cm^{-1}; EI-HR-MS (m/z): [M]$^+$ calcd for C$_{27}$H$_{34}$N$_4$O$_7$, 526.2428, found, 526.2422.

4.2.9   2-Benzyloxyethyl 2,3,4,6-tetra-O-[3-N-(tert-butyloxycarbonyl)aminopropyl]-α-D-mannopyranoside (**20**)

A solution of nitrile **19** (198 mg, 376 µmol, 1.0 eq) in MeOH (10 mL) was transferred to an autoclave vessel and aq. ammonia (25%, 10 mL), palladium on charcoal (10%, 50 mg) and Raney®-nickel (1 tip of a spatula, slurry in water) were added. After flushing several times with hydrogen, the suspension was stirred for 5 d at 45 °C and a hydrogen pressure of 100 bar. The reaction mixture was allowed to attain room temperature and was filtered over Celite®, which afterwards was thoroughly washed with a 1:1 mixture of MeOH and aq. ammonia (25%). The filtrate was concentrated under reduced pressure and the residue was suspended in MeOH (20 mL). Subsequently, TEA (208 µL, 1.50 mmol, 4.0 eq) was added and the suspension was stirred for 30 min at room temperature, when di-tert-butyl dicarbonate (657 mg, 3.01 mmol, 8.0 eq) was added. After stirring for 16 h at room temperature, quenching of the reaction was induced by addition of satd. aq. NH$_4$Cl solution and the aqueous phase was extracted three times with CH$_2$Cl$_2$. The combined organic phases were subsequently washed with water and brine, dried over MgSO$_4$, filtered and the filtrate was concentrated under reduced pressure. Purification of the crude mixture by column chromatography (cyclohexane/EtOAc, 1:1) gave product **20** (196 mg, 208 µmol, 55%) as a colourless syrup: [α]$_{25}$^{D} +15.1 (c 1.0, CH$_2$Cl$_2$); R_f = 0.29 (cyclohexane/EtOAc, 1:1); ^{1}H NMR (500 MHz, CDCl$_3$): δ 7.36-7.27 (m, 5H, Ar-H), 4.88 (d, $J_{1,2}$ = 1.4 Hz, 1H, H-1), 4.57 (d, $J_{OCHPh,OCH'Ph}$ = 12.1 Hz, 1H, OC$\underline{H}$'HPh), 4.53 (d, $J_{OCHPh,OCH'Ph}$ = 12.2 Hz, 1H, OCH'$\underline{H}$Ph), 3.84-3.76 (m, 2H, OC$\underline{H}$'HCH$_2$CH$_2$NHBoc, OC$\underline{H}$'HCH$_2$OBn), 3.71-3.48 (m, 16H, OCH'$\underline{H}$CH$_2$CH$_2$NHBoc, OCH'$\underline{H}$CH$_2$OBn, OCH$_2$C$\underline{H}$$_2$OBn, H-2, H-3, H-4, H-5, H-6a, H-6b, 3 OC$\underline{H}$$_2CH_2CH_2$NHBoc), 3.30-3.14 (m, 8H, 4 OCH$_2$CH$_2$C$\underline{H}$$_2$NHBoc), 1.85-1.68 (m, 8H, 4 OCH$_2$C$\underline{H}$$_2CH_2$NHBoc), 1.43 (s, 18H, 2 NHC(O)OC(C$\underline{H}$$_3$)$_3$), 1.43 (s, 9H, NHC(O)OC(C$\underline{H}$$_3$)$_3$), 1.42 (s, 9H, NHC(O)OC(C$\underline{H}$$_3$)$_3$); ^{13}C NMR (125 MHz, CDCl$_3$): δ 156.3, 156.2, 156.2, 156.2 (4 NH$\underline{C}$(O)OC(CH$_3$)$_3$), 138.2 (Ar-C$_{quart}$) 128.6, 127.9 (3 Ar-C), 97.6 (C-1), 79.9 (C-3), 76.2 (C-2), 75.2 (C-4), 73.4 (O$\underline{C}$H$_2$Ph), 71.9 (C-5), 71.1 (O$\underline{C}$H$_2$CH$_2$CH$_2$NHBoc), 70.0, 69.8 (2 O$\underline{C}$H$_2$CH$_2$CH$_2$NHBoc), 69.6 (C-6), 69.2 (OCH$_2\underline{C}$H$_2$OBn), 68.1 (O$\underline{C}$H$_2$CH$_2$CH$_2$NHBoc), 66.8 (O$\underline{C}$H$_2$CH$_2$OBn), 38.7, 38.4 (4 OCH$_2$CH$_2\underline{C}$H$_2$NHBoc), 30.4, 30.3, 29.9, 29.7 (4 OCH$_2\underline{C}$H$_2$CH$_2$NHBoc), 28.7, 28.6, 28.6

(4 NHC(O)OC(C$\underline{\text{H}}_3$)$_3$); IR (ATR) ṽ: 3357, 2975, 2929, 2870, 1690, 1513, 1365, 1248, 1167, 1103, 1063 cm^{-1}; ESI-MS (*m/z*): [M + Na]$^+$ calcd for C$_{47}$H$_{82}$N$_4$O$_{15}$, 943.585, found, 943.612.

4.2.10 2-Hydroxyethyl 2,3,4,6-tetra-*O*-[3-*N*-(*tert*-butyloxycarbonyl)aminopropyl]-α-D-mannopyranoside (**21**)

The benzyl ether **20** (1.57 g, 1.66 mmol, 1.0 eq) was dissolved in MeOH (25 mL) and palladium on charcoal (10%, 200 mg) was added. Under vigorous stirring, triethylsilane (795 µL, 4.98 mmol, 3.0 eq) was added in portions and stirring was continued for 16 h at room temperature. Subsequently, the catalyst was removed by filtration over Celite® and the filtrate was concentrated under reduced pressure. The residue was dissolved in EtOAc and then filtered through a pad of silica. Removal of the solvent yielded pure debenzylated compound **21** (1.39 g, (1.63 mmol, 98%) as a colourless syrup: [α]$_{25}^D$ +7.2 (*c* 1.1, CH$_2$Cl$_2$); R_f = 0.16 (cyclohexane/EtOAc, 1:4); ^{1}H NMR (600 MHz, CDCl$_3$): δ 5.37, 5.09, 4.96 (each br s, each 1H, 3 N$\underline{\text{H}}$Boc), 4.88 (d~s, 1H, H-1), 3.81 (m$_c$, 1H, OC$\underline{\text{H}}$´HCH$_2$CH$_2$NHBoc), 3.75-3.51 (m, 16H, OCH´$\underline{\text{H}}$CH$_2$CH$_2$NHBoc, 3 OC$\underline{\text{H}}_2$CH$_2$CH$_2$NHBoc, OC$\underline{\text{H}}_2$CH$_2$OH, OCH$_2$C$\underline{\text{H}}_2$OH, H-2, H-3, H-5, H-6a, H-6b), 3.45 (mc, 1H, H-4), 3.25-3.20 (m, 8H, 4 OCH$_2$CH$_2$C$\underline{\text{H}}_2$NHBoc), 1.84-1.71 (m, 8H, 4 OCH$_2$C$\underline{\text{H}}_2$CH$_2$NHBoc), 1.43 (br s, 36H, 4 NHC(O)OC(C$\underline{\text{H}}_3$)$_3$); ^{13}C NMR (125 MHz, CDCl$_3$): δ 156.3, 156.2, 156.2 (4 NH$\underline{\text{C}}$(O)OC(CH$_3$)$_3$), 98.3 (C-1), 79.9 (C-3), 76.4 (C-2), 75.5 (C-4), 72.0 (C-5), 71.1 (O$\underline{\text{C}}$H$_2$CH$_2$OH, O$\underline{\text{C}}$H$_2$CH$_2$CH$_2$NHBoc), 70.3 (O$\underline{\text{C}}$H$_2$CH$_2$CH$_2$NHBoc), 69.9 (C-6), 69.7 (2 O$\underline{\text{C}}$H$_2$CH$_2$CH$_2$NHBoc), 68.2 (O$\underline{\text{C}}$H$_2$CH$_2$CH$_2$NHBoc), 62.1 (OCH$_2$$\underline{\text{C}}H_2$OH), 38.6, 38.3 (4 OCH$_2CH_2$$\underline{\text{C}}H_2$NHBoc), 30.5, 30.4, 29.8 (4 OCH$_2$$\underline{\text{C}}H_2CH_2$NHBoc), 28.7, 28.6, 27.0 (4 NHC(O)OC($\underline{\text{C}}$H$_3$)$_3$); IR (ATR) ṽ: 3351, 2976, 2930, 2872, 1687, 1514, 1365, 1249, 1167, 1106, 1049, 985 cm^{-1}; ESI-MS (*m/z*): [M + Na]$^+$ calcd for C$_{40}$H$_{76}$N$_4$O$_{15}$, 875.5, found, 875.7.

4.2.11 2-Azidoethyl 2,3,4,6-tetra-*O*-[3-*N*-(*tert*-butyloxycarbonyl)aminopropyl]-α-D-mannopyranoside (**22**)

Mannoside **21** (314 mg, 368 µmol, 1.0 eq) and triphenylphosphine (145 mg, 552 µmol, 1.5 eq) were dissolved in dry THF (10 mL). Then, DIAD (181 µL, 920 µmol, 2.5 eq) was added at -15 °C and the reaction mixture was stirred for 30 min at this temperature. The solution was warmed to 0 °C and DPPA (119 µL, 552 µmol, 1.5 eq) was added. After stirring for 30 min at this temperature the reaction mixture was allowed to attain room temperature and was stirred for further 16 h. Afterwards, the solution was concentrated under reduced pressure and the crude mixture was purified by column chromatography (cyclohexane/EtOAc, 1:1 to 1:2).

Azide **22** (314 mg, 358 µmol, 97%) was obtained as a colourless syrup: $[\alpha]_{25}{}^{D}$ +14.0 (c 1.0, CH$_2$Cl$_2$); R_f = 0.20 (cyclohexane/EtOAc, 1:1); ^{1}H NMR (600 MHz, CDCl$_3$): δ 5.40, 5.09, 5.02, 4.93 (each br s, each 1H, 4 NHBoc), 4.89 (d~s, 1H, H-1), 3.88-3.81 (m, 2H, OCH´HCH$_2$N$_3$, OCH´HCH$_2$CH$_2$NHBoc), 3.73-3.50 (m, 14H, OCH´HCH$_2$CH$_2$NHBoc, OCH´HCH$_2$N$_3$, H-2, H-3, H-4, H-5, H-6a, H-6b, 3 OCH$_2$CH$_2$CH$_2$NHBoc), 3.43-3.35 (m, 2H, OCH$_2$CH$_2$N$_3$), 3.25-3.20 (m, 8H, 4 OCH$_2$CH$_2$CH$_2$NHBoc), 1.80-1.73 (m, 8H, 4 OCH$_2$CH$_2$CH$_2$NHBoc), 1.43 (s, 36H, 4 NHC(O)OC(CH$_3$)$_3$); ^{13}C NMR (125 MHz, CDCl$_3$): δ 156.3, 156.2, 156.2 (3 NHC(O)OC(CH$_3$)$_3$), 97.9 (C-1), 79.8 (C-3), 76.1 (C-2), 75.1 (C-4), 72.2 (C-5), 71.2 (OCH$_2$CH$_2$CH$_2$NHBoc), 69.9 (C-6, 2 OCH$_2$CH$_2$CH$_2$NHBoc), 68.1 (OCH$_2$CH$_2$CH$_2$NHBoc), 66.7 (OCH$_2$CH$_2$N$_3$), 50.6 (OCH$_2$CH$_2$N$_3$), 38.5, 38.4, 38.3 (4 OCH$_2$CH$_2$CH$_2$NHBoc), 30.4, 30.3, 29.8 (4 OCH$_2$CH$_2$CH$_2$NHBoc), 28.6, 28.6 (4 NHC(O)OC(CH$_3$)$_3$); IR (ATR) ṽ: 3357, 2975, 2926, 2871, 2104, 1689, 1513, 1365, 1270, 1249, 1167, 1105, 1069, 992 cm^{-1}; ESI-MS (m/z): [M + H]$^+$ calcd for C$_{40}$H$_{75}$N$_7$O$_{14}$, 878.5450, found, 878.5445.

4.2.12 2-Isothiocyanatoethyl 2,3,4,6-tetra-O-[3-N-($tert$-butyloxycarbonyl)aminopropyl]-α-D-mannopyranoside (**23**)

The azide **22** (105 mg, 120 µmol, 1.0 eq) and carbon disulfide (290 µL, 4.80 mmol, 40 eq) were dissolved in CHCl$_3$ (10 mL). Triphenylphosphine (126 mg, 480 µmol, 4.0 eq) was then added to the solution and the reaction mixture was stirred for 16 h at room temperature. The solution was concentrated under reduced pressure and the crude mixture was purified by column chromatography (cyclohexane/EtOAc, 1:1 to 1:2). The isothiocyanate **23** (98.4 mg, 110 µmol, 92%) was obtained as a colourless syrup: $[\alpha]_{25}{}^{D}$ +11.5 (c 1.0, CH$_2$Cl$_2$); R_f = 0.25 (cyclohexane/EtOAc, 1:1); ^{1}H NMR (500 MHz, CDCl$_3$): δ 5.38, 5.07, 5.00 (each br s, each 1H, 3 NHBoc), 4.90 (d~s, 1H, H-1), 3.87-3.80 (m, 2H, OCH´HCH$_2$NCS, OCH´HCH$_2$CH$_2$NHBoc), 3.76-3.50 (m, 16H, OCH´HCH$_2$CH$_2$NHBoc, OCH´HCH$_2$NCS, H-2, H-3, H-4, H-5, H-6a, H-6b, 3 OCH$_2$CH$_2$CH$_2$NHBoc, OCH$_2$CH$_2$NCS), 3.25-3.20 (m, 8H, 4 OCH$_2$CH$_2$CH$_2$NHBoc), 1.83-1.69 (m, 8H, 4 OCH$_2$CH$_2$CH$_2$NHBoc), 1.43 (s, 36H, 4 NHC(O)OC(CH$_3$)$_3$); ^{13}C NMR (125 MHz, CDCl$_3$): δ 156.3, 156.2, 156.2 (3 NHC(O)OC(CH$_3$)$_3$), 98.2 (C-1), 79.7 (C-3), 76.1 (C-2), 75.1 (C-4), 72.4 (C-5), 71.1, 70.0 (3 OCH$_2$CH$_2$CH$_2$NHBoc), 69.9 (C-6), 68.2 (OCH$_2$CH$_2$CH$_2$NHBoc), 66.0 (OCH$_2$CH$_2$NCS), 45.5 (OCH$_2$CH$_2$NCS), 38.6, 38.5, 38.4, 38.3 (4 OCH$_2$CH$_2$CH$_2$NHBoc), 30.4, 30.3, 29.8, 29.8 (4 OCH$_2$CH$_2$CH$_2$NHBoc), 28.7, 28.6, 28.6, 28.6 (4 NHC(O)OC(CH$_3$)$_3$); IR (ATR) ṽ: 3356, 2975, 2930, 2871, 2088, 1689, 1513, 1365,

1248, 1166, 1106, 1062, 984 cm^{-1}; ESI-MS (*m/z*): [M + Na]$^+$ calcd for C$_{41}$H$_{75}$N$_5$O$_{14}$S, 916.4929, found, 916.4924.

4.2.13 2-{(*E*)-*p*-[*p*´-(Propargyloxy)phenylazo]phenyloxy}ethyl 2,3,4,6-tetra-*O*-[3-*N*-(*tert*-butyloxycarbonyl)aminopropyl]-α-D-mannopyranoside (25)

A solution of DIAD in dry THF (5.0 mL) was added dropwise to a solution of mannoside **21** (106 mg, 124 μmol, 1.0 eq), azobenzene **24** (46.9 mg, 186 μmol, 1.5 eq) and triphenylphosphine (42.2 mg, 161 μmol, 1.3 eq) in dry THF (5.0 mL) at 0 °C. The reaction mixture was then stirred for 24 h at room temperature. Afterwards, the solution was concentrated under reduced pressure and the crude mixture was purified by column chromatography (cyclohexane/EtOAc, 1:1 to 2:3). Scaffold compound **25** (92.5 mg, 85.1 μmol, 69%) was obtained as an orange syrup: [α]$_{25}^{D}$ +12.4 (*c* 0.29, CH$_2$Cl$_2$); R_f = 0.25 (cyclohexane/EtOAc, 1:1); ^{1}H NMR (600 MHz, CDCl$_3$): δ 7.88 (m$_c$, 4H, H-8, H-12, H-15, H-17), 7.08 (m$_c$, 2H, H-14, H-18), 7.01 (m$_c$, 2H, H-9, H-11), 5.41, 5.10, 5.00, (each br s, each 1H, 3 NHBoc), 4.95 (d~s, 1H, H-1), 4.77 (d, $J_{OCH,C≡CH}$ = 2.5 Hz, 2H, OCH$_2$C≡CH), 4.24-4.19 (m, 2H, OCH$_2$CH$_2$Ar), 4.03-3.99 (m, 1H, OCH´HCH$_2$Ar), 3.89-3.81 (m, 2H, OCH´HCH$_2$Ar, OCH´HCH$_2$CH$_2$NHBoc), 3.74-3.51 (m, 13H, H-2, H-3, H-4, H-5, H-6a, H-6b, OCH´HCH$_2$CH$_2$NHBoc, 3 OCH$_2$CH$_2$CH$_2$NHBoc), 3.29-3.15 (m, 8H, 4 OCH$_2$CH$_2$CH$_2$NHBoc), 2.56 (dd~t, $J_{OCH,C≡CH}$ = 2.3 Hz, 1H, OCH$_2$C≡CH), 1.82-1.68 (m, 8H, 4 OCH$_2$CH$_2$CH$_2$NHBoc), 1.43 (m, 36H, 4 NHC(O)OC(CH$_3$)$_3$)); ^{13}C NMR (125 MHz, CDCl$_3$): δ 160.9 (C-7), 159.6 (C-16), 156.3, 156.2, 156.2 (3 NHC(O)OC(CH$_3$)$_3$), 147.7 (C-13), 147.4 (C-10), 124.6 (C-14, C-18), 124.4 (C-9, C-11), 115.3 (C-15, C-17), 115.0 (C-8, C-12), 98.0 (C-1), 79.9 (C-3), 76.1 (C-2), 75.2 (C-4), 72.1 (C-5), 71.1 (OCH$_2$CH$_2$CH$_2$NHBoc), 70.0 (OCH$_2$CH$_2$CH$_2$NHBoc), 69.9 (C-6), 69.8 (OCH$_2$CH$_2$CH$_2$NHBoc), 68.2 (OCH$_2$CH$_2$CH$_2$NHBoc), 67.4 (OCH$_2$CH$_2$Ar), 66.1 (OCH$_2$CH$_2$Ar), 56.2 (OCH$_2$C≡CH), 38.7, 38.6, 38.4, 38.3 (4 OCH$_2$CH$_2$CH$_2$NHBoc), 30.4, 30.4, 29.9 (3 OCH$_2$CH$_2$CH$_2$NHBoc), 28.7, 28.6 (2 NHC(O)OC(CH$_3$)$_3$)); IR (ATR) ṽ: 3352, 2974, 2929, 2871, 1691, 1499, 1365, 1247, 1167, 1148, 1106, 1023, 841, 649, 601 cm^{-1}; ESI-MS (*m/z*): [M + H]$^+$ calcd for C$_{55}$H$_{86}$N$_6$O$_{16}$, 1087.6179, found, 1087.6168.

4.2.14 2-Azidoethyl 2,3,4,6-tetra-*O*-{3-*N*´-(2,3,4,6-tetra-*O*-acetyl-α-D-mannopyranosyl)-thioureidopropyl}-α-D-mannopyranoside (27)

Trifluoroacetic acid (3.0 mL) was added dropwise to a solution of the scaffold mannoside **22** (532 mg, 606 μmol, 1.0 eq) in CH$_2$Cl$_2$ (18 mL) and the mixture was stirred for 1 h at room

temperature. Evaporation of the solvent yielded a colourless syrup which was taken up in a small amount of MeOH and codistilled with toluene in order to remove residual trifluoroacetic acid. After codistillation, the residue was taken up in CH_2Cl_2 (10 mL) and diisopropylethylamine (825 μL, 4.85 mmol, 8.0 eq) was added, the reaction mixture was stirred for 1 h at room temperature. Then, a solution of the tetra-O-acetylated mannopyranosyl isothiocyanate **26**[30] (1.42 g, 3.64 mmol, 6.0 eq) in CH_2Cl_2 (30 mL) was slowly added at 0 °C and the solution was refluxed for 6 h. The solution was concentrated under reduced pressure and the crude mixture was purified by column chromatography (CH_2Cl_2/MeOH, 25:1). An inseparable mixture of glycocluster **27** and side products (986 mg) was obtained as a colourless syrup.

4.2.15 2-Azidoethyl 2,3,4,6-tetra-O-{3-N'-(α-D-mannopyranosyl)thioureidopropyl}-α-D-mannopyranoside (**28**)

The crude protected glycocluster **27** (986 mg) was dissolved in MeOH (40 mL) and a freshly prepared NaOMe solution (1 M, 3.88 mL, 8.0 eq) was added at 0 °C. After stirring for 60 min at this temperature, water (6.7 mL) was added to dissolve the precipitated solid and stirring was continued for 15 min. Then, the reaction mixture was neutralized with Amberlite® IR 120 ion exchange resin, filtered and the resin was washed extensively with water. The filtrate was then concentrated under reduced pressure and the crude was purified by reversed phase column chromatography (C-18, water/acetonitrile), yielding glycocluster **29** (519 mg, 381 μmol, 63% over three steps) as a colourless amorphous solid: $[\alpha]_{25}^{D}$ +23.8 (c 0.8, DMSO); R_f = 0.52 (^{i}PrOH/H$_2$O/EtOAc/NH$_3$ (aq.), 5:3:1:1); ^{1}H NMR (500 MHz, DMSO-d_6): δ 8.08-7.94 (m, 4H, 4 NH), 7.70-7.55 (m, 4H, 4 NH), 5.52 (br s, 3H, 3 H-1´), 5.01 (br s, 3H, 3 OH), 4.90 (d~s, 1H, H-1), 4.87 (m$_c$, 1H, OH), 4.81 (br s, 4H, 4 OH), 4.68 (br s, 4H, 4 OH), 4.47-4.37 (m, 4H, 4 OH), 3.78-3.72 (m, 2H, OC$\underline{H}$´HCH$_2$N$_3$, OC$\underline{H}$´HCH$_2$CH$_2$NH), 3.65-3.41 (m, 37H, H-2, H-3, H-4, 4 H-4´, H-5, H-6a, H-6b, 4 H-6a, 4 H-6b, OCH´$\underline{H}$CH$_2$N$_3$, OCH$_2$C$\underline{H}_2$N$_3$, 4 OC$\underline{H}_2$CH$_2$CH$_2$NH, 4 OCH$_2$CH$_2$C$\underline{H}_2$NH), 3.35-3.28 (m, overlap with HDO, 4 H-2´, 4 H-5´), 3.04 (br s, 3H, 3 H-3´), 1.77-1.66 (m, 8H, 4 OCH$_2$C$\underline{H}_2$CH$_2$NH); ^{13}C NMR (125 MHz, DMSO-d_6): δ 182.8, 182.5, 182.4, 182.3 (4 C=S), 97.2 (C-1), 81.6, 81.5 (2 C-1´), 79.4 (C-3), 78.5 (C-3´), 75.2 (C-2), 74.6 (C-4), 74.2 (C-2´), 71.3 (C-5), 70.9, 70.7 (2 C-4´), 69.9 (O$\underline{C}$H$_2$CH$_2$CH$_2$NH), 69.8 (C-6), 68.2 (O$\underline{C}$H$_2$CH$_2$CH$_2$NH), 66.8, 66.6 (2 C-5´), 65.9 (O$\underline{C}$H$_2$CH$_2$N$_3$), 61.2, 61.0 (2 C-6´), 49.9 (OCH$_2$$\underline{C}H_2N_3$), 41.3, 41.2 (2 OCH$_2CH_2$$\underline{C}H_2$NH), 29.6, 29.3, 29.2, 28.9 (4 OCH$_2$$\underline{C}H_2CH_2$NH); IR (ATR) ṽ: 3295, 2923, 2103, 1544, 1346, 1276, 1203, 1068, 936, 888 cm^{-1}; ESI-MS (m/z): $[M + H]^+$ calcd for $C_{48}H_{87}N_{11}O_{26}S_4$, 1362.4785, found, 1362.4780.

Acknowledgements

References

1. Roy, R.; Shiao, T. C. *Chem. Soc. Rev.* **2015**, *44*, 3924-3941.

2. (a) Wang, L.-X.; Ni, J.; Singh, S. *Bioorg. Med. Chem.* **2003**, *11*, 159-166; (b) Simerska, P.; Moyle, P. M.; Toth, I. *Med. Res. Rev.* **2011**, *31*, 520-547.

3. (a) Meutermans, W.; Le, G. T.; Becker, B. *ChemMedChem* **2006**, *1*, 1164-1194; (b) Zuegg, J.; Muldoon, C.; Adamson, G.; McKeveney, D.; Le Thanh, G.; Premraj, R.; Becker, B.; Cheng, M.; Elliott, A. G.; Huang, J. X.; Butler, M. S.; Bajaj, M.; Seifert, J.; Singh, L.; Galley, N. F.; Roper, D. I.; Lloyd, A. J.; Dowson, C. G.; Cheng, T. J.; Cheng, W. C.; Demon, D.; Meyer, E.; Meutermans, W.; Cooper, M. A. *Nat. Commun.* **2015**, *6*, 7719, doi:10.1038/ncomms8719.

4. (a) Papin, C.; Doisneau, G.; Beau, J.-M. *Chem. Eur. J.* **2009**, *15*, 53-57; (b) Gerland, B.; Goudot, A.; Pourceau, G.; Meyer, A.; Dugas, V.; Cecioni, S.; Vidal, S.; Souteyrand, E.; Vasseur, J.-J.; Chevolot, Y.; Morvan, F. *Bioconj. Chem.* **2012**, *23*, 1534-1547; (c) Lindhorst, T. K.; Dubber, M. *Carbohydr. Res.* **2015**, *403*, 90-97.

5. (a) Opatz, T.; Kallus, C.; Wunberg, T.; Schmidt, W.; Henke, S.; Kunz, H. *Eur. J. Org. Chem.* **2003**, 1527-1536; (b) Hünger, U.; Ohnsmann, J.; Kunz H. Angew. Chem. **2004**, 1125-1128; *Angew. Chem. Int. Ed.* **2004**, *43*, 1104-1104

6. (a) Dubber, M.; Lindhorst, T. K. *J. Org. Chem.* **2000**, *65*, 5275-5281; (b) Ni, J.; Song, H.; Wang, Y.; Stamatos, N. M.; Wang, L.-X. *Bioconj. Chem.* **2006**, *17*, 493-500; (c) Sperling, O.; Dubber, M.; Lindhorst, T. K. *Carbohydr. Res.* **2007**, *342*, 696-703; (d) Zhong, W.; Skwarczynski, M.; Simerska, P.; Good, M. F.; Toth, I. *Tetrahedron* **2009**, *65*, 3459-3464; (e) Fagan, V.; Toth, I.; Simerska, P. *Beilstein J. Org. Chem.* **2014**, *10*, 1741-1748.

7. Horlacher, T.; Seeberger, P. H. *Chem. Soc. Rev.* **2008**, *37*, 1414-1422.

8. (a) Kolb, H. C.; Finn, M. G.; Sharpless, K. B. *Angew. Chem.* **2001**, *113*, 2056-2075; *Angew. Chem. Int. Ed.* **2001**, *40*, 2004-2021; (b) Meldal, M.; Tornøe, C. W. *Chem. Rev.* **2008**, *108*, 2952-3015.

9. (a) Saxon, E.; Bertozzi, C. R. *Science* **2000**, *287*, 2007-2010; (b) Köhn, M.; Breinbauer, R. *Angew. Chem.* **2004**, *116*, 3168-3178; *Angew. Chem. Int. Ed.* **2004**, *43*, 3106-3116.

10. (a) Lindhorst, T. K.; Kieburg, C. *Angew. Chem.* **1996**, *118*, 2083-2086; *Angew. Chem. Int. Ed.* **1996**, *35*, 1953-1956; (b) Ortiz Mellet, C.; Defaye, J.; Garcia Fernandez, J. M. *Chem. Eur. J.* **2002**, *8*, 1982-90; (c) Köhn, M.; Benito, J. M.; Ortiz Mellet, C.; Lindhorst, T. K.; García Fernández, J. M., *ChemBioChem* **2004**, *5*, 771-777; (d) Grabosch, C.; Kleinert, M.; Lindhorst, T. K. *Synthesis* **2010**, 828-836; (e) Grabosch, C.; Kind, M.; Gies, Y.; Schweighöfer, F.; Terfort, A.; Lindhorst, T. K., *Org. Biomol. Chem.* **2013**, *11*, 4006-4015.

11. (a) Wrodnigg, T. M.; Kartusch, C.; Illaszewicz, C. *Carbohydr. Res.* **2008**, *343*, 2057-2066; (b) Gallas, K.; Pototschnig, G.; Adanitsch, F.; Stütz, A. E.; Wrodnigg, T. M., *Beilstein J. Org. Chem.* **2012**, *8*, 1619-1629.

12. Chernyak, A. Y.; Sharma, G. V. M.; Kononov, L. O.; Krishna, P. R.; Levinsky, A. B.; Kochetkov, N. K.; Rama Rao, A. V. *Carbohydr. Res.* **1992**, *223*, 303-309.

13. Dubber, M.; Lindhorst, T. K. *Carbohydr. Res.* **1998**, *310*, 35-41.

14. McGeary, R. P.; Jablonkai, I.; Toth, I. *Tetrahedron* **2001**, *57*, 8733-8742.

15. Newkome, G. R.; Lin, X.; Young, J. K. *Synlett* **1992**, 53-54.

16. Schmidle, C. J.; Mansfield, R. C. *Ind. Eng. Chem.* **1952**, *44*, 1388-1390.

17. Saneyoshi, H.; Seio, K.; Sekine, M., *J. Org. Chem.* **2005**, *70*, 10453-10460.

18. Dubber, M.; Lindhorst, T. K. *Org. Lett.* **2001**, *3*, 4019-4022.

19. (a) Heidecke, C. D.; Lindhorst, T. K. *Chem. Eur. J.* **2007**, *13*, 9056-9067; (b) Dubber, M.; Sperling, O.; Lindhorst, T. K. *Org. Biomol. Chem.* **2006**, *4*, 3901-3912.

20. Salmon, A.; Carboni, B. *J. Organomet. Chem.* **1998**, *567*, 31-37.

21. Dondoni, A.; Marra, A. *Chem. Soc. Rev.* **2012**, *41*, 573-586.

22. Šardzík, R.; Noble, G. T.; Weissenborn, M. J.; Martin, A.; Webb, S. J.; Flitsch, S. L. *Beilstein J. Org. Chem.* **2010**, *6*, 699-703.

23. Yang, L.-Y.; Kawada, Y.; Bai, L.; Kubota, D.; Yuasa, H. *Org. Biomol. Chem.* **2011**, *9*, 6579-6586.

24. Jung, K.-H.; Hoch, M.; Schmidt, R. R. *Liebigs Ann. Chem.* **1989**, 1099-1106.

25. Zemplén, G.; Pacsu, E. *Ber. Dtsch. Chem. Ges. B* **1929**, *62*, 1613-1614.

26. Mandal, P. K.; McMurray, J. S. *J. Org. Chem.* **2007**, *72*, 6599-6601.

27. (a) Mitsunobu, O. *Synthesis* **1981**, 1-28; (b) Fletcher, S. *Org. Chem. Front.* **2015**, *2*, 739-752.

28. Patra, P. K.; Nishide, K.; Fuji, K.; Node, M. *Synthesis* **2004**, 1003-1006.

29. Weber, T.; Chandrasekaran, V.; Stamer, I.; Thygesen, M. B.; Terfort, A.; Lindhorst, T. K. *Angew. Chem.* **2014**, *126*, 14812-14815; *Angew. Chem. Int. Ed.* **2014**, *53*, 14583-14586.

30. Lindhorst, T. K.; Kieburg, C. *Synthesis* **1995**, 1228-1230.

Supporting Information

for

Synthesis of AB$_4$-type carbohydrate scaffolds as branching units in the glycosciences

Tobias-Elias Gloe[1], Anne Müller[1], Anna Ciuk[1], Tanja M. Wrodnigg[2], Thisbe K. Lindhorst[1*]

[1] *Christiana Albertina University of Kiel, Otto Diels Institute of Organic Chemistry, Otto-Hahn-Platz 3/4, D-24118 Kiel, Germany, Fax: +49 431 8807410, E-mail: tklind@oc.uni-kiel.de*
[2] *Glycogroup, Institute of Organic Chemistry, Technical University Graz, Stremayrgasse 9, A-8010 Graz, Austria*

Email: Thisbe K. Lindhorst - tklind@oc.unikiel.de

*Corresponding author

^{1}H and ^{13}C NMR spectra of synthesized compounds
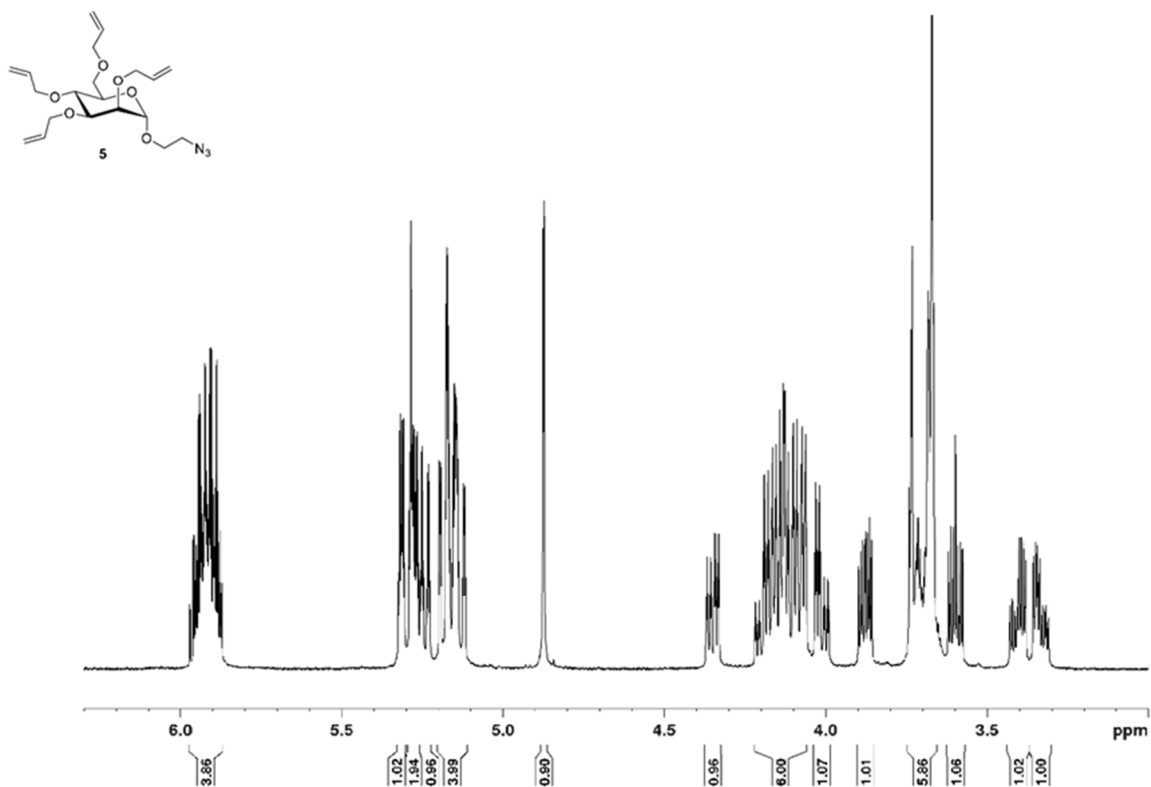
Figure S1. ^{1}H NMR spectrum of **5** (500 MHz, CDCl$_3$, 300 K).
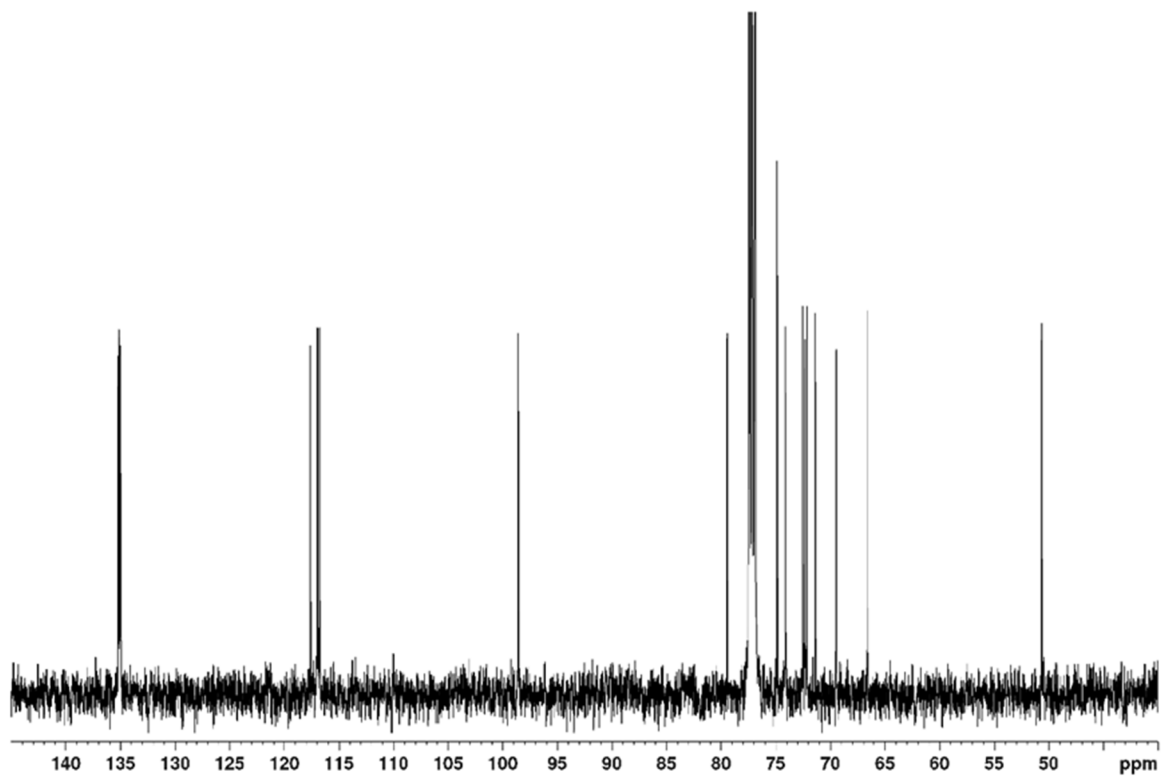
Figure S2. ^{13}C NMR spectrum of **5** (126 MHz, CDCl$_3$, 300 K).
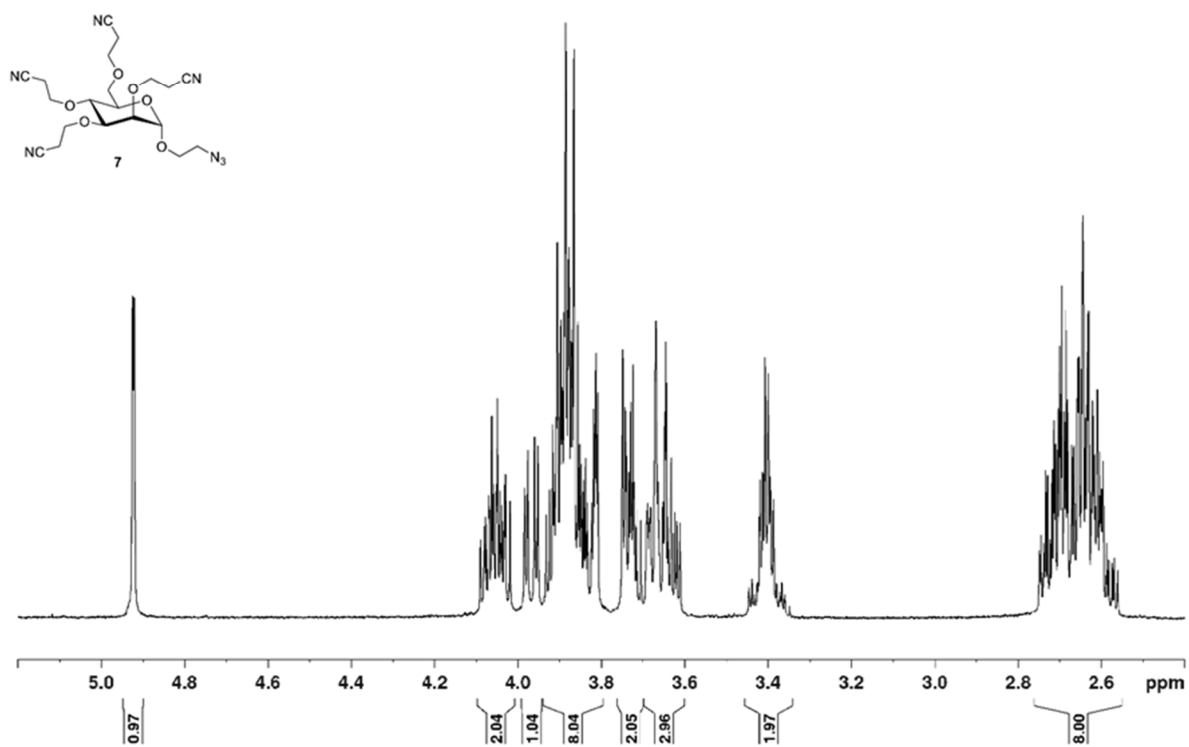
Figure S3. ^{1}H NMR spectrum of **7** (500 MHz, CDCl$_3$, 300 K).
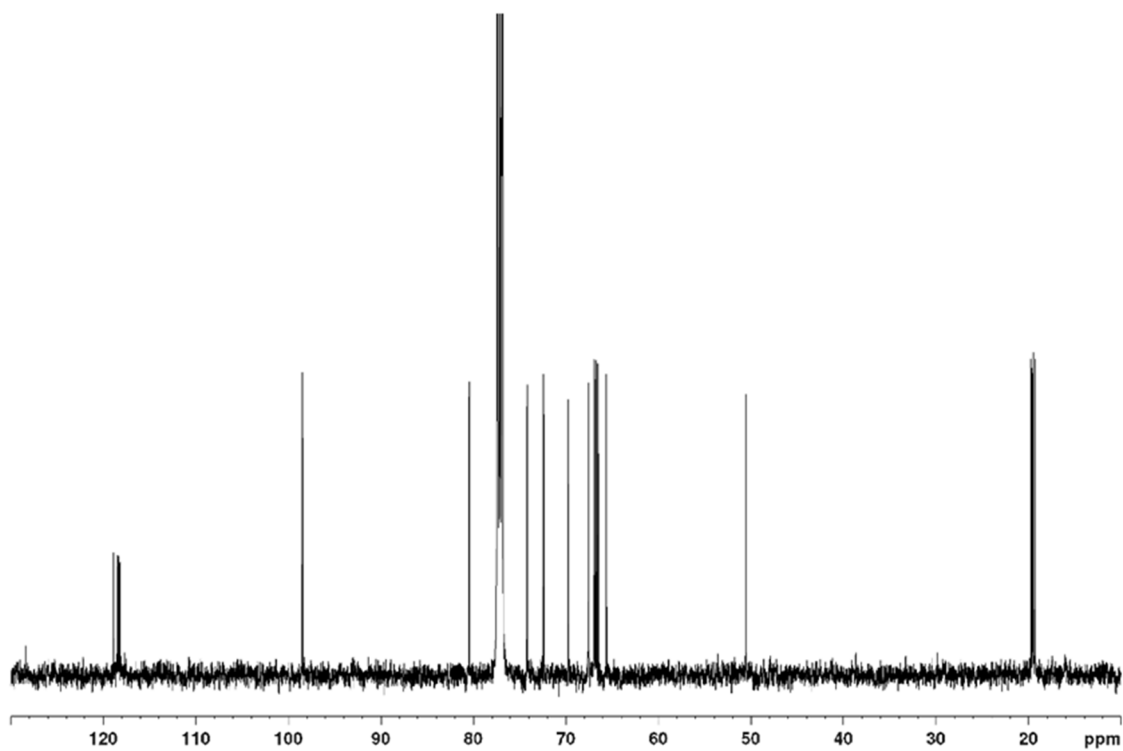
Figure S4. ^{13}C NMR spectrum of **7** (126 MHz, CDCl$_3$, 300 K).
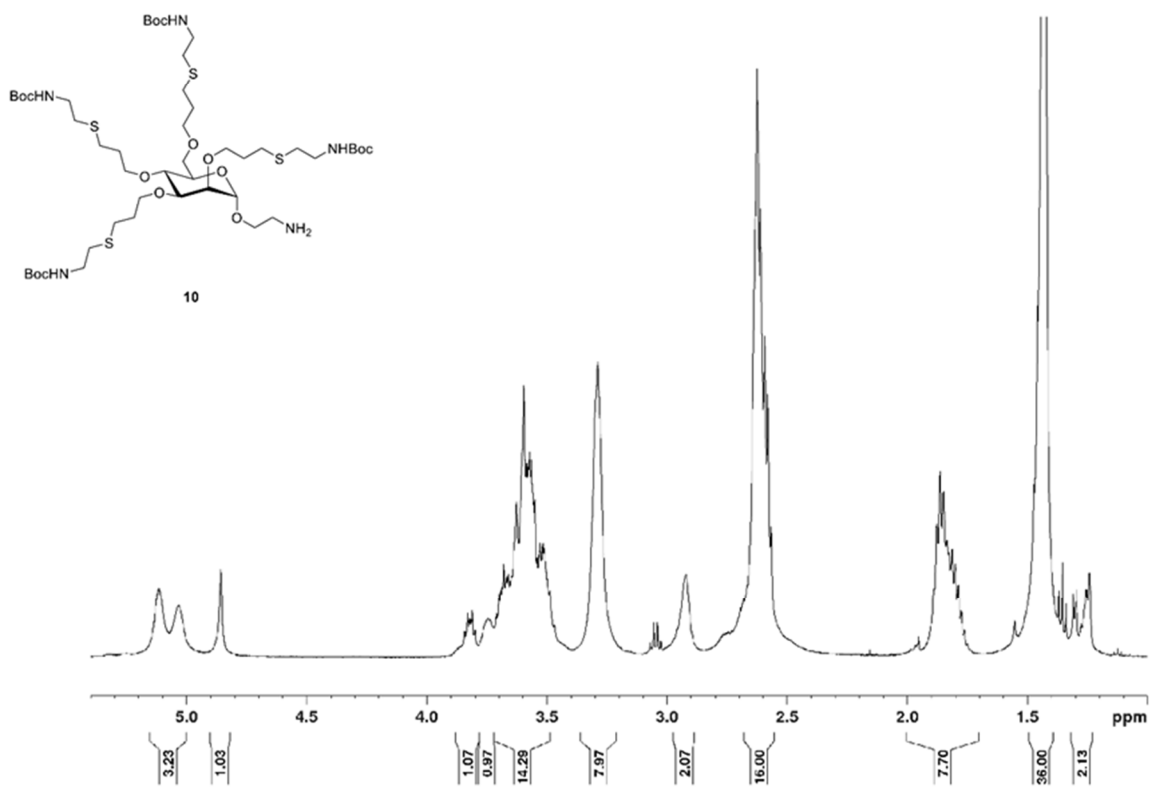
Figure S5. ^{1}H NMR spectrum of **10** (500 MHz, CDCl$_3$, 300 K).
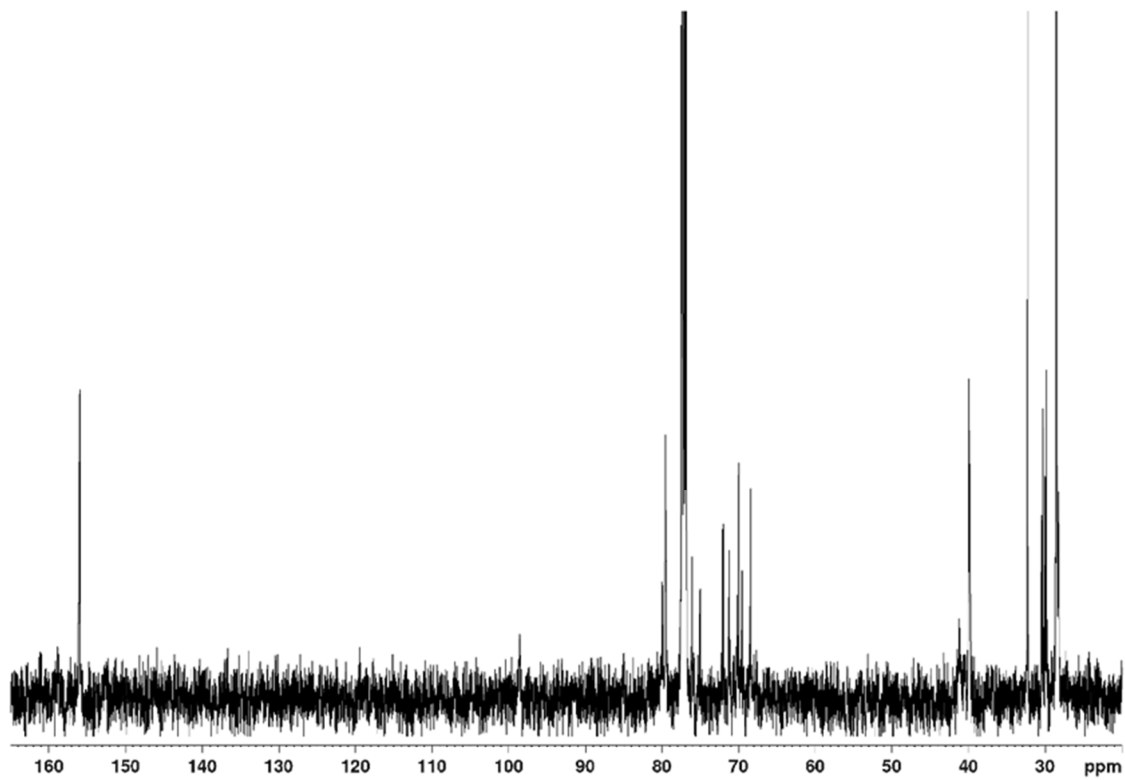
Figure S6. ^{13}C NMR spectrum of **10** (126 MHz, CDCl$_3$, 300 K).
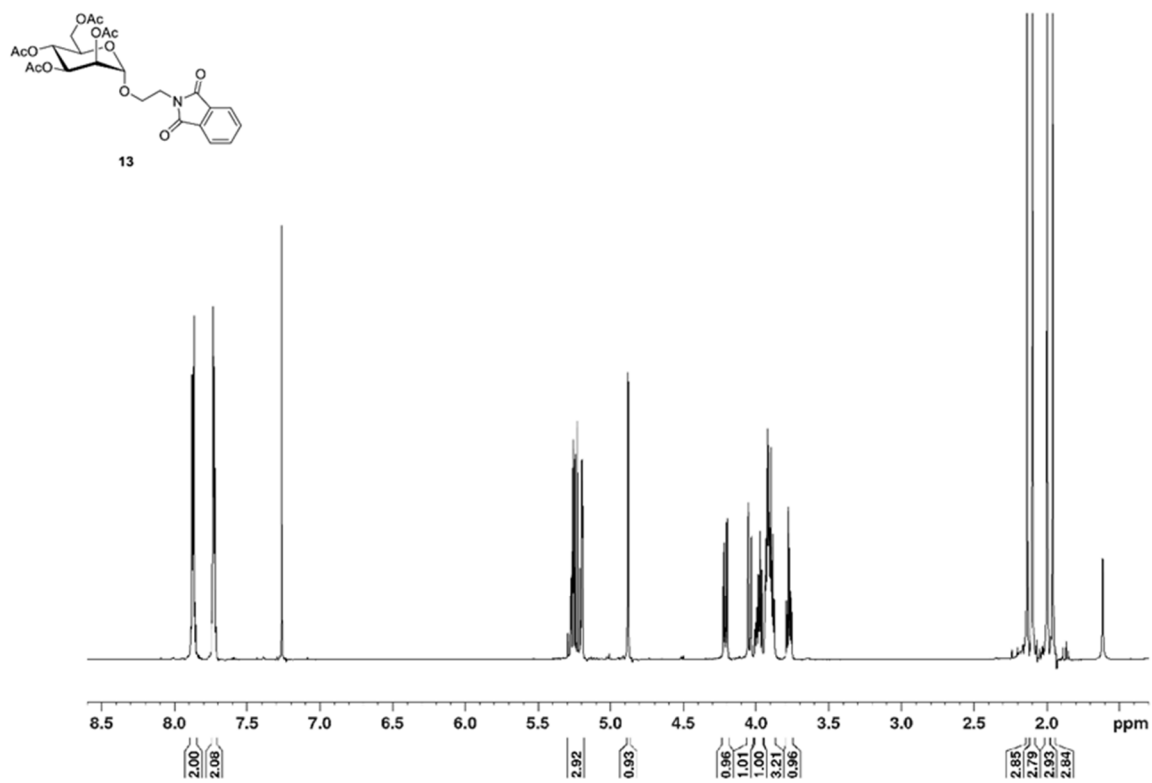
Figure S7. ^{1}H NMR spectrum of **13** (600 MHz, CDCl$_3$, 300 K).
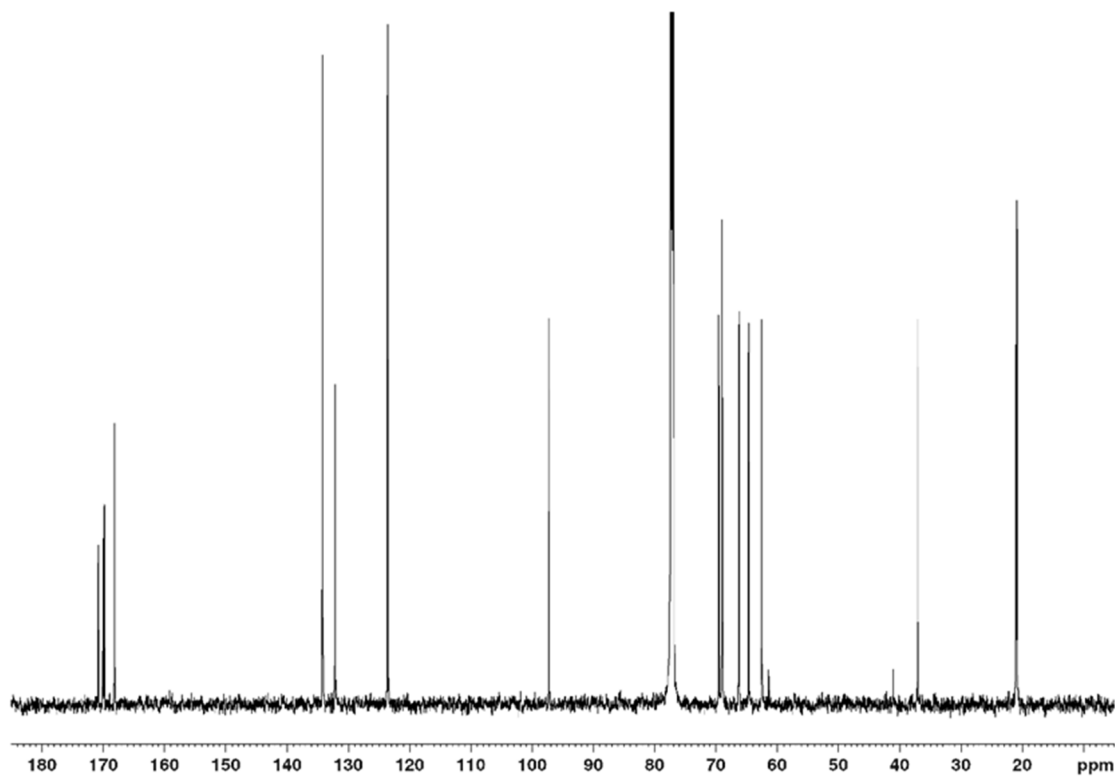
Figure S8. ^{13}C NMR spectrum of **13** (126 MHz, CDCl$_3$, 300 K).
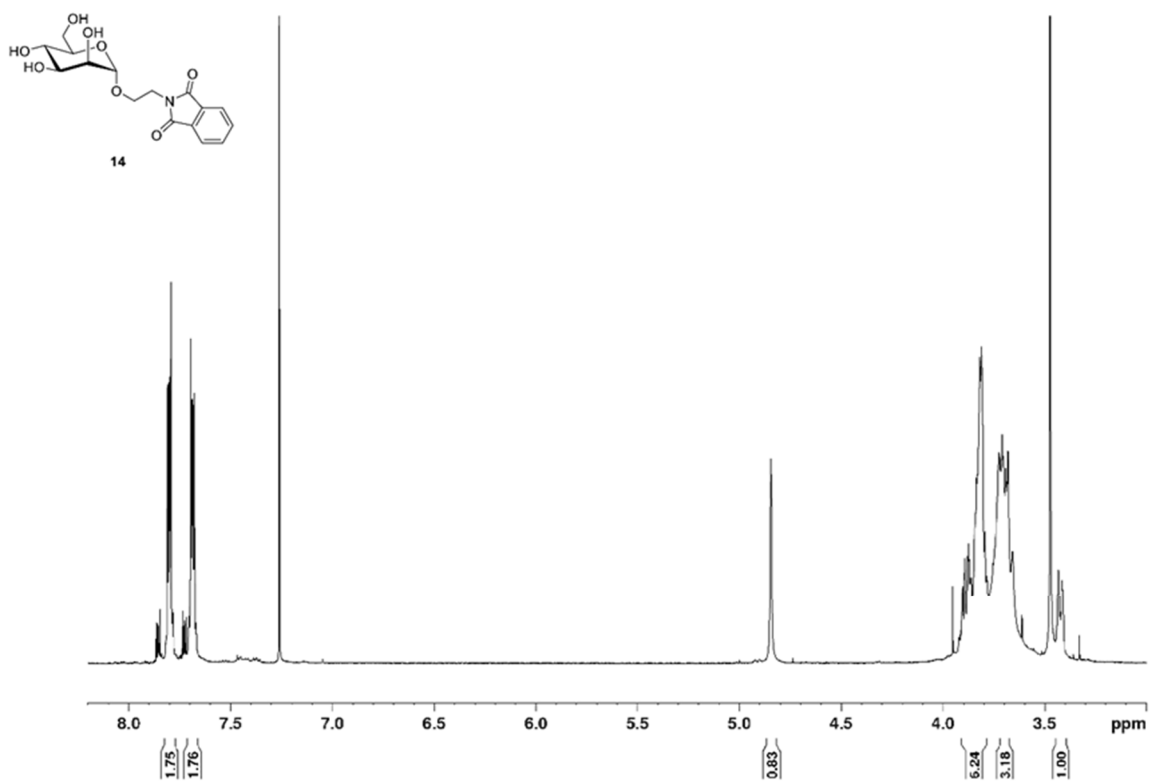
Figure S9. ^{1}H NMR spectrum of **14** (500 MHz, CDCl$_3$, 300 K).
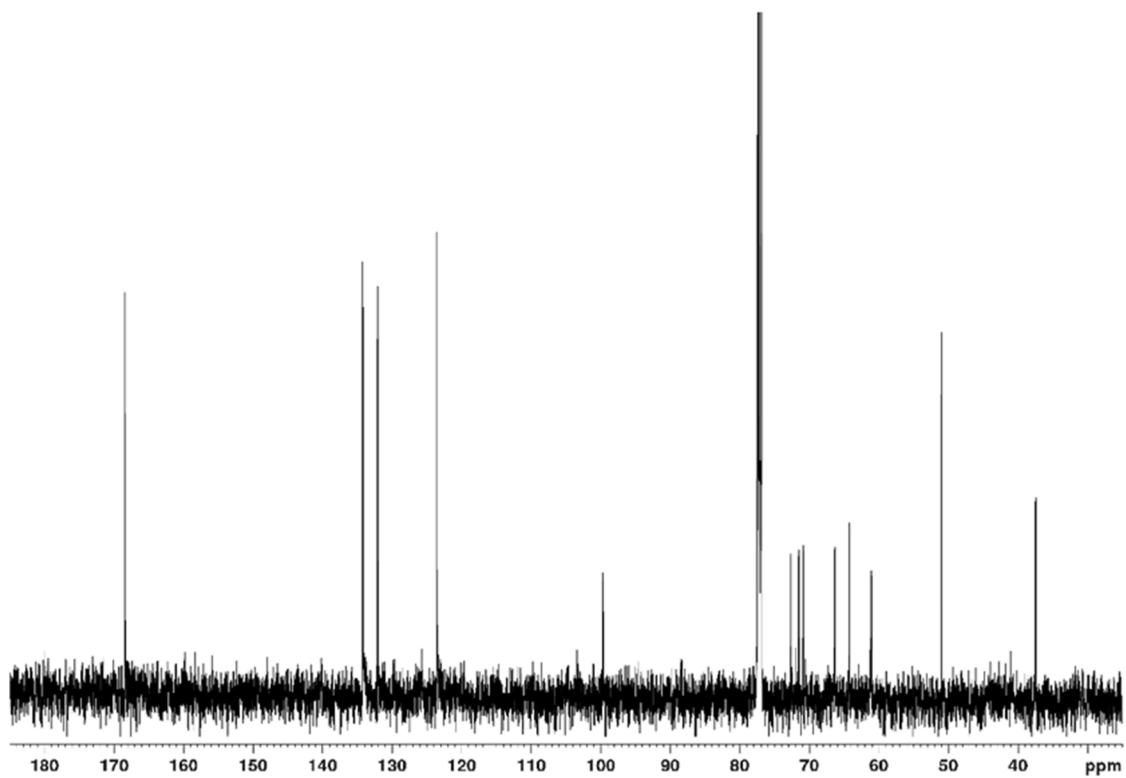
Figure S10. ^{13}C NMR spectrum of **14** (126 MHz, CDCl$_3$, 300 K).
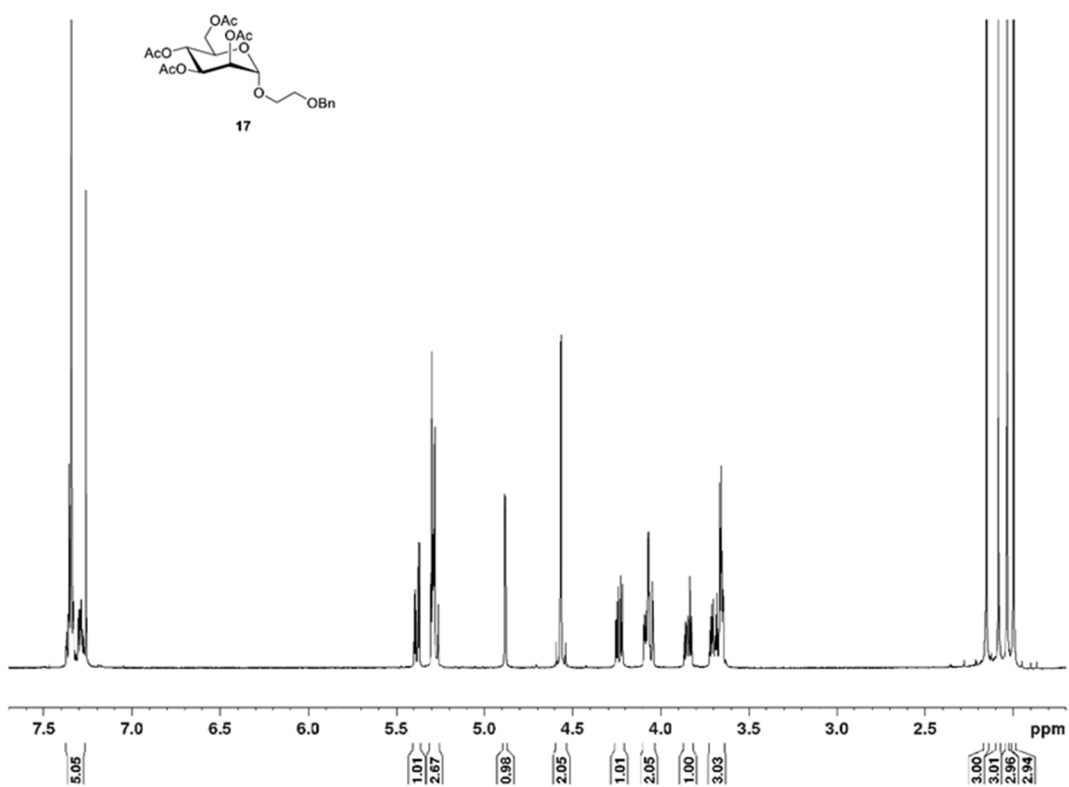
Figure S11. ^{1}H NMR spectrum of **17** (500 MHz, CDCl$_3$, 300 K).
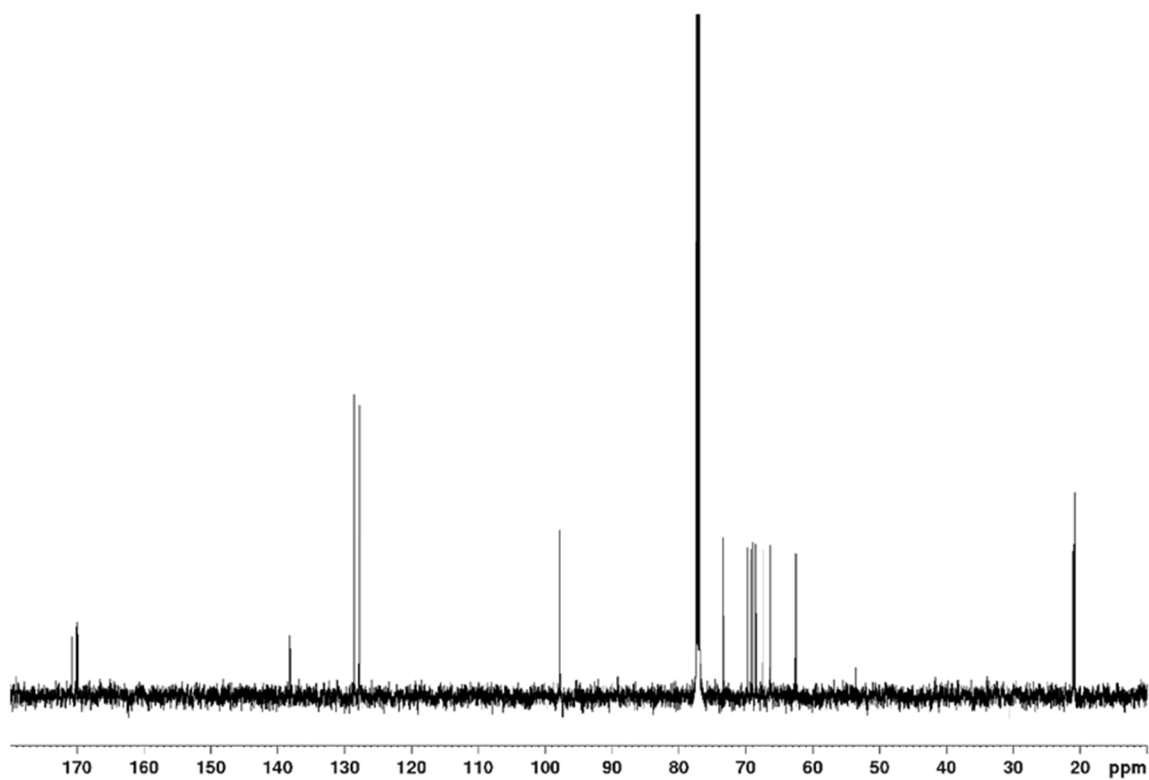
Figure S12. ^{13}C NMR spectrum of **17** (126 MHz, CDCl$_3$, 300 K).
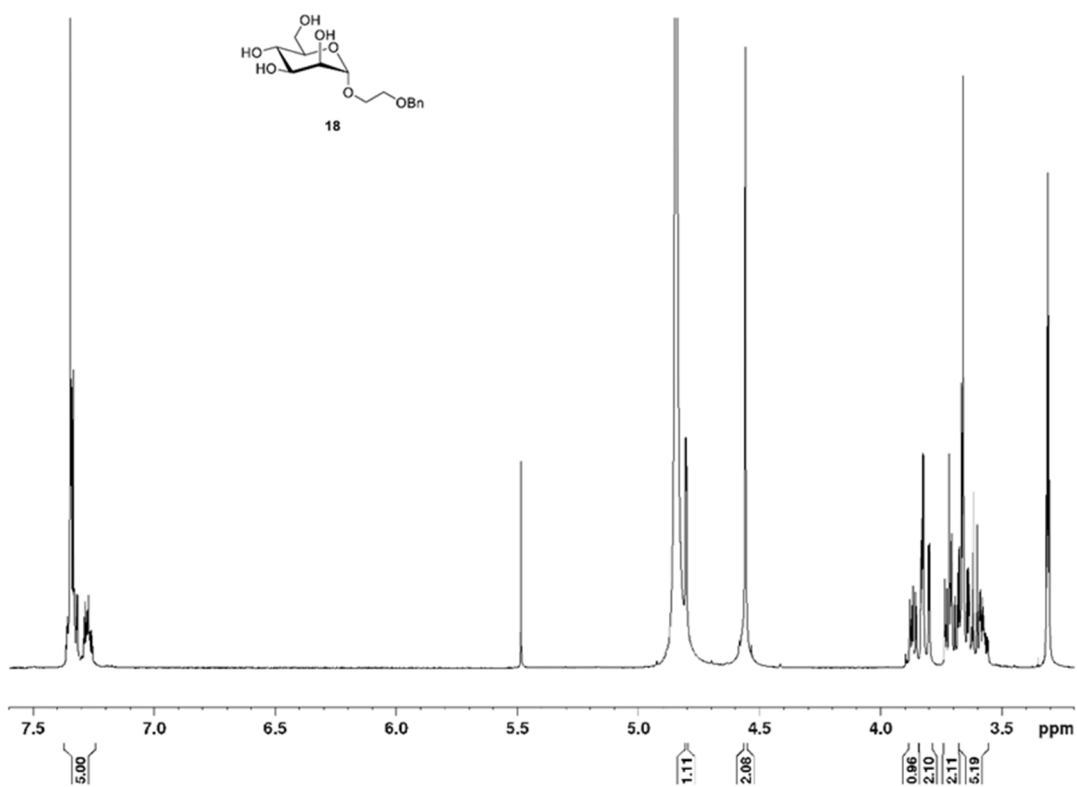
Figure S13. ^{1}H NMR spectrum of **18** (500 MHz, MeOD-d$_4$, 300 K).
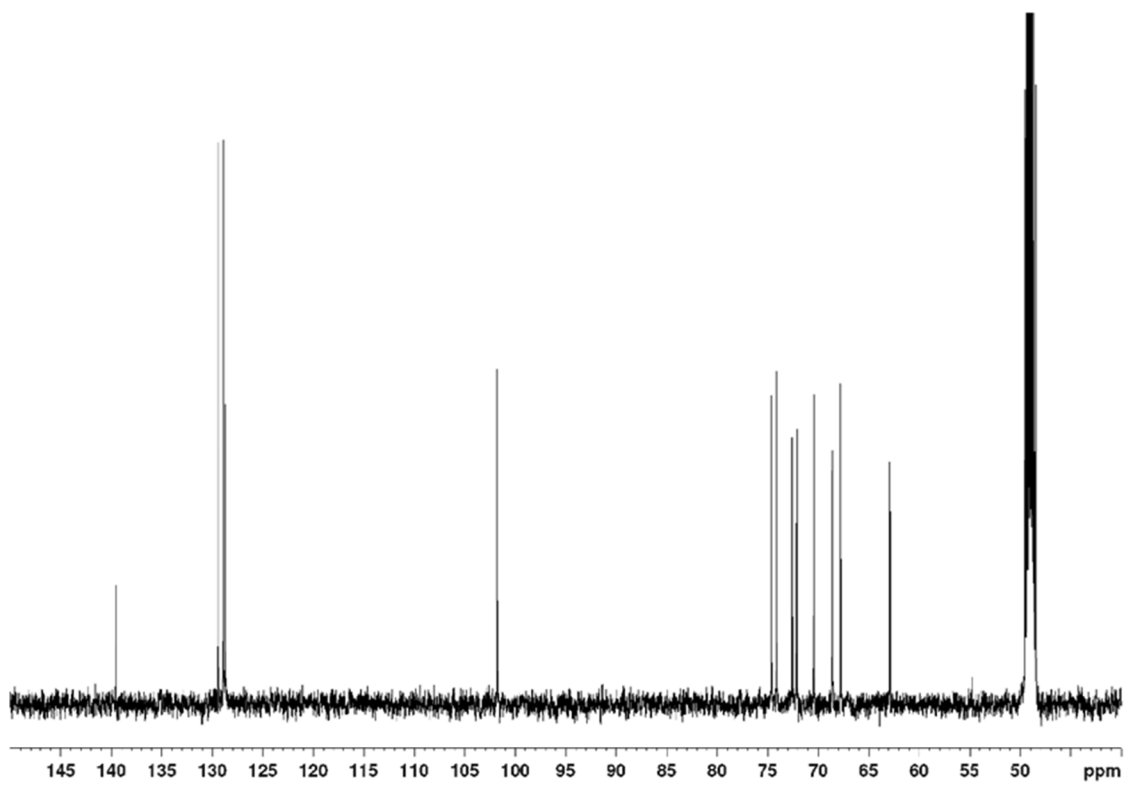
Figure S14. ^{13}C NMR spectrum of **18** (126 MHz, MeOD-d$_4$, 300 K).
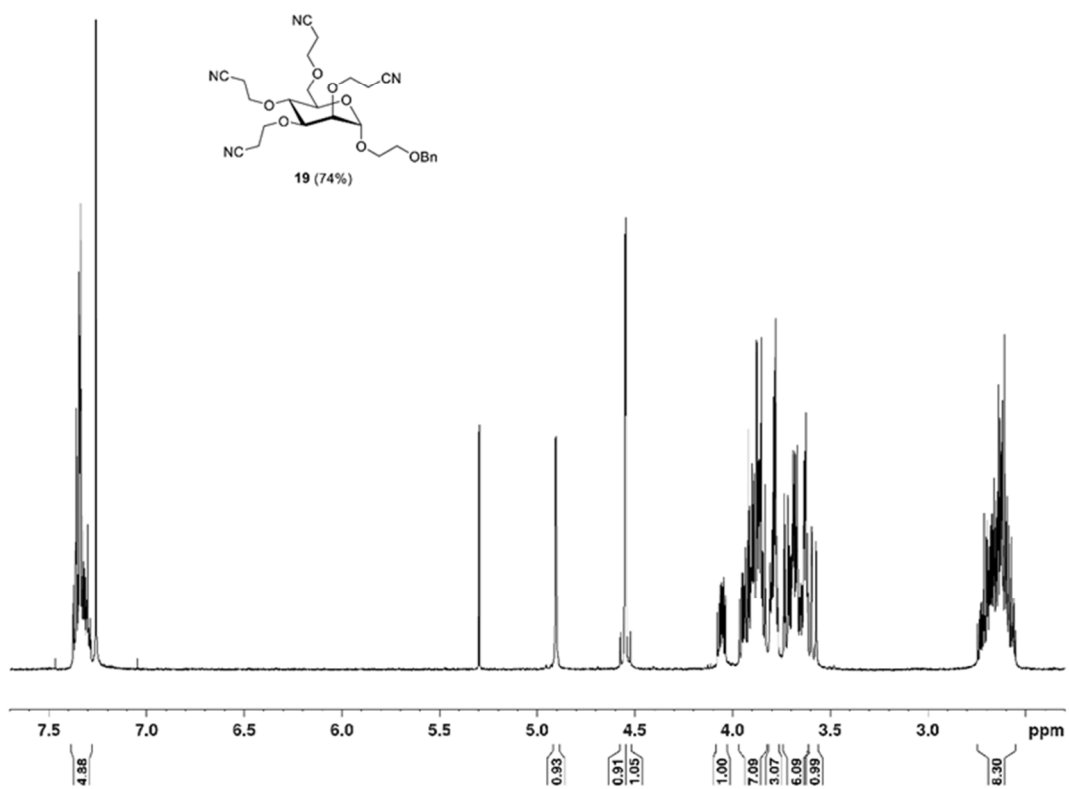
Figure S15. ^{1}H NMR spectrum of **19** (500 MHz, CDCl$_3$, 300 K).
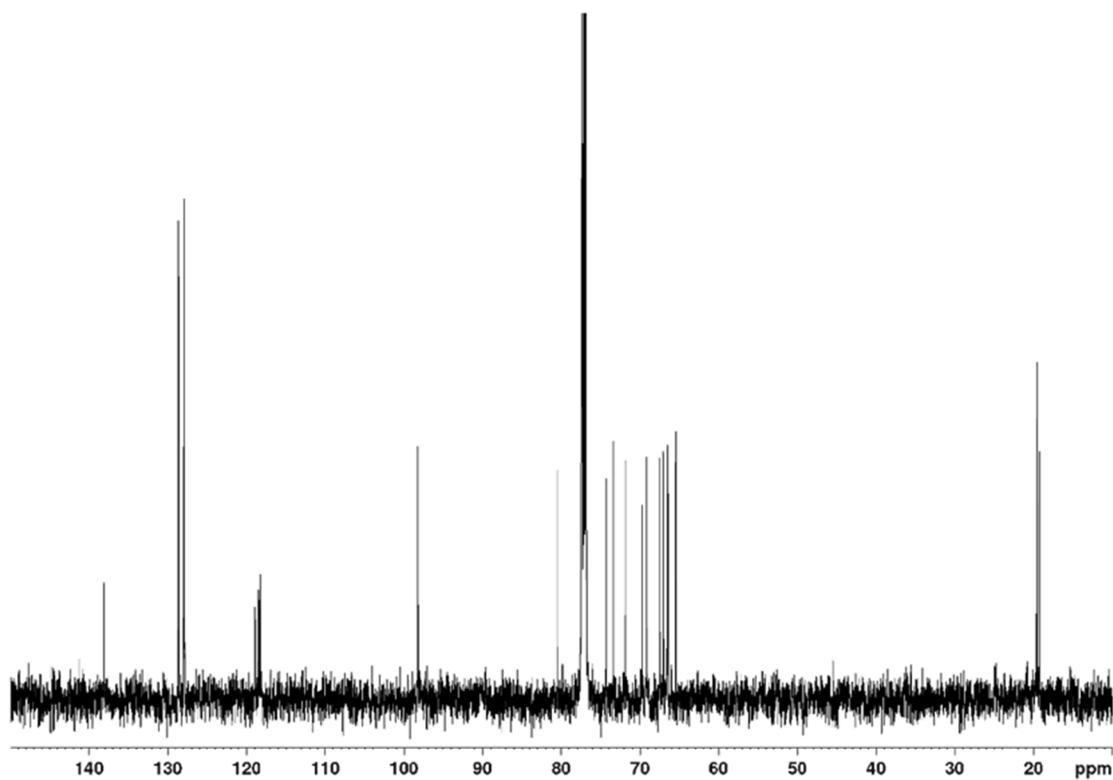
Figure S16. ^{13}C NMR spectrum of **19** (126 MHz, CDCl$_3$, 300 K).
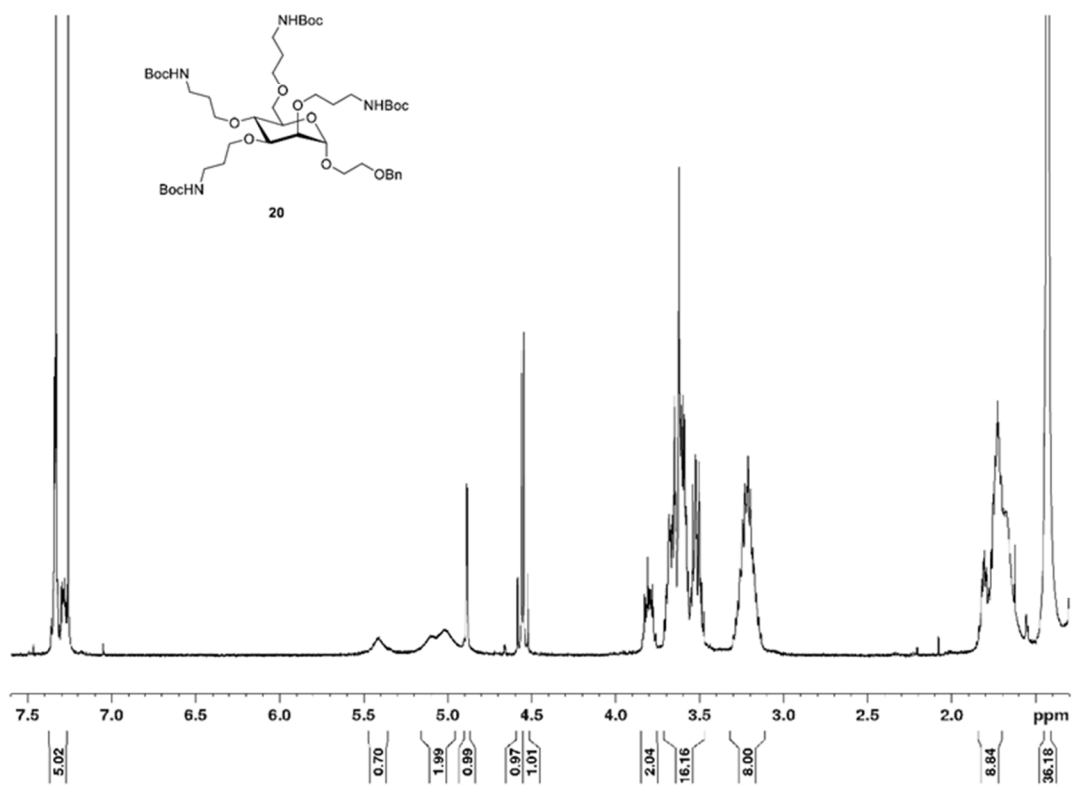
Figure S17. ^{1}H NMR spectrum of **20** (500 MHz, CDCl$_3$, 300 K).
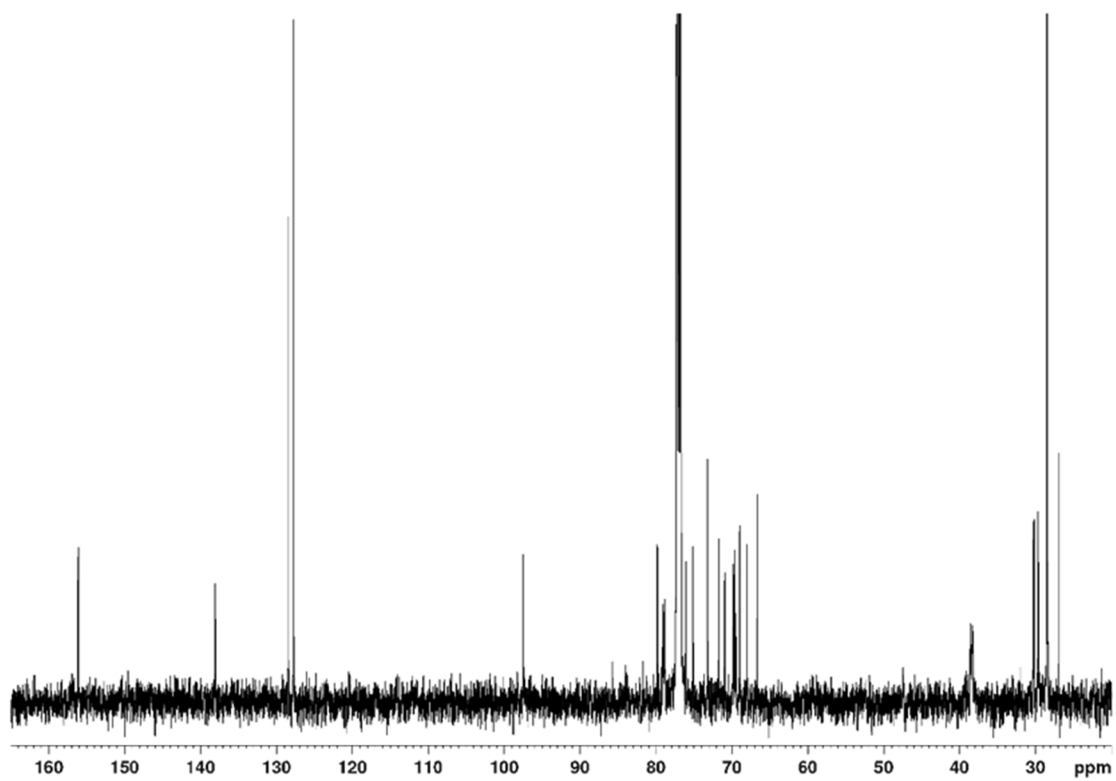
Figure S18. ^{13}C NMR spectrum of **20** (126 MHz, CDCl$_3$, 300 K).
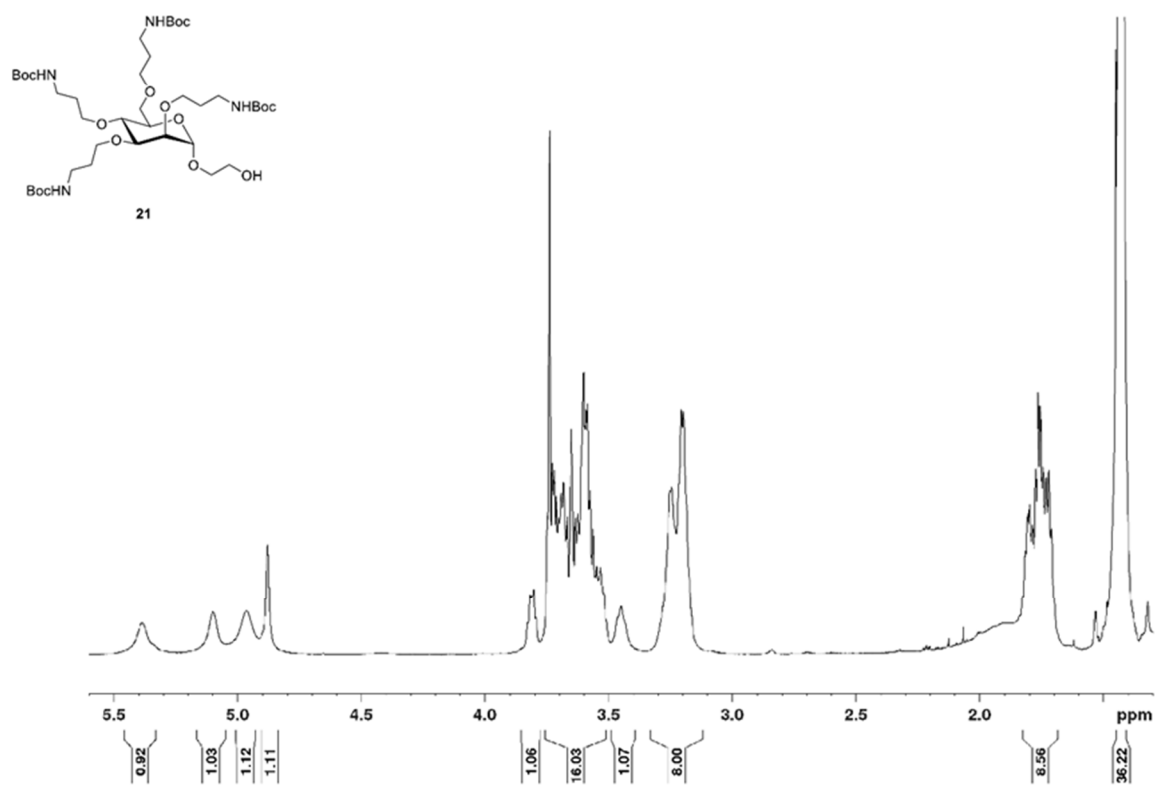
Figure S19. ^{1}H NMR spectrum of **21** (500 MHz, CDCl$_3$, 300 K).
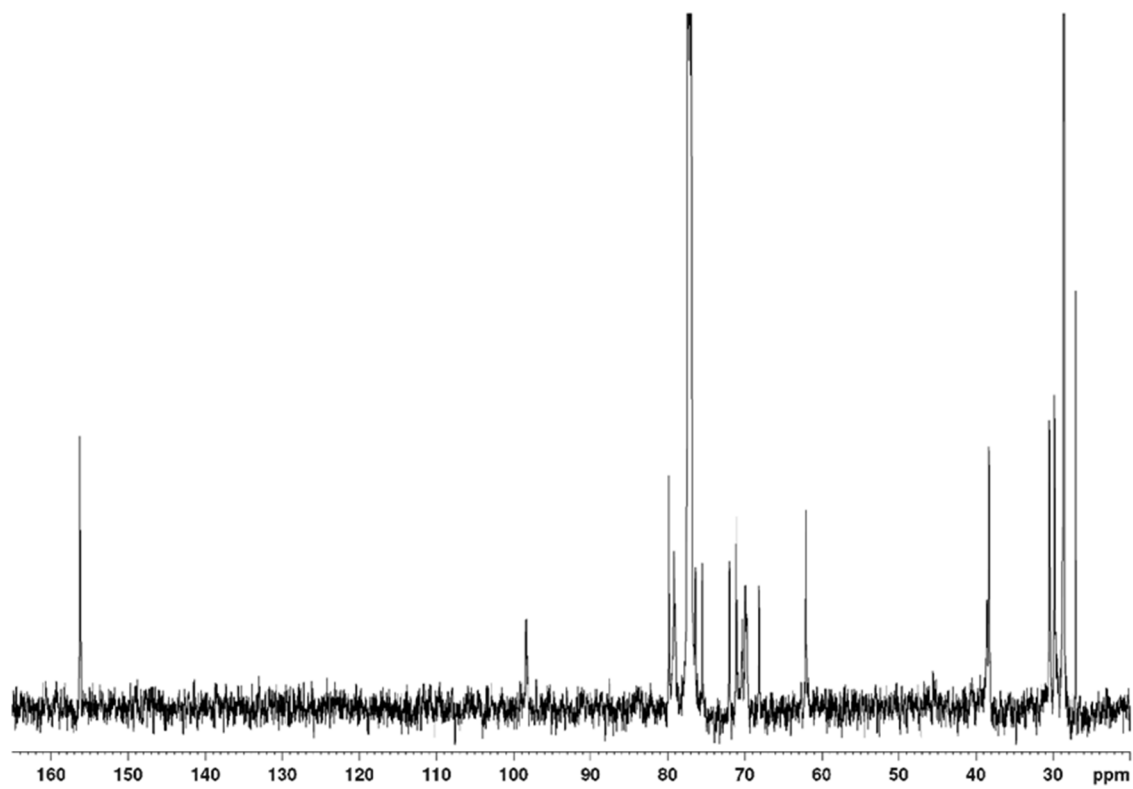
Figure S20. ^{13}C NMR spectrum of **21** (126 MHz, CDCl$_3$, 300 K).
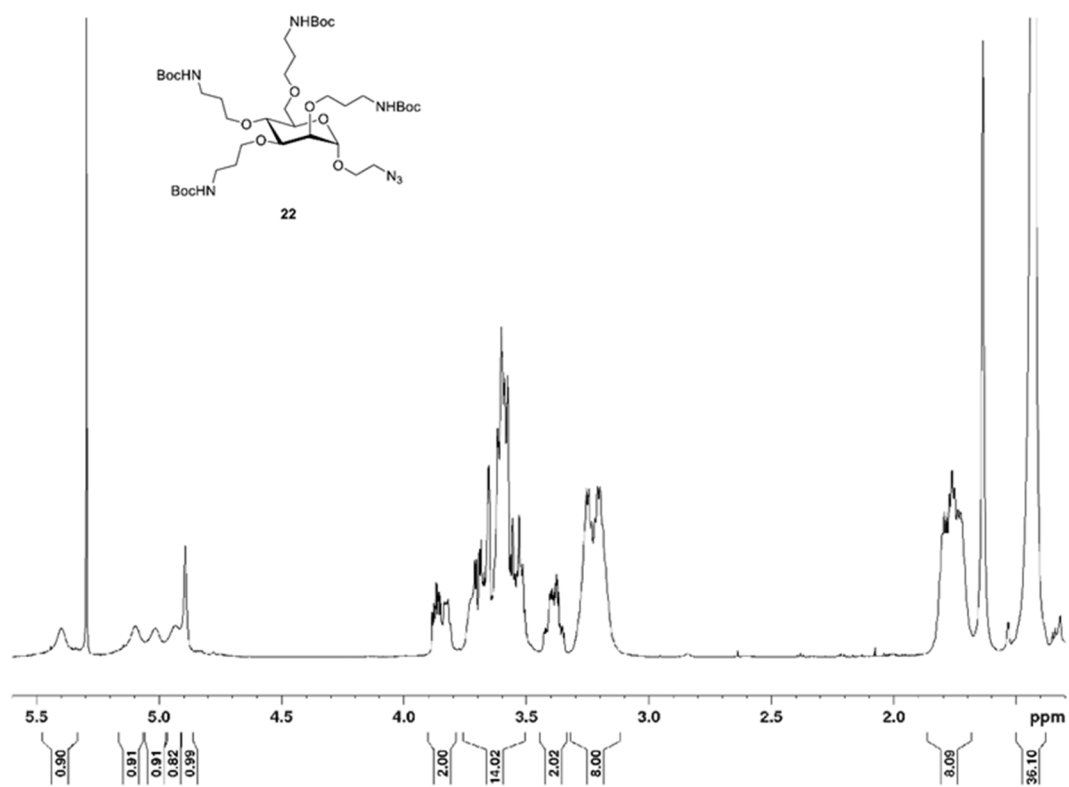
Figure S21. ^{1}H NMR spectrum of **22** (500 MHz, CDCl$_3$, 300 K).
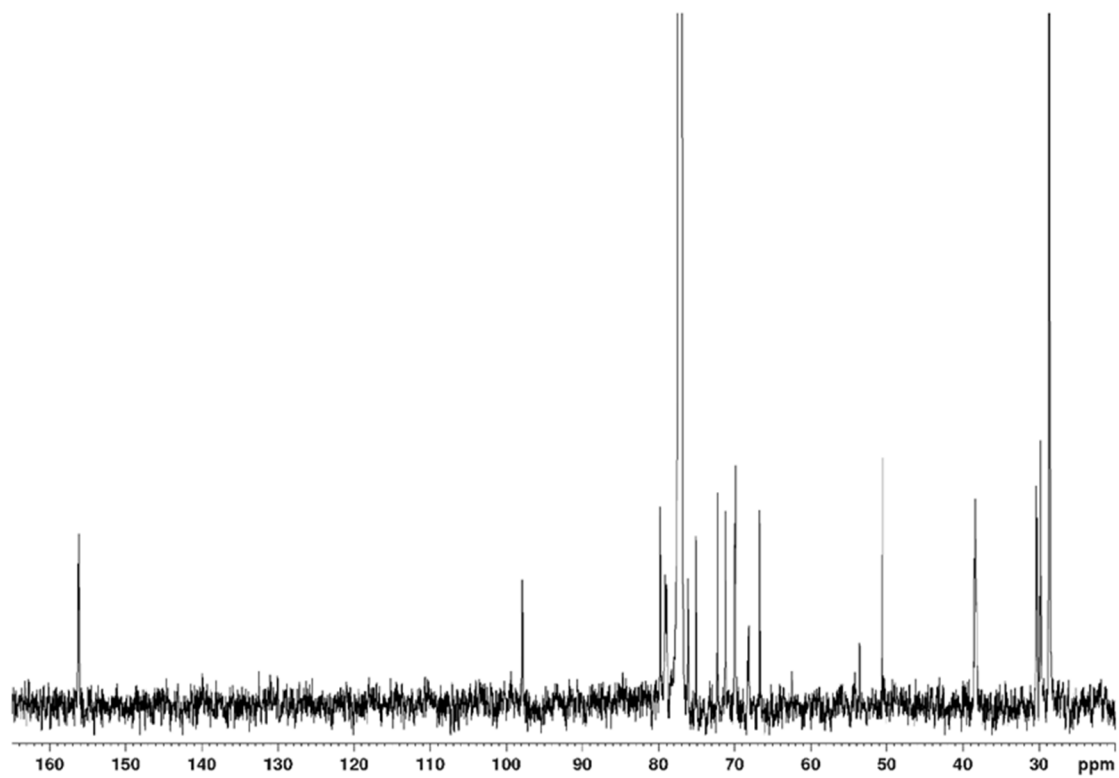
Figure S22. ^{13}C NMR spectrum of **22** (126 MHz, CDCl$_3$, 300 K).

S12
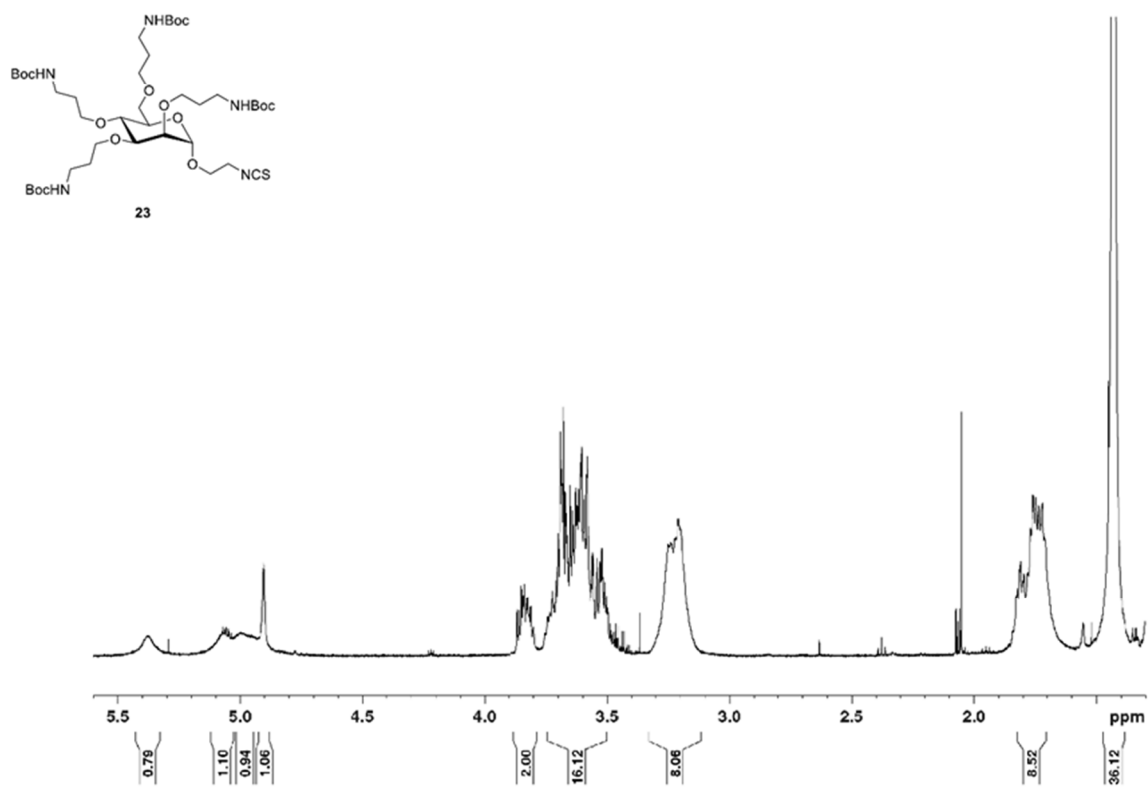
Figure S23. ^{1}H NMR spectrum of **23** (500 MHz, CDCl$_3$, 300 K).
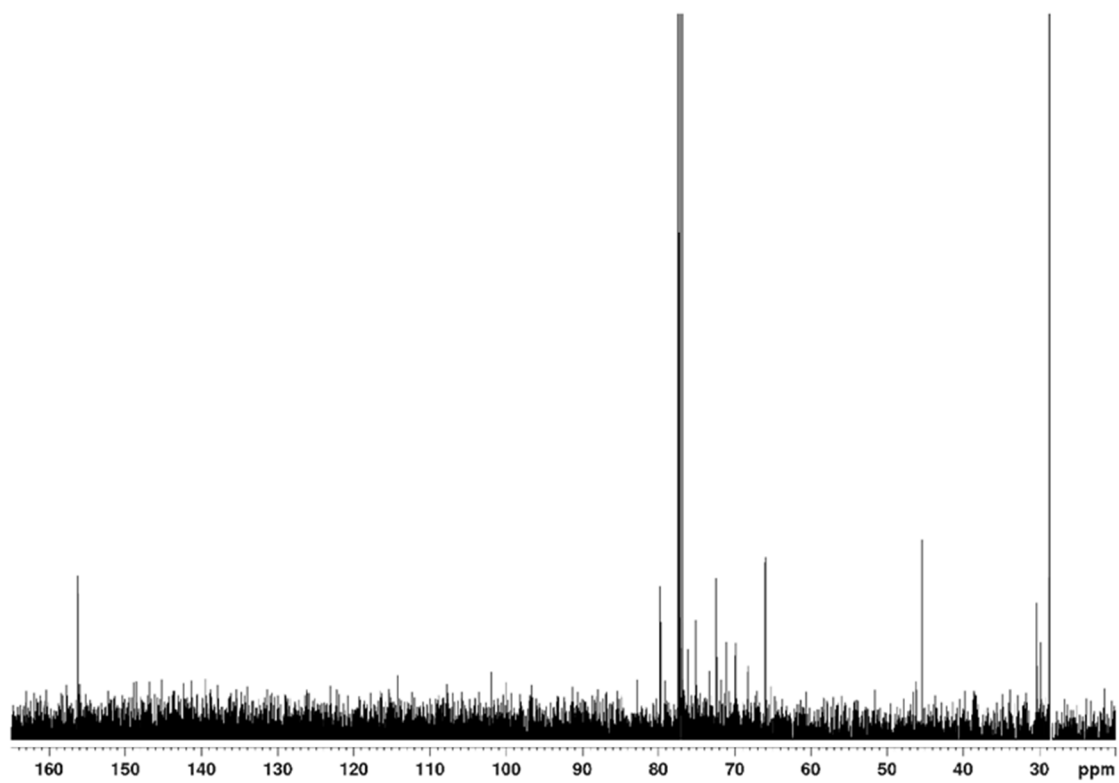
Figure S24. ^{13}C NMR spectrum of **23** (126 MHz, CDCl$_3$, 300 K).

S13
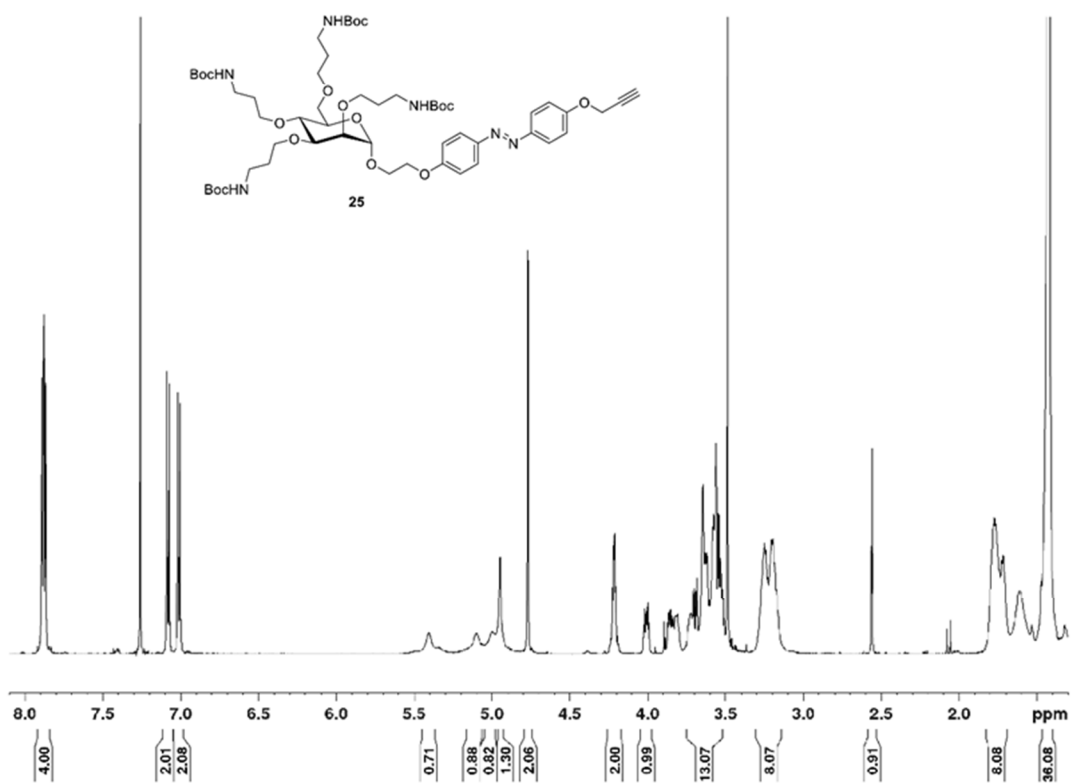
Figure S25. ^{1}H NMR spectrum of **25** (500 MHz, CDCl$_3$, 300 K).
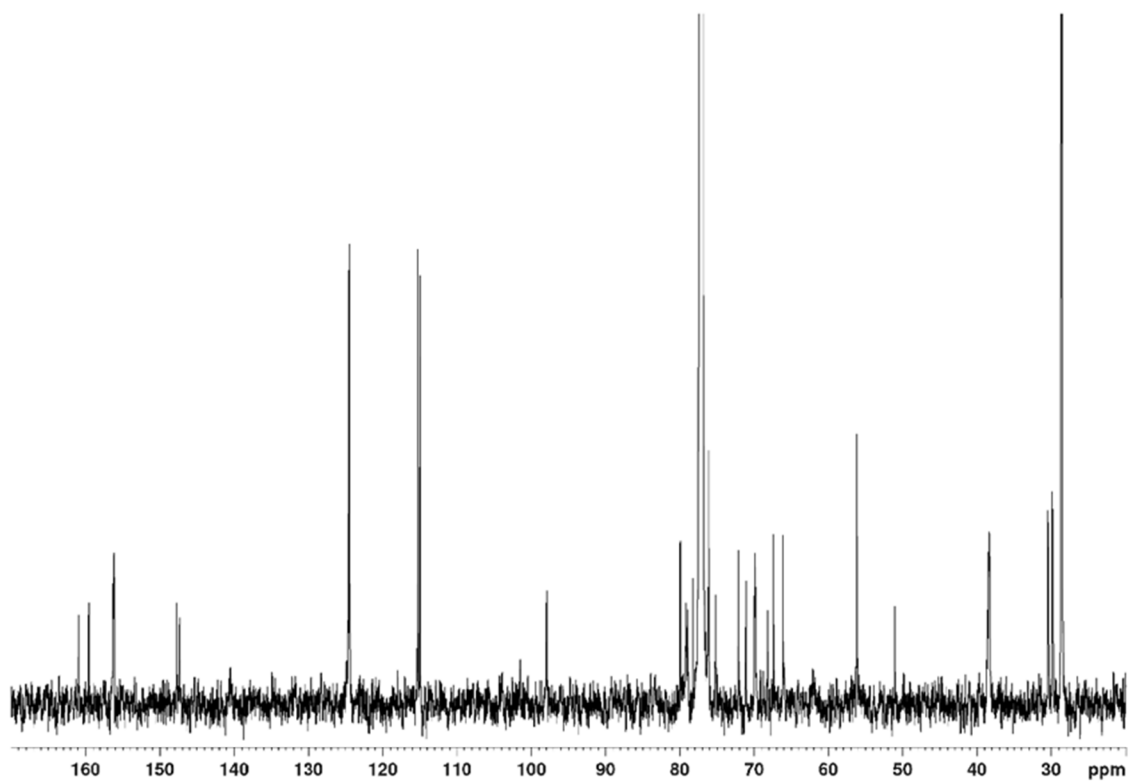
Figure S26. ^{13}C NMR spectrum of **25** (126 MHz, CDCl$_3$, 300 K).

S14
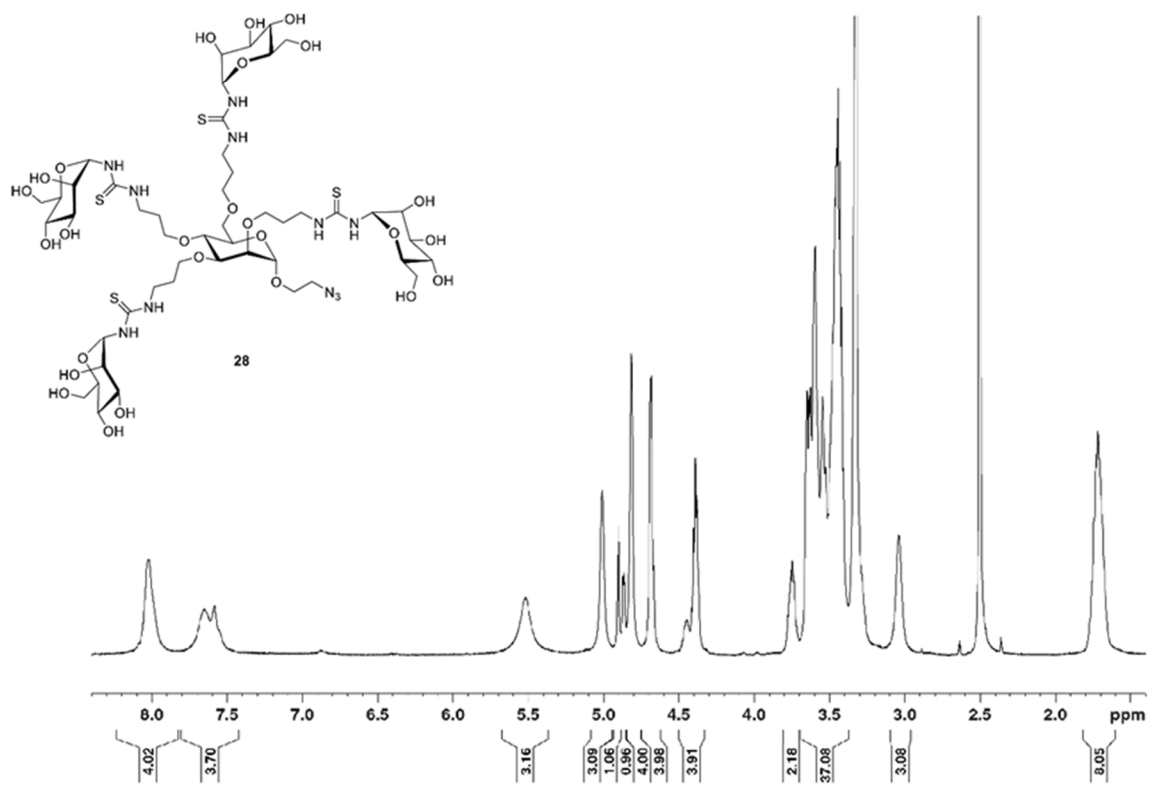
Figure S27. ^{1}H NMR spectrum of **28** (500 MHz, DMSO-d$_6$, 300 K).
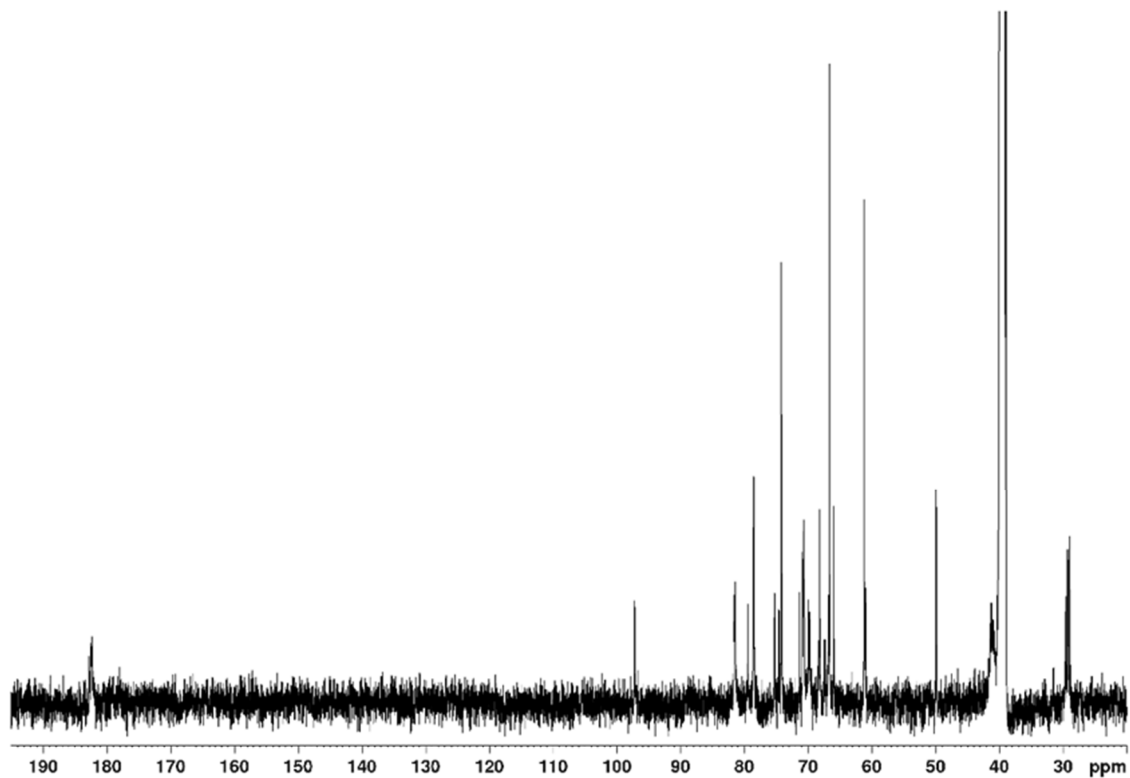
Figure S28. ^{13}C NMR spectrum of **28** (126 MHz, DMSO-d$_6$, 300 K).

4.3   Investigation of Type 1 Fimbriae-mediated Bacterial Adhesion to Tetravalent Glycoclusters

In Chapter 4.2, the synthesis of a tetravalent homoglycocluster **41** was reported, which bears four mannose portions and, in addition, an azido group in its aglycone. This functional group can be addressed for further functionalization by either conversion of the azide group, cycloaddition of an appropriate carbohydrate moiety, or by coupling to an activated surface for adhesion studies (Scheme 4.6). The latter approach is of particular interest because it allows for tests with tetravalent carbohydrate-centered glycoclusters.
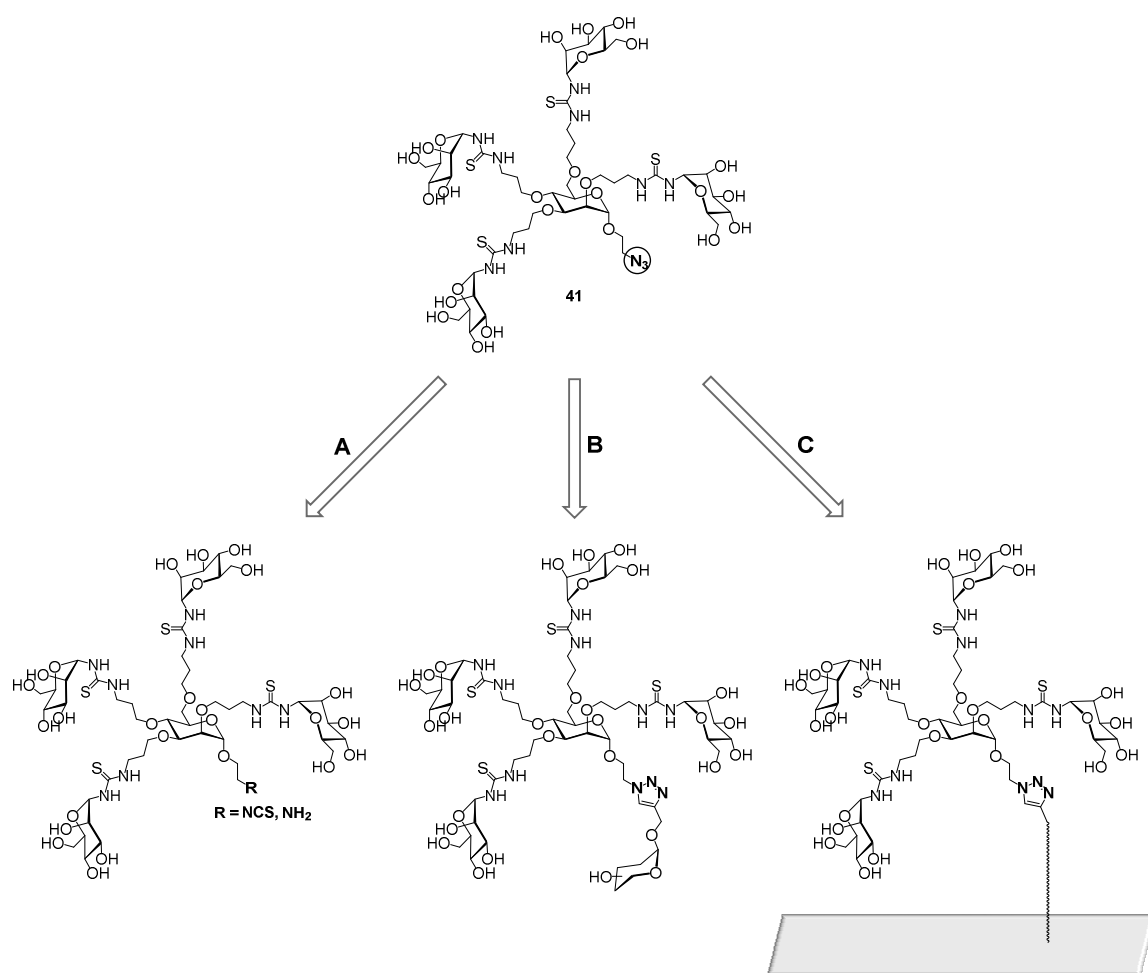
Scheme 4.6: The azide group (circle) in glycocluster **41** can be addressed in three different functionalization pathways: conversion to an isothiocyanate or amino group (A), cycloaddition of an appropriate carbohydrate moiety (B) or immobilization onto a suitable prefunctionalized surface (C).

Closer inspection of the azido function in the cluster **41** reveals that it is rather shielded by the surrounding carbohydrate moieties due to the relatively short ethyl linker connecting it to the carbohydrate scaffold. Its concealed position might hamper the immobilization process so that it was decided to attach a biorepulsive oligo ethylene glycol (OEG) linker to the cluster. The linker consists of an amino group for the actual surface coupling as well as an alkyne portion for attachment with the glycoclusters azido group by a CuAAC cycloaddition reaction. In addition to the facilitation of the immobilization process, attachment of such a biorepulsive linker is expected to decrease or eliminate unspecific adhesion of bacteria to, for example, polystyrene surfaces functionalized with this glycocluster.

Results and Discussion

4.3.1   Synthesis of OEG Linker **46** and Attachment to Glycocluster **41**

OEG linker **46**[77] was synthesized following a procedure of Norberg *et al.*[77b] starting from plain triethylene glycol (**42**), which in the initial step was alkylated with propargyl bromide. The remaining hydroxyl group of the resulting alkyne **43** was then converted into the respective tosylate **44** in order to serve as a leaving group in the next step. Treatment with sodium azide resulted in substitution of the tosylate, giving azide **45**, which was finally reduced to the targeted amine **46** under the conditions of Staudinger reduction (Scheme 4.7).
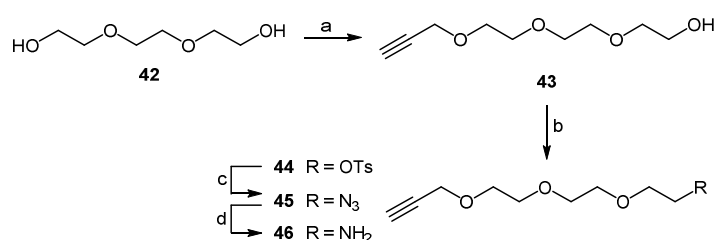
Scheme 4.7: Synthesis of OEG linker **46**. a) KOH, propargyl bromide, 60 °C, 3 h, 34%; b) TsCl, KOH, CH_2Cl_2, 0 °C, 2 h, 84%; c) NaN_3, TBAI, DMF, 70 °C, 4 h, 76%; d) PPh_3, NH_4OH, THF, rt, 16 h, 82%.

For conjugation of the OEG linker **46** with the azido-functionalized glycocluster **41**, CuAAC reaction conditions were applied according to a variant that generates the required copper(I) species *in situ* by reduction of copper(II) with sodium ascorbate.[30b] Although this variant of the click reaction is frequently used in complex organic synthesis due to its efficiency and, most importantly, its specificity, problems were encountered when applied to the glycocluster **41**. It was found that the reaction was always incomplete (irrespective of the conditions applied), even when an excess of the linker **46** and/or the copper catalyst was

added after the initial reaction. Additionally, the highly polar nature of the click product precluded the separation from the high amount of remaining starting material. Finally the desired product **47** was obtained by utilization of copper(I) bromide and N,N,N',N'',N''-pentamethyldiethylenetriamine (PMDTA) as a complexing agent, which stabilizes the copper(I) species (Scheme 4.8). Although the conversion of **41** was still incomplete, it was significantly higher than in the previous method, thus, enabling purification of the product **47** by reverse phase (RP) chromatography. Since it was necessary to use formic acid as a solvent additive, the product was obtained as the respective formic acid salt **47** in a yield of 50% (71% based on conversion, 21% starting material reisolated).
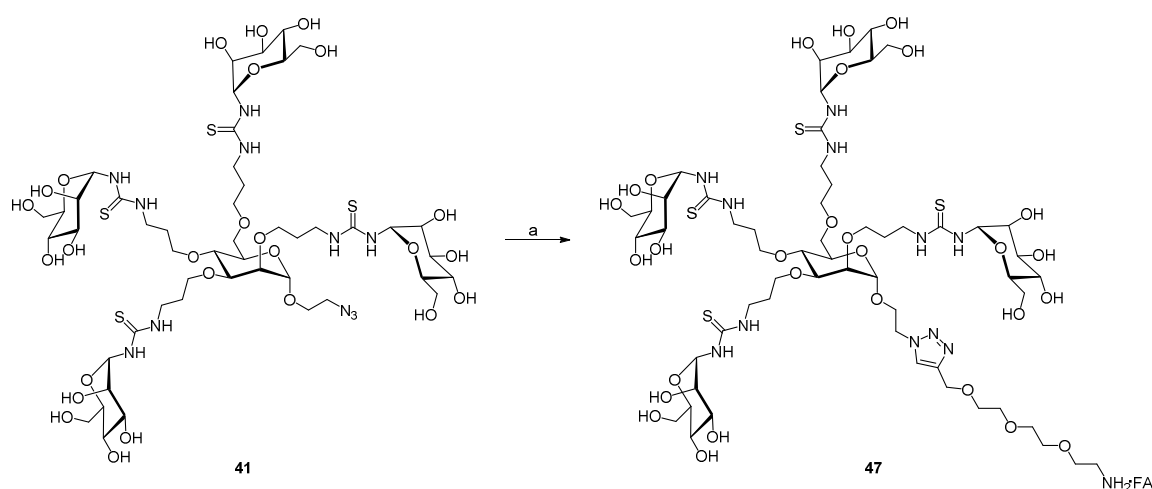
Scheme 4.8: Synthesis of glycocluster OEG conjugate **47** by means of CuAAC reaction conditions. a) **46**, CuBr, PMDTA, DMF, rt, 16 h, 50%.

4.3.2   Adhesion-Inhibition Assay with Glycocluster **41**

In order to pave the way towards adhesion studies on glycoarrays fabricated from glycocluster **47**, the inhibitory potency of glycocluster **41** towards type 1 fimbriae-mediated bacterial adhesion was investigated by performance of an adhesion-inhibition assay. For this, microtiter plates were coated with mannan, incubated with GFP-transfected *E. coli* (pPKL1162) and serial dilutions of glycocluster **41** and methyl α-D-mannoside (MeMan) were employed on the plates. After washing, fluorescence of adhering bacteria was detected, delivering inhibition curves, from which IC_{50} values were deduced (Figure 4.1).
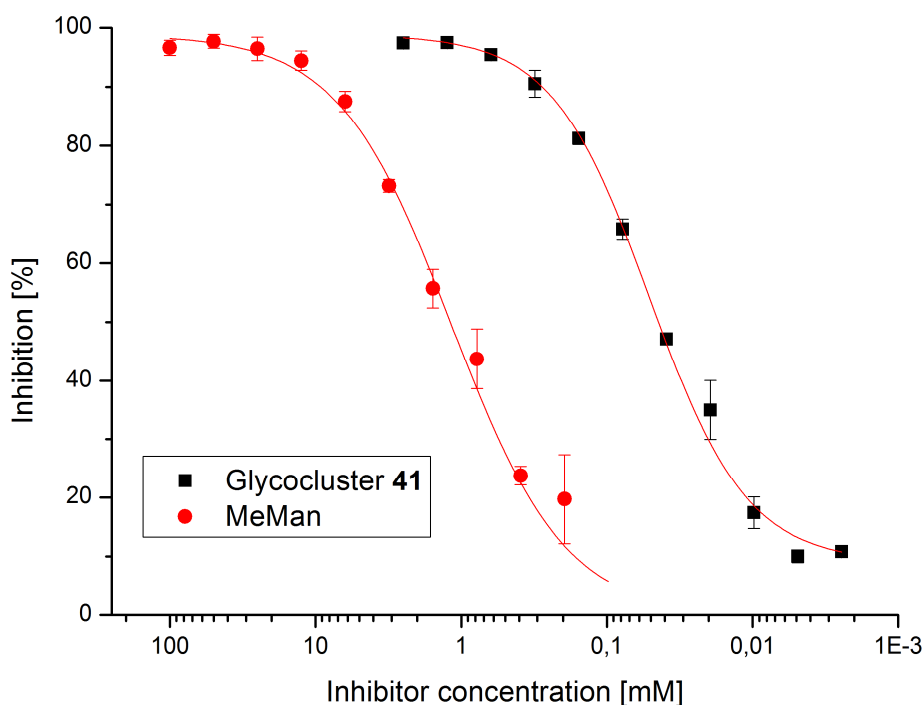
Figure 4.1: Inhibition curves obtained with glycocluster **41** from inhibition of type 1 fimbriae-mediated bacterial adhesion to mannan. The depicted inhibition curves are representative examples from three independent experiments. MeMan was tested on the same microtiter plate. Error bars are standard deviations from three testing results on one plate.

An inhibitor's IC_{50} value represents the concentration at which it prevents 50% of bacterial adhesion. Comparison to the IC_{50} value of a standard inhibitor (in this case MeMan), which is tested on the same microtiter plate, allows for direct correlation of different inhibitors by comparing their so-called relative inhibitory potencies (RIP values), even if they were not tested on the same plate. In case of multivalent inhibitors, such as the glycocluster **41**, a multivalency-corrected RIP value, RIP_{vc}, has to be taken into account in order to receive its "true" inhibitory potency. The results obtained from the adhesion-inhibition assay are listed in Table 4.1.

In the performed adhesion-inhibition assay, the RIP (based on MeMan) of glycocluster **41** was determined as approximately 26 and the RIP_{vc} as 6.4. When the RIP_{vc} value equals 1, no multivalency effect is observed so that the higher relative inhibitory potency results from a purely statistical advantage by the presence of multiple mannose residues available for lectin binding (cf. Chapter 1.4). Thus, in the case of glycocluster **41**, a small multivalency effect was determined. However, this effect is not as pronounced as for similar carbohydrate-centered glycoclusters that have been reported, showing RIP_{vc} values in the range of 16 to 36.[66b, 78]

Table 4.1: Inhibition of bacterial adhesion (*E. coli*) to a mannan-coated surface. The inhibitory potency of glycocluster **41** is compared to the standard inhibitor MeMan.[a]

	MeMan	Glycocluster **41**
$IC_{50} \pm SD$ (mM)	2.357 ± 1.032	0.0920 ± 0.0489
RIP (MeMan)	1.0	25.6
RIP_{vc}	–	6.4
[a]SD: standard deviation (from three independent assays); RIP: relative inhibitory potency referenced to MeMan (tested on the same microtiter plate); RIP_{vc}: valency-corrected RIP.		

Thiourea-bridged glycoclusters containing a non-carbohydrate core have been found to provide significantly higher binding affinities of FimH in haemagglutination assays with type 1 fimbriated *E. coli* when compared to their natural glycoside counterparts. Furthermore, comparison of big glycoclusters (tetra-, hexa- and octavalent) with smaller clusters (di- and trivalent) revealed that the latter delivered higher relative inhibition titres (RITs).[79] At first glance, these findings seem to be in contradiction to the results gathered from the testing of cluster **41**. However, carbohydrate-centered clusters containing thiourea-bridged mannose moieties have not been tested so far as inhibitors of type 1 fimbriae-mediated bacterial adhesion. Therefore, it can only be speculated what may be the reason for the cluster's reduced inhibitory potency compared to those reported containing natural glycosidic bonds. The most likely explanation seems to be a combination of both the radial arrangement of the mannose moieties fixed by the rigid mannose scaffold and the electronic and conformational properties of the thiourea groups. Furthermore, intramolecular interactions of these groups may evoke a geometric arrangement that is unfavorable for the preorganization of the presented mannose moieties as well as the recognition by the bacterial lectin. Interestingly, anomeric thiourea groups seem to mediate a strong dependence of the glycocluster-lectin recognition properties in regard to the geometrical shape of the investigated multivalent compound. This has been demonstrated by studies with the mannose-specific lectin Con A, revealing dramatic differences between thioglycoside- and glycosylthioureido- or glycosylamido-coated glycoclusters based on a cyclodextrin core[80] but also by investigation of carbohydrate-centered thioglycoside- and glycosylthioureido-glycoclusters.[74]

5.   Cyclodextrin Conjugates to Control Bacterial Adhesion

5.1   Introduction

Cyclodextrins (CDs) are cyclic oligosaccharides that are often referred to as cycloamyloses, cyclomaltoses, or Schardinger dextrins. As non-natural compounds they are obtained through enzymatic degradation of starch, one of the most essential and abundant polysaccharides found in nature. As part of the family of cage molecules, CDs have a hydrophobic cavity, which is available for inclusion or encapsulation of suitable molecules. This host-guest type relationship is often exploited in order to modify the properties of encapsulated guest molecules with regard to their biological, chemical, and physical characteristics. Besides their commercial breakthrough in the 1980s mainly in the food and pharmaceutical industry, other important fields for applications of CDs are chromatography, catalysis, biotechnology, cosmetics, agriculture, medicine, hygiene, textiles, and the environment.[81]

5.1.1   The Discovery of Cyclodextrins and Elucidation of their Structure and Properties

CDs were first discovered in the late 19th century by the French chemist Antoine Villiers when he described the fermentation of potato starch with *Bacillus amylobacter*, which under certain conditions resulted in the formation of so-called dextrins.[82] While their structure at that time was unknown, the term "dextrins" had been used to generally describe (intermediate) degradation and/or decomposition products of starch.[83] In the same year, Villiers proposed the name "cellulosine" due to the similar properties compared to cellulose, which – like cellulosine – is also resistant to acid hydrolysis and lacks reducing sugars.[84]

In the early 20th century, the Austrian chemist and bacteriologist Franz Schardinger rediscovered the cellulosines reported by Villiers as crystalline side products of starch ingestion with a heat-resistant microorganism.[85] He investigated the polysaccharides employing a colorimetric iodine test and was able to distinguish between two crystalline dextrins A and B,[86] which he later named α- and β-dextrin.[87] Although Villiers is known as the discoverer of CDs, Schardinger is acknowledged as being the "Founding Father" of CD chemistry, which is why they were called Schardinger dextrins until the 1970s. One of his most remarkable achievements, however, was the isolation of the microorganism that expresses the enzyme responsible for CD synthesis by degradation of starch. This novel

microorganism, namely *Bacillus macerans*, gave the same dextrins as before but in contrast to Villiers' *Bacillus amylobacter* produced the crystalline polysaccharides in a 10-fold higher yield.[88] Astonished about this result, Schardinger identified an explanation for his findings in the work of Robert Koch, a German physician and microbiologist, who had already stated that the bacillus Villiers employed for starch digestion was probably contaminated with *Bacillus macerans* due to the sterilization conditions he applied.[89]

Although Schardinger never elucidated the structure of α- and β-dextrin, his hypothesis that they are cyclic polysaccharides was later confirmed by Karl Johann Freudenberg,[90] who used a cryoscopic method for the determination of their molecular weights, being five glucose units for α- and six for β-dextrin.[91] His findings, however, were placed in doubt by Dexter French, claiming that the method used by Freudenberg would have been inappropriate for determination of high molecular weights due to interference of impurities that have low molecular weights. Together with Robert E. Rundle, French determined the correct molecular weights of α- and β-dextrin by applying X-ray diffraction and crystal density measurements, revealing the numbers of glucose units as six for α- and seven for β-dextrin.[92] Furthermore, he isolated γ-dextrin and determined its molecular size and structure using X-ray experiments and paper chromatography after partial acid hydrolysis and enzyme digestion. French's experiments revealed eight joined glucose units for this dextrin.[93]

Although French was the first to correctly describe the molecular composition of α-, β-, and γ-CD, it was Freudenberg who initially reported their molecular structure by studying the chemical as well as enzymatic hydrolysis and acetolysis of permethylated dextrins. As a result of his experiments, he could demonstrate that the investigated dextrins had a cyclic structure composed of glucose units joined by α-(1→4) glycosidic linkages.[94] This type of connection forces the glucose units to arrange in a cone shape. While the conus contains an apolar cavity due to the carbohydrate carbon skeleton, the hydroxyl groups are located at the rims of the conus, giving these areas hydrophilic properties. In this context, a distinction can be drawn between the narrow edge (primary face) at which the primary hydroxyl groups are located, and the wide edge (secondary face, cf. Figure 5.1A) carrying the secondary hydroxyl groups. With increasing number of glucose units, the diameter of the conus increases from α- (0.57 nm) over β- (0.78 nm) to γ-CD (0.95 nm), giving rise to encapsulation of different guest molecules with varying sizes (Figure 5.1B).
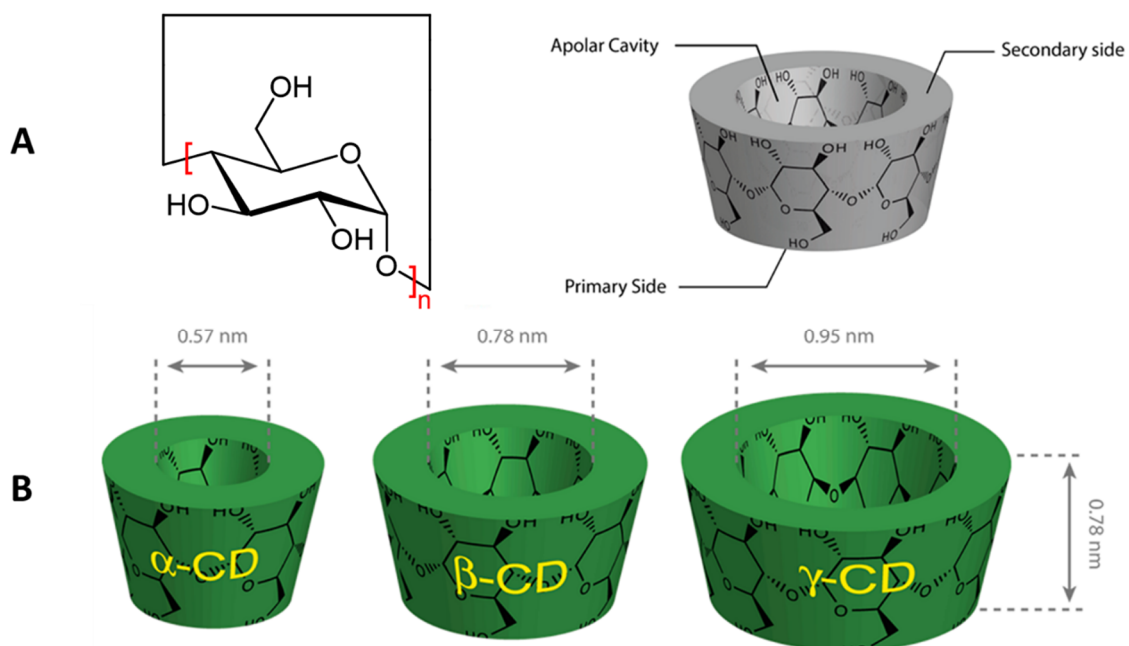
Figure 5.1: (A) Arrangement of glucose units in a circular fashion due to α-(1→4) glycosidic linkages results in the cone-shaped molecular structure of CDs. The narrow edge contains the primary hydroxyl groups (primary face) while the secondary hydroxyl groups are located at the wide edge (secondary face). (B) Geometric dimensions of α-CD (n = 6), β-CD (n = 7), and γ-CD (n = 8).[81] Modified from reference 81.

An outstanding feature of CDs is their ability to encapsulate various (mainly) hydrophobic guest molecules. Already hypothesized by Schardinger in the early 20th century, this property was extensively researched later by Friedrich Cramer, who performed studies in solution as well as in the solid state. He discovered that the CDs toroidal form allows them to complex a variety of guest molecules in their apolar cavity (Figure 5.2).[95] Moreover, Cramer reported that the inclusion of guest molecules is a reversible process based on an equilibrium between the association and dissociation of host and guest.[96] The reason for the reversibility of this process are the rather weak forces involved in encapsulation, such as hydrophobic interactions, van der Waals forces, and hydrogen bonding. Using kinetic, spectroscopic and competitive inhibition methods, Cramer determined the dissociation constants of CD complexes with various guests and showed that not only highly apolar, aliphatic and aromatic hydrocarbons can be complexed but also polar substances, such as acids, amines, halogens, and, interestingly, even (noble) gases.[95-97]
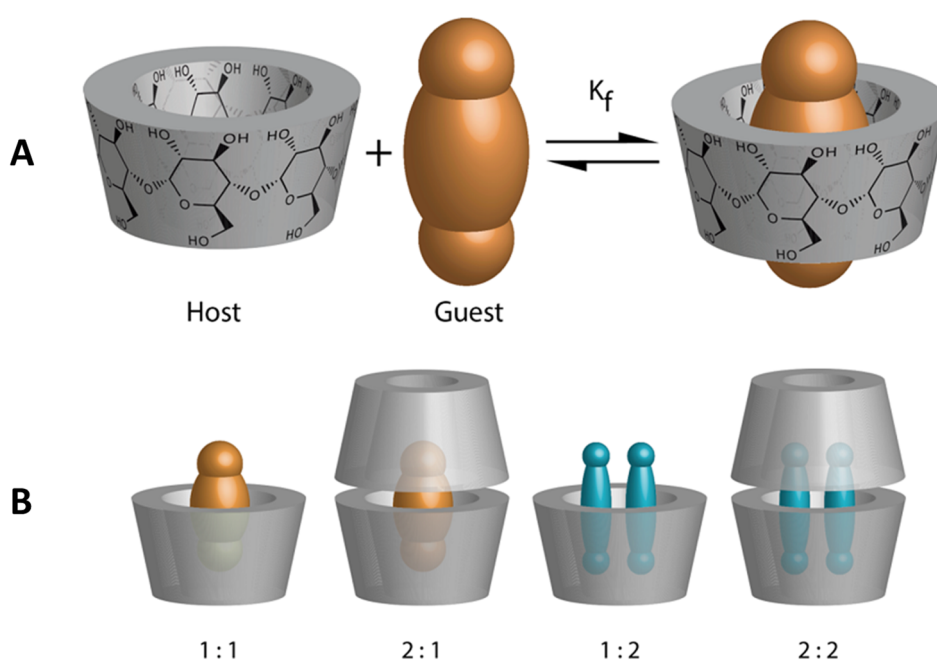
Figure 5.2: (A) Inclusion of guest molecules into the CD cavity is a reversible process based on an equilibrium between the association and dissociation of host and guest. (B) Inclusion complexes exist in different stoichiometric proportions depending on the size and structure of the guest as well as the host.[81]

5.1.2   Cyclodextrins and Their Applications

Cramer's investigations about CD inclusion complexes are acknowledged as the origin from which various applications resulted in research as well as in the chemical and pharmaceutical industry. The first patent for CD application was filed in 1953 as a collaboration of Karl Freudenberg, Friedrich Cramer, and Hans Plieninger, comprising the most important characteristics of CDs as protective agents for air-sensitive substances and for enhancing the water-solubility of hydrophobic substances.[98] With this patent, the foundation stone for the pharmaceutical application of CDs was laid, which, however, did not start until the 1970s because of their suspected toxicity French reported on.[99] Interestingly, this issue was resolved in the mid-1960s by reports revealing that the true toxicity was due to impurities trapped inside the CDs.[100] After the non-toxicity of CDs was progressively accepted by the pharmaceutical and chemical industry, high-scale production led to a significant price drop of CDs and increased their further application until today.

In the chemical industry, CDs have been produced, for instance, as stationary phases for high performance liquid chromatography (HPLC) and gas chromatography (GC). As immobilized chiral architectures, they offer the possibility to separate enantiomers and diastereomers, which is quite demanding and often impossible by the use of standard column materials.[101] Another interesting application of CDs lies in their utilization as catalysts of chemical

reactions in a similar manner as enzymes. Although Cramer had already given the base for supramolecular catalysis through CDs,[102] this field was extensively researched by Myron Lee Bender, who, for example, studied the influence of CDs on the cleavage of functional groups, such as esters, amides, phosphates, carbonates, and sulfates, but also other chemical reactions like acyl migration and decarboxylation.[103] CDs also play an important role in environmental sciences, where they find application as solubilization agents for organic pollutants but also in accumulation and removal of organic contaminants and heavy metals from water, soil, and atmosphere.[104]

There is a large number of pharmaceutical applications for CDs. In most cases, they are utilized as drug carriers when the water solubility of a drug is restricted. In this aspect, the drug's inclusion into the CD cavity enhances the transport through the cellular membrane, which it has to cross in order to develop its effect. Importantly, the lipophilic membrane only has a low affinity for the hydrophilic CD[105] so that it remains outside of the cell while the drug passes the membrane. Not only does the complexation of a drug improve its delivery, it also facilitates the administration of volatile compounds, for instance, in the form of tablets.[106] Moreover, CDs are often applied to mask the bitter or irritant taste of drugs and, in some cases, can also reduce their unpleasant odors.[107]

The latter example especially points out the accessibility of CDs for general consumers in everyday life. Here, they are frequently applied for stabilization, odor control, and conversion of liquid ingredients into a solid form. Preventing unpleasant odors, for example, in diapers, female hygiene products, or paper towels is often achieved by dry CD powder, which reduces the volatility of smelly mercaptans, and addition of a hydroxypropyl β-CD surfactant provides antimicrobial activity.[108] Long-lasting fragrances have been produced by complexation with CDs, increasing the energy barrier for evaporation of volatile compounds so that they are slowly released over a long period of time.[109] Other interesting sectors of application are foods and flavors, where CDs are often utilized for flavor protection and flavor delivery but they have also become popular in food processing for removal of cholesterol from animal products and masking of bitter components in citrus fruit juices.[107]

Furthermore, azobenzene derivatives have been widely investigated as guest molecules, which form stable inclusion complexes with CDs. Interestingly, encapsulation of these guests preferentially occurs in the *E* form while the *Z* isomer is not capable of entering the CD cavity or is expelled after photoisomerization of the encapsulated *E* form.[110] This property has been exploited in many studies in order to influence supramolecular assembly processes but also gated-ion channels have been created, whose function relies on CD-azobenzene inclusion complexes.[111]

Samanta *et al.* reported on a dynamic supramolecular system, which is able to capture and release different lectins in response to irradiation with UV light.[112] Here, vesicles that have been created from amphiphilic CDs acted as hosts for cross-linkers with an azobenzene and a carbohydrate moiety. After inclusion of the azobenzene present in the *E* form, binding of an azobenzene lactoside by peanut agglutinin (PNA) resulted in crosslinking of the complexes. Exposing the dense multilamellar complexes to UV light effected photoisomerization of the azobenzene moiety and, consequently, led to the transition from a high-affinity, multivalent state to a low-affinity, monovalent state (Figure 5.3).
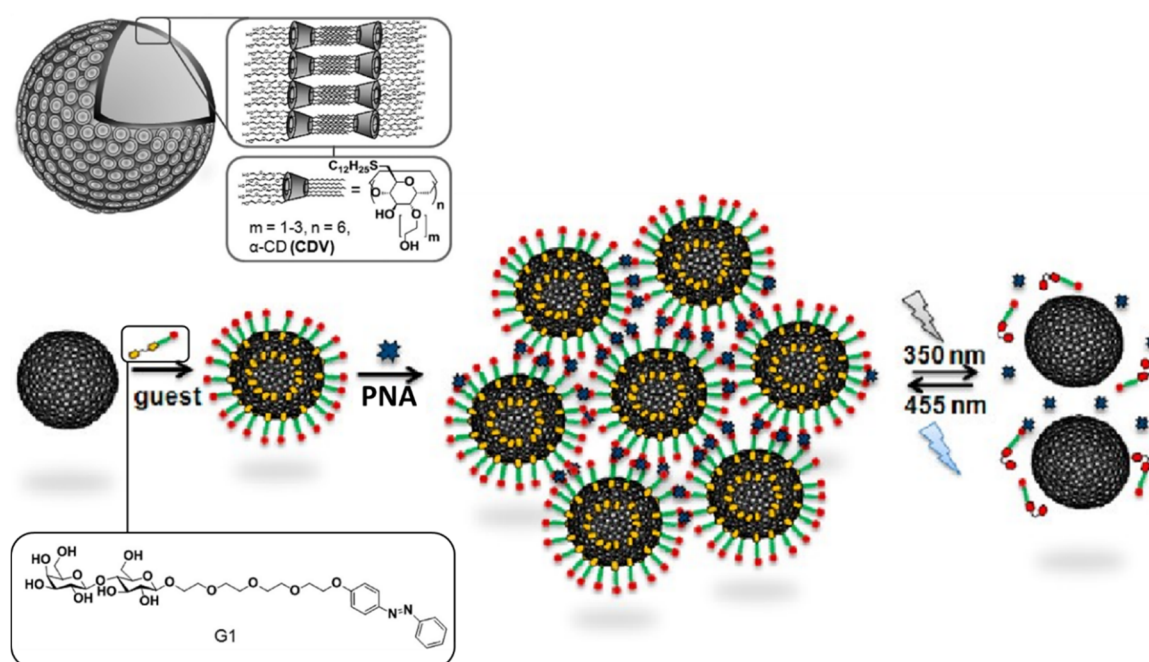
Figure 5.3: Assembly of amphiphilic CD vesicles, noncovalent cross-linkers with an azobenzene and a carbohydrate moiety (G1), and the lectin PNA leads to dense multilamellar complexes. Irradiation with UV light results in isomerization of the azobenzene units, causing the transition from a high-affinity, multivalent state to a low-affinity, monovalent state.[112] Modified from reference 112.

In another example, the Harada group reported a thermo- and light-responsive azobenzene CD complex, which consists of a CD host covalently bound to a hydrocinnamoyl linker *via* a polyethylene glycol spacer, which is terminated with an azobenzene guest moiety (6-Az-PEG600-HyCiO-β-CD, cf. Figure 5.4 left).[113] The group performed 2D ROESY NMR experiments to study the conjugate's complexation behavior and observed a strong temperature and concentration dependence. Recording NMR spectra at 30 °C revealed that a self-inclusion complex was formed, where the CD cavity alternatively encapsulates the aromatic part of the hydrocinnamoyl linker and the azobenzene moiety. However, when measured at 1 °C, only the aromatic part of the linker was included while exclusive inclusion of the azobenzene unit occurred at 60 °C. Furthermore, it was reported that the complex existed in a dethreaded form

at 80 °C and intermolecular complexes preferentially formed at high concentrations. Interestingly, UV light irradiation caused a conformational change to a self-inclusion complex, in which the CD cavity includes the azobenzene part irrespective of the concentration applied.
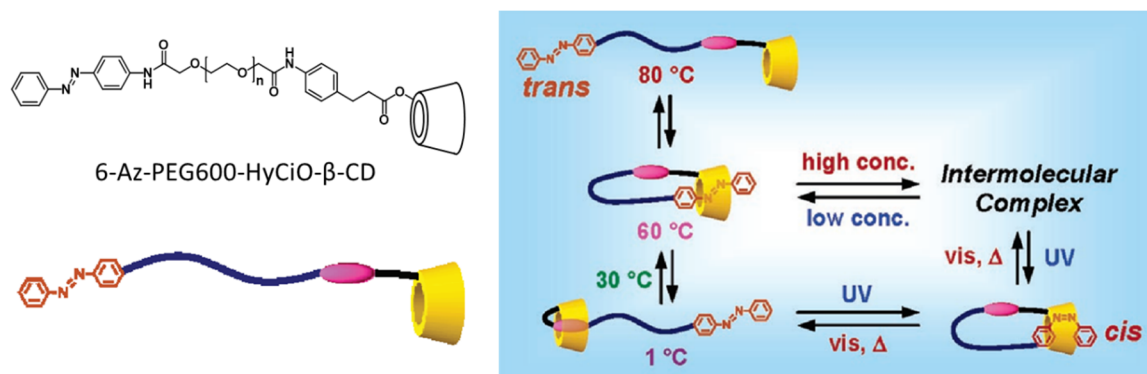
Figure 5.4: Molecular structure and schematic depiction of the CD complex (6-Az-PEG600-HyCiO-β-CD, left). Proposed conformational changes of the CD complex in aqueous solution by external stimuli (right).[113] Modified from reference 113.

This chapter covers different approaches for the development of a novel assay system, which enables investigation of switchable cell adhesion based on CD inclusion complexes. Research presented in Chapter 5.2 involves initial approaches concerning the assay system whereas the results mentioned in Chapter 5.2.1 are part of the bachelor thesis of V. Thoms.[114] Chapter 5.2.2 contains results gathered from a short term scientific mission at the CSIC – University of Seville. Advanced research on the assay system is described in Chapter 5.3 while parts of this chapter are reported in the bachelor thesis of S. O. Jaeschke.[115] The preparation of compounds and performance of biological tests described in Chapter 5.3 was done in collaboration with A. Müller.

5.2 Covalent and Non-covalent Immobilization of Cyclodextrin Derivatives for Investigation of Bacterial Adhesion

Due to their remarkable ability to form inclusion complexes with suitable, mainly hydrophobic guest molecules, CDs can not only be utilized for this purpose in solution but also when assembled on surfaces.[116] While this property has been researched particularly in the field of supramolecular chemistry, it has also become an important issue for biochemistry and bioorganic chemistry. As mentioned in Chapter 5.1.2, CDs have been successfully employed for inclusion of azobenzene glycoconjugates in order to achieve switching of processes such as lectin binding. In analogy, switching of bacterial adhesion may be a feasible approach as well. Therefore, I designed a new type of binding assay, which allows for switchable cell adhesion to photoresponsive ligands that are assembled on supramolecular surfaces.

For the development of the assay system, two approaches were pursued, which differ in the nature of the employed CD hosts as well as the glycoconjugate guest molecules. While the first approach involved covalent immobilization of amino-functionalized CD derivatives onto activated microtiter plates (cf. Chapter 5.2.1), in the second approach, supramolecular surfaces were created by non-covalent immobilization of amphiphilic CD derivatives (cf. Chapter 5.2.2). In order to effect inclusion complex formation, the fabricated CD surfaces were subsequently treated with the respective guest molecule, which, besides the mannose moiety, bears a hydrophobic portion (azobenzene or adamantane; detailed molecular structures are discussed in the respective chapter), allowing for inclusion into the CD cavity. As a result, mannose moieties are presented on the supramolecular surface and are available for binding by the bacterial lectin FimH.

There are two ways to achieve reversible adhesion of bacteria to the supramolecular surface. One is the competitive displacement of the encapsulated guest molecule with a guest which undergoes stronger interactions with the CD cavity. Since inclusion complex formation is a reversible process, which is influenced by an equilibrium, competitive displacement can be controlled by adjusting the concentration of the competing guest molecule (in case both guests have a similar molecular structure). The other possibility, which is also more elaborate since a competitive guest is not needed, is photo-switchable displacement of the encapsulated guest molecule. For this, a photoresponsive azobenzene guest is required. As described in the introduction, exclusively the *E* isomer can insert into the CD cavity while the bulkier, more hydrophilic *Z* isomer does only show weak inclusion properties. This, of course, offers the opportunity to convert an already included azobenzene glycoconjugate into its *Z* isomer by photoirradiation, resulting in disruption of the inclusion complex. As a consequence, adhesion

of bacteria to the supramolecular surface is attenuated, as no mannose moieties are available for binding (Figure 5.5).
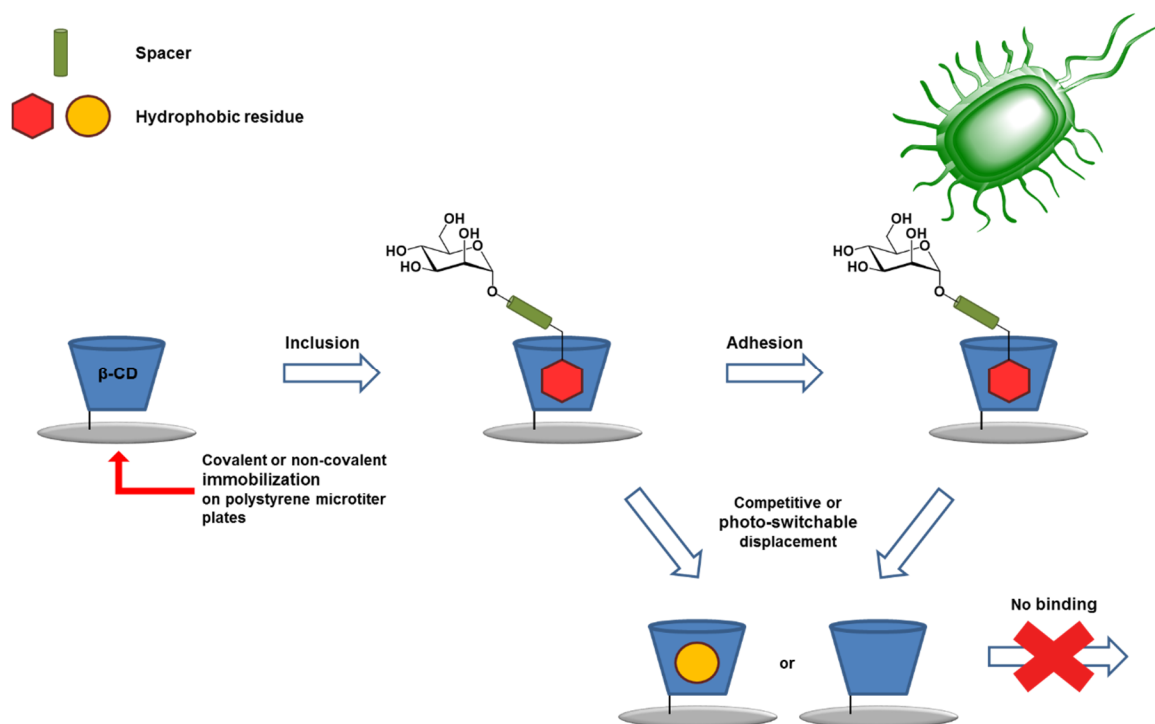
Figure 5.5: Outline for CD-based adhesive surfaces. CD derivatives that are covalently or non-covalently immobilized onto a polystyrene surface are capable of forming inclusion complexes with carbohydrate-ligands containing a hydrophobic residue. Once inclusion complexes are formed, the carbohydrate can be bound by type 1 fimbriated *E. coli*. Competitive or photo-switchable displacement of the guest encapsulated in the CD cavity results in attenuation of bacterial binding.

5.2.1 Bacterial Adhesion by Application of Covalently Immobilized Cyclodextrins

5.2.1.1 Synthesis of Cyclodextrin Derivatives and Azobenzene Guest Molecules

For proper functionalization of activated microtiter plates with CDs, an appropriate CD precursor was needed. The well-known mono-6-azido-6-deoxy-β-CD (**50**)[117] was chosen for this purpose. Applying this CD derivative in a 1,3-dipolar cycloaddition with propargylamine creates a suitable compound for surface immobilization *via* the amino group. The synthesis of this amino-functionalized CD **51** is not only straight-forward but can also be commenced from inexpensive β-CD (**48**).

First, one of the primary hydroxyl groups of β-CD (**48**) was tosylated by utilization of 1-(*p*-toluenesulfonyl)imidazole,[118] giving the corresponding tosylate **49**.[119] The azido-β-CD **50** was then obtained by simple nucleophilic substitution with sodium azide. Copper catalyzed 1,3-

dipolar cycloaddition with propargylamine gave the amino-functionalized CD **51**, which was used for immobilization without further purification (Scheme 5.1A).

In order to compare the immobilization of CD **51** with that of a standard mannoside, an amino functionalized mannoside **53** was prepared. Therefore, 2-azidoethyl α-D-mannoside (**52**)[120] and propargylamine were reacted in a copper-catalyzed cycloaddition, giving mannoside **53**, which was also used without further purification for the immobilization process (Scheme 5.1B).
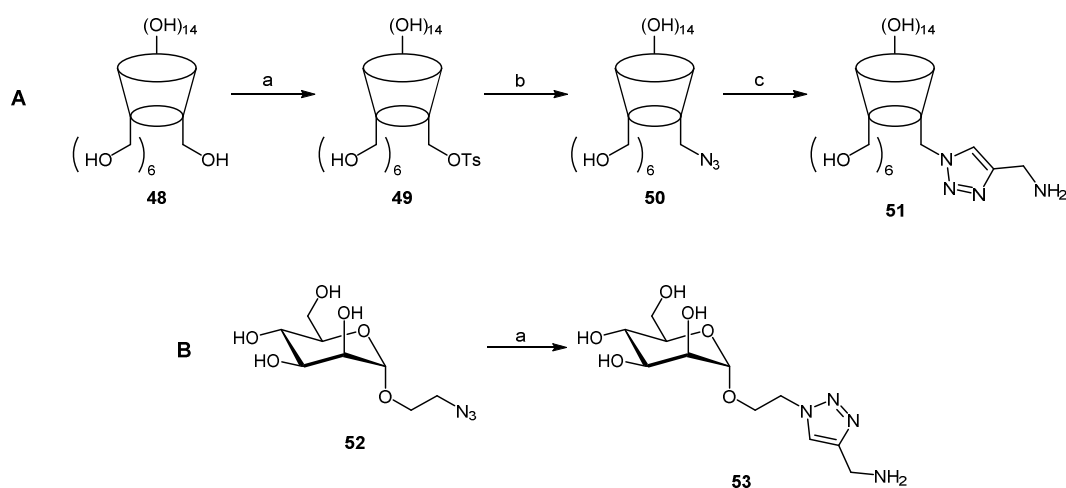
Scheme 5.1: A) Synthesis of CD derivative **51**. a) 1-(*p*-toluenesulfonyl)imidazole, H$_2$O, rt, 2 h, 32%; b) NaN$_3$, H$_2$O, 120 °C, 16 h, 42%; c) propargylamine, CuSO$_4$·5 H$_2$O, sodium ascorbate, DMF/H$_2$O (3:1), rt, 2 h, crude product. B) Synthesis of mannoside **53**. a) propargylamine, CuSO$_4$·5 H$_2$O, sodium ascorbate, DMF/H$_2$O (3:1), rt, 2 h, crude product.

After synthesis of CD **51** and mannoside **53**, an appropriate photoresponsive guest molecule was synthesized. Here, the choice fell upon a simple azobenzene mannoside **59**, which contains a triethylene glycol spacer between the mannose moiety and the azobenzene. This spacer was added to the glycoconjugate in order to improve its water solubility since it has been found earlier that plain azobenzene mannosides tend to show decreased water solubility.[121]

The synthesis was started with the preparation of the azobenzene triethylene glycol ether **56** by a nucleophilic substitution reaction with *p*-phenylazophenol (**55**) and chloride **54**. The resulting alcohol **56** was then glycosylated with trichloroacetimidate **57**[122] employing BF$_3$-etherate as a promoter, yielding the unprotected mannoside **59** after subsequent Zemplén[123] deacetylation of mannoside **58** (Scheme 5.2).
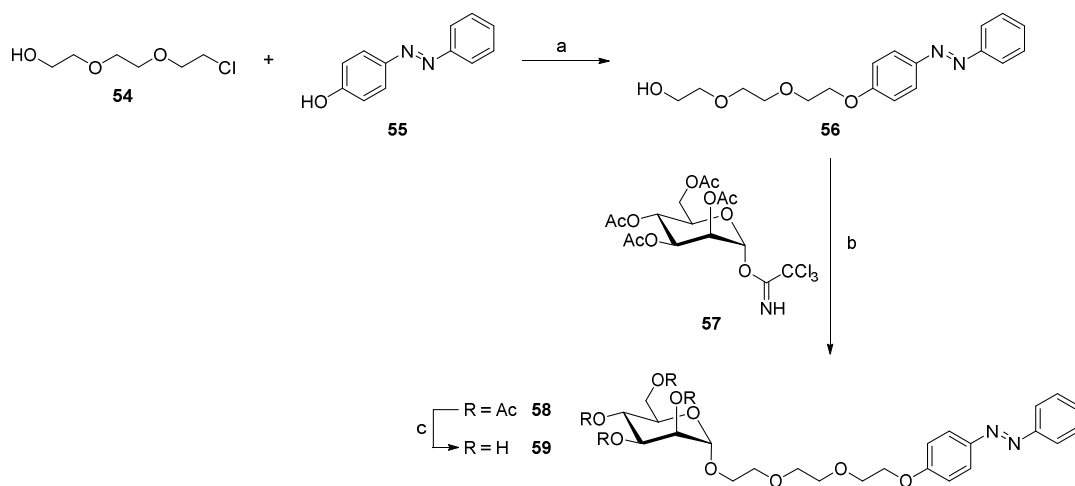
Scheme 5.2: Synthesis of azobenzene mannoside **59**. a) KOH, *n*-BuOH, 140 °C, 3 d, 70%; b) BF$_3$·Et$_2$O, CH$_2$Cl$_2$, rt, 16 h, 42%; c) NaOMe, MeOH, rt, 16 h, 92%.

5.2.1.2 Validating Surface Functionalization

Before the biological testing, the immobilization of CD **51** was validated and compared to that of mannoside **53**. For this purpose, a phenol-sulfuric acid assay[124] was performed after both compounds had been covalently immobilized onto activated microtiter plates. This assay offers the possibility to determine the concentration of immobilized glycoconjugates on the surface *via* photometric detection of the absorbance at 490 nm. Therefore, calibration lines were deduced from dilution series of azido CD **50** as well as 2-azidoethyl α-D-mannoside (**52**) (Figure 5.6).
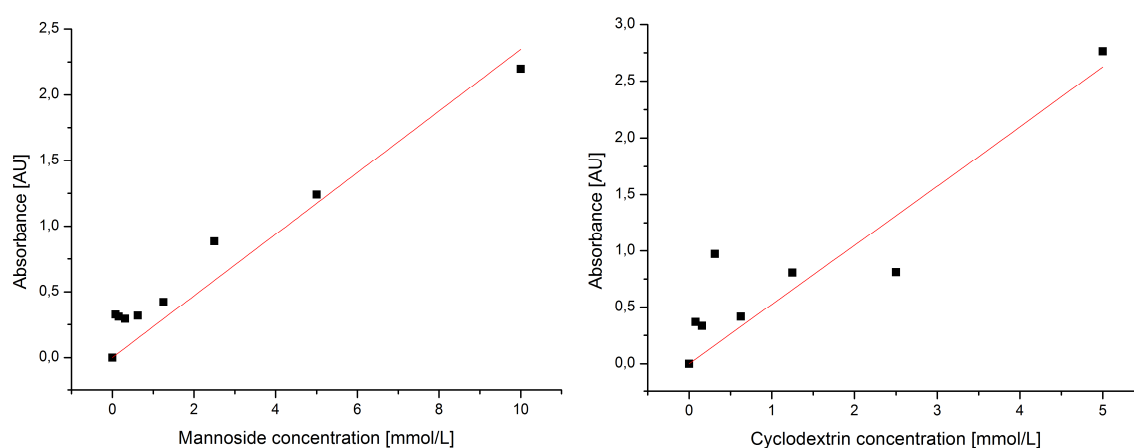
Figure 5.6: Phenol-sulfuric acid assay. Calibration lines were deduced from dilution series of 2-azidoethyl α-D-mannoside (**52**, left) and azido-CD **50** (right).

Using the functional equation of the CD **50** calibration line considers the 7-fold valency of the CD. In this way, the concentrations of both immobilized compounds **51** and **53**, as calculated from the calibration lines, can be directly compared (Table 5.1).

Table 5.1: Results from the phenol-sulfuric acid assay of mannoside **53** and CD **51** immobilized onto polystyrene.

	Average value of absorbance	Calculated concentration [mmol/L]
Mannoside **53**	0.164 ± 0.043	0.598 ± 0.162
CD **51**	0.151 ± 0.030	0.208 ± 0.058

Comparing the calculated concentrations reveals that immobilization of mannoside **53** is more efficient than that of CD **51**, resulting in a higher concentration on the surface. Despite the limited sensibility of the phenol-sulfuric acid assay, the results show a successful immobilization of CD **51**.

5.2.1.3   Biological Testing

Before testing the inclusion of the synthesized azobenzene guest molecule **59**, followed by bacterial adhesion to the mannose moieties presented, the functional surface itself was first investigated towards type 1 fimbriae-mediated bacterial adhesion in order to preclude unspecific interactions of bacteria with the CD surface. Therefore, mannoside **53**, CD **51** as well as propargylamine were immobilized on activated microtiter plates by application of 10 mM solutions of the respective compound. Then, the plates were incubated with GFP-transfected *E. coli* (pPKL1162) and after washing, bacterial adhesion was measured by readout of the fluorescence intensity (Figure 5.7).
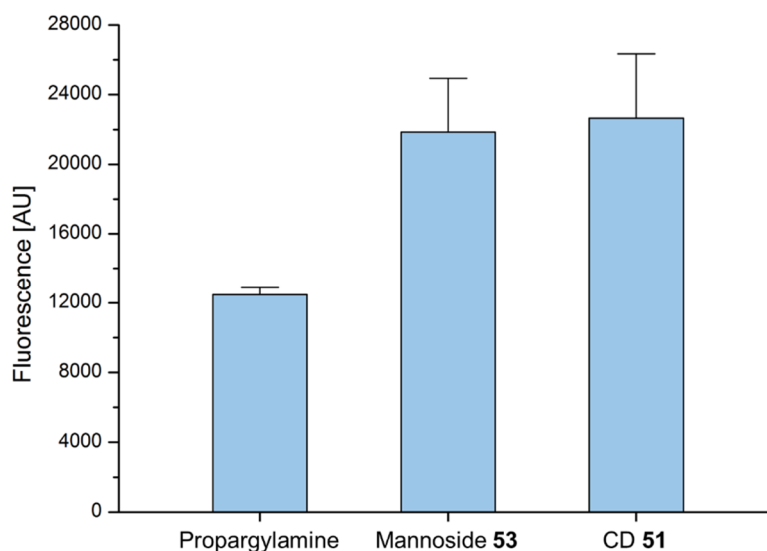
Figure 5.7: Bacterial adhesion to microtiter plates functionalized with propargylamine (left), mannoside **53** (middle) and CD **51** (right). The fluorescence values shown resulted from incubation with a bacteria suspension of 2 mg/mL.

The adhesion studies show that immobilization of propargylamine alone resulted in more than 50% of bacterial binding when compared to CD **51** which gave the highest fluorescence value. Unfortunately, both values for mannoside **53** and CD **51**, respectively, are in the same range. It can be speculated that the *E. coli* strain used for the experiments is not only capable of specific binding to mannose residues but also shows similar adhesion properties towards glucose units of the β-CD derivatives.

For further investigation of bacterial binding, plain β-CD (**48**) was used as an inhibitor of type 1 fimbriae-mediated bacterial adhesion. Performance of an adhesion-inhibition assay was very important at this point since the previously observed binding behavior could also be a result of unspecific binding to the supramolecular surface. Thus, mannan-coated microtiter plates were prepared, incubated with fluorescent *E. coli* and subsequently, serial dilutions of β-CD (**48**) and MeMan were employed on the plate. After washing, fluorescence was detected, delivering inhibition curves from which IC_{50} values were deduced where possible (Figure 5.8).
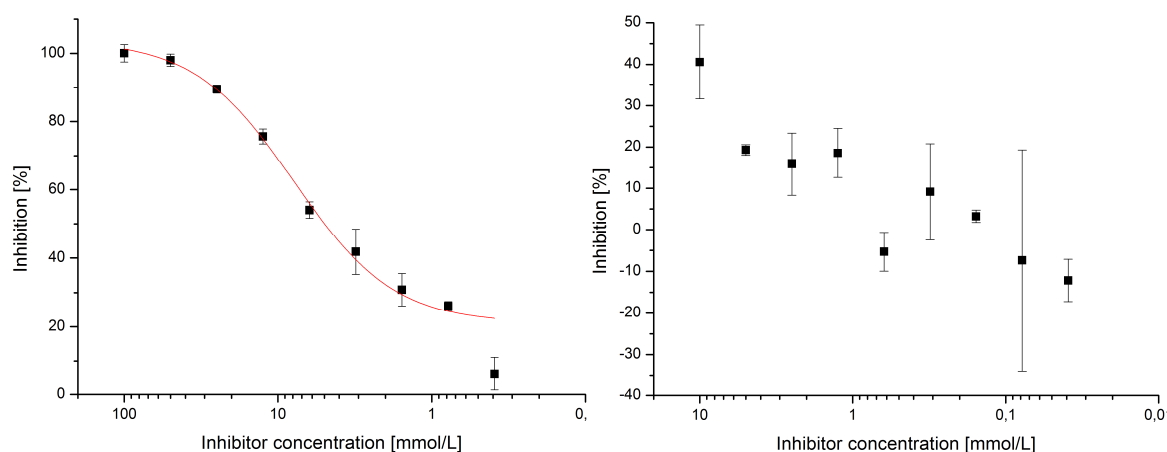
Figure 5.8: Inhibition curves obtained with MeMan (left) and β-CD (**48**, right) from inhibition of type 1 fimbriae-mediated bacterial adhesion to mannan-coated microtiter plates. Non-linear regression gave the sigmoidal concentration-response curve for MeMan while this was not possible for β-CD (**48**). Error bars result from triplicate values on one plate.

While the inhibition curve of MeMan shows a sigmoidal shape and delivers an IC_{50} value of 4.20 mM, non-linear regression was not possible for the inhibition curve of β-CD (**48**). Presumably, a sigmoidal shape might be observed when testing higher concentrations, though this was not possible due to the restricted water solubility of β-CD (**48**).

Although inhibition of bacterial adhesion by β-CD (**48**) did not result in a sigmoidal curve and the respective IC_{50} value could not be deduced, it is apparent that MeMan is a better inhibitor. This raises the question, why bacterial adhesion to the supramolecular surface was observed in the previous experiments. The results gathered from the adhesion-inhibition assay suggest that a possible affinity of FimH for glucose (as in CD **51**) can be ruled out as a reason for this adhesion behavior. More likely, the observed adhesion could be a result of unspecific interactions of the lectin with the supramolecular surface or with unfunctionalized parts of the polystyrene surface, resulting from incomplete immobilization.

To conclude, the approach described in this chapter turned out to be not as promising as expected. In order to further investigate this assay system, the nature of the supramolecular surface needs to be modified so that unspecific binding of bacteria to the surface can be precluded. Therefore, a different approach, which involves the non-covalent immobilization of amphiphilic CD derivatives, will be discussed in the following chapter. Furthermore, application of the azobenzene guest molecule **59** will be demonstrated as well.

5.2.2 Application of Amphiphilic Cyclodextrins for Non-covalent Immobilization

It was described earlier that substrates with long alkyl chains can be immobilized on polystyrene microtiter plates due to their ability of undergoing hydrophobic interactions with the surface. Using this approach, glycoSAMs were fabricated by non-covalent immobilization of amphiphilic substrates.[125] Furthermore, SAMs of amphiphilic CDs on hydrophobic and hydrophilic substrates have been established.[126] Applying this approach to the investigated assay system will be discussed in this chapter. Thus, not only the targeted CDs were modified but also two different mannosides were chosen as guest molecules for inclusion complex formation. Furthermore, it was decided to perform an ELLA-type (enzyme-linked lectin assay) variation of the assay by using an HRP (horseradish peroxidase) conjugate of the mannose-specific lectin Con A before investigating type 1 fimbriae-mediated bacterial adhesion.

The CD derivatives chosen for immobilization were modified with either C_6, C_{12}, or C_{14} alkyl chains on the primary face and were compared towards their applicability in the binding assay. While one of the guest molecules employed was azobenzene glycoconjugate **59** (cf. Chapter 5.2.1), a different guest molecule in this chapter consists of three portions, which each serve a different purpose: a hydrophobic adamantane residue, a guaiazulene moiety and a mannose portion.

Adamantane derivatives are known to form very stable inclusion complexes with CDs and have been widely used in the field of supramolecular chemistry as guest molecules.[127] Therefore, this portion was incorporated into the guest molecule for undergoing strong interactions with the hydrophobic CD cavity. While the mannose portion will be used for the actual binding of the mannose-specific lectin Con A, the guaiazulene portion serves a completely different purpose. As already described in Chapter 3.3, guaiazulene – as an azulene derivative – has a strong blue color and was previously used in the CSP methodology as a color tag. In this approach, however, the color of the guaiazulene tag is exploited for photometric determination of the actual concentration of ligands on the supramolecular surface.

With these components at hand, the concept can be understood as explained in Chapter 5.2, considering investigation of lectin binding instead of bacterial adhesion (Figure 5.9).
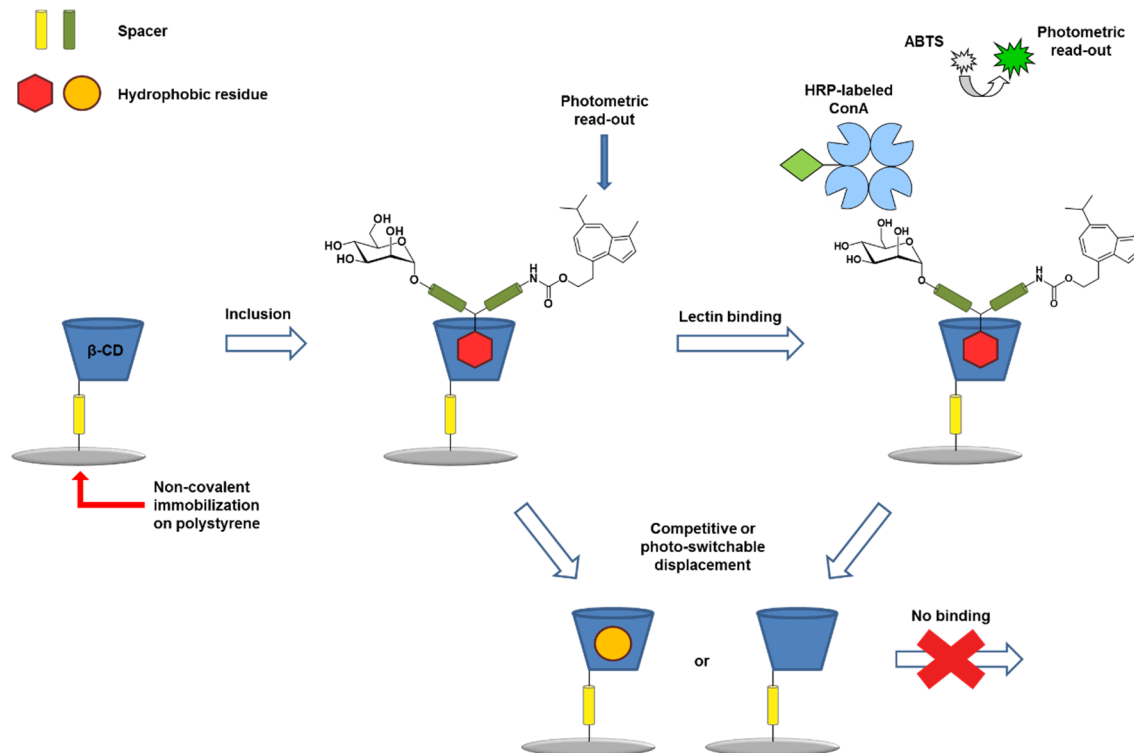
Figure 5.9: Amphiphilic CD derivatives that are non-covalently immobilized to a polystyrene surface are capable of forming inclusion complexes with carbohydrate-ligands containing a hydrophobic residue. The extent of host-guest-complex formation can be monitored by guaiazulene supported photometric read-out. Once inclusion complexes are formed, the carbohydrate can be bound by lectin Con A. Depending on its chemical structure the ligand can be removed from the CD cavity by competitive or photo-switchable (in case of an azobenzene guest molecule) displacement, thus, attenuating lectin binding.

The following work was done in collaboration with the research group of Jose Manuel García Fernández during a short term scientific mission at the CSIC – University of Seville.[128]

Results and Discussion

5.2.2.1   Synthesis of Cyclodextrin Derivatives and Mannoside Guest Molecule 64

For non-covalent immobilization on polystyrene microtiter plates, three amphiphilic CD derivatives 61,[129] 62, and 63 were synthesized, which differ in the length of the alkyl chains that are connected to the primary face of the CD. For better comparison of how different lengths affect the immobilization, C_6, C_{12}, and C_{14} alkyl chains were chosen.

The synthesis of the amphiphilic CD derivatives was started from plain β-CD (48) in an Appel-analogous reaction with triphenylphosphine and *N*-bromosuccinimide, which furnished heptakisbromo CD 60.[130] Then, a nucleophilic substitution reaction with carboxylates of the respective fatty acids hexanoic, dodecanoic, and tetradecanoic acid, respectively, was

performed, giving the targeted amphiphilic CD derivatives **61-63** in moderate to low yields. Since long alkyl chains promote micelle formation, precipitation and filtration of the products was getting more problematic when heading towards higher chain lengths, resulting in a significant drop in yield.
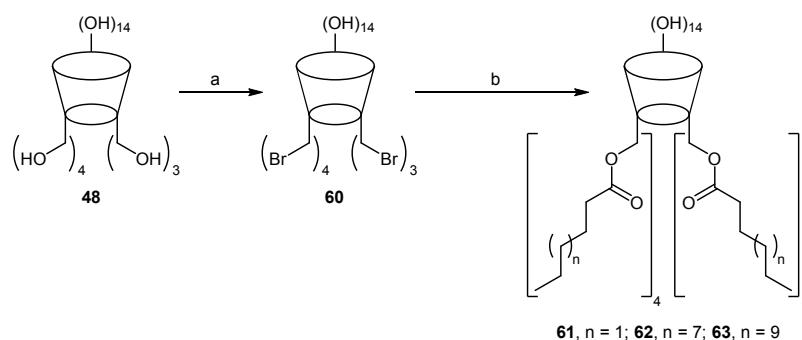
Scheme 5.3: Synthesis of amphiphilic CD derivatives **61-63**. a) 1. PPh$_3$, NBS, DMF, 80 °C, 16 h; 2. NaOMe, MeOH, rt, 2 h, 96%; b) n = 1, hexanoic acid, Cs$_2$CO$_3$, DMF, 50 °C, 72 h, 60%; n = 7, dodecanoic acid, Cs$_2$CO$_3$, DMF, 50 °C, 72 h, 38%; n = 9, tetradecanoic acid, Cs$_2$CO$_3$, DMF, 50 °C, 72 h, 9%.

Next, the synthesis of mannoside guest molecule **64** was performed. Retrosynthetic analysis reveals that all three portions can be easily connected through a branching unit that contains three different functional groups (Scheme 5.4).
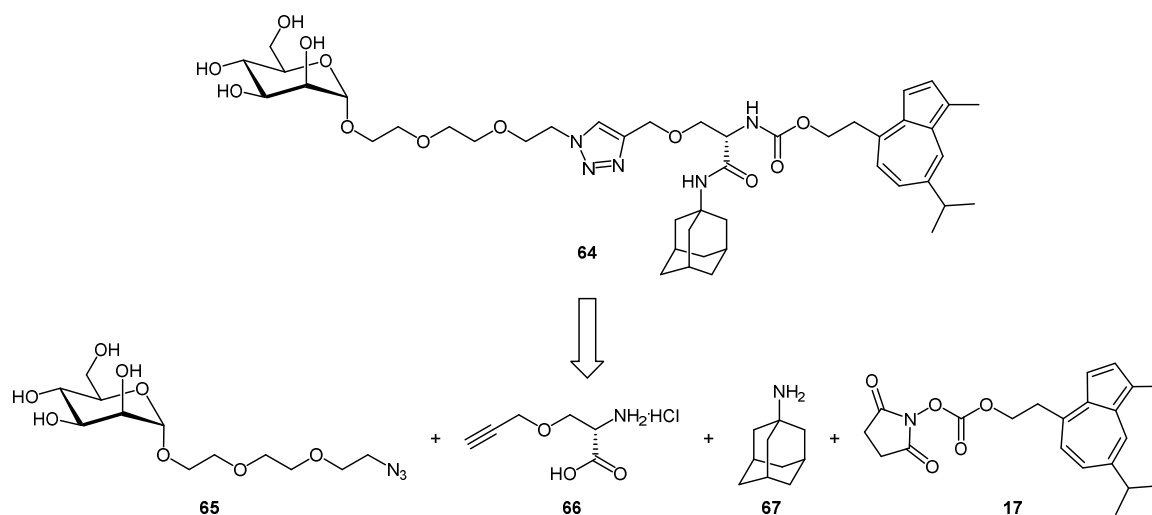
Scheme 5.4: Retrosynthetic analysis of mannoside guest molecule **64**. Disconnection results in three precursor molecules **17**, **65** and **67** that can be joined with each other through *O*-propargyl-L-serine hydrochloride **66** as the branching unit.

For this, *O*-propargyl-L-serine hydrochloride **66**[131] is perfectly suited since the alkyne can be addressed for cycloaddition with mannose conjugated azide **65**,[132] the amino group can form a carbamate by reaction with guaiazulene carbonate **17** (cf. Chapter 3.3) and the carboxylic acid can be joined with adamantylamine (**67**). The synthesis of *O*-propargyl-L-serine hydrochloride **66** was commenced by base promoted alkylation of Boc-protected L-serine **68** with sodium hydride and propargyl bromide, giving alkyne **69** in excellent yield. *O*-propargyl-L-serine hydrochloride **66** was then obtained in good yield by Boc-deprotection with hydrochloric acid (Scheme 5.5).
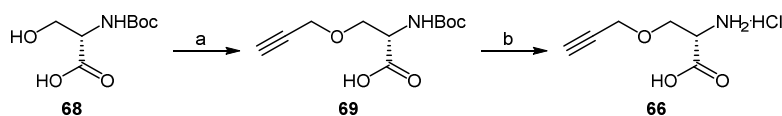
Scheme 5.5: Synthesis of *O*-propargyl-L-serine hydrochloride **66**. a) propargyl bromide, NaH, DMF, rt, 16 h, 96%; b) HCl (aq.), EE, rt, 1 h, 84%.

Next, the well-known mannoside **65** was prepared for further linkage with the branching element. Lewis-acid promoted glycosylation of triethylene glycol **54** with pentaacetyl α-D-mannose (**70**)[133] was performed, giving chloride **71**[134] in moderate yield. Then, by nucleophilic substitution with sodium azide, azide **72** was obtained in good yield and subsequent Zemplén deacetylation furnished mannoside **65**.
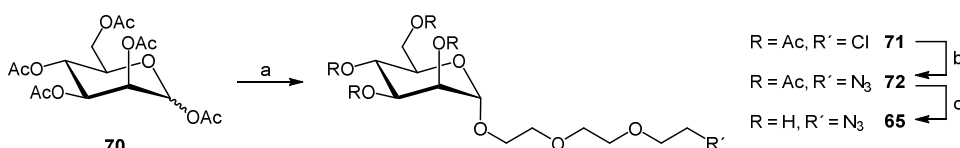
Scheme 5.6: Synthesis of mannoside **65**. a) **54**, BF$_3$·Et$_2$O, CH$_2$Cl$_2$, rt, 16 h, 63%; b) NaN$_3$, TBAI, DMF, 60 °C, 16 h, 89%; c) NaOMe, MeOH, rt, 16 h, 96%.

In order to facilitate and accelerate the further synthesis of guest molecule **64** by taking advantage of the intense blue color of guaiazulene, carbonate **17** (cf. Chapter 3.3) was first coupled to the branching unit before the other required portions. Then, the adamantyl residue was introduced by HBTU- and HOBt-promoted amide coupling of adamantylamine (**68**) and carboxylic acid **73**, giving amide **74** in good yield. The last step in this pathway was the connection of unprotected mannoside **65** to the branching element in a 1,3-dipolar cycloaddition. However, experiments revealed that this reaction resulted in formation of side products, which were not separable from the desired product **64**. Therefore, it was preferred

to couple the acetyl-protected mannoside **72** instead, giving the acetylated product **75** in a moderate yield of 50% (55% based on conversion, 5% starting material reisolated). Since the reaction was accommodated by formation of diversely colored side products, the guaiazulene portion may have suffered from decomposition or substitution, which explains the drop in yield. The mannoside guest molecule **64** was then finally obtained by employing Zemplén conditions for deacetylation of precursor **75**.
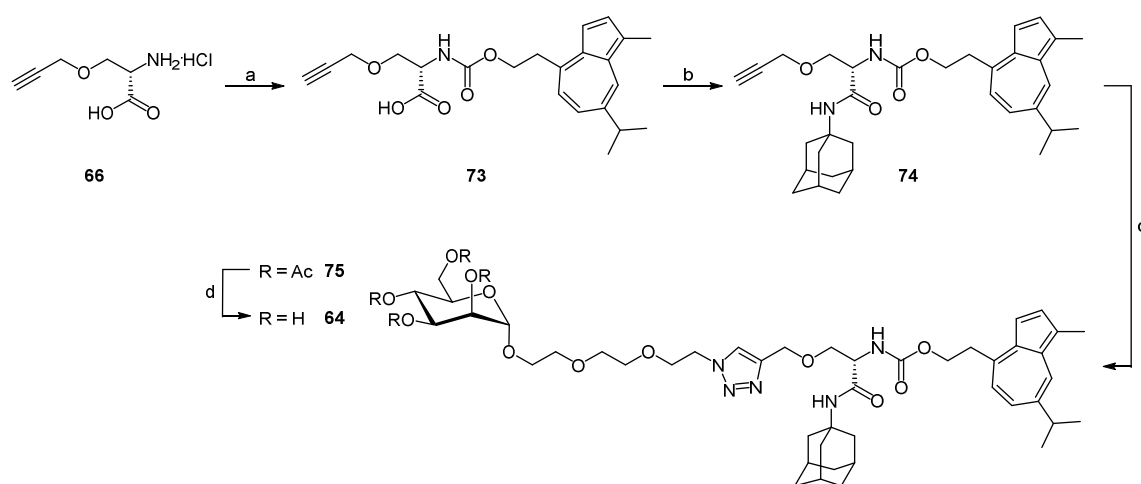
Scheme 5.7: Synthesis of mannoside guest molecule **64**. a) **17**, NaHCO₃, THF/H₂O (1:1), rt, 16 h, 90%; b) **67**, HBTU, HOBt, DIPEA, DMF, rt, 16 h, 89%; c) **72**, CuSO₄·5 H₂O, sodium L-ascorbate, DMF/H₂O (3:1), rt, 16 h, 50%; d) NaOMe, MeOH, rt, 16 h, 88%.

5.2.2.2   Lectin Binding Assay

For investigation of the previously synthesized compounds in the ELLA-type assay, the initial step performed was employing amphiphilic CDs **61-63** on polystyrene microtiter plates in order to achieve non-covalent immobilization onto the surface. Since the solubility of these compounds in PBS (phosphate buffered saline) dropped significantly with increasing alkyl chain length, CD solutions were prepared from respective DMSO stock solutions with a maximum DMSO content of 1%. The standard procedure reported by Lindhorst *et al.* for immobilization of amphiphilic substrates on polystyrene surfaces[125] is desiccation of the substrate solution on the plate. Due to the DMSO content, however, this procedure could not be applied since immobilized CDs could possibly redissolve in DMSO and, thus, be removed by washing afterwards. Instead, the plates were incubated overnight and subsequently washed several times to remove excess CD solution. At this point it was essential to avoid buffers containing detergents in order to ensure that already immobilized CDs were not removed from the surface.

Then, inclusion of mannoside guest **64** as well as azobenzene mannoside **59** (cf. Chapter 5.2.1.1), respectively, into the CD cavity was performed. Therefore, serial dilutions of ligand solutions were applied on the CD-covered plates. Due to the poor water solubility of mannoside **64**, respective ligand solutions were prepared from DMSO stock solutions as explained earlier. After washing and blocking with bovine serum albumin (BSA), absorbance at 600 nm was measured for photometric determination of the ligand concentration on the surface of the plates that were incubated with guaiazulene derivative **64**. Interestingly, no absorbance could be detected at this wavelength, indicating that the concentration of ligand was below the limit of detection. Nevertheless, the plates were finally incubated with peroxidase-labeled Con A and after washing, ABTS (2,2´-azino-bis(3-ethylbenzo-thiazoline-6-sulphonic acid) was added, resulting in a color reaction. In this way, the extent of lectin bound to the ligands on the surface could be monitored by measuring the absorbance at 405 nm, giving the respective binding curves (Figure 5.10).
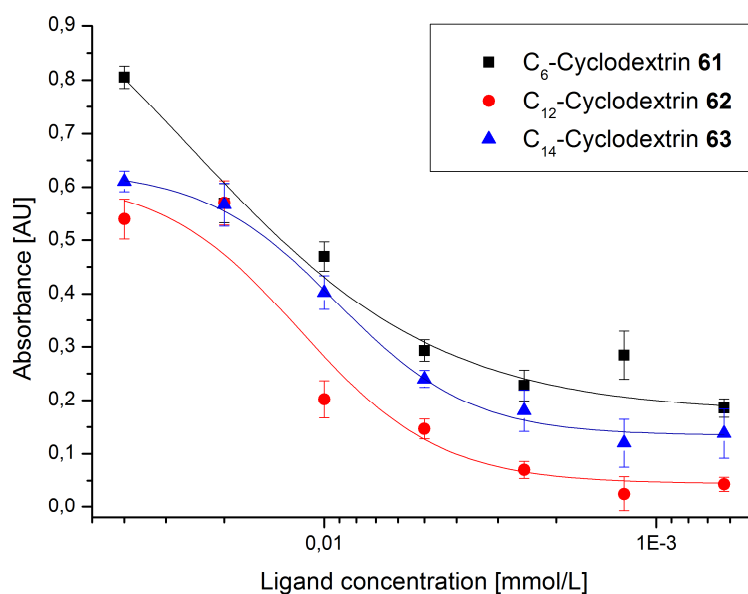
Figure 5.10: Lectin binding to microtiter plates covered with CDs **61** (black), **62** (red), and **63** (blue). While the concentration for CD immobilization was kept at 5 μM, the concentration of ligand **64** for inclusion complex formation was varied. Error bars result from duplicate values on one plate.

The binding curves obtained from the plates incubated with mannoside **64** show an increase of absorbance with increasing concentrations of ligand. This confirms that the inclusion of ligands into the immobilized CDs was successful and, hence, the actual immobilization process as well. On closer inspection, it becomes evident that the functionalization of the surfaces was differently efficient depending on which CD was used. CDs **62** and **63**, which both have relatively long alkyl chains in comparison to **61**, show similar curves. However, the curve of CD **61** has a higher absorbance value at the highest ligand concentration, indicating that

immobilization seems to be more effective in this case. Nevertheless, the ligand concentrations used for testing were too low because the rising absorbance had not yet reached a plateau. Therefore, higher concentrations were to be tested in the following experiments.

In order to investigate if photo-induced isomerization of azobenzene mannoside **59** results in disruption of the inclusion complex and, thus, switches lectin binding, the plates were treated with this ligand as well. However, this did not result in observable lectin binding, no matter which CD derivative was used for immobilization. It appears that inclusion of the azobenzene residue is not as efficient as that of the adamantane residue in **64**. However, application of higher ligand concentrations may result in better inclusion and detectable lectin binding.

Although it was planned to perform further experiments concerning the improvement of the assay as well as investigation of bacterial adhesion in this format, future research on this topic was terminated. The reason for this was a publication by Jonkheijm *et al.*[135], which was published shortly after the initial experiments were performed. In this publication, an assay system is described which is similar to the one discussed here and involves switching of lectin and bacterial binding to azobenzene glycoconjugates that are assembled on a supramolecular surface. Jonkheijm and coworkers succeeded in fabricating a surface of amphiphilic CDs and induced inclusion complex formation with azobenzene mannosides. Lectin as well as bacterial binding to the surface was then measured and later attenuated by irradiation with UV light, causing isomerization of the azobenzene moiety and, thus, disruption of the previously formed inclusion complexes. Jonkheijm employed an imprinting technique for immobilizing the amphiphilic CD derivatives onto different surfaces, which presumably facilitated and enhanced this process.

Although Jonkheijm succeeded in an early publication of his results, the feasibility of this approach could be confirmed and investigation of this assay format from a different point of view may be promising. Therefore, A. Müller and I initiated another project, which deals with a variation of the assay described in this chapter.

5.3 Switching Bacterial Adhesion by Means of Cyclodextrin Inclusion Complexes on Photoresponsive Surfaces

In another approach, a reversed variant of the binding assay that was discussed in the previous chapters was investigated. The basic concept therein is the same, however, the inclusion scenario between the azobenzene and the CD takes place on a photoresponsive surface of covalently immobilized azobenzene derivatives either on polystyrene microtiter plates or magnetic polyethylene glycol (PEG) beads. For this purpose, two azobenzene derivatives were employed, which, despite their similar molecular structure, greatly differ in their photochemical properties, giving rise to two different types of photoresponsive surfaces. For inclusion complex formation, two CD conjugates are employed, which contain an alkyl or an aromatic mannoside connected to the β-CD *via* a triazole linkage. Once the azobenzene moiety is encapsulated, the mannose unit of the respective CD conjugate is presented on the surface and accessible for type 1 fimbriae-mediated bacterial adhesion. In order to prove the switching of bacterial binding, the surface can be exposed to UV light prior to incubation with the fluorescent bacteria. In this way, disruption of the inclusion complexes is induced and the CD conjugate is released, thus, making the surface inadhesive (Figure 5.11).
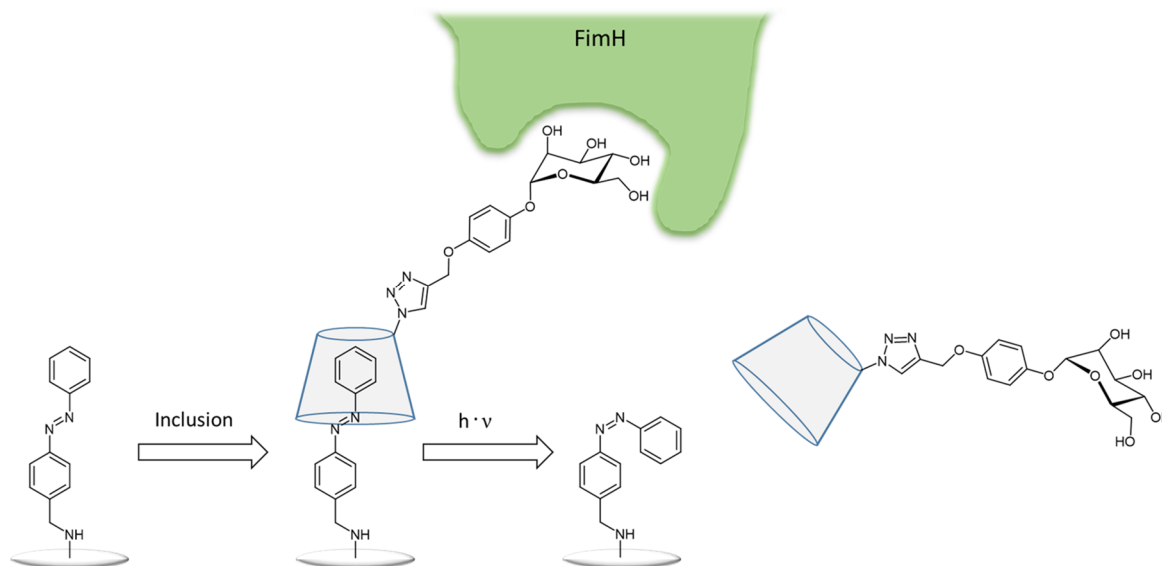
Figure 5.11: Inclusion of a mannose CD conjugate occurs on a photoresponsive surface of a covalently immobilized azobenzene derivative. Binding of the mannose moiety of the CD conjugate by the bacterial lectin FimH results in bacterial adhesion to the supramolecular surface. Exposure to UV light leads to disruption of the inclusion complexes, thus, making the surface non adhesive.

The procedure described above proves the inclusion complex formation as well as the switching process just in an indirect way since the fluorescence measurement is not possible until the performance of bacterial binding. To overcome this hurdle and directly prove the inclusion on the surface, a fluorescein-tagged CD derivative was prepared and employed as a host. In this way, the inclusion complex formation as well as the UV light mediated disruption of the complex can be directly validated through fluorescence read-out.

For this project, A. Müller synthesized precursor mannoside **89** and azobenzene derivative **82** while I performed the synthesis of all CD-derived compounds (for precursors cf. Chapter 5.2) and azobenzene derivative **83**. Both of us performed the biological tests and interpreted the obtained data.

Results and Discussion

5.3.1   Synthesis of Azobenzene Guest Molecules and CD Hosts

Since the surfaces used for the assays were prefunctionalized with either carboxylate groups or activated functional groups, such as active esters, azobenzene derivatives that bear an alkyl amino group were needed for covalent immobilization. Therefore, two different azobenzene derivatives **82** and **83** were synthesized, which differ in the substitution of the aromatic system but have both a methylene amino group available for coupling with the respective surface.

The first step in the synthesis of azobenzene derivative **82** was the condensation of 4-[*N*-Boc-aminomethyl]aniline (**76**) with nitrosobenzene (**77**) employing Mills reaction[136] conditions, giving the Boc-protected product **80** in good yield. Final deprotection with trifluoroacetic acid gave the target compound **82** quantitatively. For the synthesis of azobenzene derivative **83**, nitroso compound **78**[137] was prepared from 4-[*N*-Boc-aminomethyl]aniline (**76**) by oxidation with Oxone®. The crude product was obtained as a mixture of the nitroso compound **78** and the respective nitro derivative, which, however, was unproblematic for direct use in the next step. Condensation of crude **78** and *p*-anisidine (**79**) was performed also by employing Mills reaction conditions, giving the product **81** in a moderate yield. The target compound **82** was then obtained by quantitative deprotection with trifluoroacetic acid (Scheme 5.8).

Additionally, the Boc-group of **80** was cleaved with concentrated aqueous hydrochloric acid, giving the respective ammonium hydrochloride **20** in a quantitative yield. This azobenzene derivative was, however, not used for surface immobilization but as a reactant for an Amadori rearrangement reaction (cf. Chapter 3.3).
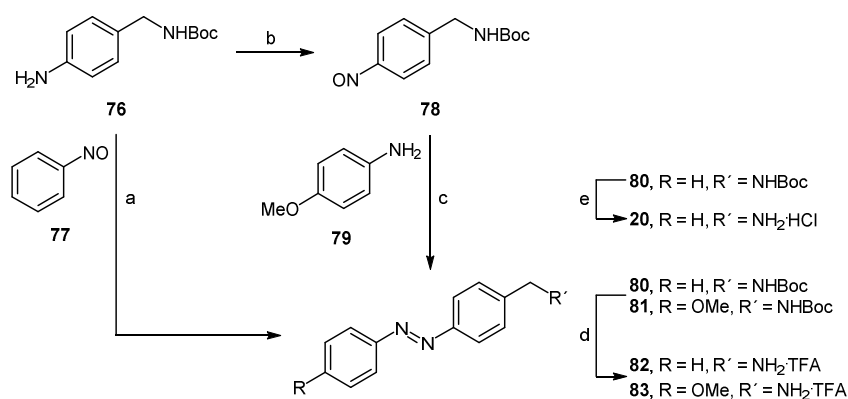
Scheme 5.8: Synthesis of azobenzene derivatives **82** and **83**. a) DMSO, AcOH, rt 16 h, 75%; b) Oxone®, H_2O, CH_2Cl_2, rt, 16 h, 48%; c) DMSO, AcOH, rt, 16 h, 82%; d) TFA, CH_2Cl_2, rt, 1 h, R = H, quant., R = OMe, quant; e) CH_2Cl_2, HCl_{aq}, rt, 4 h, quant.

For the synthesis of CD conjugates **85** and **90** it was decided to couple azido-β-CD **50** (cf. Chapter 5.2.1.1) with two precursor mannosides in a simple CuAAC reaction. Therefore, it was required that both mannosides contain a propargyl function accessible for the cycloaddition. The choice herein fell upon propargyl α-D-mannoside (**84**)[138] and an aromatic mannoside **89**, in which the propargyl function is located at the opposite side of the phenyl ring.

CD conjugate **85** was prepared by directly coupling propargyl α-D-mannoside (**84**) with azido-β-CD **50** under CuAAC conditions. The pure product **85** could be isolated after purification by gel permeation chromatography in a very good yield (Scheme 5.9A).

The first step of the synthesis of aromatic CD conjugate **90** was Lewis acid-promoted glycosylation of mannose pentaacetate (**70**) with hydroquinone (**86**), giving the aromatic mannoside **87** in a good yield. In the next step, the propargyl function was introduced at the phenolic position by alkylation with propargyl bromide. The resulting acetyl-protected mannoside **88** was obtained in a fair yield and was then deacetylated. Final coupling of azido-β-CD **50** with mannoside **89** by means of CuAAC gave the targeted CD conjugate **90** in a good yield after purification through RP chromatography (Scheme 5.9B).
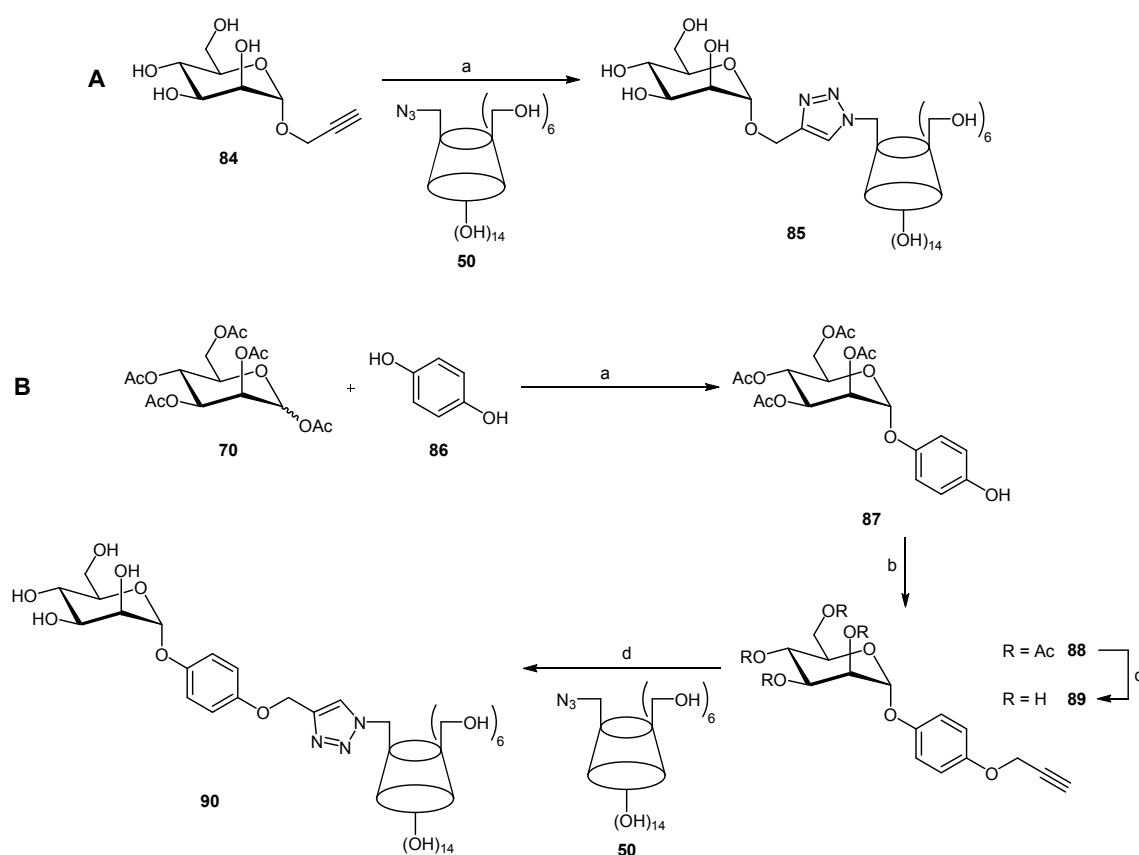
Scheme 5.9: A) Synthesis of CD conjugate **85**: a) CuSO$_4$ · 5 H$_2$O, sodium ascorbate, DMF/H$_2$O (3:1), rt, 16 h, 92%; B) Synthesis of CD conjugate **90**: a) BF$_3$ · Et$_2$O, CH$_2$Cl$_2$, MeCN, rt, 48 h, 71%; b) propargyl bromide, K$_2$CO$_3$, KI, MeCN, 70 °C, 16 h, 65%; c) NaOMe, MeOH, rt, 16 h, 81%; d) CuSO$_4$ · 5 H$_2$O, sodium ascorbate, DMF/H$_2$O (3:1), rt, 16 h, 78%.

As a precursor for the CD derivative **93**, amino-β-CD **91**[139] was prepared by reducing azido-β-CD **50** under Staudinger reduction conditions following a procedure from Tang *et al.*[140] Thiourea bridging with fluorescein isothiocyanate **92** finally gave the fluorescein-tagged CD derivative as the corresponding spiro form **93** in a fair yield (Scheme 5.10).
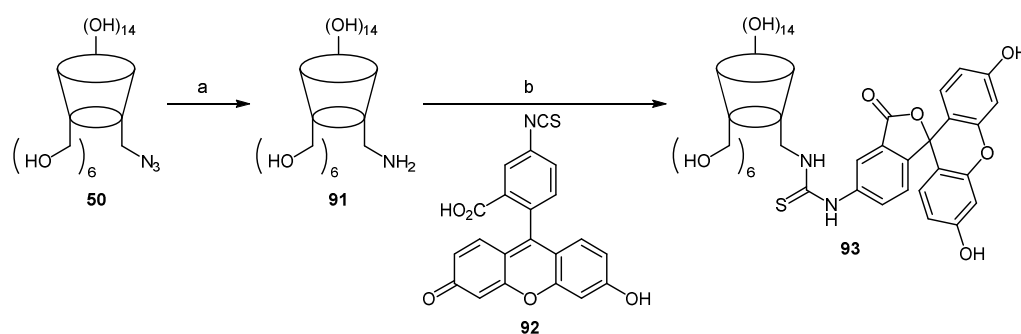
Scheme 5.10: Synthesis of fluorescein-tagged CD derivative **93**. a) 1. PPh$_3$, DMF, rt, 2 h; 2. H$_2$O, 90 °C, 2 h, 91%; b) DIPEA, DMF, rt, 16 h, 64%.

5.3.2   Biological Testing on Polystyrene Microtiter Plates

For investigation of bacterial adhesion to the CD conjugates, the photoresponsive surface of azobenzene guest molecules had to be fabricated. In the initial experiments only azobenzene derivative **82** was tested while testing of azobenzene derivative **83** as well as the validation of inclusion complex formation with fluorescein-tagged CD derivative **93** will be discussed in Chapter 5.3.3.

For fabrication of the photoresponsive surface, a 10 mM solution of azobenzene derivative **82** in carbonate buffer (pH 9.6) was incubated on polystyrene microtiter plates. Subsequently, the plates were washed for removal of unreacted azobenzene and deactivated with an ethanolamine solution. To induce inclusion complex formation on the surface, the microtiter plates were incubated with CD conjugates **85** and **90**, respectively, and excess CD conjugate was removed by washing. After incubation with fluorescent *E. coli* (PKL1162), fluorescence was measured for quantification of bacterial adhesion. As a reference, *p*-aminophenyl α-D-mannoside (*p*APMan) was always tested on the same plate. The obtained adhesion curves are shown in Figure 5.12.
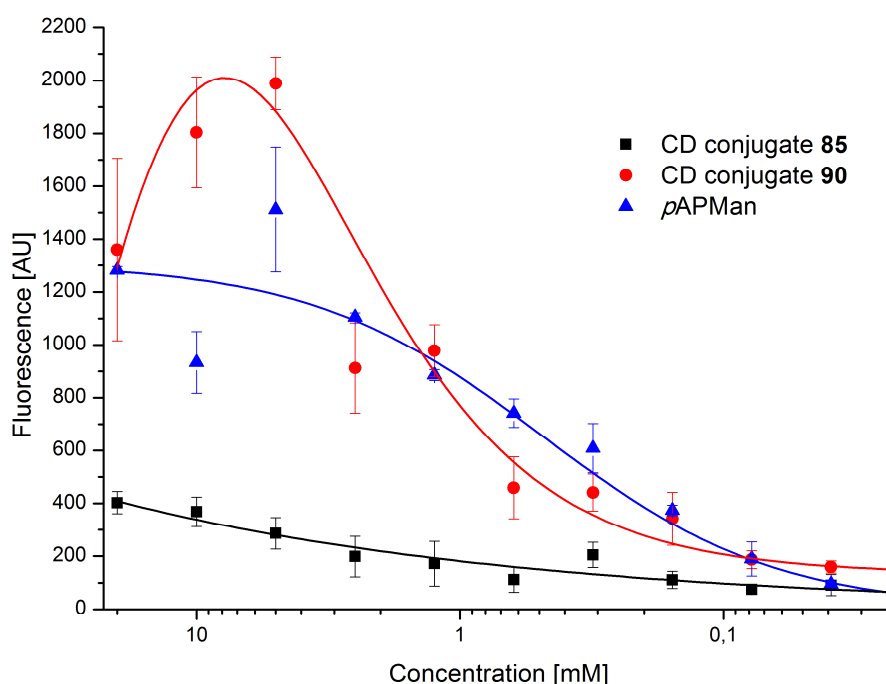
Figure 5.12: Bacterial adhesion to microtiter plates immobilized with azobenzene derivative **82**. While the concentration for immobilization was kept at 10 mM, the concentration of CD conjugates **85** and **90** for inclusion complex formation was varied. Error bars result from duplicate values on one plate.

The adhesion curves obtained from the initial experiments reveal that bacterial binding occurs in varying degrees depending on the inclusion complex present on the surface. Application of the aliphatic CD conjugate **85** resulted in low bacterial binding, which only moderately increases towards higher CD concentrations. The binding curve obtained from aromatic CD conjugate **90**, on the other hand, shows much higher bacterial binding and in its maximum even surpasses the binding curve of *p*APMan. As described in the general introduction (cf. Chapter 1.3), aromatic mannosides show a stronger binding to the bacterial lectin FimH due to additional interactions with the tyrosine gate near the CRD. These interactions also seem to be responsible for the stronger adhesion obtained from surfaces that were treated with the aromatic CD conjugate **90**. Furthermore, bacterial binding decreases substantially at higher CD concentrations, suggesting an increase of steric hindrance on the surface so that either inclusion complex formation is hampered or the bacterial adhesion itself.

These binding assays confirm that the overall concept is feasible and provides a solid foundation for further experiments involving irradiation with UV light for switching the surface's adhesive properties. Due to the low bacterial binding resulting from the aliphatic CD conjugate **85**, only the aromatic CD conjugate **90** was utilized in the following experiments.

In order to switch the adhesive properties of the photoresponsive surface, azobenzene-covered microtiter plates were fabricated according to the protocol described above. The microtiter plate was then divided into two parts whereby one part was exposed to UV light and the other was kept covered so that no irradiation could take place. Incubation with GFP-transfected *E. coli* was followed by fluorescence measurement. *p*APMan was immobilized on both parts of the plate as a control to ensure that the UV light does not influence the surface's integrity.

The obtained data (not shown) revealed that the part of the plate exposed to UV light irradiation showed decreased bacterial binding but had very strong internal fluctuations. It appears that photoisomerization of the azobenzene molecules on the surface indeed lead to disruption of the formed inclusion complexes and, hence, less bacterial binding. The fluctuations, however, indicate that the irradiation process is not optimal, which may be due to the experimental setup. Since the UV lamp is located above the microtiter plate, shadows are casted from the wall of each well resulting in an uneven distribution of radiation and therefore incomplete photoisomerization (Figure 5.13).
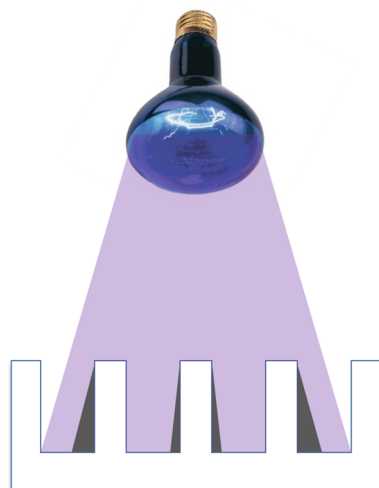
Figure 5.13: Schematic depiction of the experimental setup applied for irradiation of microtiter plates. Due to the location of the UV lamp above the plate, the walls cast a shadow on each well. As a result, not every well receives the same amount of radiation leading to incomplete photoisomerization.

The control wells that were treated with *p*APMan, however, also showed decreased bacterial binding after irradiation. This suggests that the surface's integrity had been influenced by the exposure with UV light. In this context, it has been reviewed earlier that polystyrene like many other polymers degrades when subjected to UV irradiation in the presence of air due to attack of free radicals formed in the polymer matrix.[141] Degradation of the polystyrene surface is a serious issue since it may have resulted in a change of the surface's functionalization and, thus, a decrease in the number of binding partners available for bacterial adhesion. At this point, it cannot be precluded that the decreased bacterial binding, which was detected in the wells treated with CD conjugate **90**, is not due to the collaps of the inclusion complexes after photoisomerization but may possibly be a consequence of surface degradation.

The results from the performed assays demonstrate that experiments involving irradiation on microtiter plates require a special setup since all wells must receive the same amount of radiation to ensure effective photoisomerization. It was speculated that shadows are casted on the wells due to the location of the UV lamp above the plate. Therefore, irradiation from under the plate might be a way to solve this problem. However then, transparent microtiter plates must be utilized, which, on the other hand, cannot be used for fluorescence measurements due to "crosstalk" interference between the wells. Instead, other options including HRP conjugated lectins or application of streptavidin/biotin-systems may be employed in this case.

More importantly, however, the material of the microtiter plates must be chosen with caution since irradiation with UV light seemed to have degraded the surface and supposedly changed

its functionalization. Fine-tuning of the azobenzene's substitution may be another option since certain substituents have been known to shift the wavelength for photoisomerization from shorter wavelengths in the UV region to longer wavelengths in the red to near-infrared (near-IR) region, which are less aggressive owing to their lower energy.[142]

On the basis of these facts, experiments on polymer-based microtiter plates were not further pursued. Instead, it was preferred to perform assays with magnetic PEG beads, which will be discussed in the following chapter.

5.3.3   Biological Testing on Magnetic PEG Beads

In further assays, PEG beads, which contain a magnetic core, were used as a replacement for the employed polystyrene microtiter plates since, besides their UV light compatibility, they offer interesting applications. Carbohydrate-functionalized PEG beads, for example, have been efficiently employed in the isolation and removal of bacteria from solution.[143] Acting as sensitive sensors for detection of *E. coli* bacteria, antibody-functionalized beads have been utilized for capturing bacteria, which subsequently initiated an electric detection mechanism by binding of guanine-labeled beads.[144]

Prior to bacterial adhesion experiments, the inclusion complex formation on the beads' surface was validated by utilizing the fluorescein-tagged CD **93**. Since the beads were prefunctionalized with carboxylate groups, the corresponding active esters had to be created by treatment with 1-ethyl-3-(3-dimethylaminopropyl)carbodiimide (EDC) and *N*-hydroxyl succinimide (NHS). Then, azobenzene derivatives **82** and **83**, respectively, were coupled to the beads' surface by incubation with a 10 mM solution of the respective azobenzene in carbonate buffer (pH 9.6). Subsequently, the beads were washed for removal of unreacted azobenzene and deactivated with an ethanolamine solution. Inclusion complex formation was induced by incubation with an 8 mM solution of fluorescein-tagged CD **93** and excess CD was removed by washing. The functionalized beads were then separated into two portions while one portion was irradiated with UV light (365 nm) and the other portion was kept in the dark. Then, inclusion of the CD derivative **93** as well as the disruption of the complexes was quantified by fluorescence detection (Figure 5.14). The obtained results from the fluorescence measurement are depicted in Figure 5.15A.
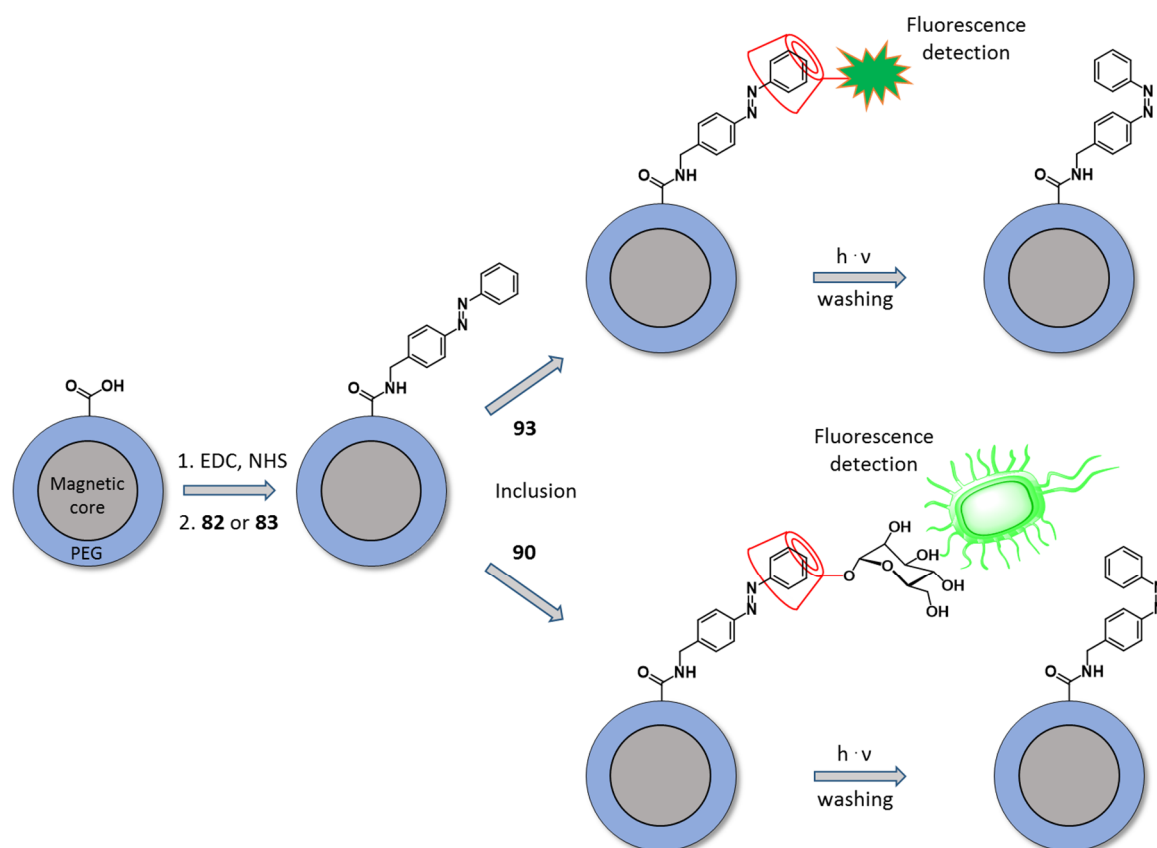
Figure 5.14: Outline for a protocol of photo-switchable cell adhesion to functional PEG beads, exemplified by beads functionalized with azobenzene **82**. Activation of the carboxylate groups on the beads' surface allows for immobilization of azobenzene derivatives **82** and **83**, respectively. Treatment with fluorescent CD conjugate **93** enables the validation of inclusion complex formation by direct fluorescence detection. Photoisomerization of the azobenzene units results in disruption of the complexes and, consequently, a decrease in fluorescence intensity. Bacterial adhesion can be investigated by treating the photoresponsive beads with CD conjugate **90** and incubating with fluorescent *E. coli*. Decreased bacterial adhesion can be achieved by photoirradiation, expelling the CD conjugate **90**.

For investigation of bacterial adhesion, functionalized beads were prepared according to the protocol described above. Therefore, the beads were treated with an 8 mM solution of CD conjugate **90**. Since irradiation with UV light would harm the bacteria and, thus, alter the result of the assay, irradiation of the beads was performed prior to incubation with the bacteria. For this, the functionalized beads were again separated into two portions while one portion was irradiated with UV light (365 nm) and the other portion was kept in the dark. Finally, both portions were incubated with GFP-transfected *E. coli* (PKL1162), subsequently washed and fluorescence was measured for quantification of adhesion. The obtained results are depicted in Figure 5.15B whereby the highest fluorescence value of each assay (at least three independent experiments) was normalized to 1.
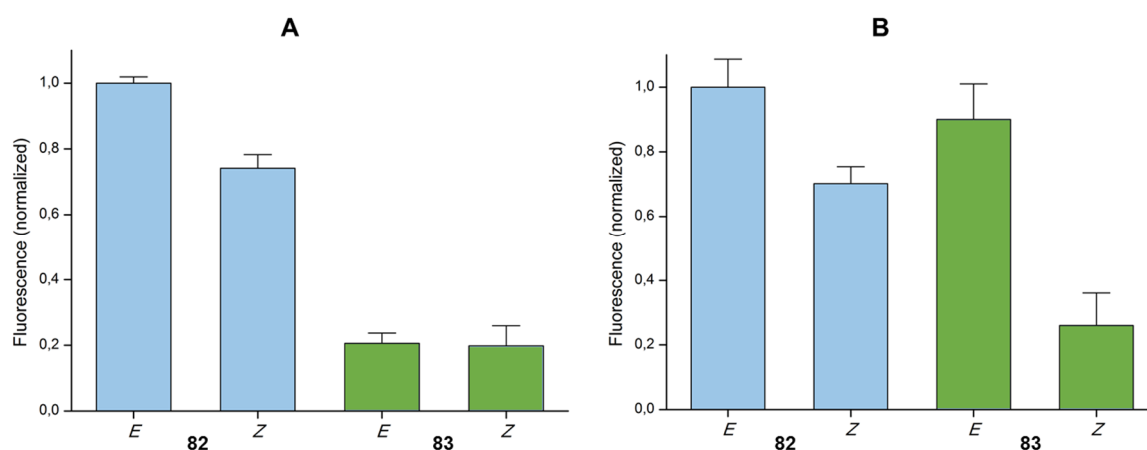
Figure 5.15: A) Measured fluorescence from inclusion of fluorescein-tagged CD **93** on magnetic PEG beads functionalized with azobenzene derivatives **82** (blue) and **83** (green), respectively, and the corresponding fluorescence after irradiation at 365 nm. B) Detected fluorescence resulting from bacterial adhesion to CD conjugate **90** on beads functionalized with azobenzene derivatives **82** (blue) and **83** (green), respectively, and after irradiation at 365 nm. The shown data sets represent average values from several (at least three) independent experiments.

Comparing the results depicted in Figure 5.15A reveals that inclusion complex formation is much more pronounced on beads functionalized with azobenzene derivative **82**, resulting in an almost fivefold higher detected fluorescence value compared to those treated with **83**. As far as the efficiency of photoinduced complex disruption is concerned, azobenzene **82** shows nearly 26% of decrease in fluorescence while in the case of azobenzene **83** no mentionable difference between both isomers could be observed. Keeping these results in mind, interpretation of the data obtained from bacterial adhesion studies (Figure 5.15B) shows a different scenario. Here, adhesion is almost equally efficient on both types of functionalized beads. Comparing the efficiency of photoinduced complex disruption, however, reveals that prior irradiation prevents bacterial adhesion by 30% for azobenzene **82** and by 74% for azobenzene **83**. These findings are in accordance with the compounds' individual *E/Z* ratio in the photostationary state (cf. Experimental Section) whereas azobenzene derivative **83** has a higher *Z* amount than **82**.

The obtained results raise the question why inclusion complex formation with fluorescein-tagged CD **93** was very low on beads functionalized with azobenzene derivative **83**. It could be argued that an insufficient immobilization of the azobenzene was the reason for this issue. However, the same beads were used in the bacterial adhesion studies, which, on the contrary, provided good results. One possible reason for the hampered inclusion can be related to the rather bulky fluorescein residue, which is located quite close to the primary face of the CD and may have caused steric clash with the azobenzene's methoxy group.

6. Conclusions

Exploration of the Amadori Rearrangement for Bioconjugation of Carbohydrates

Since it was previously demonstrated that the Amadori rearrangement has potential as a selective ligation method for efficient conjugation of unprotected sugars and amines, the aim of this project was to further investigate this reaction by employing different substrates. The article "Are D-*manno*-configured Amadori Products Ligands of the Bacterial Lectin FimH?" focused on the evaluation of the Amadori rearrangement for the preparation of ligands for the bacterial lectin FimH (Figure 6.1). The synthesis of an appropriate heptopyranose as a starting material for the synthesis of *manno*-configured Amadori products was reported. Aniline and propargylamine were reacted with this heptose to yield the respective *C*-glycosyl-type hexoses, revealing that Amadori rearrangement of aniline turned out to be less efficient as that of propargylamine due to the less nucleophilic, aromatic amino group of aniline. Furthermore, molecular docking of both Amadori products was performed in order to investigate the influence of the alkyl/aryl aminomethyl group at the β-face of the sugar ring on the complexation of the glycoconjugates in the CRD of FimH. The studies suggested a reasonable binding mode, however, biological testing of the Amadori products revealed 0.2–0.4 fold weaker potencies towards inhibition of type 1 fimbriae-mediated bacterial adhesion compared to MeMan.
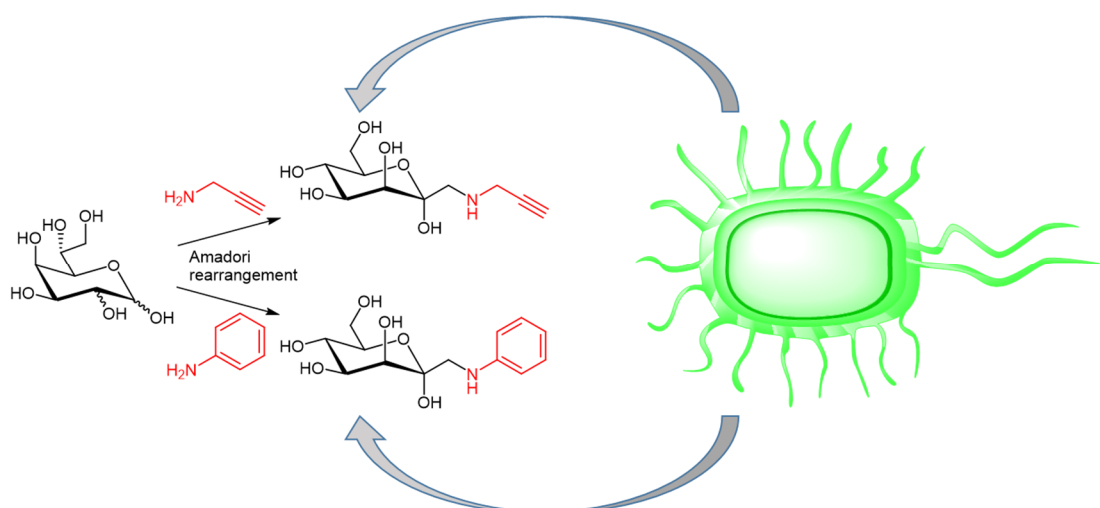
Figure 6.1: Amadori rearrangement of a suitable heptose with different amines results in *C*-glycosyl type D-mannoside analogues. The potency of these compounds for inhibition of type 1 fimbriae-mediated bacterial adhesion is in the range of MeMan.

A possible explanation for this issue may be found in the tilted arrangement of the Amadori products while being complexed in the CRD of FimH, resulting in compromised H-bonding, which weakens the affinity. Hence, it was shown that the utilization of the Amadori rearrangement for the synthesis of FimH ligands is critical since the resulting products have a limited fit in the CRD as a consequence of the sterically challenging aglycone.

The chromatographic purification of Amadori products is quite cumbersome and in some cases can be even impossible due to the high polarity of the employed starting materials as well as the product itself. Because of this, the second chapter focused on application of the CSP methodology on amine substrates as starting materials in the Amadori rearrangement (Figure 6.2). A known guaiazulene carbonate was employed to synthesize a guaiazulene-tagged amine **18** for Amadori rearrangement reactions. Employing two different heptoses **20** and **21a/b**, the corresponding *gluco*- and *manno*-configured products were prepared without any observable difference in the efficiency of the reaction. However, it turned out that several side products had been formed in both cases, which, nevertheless, could be easily removed through chromatography facilitated by the guaiazulene moiety.
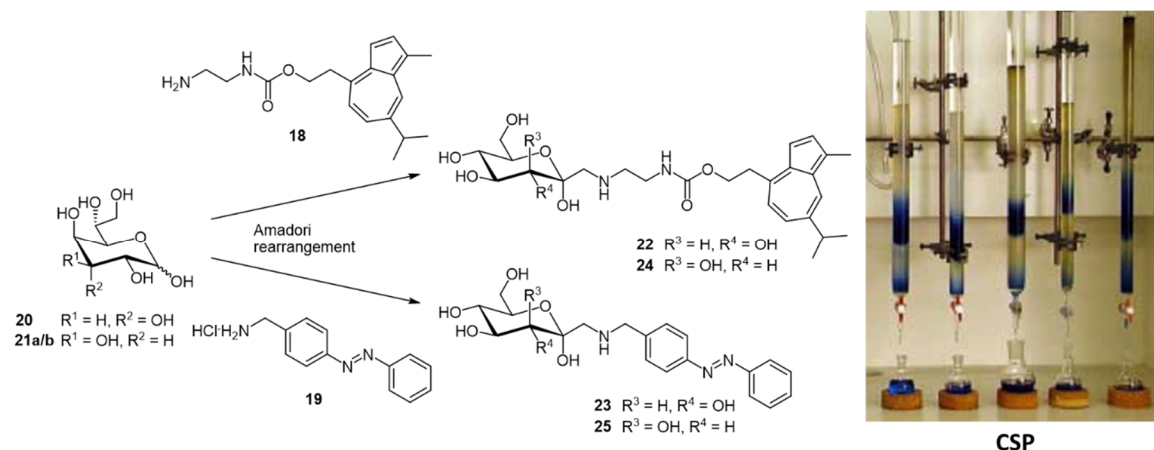
Figure 6.2: Application of different colored amines in the Amadori rearrangement resulted in chromophore-tagged Amadori products **22-25**. Utilization according to the CSP methodology revealed that guaiazulene-derived compounds **22** and **24** were suited best for this purpose.

Besides the guaiazulene-tagged amino compound **18**, an aminomethylazobenzene **19** was applied in the Amadori rearrangement reactions with both heptopyranoses. In both cases, the reaction emerged as highly inefficient as only the *gluco*-configured product **23** was obtained in a very low yield while the *manno*-configured product **25** remained heavily contaminated. Since the hydrochloride **20**, instead of the free amine, was employed for the reaction, it was suspected that the pH value of the solution may have been unfavorable for the reaction, resulting in low reactivity of the azobenzene derivative. Additionally, the chromatographic

purification did not proceed well enough due to extensive tailing, which significantly affected the purity of the obtained products.

Taken together, it could be demonstrated that the Amadori rearrangement can be efficiently employed as a ligation method for conjugation of carbohydrates. This, however, requires that the compatibility of the starting materials (especially regarding their reactivity) is provided. Although Amadori products did not deliver high potencies towards inhibition of bacterial adhesion, the reaction may be used to generate ligands for lectins other than FimH. The general applicability of this reaction as a bioconjugation method, however, remains uncertain and requires further investigation. Especially concerning the amount of formed side products as well as the incomplete conversion, which was observed in some examples described herein, points out the necessity of improving the reaction's efficiency. Solutions to these issues may be adjustment of the utilized reactants or, more elegantly, tuning of the reactions conditions. Although the Amadori rearrangement may not be generally applicable yet, the Glycogroup at the TU Graz successfully investigated different mono- but also multivalent rearrangement reactions, demonstrating the potential of this reaction for special applications.

Bacterial Adhesion to Carbohydrate Scaffold-Based Glycoclusters

In the first part of this chapter, the manuscript "Synthesis of AB$_4$ Carbohydrate Scaffolds as Branching Units in the Glycosciences" was presented. Therein, the synthesis of a carbohydrate scaffold bearing an AB$_4$-type functionalization was discussed following a retrosynthetic approach. Performance of different pathways revealed that the azido group in the aglycone of the scaffold had to be introduced at an advanced stage in order to avoid severe side reactions which were observed during most of the examined pathways. Finally, the N$_3$/(NHBoc)$_4$-functionalized target scaffold could be synthesized in 30% yield over six steps. From this compound as well as from a precursor, other valuable molecules were prepared including a photoswitchable glycoconjugate and a glycocluster **41** (Figure 6.3).
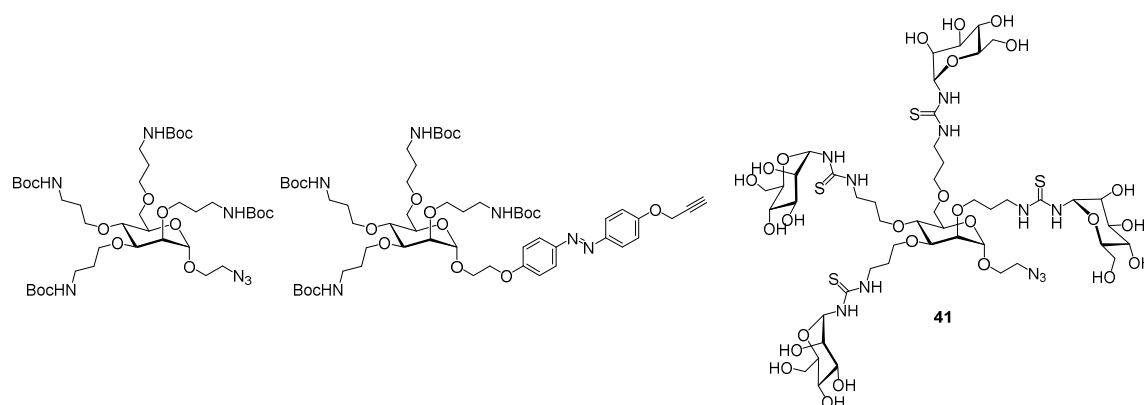
Figure 6.3: Target molecules that have been prepared in the scope of the manuscript "Synthesis of AB$_4$ Carbohydrate Scaffolds as Branching Units in the Glycosciences".

In the second part of the chapter the previously synthesized glycocluster **41** was prepared for surface functionalization by attachment of a biorepulsive OEG linker **46** through a CuAAC cycloaddition reaction. Although the click reaction at first turned out to be unexpectedly problematic due to insufficient conversion of the starting material, the target glycocluster **47** could be finally obtained in a yield of 50% (71%, based on conversion) by employing a different Cu(I) catalyst and purification by RP chromatography. Furthermore, tetravalent glycocluster **41** was tested as an inhibitor of type 1 fimbriae-mediated bacterial adhesion. An RIP value of 25.6 and a valency corrected value of 6.4 was determined, showing that the cluster **41** has a small multivalency effect, which, however, is not in the range of previously reported clusters containing a carbohydrate core. It was suspected that the geometrical shape of the glycocluster in combination with the electronic and conformational properties of the thiourea groups, which are connected to the mannose moieties, may negatively influence their preorganization as well as the recognition by the lectin. The scaffold compounds and the glycocluster **41** described in this chapter give rise to a variety of special applications as topics of future research in the Lindhorst group. Glycocluster, for instance, that arise from the photoresponsive scaffold (cf. Chapter 4.2) may be immobilized on suitable surfaces by click chemistry. Similarly, glycocluster **47**, which contains a biorepulsive linker, may be attached to surfaces *via* its amino group.
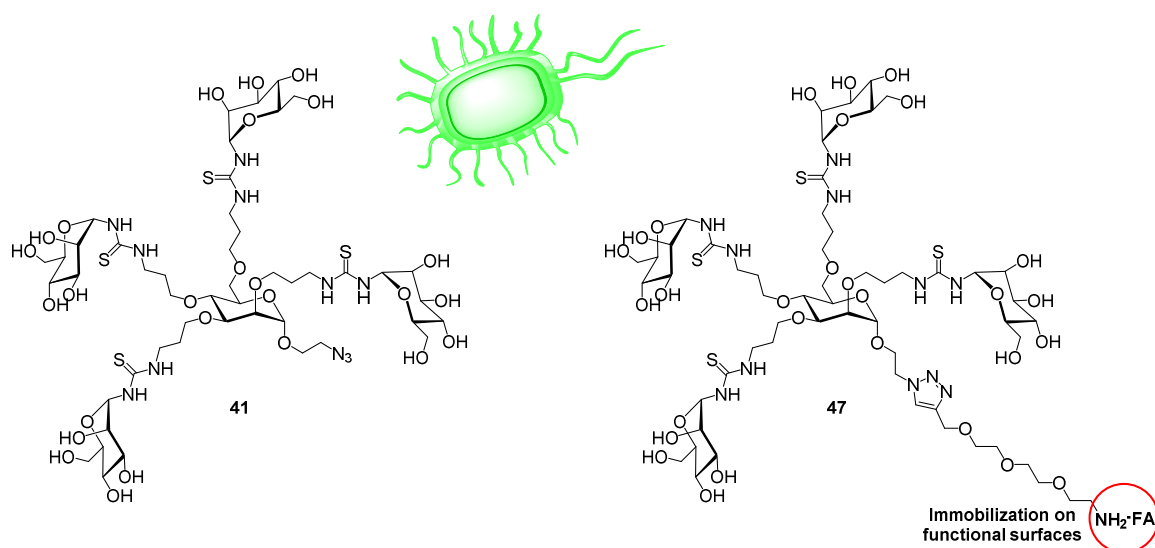
Figure 6.4: Tetravalent glycocluster **41** has been tested as an inhibitor of type 1 fimbriae-mediated bacterial adhesion. Attachment of a biorepulsive OEG linker allows for immobilization onto functional surfaces *via* the amino group (red circle).

Cyclodextrin Conjugates to Control Bacterial Adhesion

Since CDs are capable of encapsulating appropriate hydrophobic molecules, such as adamantane or azobenzene, an assay system based on this feature was developed. Two approaches were investigated, which involved different CD hosts for fabrication of a supramolecular surface. Inclusion of different glycoconjugate guest molecules on the surface was performed in order to effect switchable bacterial adhesion. The first approach involved covalent immobilization of amino-functionalized CD derivatives as a means to create the supramolecular surface. However, this approach resulted in unspecific binding of bacteria to the surface and was not further pursued. In the second approach, the supramolecular surface was fabricated by non-covalent immobilization of amphiphilic CD derivatives. The performed ELLA studies, utilizing the lectin Con A and an adamantane glycoconjugate, demonstrated that the applied conditions needed adjustment but the approach is feasible. However, this approach was also not pursued any longer since a similar assay system was published by Jonkheijm and coworkers. Based on the experiences gathered from the previous experiments, a reverse variant of this assay system was investigated which involved bacterial adhesion to CD complexes on photoresponsive surfaces (Figure 6.5).
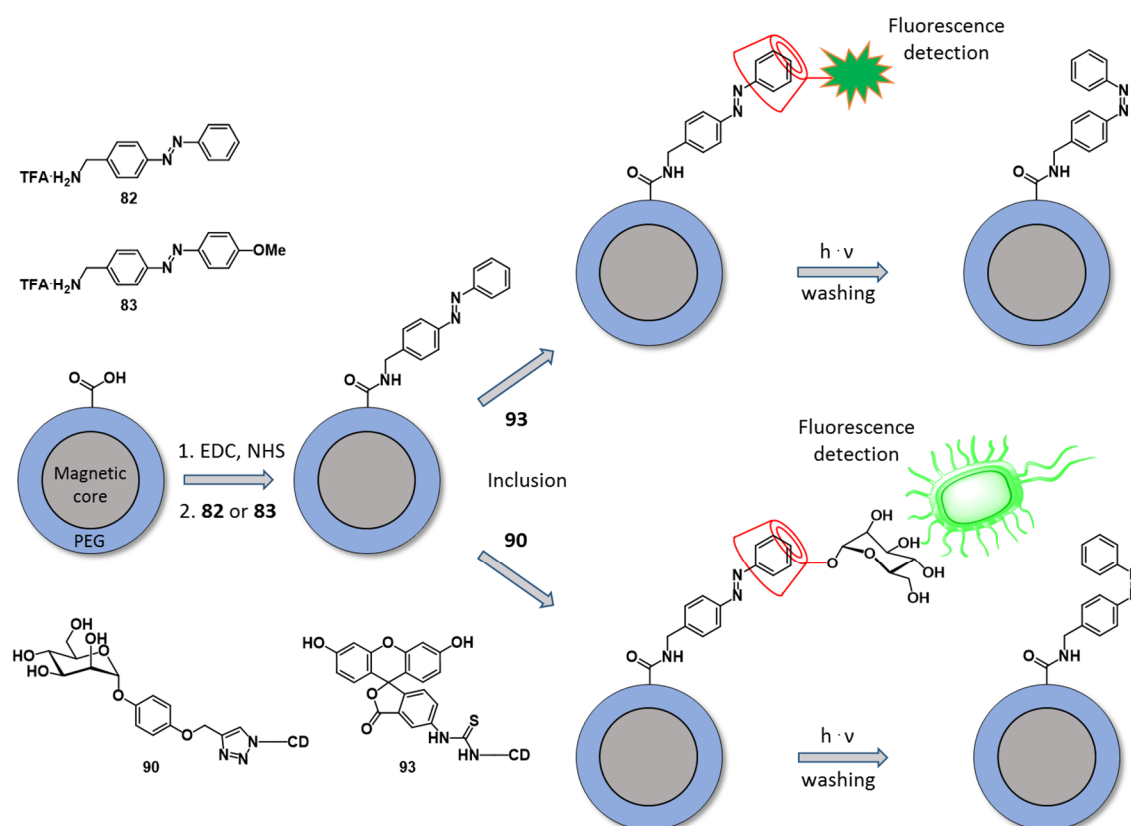
Figure 6.5: Magnetic PEG beads functionalized with azobenzene **82** and **83**, respectively, were treated with CD conjugates **90** or **93**. Switching of bacterial adhesion was effected by photoisomerization of the azobenzene units.

The photoresponsive surfaces were fabricated by immobilization of aminomethylazobenzene derivatives **82** and **83**, respectively, onto prefunctionalized microtiter plates. UV-light irradiation of polystyrene microtiter plates revealed that alteration of the functional surface took place so that the solid support was changed to UV-stable magnetic PEG beads. For these studies, two CD conjugates **90** and **93** were utilized for inclusion on the photoresponsive surface. While the fluorescein-tagged CD conjugate **93** was applied for validation of the inclusion complex formation, investigation of switchable cell adhesion was enabled by treatment with mannose CD conjugate **90**.

Inclusion of the fluorescein-tagged CD conjugate **93** turned out to be inefficient on beads functionalized with azobenzene derivative **83**. The performed bacterial adhesion assays, however, revealed that adhesion was equally pronounced on both functional surfaces (**82** and **83**). Attenuation of bacterial adhesion by photoisomerization of the azobenzene units depended greatly on the switching properties of the respective azobenzene. While in the case of azobenzene **82**, bacterial adhesion was decreased by 30%, photoisomerization of **83** resulted in a decrease of 74%. This proof of principle paves the way towards many interesting applications in research but also in the medical sector. For instance, this system could be applied in diagnostic procedures or, in the case of the tested PEG beads, for the extraction and accumulation of pathogens from body fluids or other media.

The results presented in this thesis point out that the possibilities for investigation of bacterial adhesion can be highly diverse. Especially interdisciplinary studies and combinations of complex organic synthesis with biochemical techniques are powerful and promising tools, allowing for elucidation of biological processes in many aspects. The findings of this thesis contribute to the examination of novel targets as well as techniques for investigation of bacterial adhesion and will be topic of future research in the Lindhorst group.

7.   Experimental Section

7.1   Materials and Methods

Reactions, chemicals and solvents

All reactions were carried out under atmospheric conditions (unless indicated otherwise). Moisture-sensitive reactions were carried out under a nitrogen atmosphere in reaction vessels that were baked out before use. All chemicals were purchased from abcr, Acros, Alfa Aesar, Merck, Sigma-Aldrich or TCI and used without further purification. For extractions and column chromatography, technical grade solvents were used, which were purified by distillation before use. Dry solvents were either directly purchased from the manufacturer or dried by an Inert PureSolv MD5 solvent purification system.

Thin layer chromatography (TLC)

TLC was performed on silica gel plates (GF 254, Merck) backed with aluminum. Detection of UV-active substances was achieved by a CAMAG UV lamp (λ_1 = 254 nm, λ_2 = 366 nm). Substances that were not UV-active were detected by charring with 10% sulfuric acid in EtOH, with a vanillin staining reagent (3.0 g vanillin and 0.5 mL H_2SO_4 in 100 mL EtOH) or with a ninhydrin staining solution followed by heating at ≈ 180 °C.

Flash- and reverse phase (RP) chromatography

Flash chromatography was carried out on silica gel 60 (Merck, 230-400 mesh, particle size 0.040-0.063 mm) or by using an Interchim puriFlash®450 chromatography system with distilled solvents. RP chromatography was performed by using the same flash system with CHROMABOND® C18ec columns (Macherey Nagel).

Gel permeation chromatography (GPC)

GPC was performed on Sephadex® G-15 (Sigma Aldrich) by using a peristaltic pump with DMF as the solvent.

Nuclear magnetic resonance spectroscopy (NMR)

NMR spectra were recorded on Bruker DRX-500 (500.13 MHz for ^{1}H and 125.75 MHz for ^{13}C) and AV-600 (600.13 MHz for ^{1}H and 150.92 MHz for ^{13}C) spectrometers at 300 K. Assignment of the peaks was achieved with the aid of 2D NMR techniques (^{1}H,^{1}H-COSY, ^{1}H,^{13}C-HSQC and

^{1}H,^{13}C-HMBC). Chemical shifts are referenced to the residual proton or the carbon signal of the used deuterated solvent.

CDCl$_3$	^{1}H	7.26 ppm (s)
	^{13}C	77.16 ppm (t)
MeOH-d_4	^{1}H	3.31 ppm (quint)
	^{13}C	49.00 ppm (sept)
DMSO-d_6	^{1}H	2.50 ppm (quint)
	^{13}C	39.52 ppm (sept)

Data is presented in the following format: chemical shift (δ), multiplicity (s = singlet, d = doublet, t = triplet, q = quartet, m = multiplet and br = broad signal), coupling constant in Hertz (Hz) and integration.

Optical rotations

Optical rotations were measured on a PerkinElmer 241 polarimeter (sodium D-line: 589 nm, cell length: 1 dm) in the solvents indicated. Optical rotations of guaiazulene derivatives could not be recorded since their intense color prevents detection.

Melting points (m.p.)

Melting points were determined on a BÜCHI Melting Point M-560 apparatus.

Mass spectrometry (MS)

ESI mass spectra were recorded on a Bruker Daltonics Esquire-LC instrument. High-resolution (HR) ESI-MS was performed on an Agilent 6224 ESI-TOF instrument. EI mass spectra were recorded on a Jeol AccuTOF 4GCV instrument. MALDI-TOF spectra were measured on a Bruker Biflex III instrument with an acceleration voltage of 19 kV and 2,5-dihydroxybenzoic acid (DHB) as the matrix.

Purity of compounds

The purity of synthesized compounds was ensured by validation of the corresponding ^{1}H and ^{13}C NMR spectra in combination with the respective HR ESI-MS spectra.

Infrared (IR) spectroscopy

IR spectra were recorded on a PerkinElmer FT-IR Paragon 1000 (ATR) spectrometer. Absorption bands are presented in cm^{-1}.

Ultraviolet–visible (UV/Vis) spectroscopy

UV/Vis spectra were recorded on a Lambda-41 spectrometer from PerkinElmer equipped with Büchi thermostat. Samples were measured in fused quartz cuvettes with a diameter of 1 cm at a temperature of 20 °C ± 1 °C.

Irradiation experiments

Irradiation was performed by using an LED (λ = 365 nm) from Nichia Corporation (NC4U133A) with a full-width at half maximum (FWHM) of 9 nm and an optical power output (PO) of $\approx$ 1 W.

Microtiter plates

Adhesion-inhibition assays were performed on black Nunc MicroWell™ (MaxiSorp™) 96-well plates (Thermo Scientific™). Covalent immobilization of compounds was carried out on black Nunc Immobilizer™ Amino 96-well plates. For ELLA-type assays, transparent Nunc-Immuno™ MicroWell™ (MaxiSorp™) 96-well plates were utilized. Phenol-sulfuric acid assays were performed on transparent Nunc Immobilizer™ Amino 96-well plates.

ELISA reader

Fluorescence and absorbance was measured on a Tecan infinite® 200 multifunction microplate reader. A bandpass filter was used with 485 nm for excitation and 535 nm for emission. For the phenol-sulphuric acid assay, absorbance was measured at 492 nm.

Magnetic PEG beads

Bacterial adhesion studies were performed on micromod magnetic polystyrene beads containing a PEG-COOH coating (micromer®-M, 08-56-203).

7.2   General Synthetic Procedures

7.2.1   General Procedure A (Synthesis of amphiphilic CD derivatives **61-63**)

The preparative procedure was adapted from *J. Pharm. Sci.* **2002**, *91* (5), 1214-1224:

A solution of heptakisbromo CD **60**[130] (1.0 eq) in deoxygenated DMF was added to a solution of the respective carboxylic acid (14 eq) and Cs_2CO_3 (7.0 eq) as well in deoxygenated DMF. The reaction mixture was stirred at 50 °C for 72 h and was then filtered. The solvent was removed under reduced pressure and the residue was washed several times with water. The resulting solid was taken up in DMF and precipitated by addition of water. After filtration, the solid was washed with water followed by acetone and finally dried at 60 °C, giving the respective amphiphilic CD derivative.

7.2.2   General Procedure B (CuAAC reaction with copper(II) sulfate pentahydrate)

The preparative procedure was adapted from *Angew. Chem.* **2002**, *114* (14), 2708-2711:

The respective azide (1.0 eq) and alkyne (1.0 eq) were both dissolved in DMF and an aqueous solution of $CuSO_4 \cdot 5 H_2O$ (0.42 eq) was added. After that, an aqueous solution of sodium ascorbate (0.85 eq) was added and the reaction mixture was stirred at room temperature for 16 h. The solvent was removed under reduced pressure and the crude product was purified by the method indicated in the corresponding individual procedure.

7.2.3   General Procedure C (NaOMe promoted deacetylation)

The preparative procedure was adapted from *Chem. Ber.* **1929**, *62* (6), 1613-1614:

The respective acetyl-protected carbohydrate was dissolved in MeOH. Subsequently, a freshly prepared methanolic NaOMe solution (1 M) was added and the reaction mixture was stirred for 16 h at room temperature. The solution was then neutralized by addition of Amberlite-IR120®, the resin was filtered off, and the solvent was removed under reduced pressure to yield the pure deacetylated compound.

7.3   Individual Synthetic Procedures

4-(2-Hydroxyethyl)-7-isopropyl-1-methylazulene (16)[57]
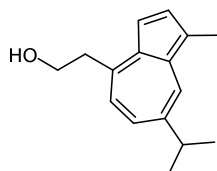
The preparative procedure was adapted from *Eur. J. Org. Chem.* **2006**, 1103-1108:

An LDA solution (25.2 mL, 50.4 mmol, 1.0 eq; 2 M) was diluted dry Et$_2$O (100 mL) and cooled to -35 °C. Then, a solution of guaiazulene **14** (10.0 g, 50.4 mmol, 1.0 eq) in Et$_2$O (30 mL) was added dropwise and the reaction mixture was stirred for 40 min at this temperature. Paraformaldehyde was added and stirring was continued for 10 min at -35 °C. The mixture was then allowed to attain room temperature and stirred for 16 h. The solution was diluted with Et$_2$O and the organic phase was washed three times with brine, dried over MgSO$_4$, filtered, and the solvent was removed under reduced pressure. The crude mixture was purified by flash chromatography (toluene/EtOAc, 6:1), giving product **16** as a blue oil.

Yield: 6.17 g, 27.0 mmol, 54%.

The obtained spectroscopic data was according to that reported in the literature.[57]

2-(7-Isopropyl-1-methylazulen-4-yl)ethyl *N*-succinimidyl carbonate (17)[59]
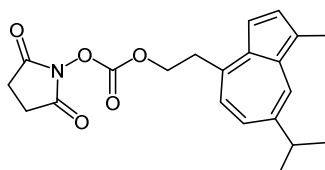
The preparative procedure was adapted from *J. Carbohydr. Chem.* **2009**, *28* (6), 330-347:

Pyridine (35.2 μL, 436 μmol, 0.2 eq) and DSC (669 mg, 2.61 mmol, 1.2 eq) were added to a solution of alcohol **16** (497 mg, 2.18 mmol, 1.0 eq) in dry DMF (3 mL). The reaction mixture was stirred at 40 °C for 16 h and the solvent was removed under reduced pressure. The residue was taken up in EtOAc (30 mL) and the organic phase was washed three times with brine. After drying over MgSO$_4$, the organic phase was filtered, and the solvent was removed

under reduced pressure. The crude product was purified by flash chromatography (cyclohexane/EtOAc, 3:1→2:1), giving carbonate **17** as a blue solid.

Yield: 736 mg, 1.99 mmol, 91%.

The obtained spectroscopic data was according to that reported in the literature.[59]

N-2-[2-(7-Isopropyl-1-methyl-azulen-4-yl)ethoxycarbonylamido]ethylamine (18)
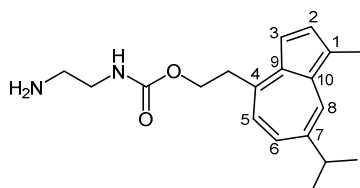
A solution of carbonate **17** (76.4 mg, 207 µmol, 1.0 eq) in $CHCl_3$ (1 mL) was added at 0 °C to a solution of ethylene diamine (373 µL, 5.59 mmol, 27 eq) in $CHCl_3$ (3.5 mL). The reaction mixture was stirred for 1 h at this temperature and stirring was continued for further 16 h at room temperature. The organic phase was washed twice with satd. aq. $NaHCO_3$ solution, brine, and water. After drying over $MgSO_4$, the organic phase was filtered and the solvent was removed under reduced pressure. The residue was purified by flash chromatography (CH_2Cl_2/MeOH, 10:1 containing 1% of TEA), giving amine **18** as a blue oil.

Yield: 61.9 mg, 197 µmol, 95%;

R$_f$: 0.26 (CH_2Cl_2/MeOH, 9:1 containing 1% of TEA);

¹H NMR (500 MHz, $CDCl_3$, 300 K): δ = 8.16 (d, $J_{6,8}$ = 1.6 Hz, 1H, H-8), 7.62 (d, $J_{2,3}$ = 3.6 Hz, 1H, H-2), 7.38 (dd, $J_{5,6}$ = 10.6 Hz, $J_{6,8}$ = 1.1 Hz, 1H, H-6), 7.31 (d, $J_{6,8}$ = 2.9 Hz, 1H, H-3), 6.96 (d, $J_{5,6}$ = 10.7 Hz, 1H, H-5), 5.62 (m$_c$, 1H, NHCO), 4.44 (dd~t, $_{OCH,CH-az}$ = 7.3 Hz, 2H, OCH$_2$CH$_2$-az), 4.23 (br s, 2H, NH$_2$), 3.42 (dd~t, $_{OCH,CH-az}$ = 7.3 Hz, 2H, OCH$_2$CH$_2$-az), 3.34 (m$_c$, 2H, H$_2$NCH$_2$CH$_2$NHCO), 3.04 (sept, $J_{isopropyl}$ = 6.7 Hz, 1H, az-CH(CH$_3$)$_2$), 2.95 (m$_c$, 2H, H$_2$NCH$_2$CH$_2$NHCO), 2.63 (s, 3H, az-CH$_3$), 1.33 (d, $J_{isopropyl}$ = 6.9 Hz, 6H, az-CH(CH$_3$)$_2$) ppm;

¹³C NMR (125 MHz, $CDCl_3$, 300 K): δ = 157.1 (C=O), 143.7 (C-7), 140.4 (C-4), 137.7 (C-10), 137.0 (C-2), 136.3 (C-9), 135.2 (C-6), 133.6 (C-8), 125.6 (C-1), 124.9 (C-5), 112.7 (C-3), 65.4 (OCH$_2$CH$_2$-az), 41.6 (H$_2$NCH$_2$CH$_2$NHCO), 41.2 (H$_2$NCH$_2$CH$_2$NHCO), 38.4 (az-CH(CH$_3$)$_2$), 37.9 (OCH$_2$CH$_2$-az), 24.8 (az-CH(CH$_3$)$_2$), 13.0 (az-CH$_3$) ppm;

ESI-MS (*m/z*): [M+H]⁺ calcd. for $C_{19}H_{27}N_2O_2$, 315.207, found, 315.183;

IR (ATR) ṽ: 3293, 2957, 1700, 1523, 1459, 1387, 1250, 1140, 1024, 921, 823, 779 cm⁻¹.

1-{*N*-2-[2-(7-Isopropyl-1-methyl-azulen-4-yl)ethoxycarbonylamido]ethyl}amino-1-deoxy α-D-*gluco*-hept-2-ulose (22)
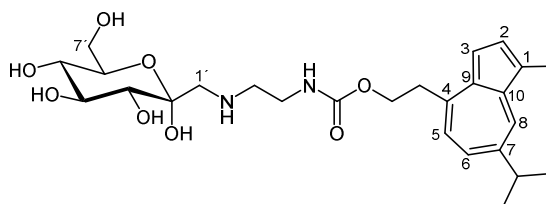
D-*Glycero*-D-*gulo*-heptopyranose (**20**, 134 mg, 638 μmol, 1.0 eq) was dissolved in a mixture of EtOH (4 mL), 1,4-dioxane (0.5 mL), and water (5 drops). Then guaiazulene-tagged amine **18** (201 mg, 638 μmol, 1.0 eq) and acetic acid (36.5 μL, 638 μmol, 1.0 eq) were added and the reaction mixture was stirred at 70 °C for 5 h. The solvent was removed under reduced pressure and the crude product was purified by flash chromatography (CHCl$_3$/MeOH, 5:1→3:1 containing 1% of conc. NH$_4$OH). Amadori product **22** was obtained as a blue syrup.

Yield: 116 mg, 328 μmol, 52% (66% based on conversion, 14% starting material reisolated).

R$_f$: 0.32 (CHCl$_3$/MeOH, 2:1 containing 1% of conc. NH$_4$OH);

^{1}H NMR (500 MHz, MeOH-d_4, 300 K): δ = 8.19 (d~s, 1H, H-8), 7.62 (d, $J_{2,3}$ = 3.6 Hz, 1H, H-2), 7.46 (dd~d, $J_{5,6}$ = 10.6 Hz, 1H, H-6), 7.32 (d, $J_{6,8}$ = 3.7 Hz, 1H, H-3), 7.06 (d, $J_{5,6}$ = 10.7 Hz, 1H, H-5), 4.44 (dd~t, $_{OCH,CH\text{-}az}$ = 7.0 Hz, 2H, OC$\underline{H}_2$CH$_2$-az), 3.82 (dd, $J_{7'a,7'b}$ = 11.6 Hz, $J_{6',7'a}$ = 2.2 Hz, 1H, H-7'a), 3.75-3.72 (m, 1H, H-4'), 3.69-3.65 (m, 2H, H-6', H-7'b), 3.46 (dd~t, $_{OCH,CH\text{-}az}$ = 7.0 Hz, 2H, OCH$_2$C$\underline{H}_2$-az), 3.33-3.27 (m, 4H, HNCH$_2$C$\underline{H}_2$NHCO, H-3', H-5'), 3.08 (sept, $J_{isopropyl}$ = 6.9 Hz, 1H, az-C$\underline{H}$(CH$_3$)$_2$), 3.02 (s, 2H, H-1'a,b), 2.94 (m$_c$, 2H, HNC$\underline{H}_2$CH$_2$NHCO), 2.63 (s, 3H, az-CH$_3$), 1.36 (d, $J_{isopropyl}$ = 6.9 Hz, 6H, az-CH(C$\underline{H}_3$)$_2$) ppm;

^{13}C NMR (125 MHz, CDCl$_3$, 300 K): δ = 159.4 (C=O), 144.9 (C-7), 141.4 (C-4), 139.0 (C-10), 137.9 (C-2), 137.7 (C-9), 136.0 (C-6), 134.0 (C-8), 126.4 (C-1), 125.8 (C-5), 113.4 (C-3), 97.0 (C-2'), 75.5 (C-6'), 74.4 (C-3'), 74.3 (C-4'), 71.6 (C-5'), 66.5 (OC$\underline{H}_2$CH$_2$-az), 62.7 (C-7'), 55.1 (C-1'), 50.1 (HNC$\underline{H}_2$CH$_2$NHCO), 39.6 (H$_2$NCH$_2$C$\underline{H}_2$NHCO), 39.4 (az-C$\underline{H}$(CH$_3$)$_2$), 38.5 (OCH$_2$C$\underline{H}_2$-az), 25.1 (az-CH(C$\underline{H}_3$)$_2$), 12.9 (az-CH$_3$) ppm;

λ$_{max}$ (ε): 349 nm (3587 L mol^{-1} cm^{-1});

ESI-MS (*m/z*): [M+H]$^+$ calcd. for C$_{26}$H$_{38}$N$_2$O$_8$, 507.270, found, 507.274;

IR (ATR) ṽ: 3318, 2960, 1698, 1525, 1456, 1255, 1034, 823 cm^{-1}.

1-{*N*-2-[2-(7-Isopropyl-1-methyl-azulen-4-yl)ethoxycarbonylamido]ethyl}amino-1-deoxy α-D-*manno*-hept-2-ulose (24)
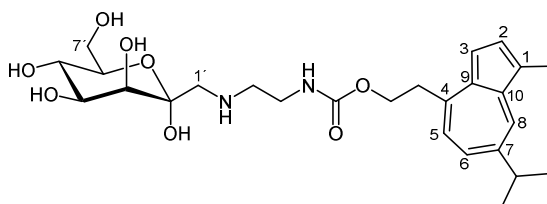
D-*Glycero*-D-*galacto*/D-*talo* heptopyranose (**21a/b**, 142 mg, 677 μmol, 1.0 eq) was dissolved in a mixture of EtOH (4 mL), 1,4-dioxane (0.5 mL), and water (5 drops). Then guaiazulene-tagged amine **18** (213 mg, 677 μmol, 1.0 eq) and acetic acid (38.7 μL, 677 μmol, 1.0 eq) were added and the reaction mixture was stirred at 70 °C for 7 h. The solvent was removed under reduced pressure and the crude product was purified by flash chromatography (CHCl$_3$/MeOH, 5:1→3:1 containing 1% of conc. NH$_4$OH). Amadori product **24** was obtained as a blue syrup.

Yield: 185 mg, 365 μmol, 54% (59% based on conversion, 5% starting material reisolated).

R$_f$: 0.35 (CHCl$_3$/MeOH, 2:1 containing 1% of conc. NH$_4$OH);

^{1}H NMR (600 MHz, CDCl$_3$, 300 K): δ = 8.19 (d~s, 1H, H-8), 7.63 (d, $J_{2,3}$ = 3.2 Hz, 1H, H-2), 7.47 (dd~d, $J_{5,6}$ = 10.5 Hz, 1H, H-6), 7.33 (d, $J_{6,8}$ = 3.4 Hz, 1H, H-3), 7.07 (d, $J_{5,6}$ = 10.6 Hz, 1H, H-5), 4.46 (dd~t, $_{OCH,CH\text{-}az}$ = 6.9 Hz, 2H, OC$\underline{H}_2$CH$_2$-az), 3.85-3.82 (m, 3H, H-3′, H-4′, H-7′a), 3.76 (dd, $J_{7'a,7'b}$ = 11.6 Hz, $J_{6',7'b}$ = 5.3 Hz, 1H, H-7′b), 3.73-3.71 (m, 1H, H-6′), 3.66-3.63 (m, 1H, H-5′), 3.47 (dd~t, $_{OCH,CH\text{-}az}$ = 6.9 Hz, 2H, OCH$_2$C$\underline{H}_2$-az), 3.37 (m$_c$, 2H, HNCH$_2$C$\underline{H}_2$NHCO), 3.27 (d, $J_{1'a,1'b}$ = 12.5 Hz, 1H, H-1′a), 3.12-3.02 (m, 4H, HNC$\underline{H}_2$CH$_2$NHCO, H-1′b, az-C$\underline{H}$(CH$_3$)$_2$), 2.63 (s, 3H, az-CH$_3$), 1.36 (d, $J_{isopropyl}$ = 6.9 Hz, 6H, az-CH(C$\underline{H}_3$)$_2$) ppm;

^{13}C NMR (150.92 MHz, CDCl$_3$, 300 K): δ = 159.6 (C=O), 144.8 (C-7), 141.4 (C-4), 139.1 (C-10), 137.9 (C-2), 137.7 (C-9), 136.0 (C-6), 134.0 (C-8), 126.5 (C-1), 125.8 (C-5), 113.5 (C-3), 96.2 (C-2′), 75.1 (C-3′), 75.0 (C-6′), 72.6 (C-4′), 67.8 (C-5′), 66.7 (O$\underline{C}$H$_2$CH$_2$-az), 62.6 (C-7′), 55.6 (C-1′), 49.9 (HN$\underline{C}$H$_2$CH$_2$NHCO), 39.4 (az-$\underline{C}$H(CH$_3$)$_2$), 38.7 (HNCH$_2$$\underline{C}H_2$NHCO), 38.5 (OCH$_2$$\underline{C}H_2$-az), 25.1 (az-CH($\underline{C}H_3$)$_2$), 12.9 (az-CH$_3$) ppm;

λ$_{max}$ (ε): 349 nm (5352 L mol^{-1} cm^{-1});

ESI-MS (*m/z*): [M+H]$^+$ calcd. for C$_{26}$H$_{38}$N$_2$O$_8$, 507.3, found, 507.2;

IR (ATR) ṽ: 3280, 2960, 1699, 1540, 1410, 1255, 1052, 1033, 922, 821 cm^{-1}.

1-[*N*-(*E*)-*p*-(Phenylazo)benzyl]amino-1-deoxy α-D-*gluco*-hept-2-ulose (23)
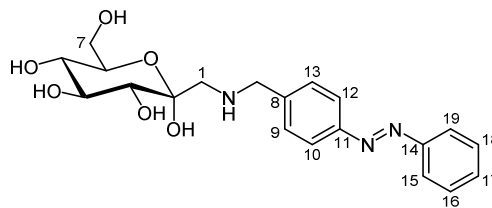
Azobenzene derivative **19** (85 mg, 0.34 mmol, 1.0 eq) was suspended in a mixture of EtOH (5 mL) and TEA (47 μL, 0.34 mmol, 1.0 eq). The suspension was stirred for 20 min at room temperature before D-*glycero*-D-*gulo*-heptopyranose (**20**, 71 mg, 0.34 mmol, 1.0 eq) as well as 1,4-dioxane (0.5 mL) and water (5 drops) were added. The reaction mixture was stirred at 70 °C for 2 h but TLC revealed only little conversion so that another 0.5 eq of azobenzene derivative **19** (43 mg, 0.17 mmol) and TEA (24 μL, 0.17 mmol) were added. Stirring was then continued for 8 h at 70 °C and the solvent was removed under reduced pressure. The crude product was purified by flash chromatography (CHCl$_3$/MeOH, 84:15 containing 1% of conc. NH$_4$OH), giving Amadori product **23** as a yellow amorphous solid.

Yield: 9 mg, 0.02 mmol, 6%;

R$_f$: 0.38 (CHCl$_3$/MeOH, 3:1 containing 1% of conc. NH$_4$OH);

$[\alpha]_D^{20}$ = +20.6 (c = 0.8, MeOH);

^{1}H NMR (500 MHz, CDCl$_3$, 300 K): δ = 7.95 (m$_c$, 2H, H-10, H-12), 7.92 (m$_c$, 2H, H-15, H-19), 7.64 (m$_c$, 2H, H-9, H-13), 7.55 (m$_c$, 2H, H-16, H-18), 7.53 (m$_c$, 1H, H-17), 4.19 (d, $J_{NCH,NCH'}$ = 13.7 Hz, 1H, HNC<u>H</u>′H-ar), 4.15 (d, $J_{NCH,NCH'}$ = 13.7 Hz, 1H, HNCH′<u>H</u>-ar), 3.85 (dd, $J_{7a,7b}$ = 11.5 Hz, $J_{6,7a}$ = 2.3 Hz, 1H, H-7a), 3.78-3.74 (m, 1H, H-4), 3.70-3.65 (m, 2H, H-6, H-7b), 3.33-3.27 (m, 2H, H-3, H-5), 3.06 (d, $J_{H-1a,H-1b}$ = 12.4 Hz, 1H, H-1a), 3.03 (d, $J_{H-1a,H-1b}$ = 12.3 Hz, 1H, H-1b) ppm;

^{13}C NMR (125 MHz, CDCl$_3$, 300 K): δ = 154.0 (C-14), 153.8 (C-11), 132.5 (C-17), 131.3 (C-9, C-13), 130.9 (C-8), 130.3 (C-16, C-18), 124.1 (C-10, C-12), 123.9 (C-15, C-19), 97.1 (C-2), 75.5 (C-6), 74.4 (C-3, C-4), 71.6 (C-5), 62.7 (C-7), 54.6 (C-1), 53.2 (HN<u>C</u>H$_2$-ar) ppm;

ESI-MS (*m/z*): [M+Na]$^+$ calcd. for C$_{20}$H$_{25}$N$_3$O$_6$, 426.2, found, 426.1.

2-(2-(2-(Prop-2-ynyloxy)ethoxy)ethoxy)ethanol (43)[77b]
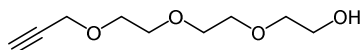
The preparative procedure was adapted from *Bioconjugate Chem.* **2009**, *20* (12), 2364-2370:

Ground potassium hydroxide (3.04 g, 54.1 mmol, 1.1 eq) was added to neat triethylene glycol (**42**, 19.8 mL, 148 mmol, 3.0 eq) and the reaction mixture was stirred at 40 °C for 30 min. Then propargyl bromide solution (4.66 mL, 49.2 mmol, 1.0 eq; 80% in toluene) was added and stirring was continued at 60 °C for 3 h. The mixture was then diluted with water (45 mL) and acidified to pH 1 with a hydrochloric acid solution (1 M). The aqueous phase was extracted three times with EtOAc and the combined organic phases were washed twice with brine. The organic phase was then dried over MgSO$_4$, filtered, and the solvent was removed under reduced pressure. The crude product was purified by flash chromatography (cyclohexane/EtOAc, 1:1), giving alkyne **43** as a colorless oil.

Yield: 3.14 g, 16.7 mmol, 34%.

The obtained spectroscopic data was according to that reported in the literature.[77b]

2-(2-(2-(Prop-2-ynyloxy)ethoxy)ethoxy)ethyl 4-methylbenzenesulfonate (44)[77b]
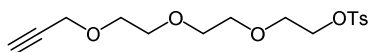
The preparative procedure was adapted from *Bioconjugate Chem.* **2009**, *20* (12), 2364-2370:

Alkyne **43** (1.03 g, 5.47 mmol, 1.0 eq) and tosyl chloride (1.15 g, 6.02 mmol, 1.1 eq) were dissolved in CH$_2$Cl$_2$ (6 mL). Ground potassium hydroxide (1.23 g, 21.9 mmol, 4.0 eq) was slowly added at 0 °C and the reaction mixture was stirred at this temperature for 3 h. The mixture was poured onto ice-cold water and the aqueous phase was extracted three times with CH$_2$Cl$_2$. The organic phase was then washed with brine, dried over MgSO$_4$, filtered, and the solvent was removed under reduced pressure. The residue was purified by flash chromatography (cyclohexane/EtOAc, 2:1), giving tosylate **44** as a colorless oil.

Yield: 1.57 g, 4.59 mmol, 84%.

The obtained spectroscopic data was according to that reported in the literature.[77b]

3-(2-(2-(2-Azidoethoxy)ethoxy)ethoxy)prop-1-yne (45)[77b]
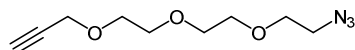
The preparative procedure was adapted from *Bioconjugate Chem.* **2009**, *20* (12), 2364-2370: Tosylate **44** (4.94 g, 14.4 mmol, 1.0 eq), sodium azide (7.48 g, 115 mmol, 8.0 eq) and TBAI (532 mg, 1.44 mmol, 0.1 eq) were dissolved in DMF (150 mL). The reaction mixture was stirred at 70 °C for 4 h. The mixture was then poured onto ice-cold water and the aqueous phase was extracted four times with CH_2Cl_2. The organic phase was dried over $MgSO_4$, filtered, and the solvent was removed under reduced pressure. The crude product was purified by flash chromatography (cyclohexane/EtOAc, 1:1), giving azide **45** as a colorless oil.

Yield: 2.34 g, 11.0 mmol, 76%.

The obtained spectroscopic data was according to that reported in the literature.[77b]

2-(2-(2-(Prop-2-ynyloxy)ethoxy)ethoxy)ethylamine (46)[77b]
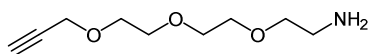
The preparative procedure was adapted from *Bioconjugate Chem.* **2009**, *20* (12), 2364-2370: PPh_3 (4.33 g, 16.5 mmol, 1.5 eq) was added to solution of azide **45** (2.34 g, 11.0 mmol, 1.0 eq) in dry THF (50 mL). The reaction mixture was stirred for 16 h at room temperature and conc. NH_4OH (35%, 5 mL) was added. Stirring was continued for another 16 h at this temperature and the solvent was removed under reduced pressure. The residue was purified by flash chromatography (CH_2Cl_2/MeOH, 90:9 containing 1% of conc. NH_4OH), giving amine **46** as a colorless oil.

Yield: 1.76 g, 9.40 mmol, 85%.

The obtained spectroscopic data was according to that reported in the literature.[77b]

2-(4-(2-(2-(2-Ammoniumethoxy)ethoxy)ethoxy)methyltriazolyl)ethyl 2,3,4,6-tetra-*O*-[3-*N′*-(α-D-mannopyranosyl)thioureidopropyl] α-D-mannopyranosyl formate (47)
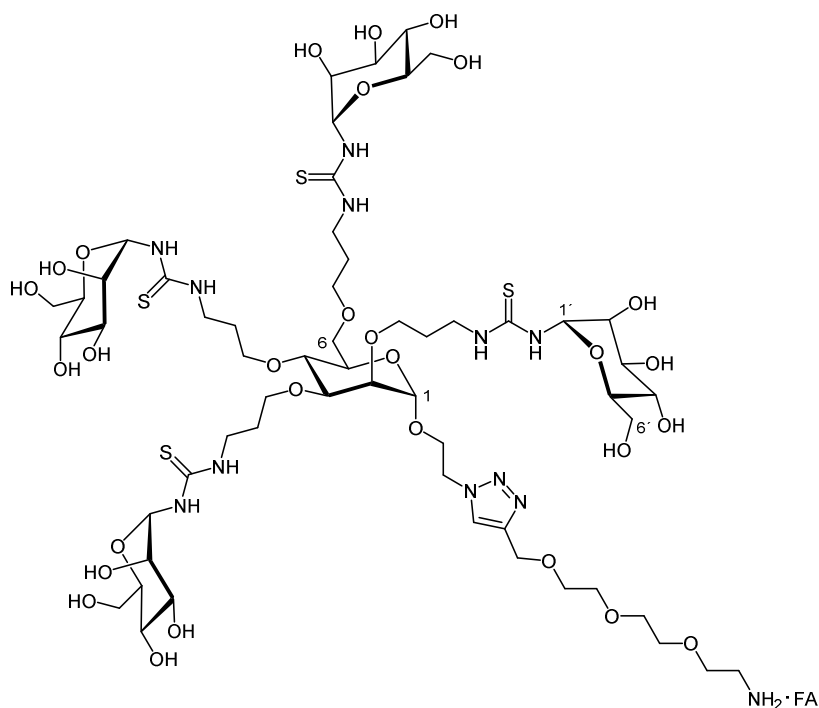
A stock solution of CuBr (7.03 mg, 49.0 µmol) and PMDETA (10.2 µL, 49.0 µmol) in dry DMF (15.8 mL) was prepared. Then, glycocluster **41** (42.2 mg, 31.0 µmol, 1.0 eq) and alkyne **46** (5.80 mg, 31.0 µmol, 1.0 eq) were dissolved in 2 mL of the stock solution and the reaction mixture was stirred for 16 h at room temperature. The solvent was removed under reduced pressure and the residue was purified by RP chromatography (ACN/ddH$_2$O containing 0.1% of formic acid, cf. Appendix), giving the product as the corresponding formate salt **47**.

Yield: 24.6 mg, 15.4 µmol, 50% (71% based on conversion, 21% starting material reisolated).

R$_f$: 0.19 (*i*PrOH/H$_2$O/EtOAc/NH$_4$OH (conc.), 5:3:1:1);

$[\alpha]_D^{20}$ = +20.8 (c = 0.3, H$_2$O);

¹H NMR (500 MHz, D$_2$O, 300 K): δ = 8.38 (s, 1H, C(O)H), 8.08 (s, 1H, H$_{triazole}$), 5.64-5.44 (m, 3H, 3 H-1′), 4.86 (d~s, 1H, H-1), 4.67 (s, 2H, triazole-C$\underline{H}_2$O), 4.64 (m$_c$, 2H, OCH$_2$C$\underline{H}_2$-triazole), 4.04-3.99 (m, 2H, OC$\underline{H}$′HCH$_2$-triazole, H-4), 3.93-3.85 (m, 7H, OCH′$\underline{H}$CH$_2$-triazole, 4 H-4′, 2 H-6′a), 3.80-3.77 (m, 4H, H-2, H-5, 2 H-6′a), 3.72-3.44 (m, 45H, triazole-CH$_2$OC$\underline{H}_2$, triazole-CH$_2$OCH$_2$C$\underline{H}_2$, OC$\underline{H}_2$CH$_2$O, OCH$_2$C$\underline{H}_2$O, OC$\underline{H}_2$CH$_2$NH$_4$⁺, 4 OC$\underline{H}_2$CH$_2$CH$_2$NH, 4 OCH$_2$CH$_2$C$\underline{H}_2$NH, 4 H-2′, 4 H-3′, H-3, 4 H-5′, 4 H-6′b, H-6a,b), 3.16 (m$_c$, 2H, OCH$_2$C$\underline{H}_2$NH$_4$⁺), 1.83 (br m$_c$, 8H, 4 OCH$_2$C$\underline{H}_2$CH$_2$NH) ppm;

¹³C NMR (125 MHz, D$_2$O, 300 K): δ = 181.6 (C=S), 170.6 (C=O), 143.9 (C$_{quart, triazole}$), 125.6 (C$_{triazole}$), 97.1 (C-1), 82.3, 81.4 (2 C-1′), 78.8 (C-3), 77.4 (C-3′), 75.2 (C-2), 73.6, 73.4 (C-2′), 70.7, 70.5 (C-5, C-4′), 69.7, 69.5, 68.9, 68.5, 67.6, 66.9, 66.5, 66.4 (triazole-CH$_2$OC$\underline{H}_2$, triazole-CH$_2$OCH$_2$C$\underline{H}_2$, OC$\underline{H}_2$CH$_2$O, OCH$_2$C$\underline{H}_2$O, OC$\underline{H}_2$CH$_2$CH$_2$NH, C-5′, C-6), 65.7 (OC$\underline{H}_2$CH$_2$-triazole), 63.1 (triazole-C$\underline{H}_2$O), 61.0, 60.8 (2 C-6′), 50.2 (OCH$_2$C$\underline{H}_2$-triazole), 42.3, 42.1 (2 OCH$_2$CH$_2$C$\underline{H}_2$NH), 39.1 (OCH$_2$C$\underline{H}_2$NH$_4^+$), 29.0, 28.7, 28.5, 28.2 (4 OCH$_2$C$\underline{H}_2$CH$_2$NH) ppm;

ESI-MS (*m/z*): [M+H]$^+$ calcd. for C$_{57}$H$_{104}$N$_{12}$O$_{29}$S$_4$, 1549.5993, found, 1549.5971.

Mono[6^A-(*p*-toluenesulfonyl)-6^A-deoxy]cyclomaltoheptaose (49)[119a]
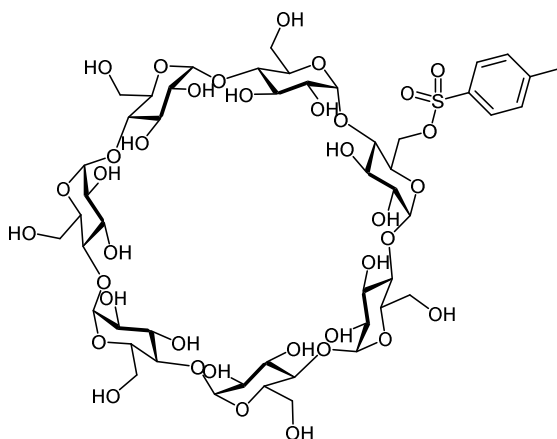
The preparative procedure was adapted from *Org. Synth.* **2000**, *77*, 225:

β-CD (**48**, 8.26 g, 7.26 mmol, 4.0 eq) was suspended in water (180 mL) and the suspension was brought to 60 °C. The resulting clear solution was cooled to room temperature and 1-(*p*-toluenesulfonyl)imidazole (6.46 g, 29.1 mmol, 4.0 eq) was added. The reaction mixture was stirred for 2 h at room temperature before aq. NaOH (3.72 g in 10 mL) was slowly added over 10 min. The suspension was then filtered and the filtrate was neutralized by addition of solid NH$_4$Cl (9.95 g). The solution was reduced to half of the initial volume by blowing a gentle stream of air over the surface of the solution for 16 h. The precipitate was collected by filtration, washed with ice-cold water, followed by acetone, and dried at 60 °C. The solid was recrystallized from water and tosylate **49** was obtained as a white solid.

Yield: 2.96 g, 2.30 mmol, 32%.

The obtained spectroscopic data was according to that reported in the literature.[119a]

Mono[6^A-azido-6^A-deoxy]cyclomaltoheptaose (50)[117]
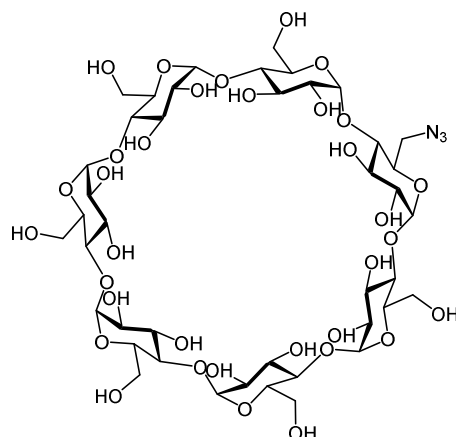
The preparative procedure was adapted from *Analyst* **2011**, *136*, 5017–5024:

NaN_3 (194 mg, 2.98 mmol, 1.2 eq) was added to a solution of tosylate **49** (3.23 g, 2.51 mmol, 1.0 eq) in DMF (30 mL) and the reaction mixture was stirred at 80 °C for 6 h. After cooling to room temperature, the solution was added dropwise to acetone and the precipitate was collected by filtration. Washing with acetone and subsequent drying at 60 °C furnished azide **50** as a white solid.

Yield: 2.96 g, 2.30 mmol, 32%.

The obtained spectroscopic data was according to that reported in the literature.[117]

Mono[6^A-(4-aminomethyl-triazolyl)-6^A-deoxy]cyclomaltoheptaose (51)
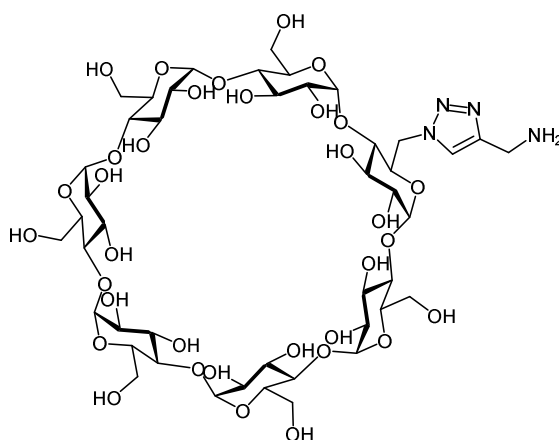
CD conjugate **51** was synthesized according to general procedure B with azide **50** (200 mg, 172 µmol), propargylamine (11.0 µL, 172 µmol), $CuSO_4 \cdot 5 H_2O$ (18.1 mg, 72.5 µmol), sodium

ascorbate (28.7 mg, 145 µmol), DMF (2 mL), and water (0.67 mL). A greenish solid (0.31 g) was obtained which was used without further purification.

2-(4-Aminomethyl-triazolyl)ethyl α-D-mannopyranoside (53)
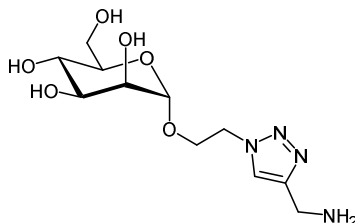
Mannoside **53** was synthesized according to general procedure B with azide **52** (42.9 mg, 172 µmol), propargylamine (11.0 µL, 172 µmol), $CuSO_4 \cdot 5\,H_2O$ (18.1 mg, 72.5 µmol), sodium ascorbate (28.7 mg, 145 µmol), DMF (2 mL), and water (0.67 mL). A greenish solid (0.11 g) was obtained which was used without further purification.

2-(2-(2-[(*E*)-*p*-(*p´*-Phenylazo)phenyloxy]ethoxy)ethoxy)ethanol (56)
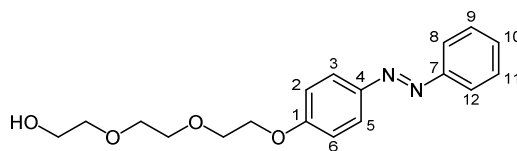
A mixture of *p*-phenylazophenol **55** (3.25 g, 16.4 mmol, 1.0 eq), potassium hydroxide (920 mg, 16.4 mmol, 1.0 eq) and 2-[2-(2-chlorethoxy)ethoxy]ethanol **54** (2.40 mL, 16.4 mmol, 1.0 eq) in *n*-Butanol (20 mL) was refluxed for 72 h. Remaining solids were filtered off, washed thoroughly with $CHCl_3$, and the solvent was removed under reduced pressure. The residue was purified by flash chromatography (Et$_2$O/EtOAc, 5:1), giving azobenzene derivative **56** as an orange solid.

Yield: 3.80 g, 11.5 mmol, 70%;

R$_f$: 0.23 (Et$_2$O/EtOAc, 5:1);

m.p.: 56 °C;

¹H NMR (500 MHz, CDCl$_3$, 300 K): δ = 7.84 (m$_c$, 2H, H-3, H-5), 7.78 (m$_c$, 2H, H-8, H-12), 7.47-7.35 (m, 3H, H-9, H-10, H-11), 6.96 (m$_c$, 2H, H-2, H-6), 4.18-4.13 (m, 2H, Ar-OC$\underline{H}_2$CH$_2$O), 3.85-

3.81 (m, 2H, Ar-OCH$_2$C$\underline{H}_2$O), 3.70-3.61 (m, 6H, OC$\underline{H}_2$CH$_2$O, OCH$_2$C$\underline{H}_2$O, OCH$_2$C$\underline{H}_2$OH), 3.58-3.53 (m, 2H, OC$\underline{H}_2$CH$_2$OH) ppm;

^{13}**C NMR** (125 MHz, CDCl$_3$, 300 K): δ = 161.2 (C-1), 152.7 (C-7), 147.1 (C-4), 130.4 (C-10), 129.0 (C-9, C-11), 124.7 (C-3, C-5), 122.6 (C-8, C-12), 114.8 (C-2, C-6), 72.5 (O$\underline{C}$H$_2$CH$_2$OH), 70.9 (O$\underline{C}$H$_2$CH$_2$O), 70.4 (O$\underline{C}$H$_2$CH$_2$O), 69.6 (Ar-O$\underline{C}$H$_2$CH$_2$O), 67.7 (Ar-O$\underline{C}$H$_2$CH$_2$O), 61.8 (O$\underline{C}$H$_2$CH$_2$OH) ppm;

ESI-MS (*m/z*): [M+Na]$^+$ calcd. for C$_{18}$H$_{22}$N$_2$O$_4$, 353.148, found, 353.144;

IR (ATR) ṽ: 3271, 2930, 2877, 1595, 1498, 1453, 1358, 1253, 1234, 1140, 1103, 1060, 1030, 923, 844, 771 cm^{-1}.

2-(2-(2-[(*E*)-*p*-(*p′*-Phenylazo)phenyloxy]ethoxy)ethoxy)ethyl 2,3,4,6-tetra-*O*-acetyl α-ᴅ-mannopyranoside (58)
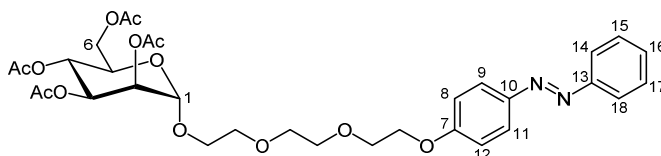
Trichloroacetimidate **57** (385 mg, 781 µmol, 1.0 eq) and azobenzene derivative **56** (310 mg, 939 µmol, 1.2 eq) were dissolved in dry CH$_2$Cl$_2$ (6 mL). Then, BF$_3$-etherate (150 µL, 1.25 mmol, 1.6 eq) was added dropwise at 0 °C and the solution was stirred for 30 min at this temperature. After stirring for 16 h at room temperature, the solution was diluted with CH$_2$Cl$_2$ and the organic phase was washed with satd. aq. NaHCO$_3$ solution until no further gas formation was observed. The organic phase was dried over MgSO$_4$, filtered and the filtrate was concentrated under reduced pressure. Purification of the crude mixture by flash chromatography (cyclohexane/EtOAc, 2:3) gave the product **58** as an orange amorphous solid.

Yield: 217 mg, 328 µmol, 42%;

R$_f$: 0.22 (cyclohexane/EtOAc, 2:3);

$[\alpha]_D^{20}$ = -0.875 (c = 0.4, CH$_2$Cl$_2$);

^{1}**H NMR** (500 MHz, CDCl$_3$, 300 K): δ = 7.91 (m$_c$, 2H, H-9, H-11), 7.87 (m$_c$, 2H, H-14, H-18), 7.49 (m$_c$, 2H, H-15, H-17), 7.43 (dd~t, $J_{15,16}$ = 7.4 Hz, $J_{16,17}$ = 7.4 Hz, 1H, H-16), 7.04 (m$_c$, 2H, H-8, H-12), 5.37 (dd, $J_{2,3}$ = 3.4 Hz, $J_{3,4}$ = 10.1 Hz, 1H, H-3), 5.30 (d, $J_{3,4}$ = 10.0 Hz, 1H, H-4), 5.28 (dd, $J_{1,2}$ = 1.8 Hz, $J_{2,3}$ = 3.5 Hz, 1H, H-2), 4.88 (d, $J_{1,2}$ = 1.6 Hz, 1H, H-1), 4.29 (dd, $J_{5,6}$ = 5.0 Hz, $J_{6a,6b}$ =

12.2 Hz, 1H, H-6a), 4.23 (m, 2H, OCH$_2$C$\underline{H}_2$-Ar), 4.10-4.05 (m, 2H, H-5, H-6b), 3.92-3.90 (m, 2H, OC$\underline{H}_2$CH$_2$-Ar), 3.85-3.80 (m, 2H, Man-OC$\underline{H}_2$CH$_2$O), 3.76-3.74 (m, 2H, Man-OCH$_2$C$\underline{H}_2$O), 3.70-3.64 (m, 4H, OC$\underline{H}_2$CH$_2$O, OCH$_2$C$\underline{H}_2$O), 2.15, 2.10, 2.02, 1.99 (each s, each 3H, 4 OAc) ppm;

^{13}C NMR (125 MHz, CDCl$_3$, 300 K): δ = 170.7, 170.0, 169.9, 169.7 (4 C=O), 161.3 (C-7), 152.7 (C-13), 147.1 (C-10), 130.4 (C-16), 129.0 (C-15, C-17), 124.7 (C-9, C-11), 122.6 (C-14, C-18), 114.9 (C-8, C-12), 97.7 (C-1), 70.9 (Man-OCH$_2$$\underline{C}H_2$O), 70.8 (O$\underline{C}H_2CH_2$O), 70.0 (OCH$_2$$\underline{C}H_2$O), 69.7 (O$\underline{C}H_2CH_2$O-Ar), 69.6 (C-5), 69.1 (C-2), 68.4 (C-4), 67.8 (OCH$_2$$\underline{C}H_2$O-Ar), 67.4 (Man-O$\underline{C}H_2CH_2$O), 66.2 (C-3), 62.4 (C-6) ppm;

ESI-MS (*m/z*): [M+Na]$^+$ calcd. for C$_{32}$H$_{40}$N$_2$O$_{13}$, 683.243, found, 683.242;

2-(2-(2-[(*E*)-*p*-(*p′*-Phenylazo)phenyloxy]ethoxy)ethoxy)ethyl α-D-mannopyranoside (59)

Deprotected mannoside **59** was synthesized according to general procedure C with acetyl-protected carbohydrate **58** (217 mg, 328 µmol), NaOMe solution (555 µL, 555 µmol) and methanol (5 mL), giving an orange amorphous solid.

Yield: 149 mg, 303 µmol, 92%;

R$_f$: 0.40 (EtOAc/MeOH, 5:1);

$[\alpha]_D^{20}$ = 26.5 (c = 0.4, CH$_2$Cl$_2$);

m.p.: 101 °C;

^{1}H NMR (500 MHz, D$_2$O, 300 K): δ = 7.46 (m$_c$, 2H, H-9, H-11), 7.42 (m$_c$, 2H, H-14, H-18), 6.96-6.94 (m, 2H, H-15, H-17), 6.88 (m$_c$, 1H, H-16), 6.50 (m$_c$, 2H, H-8, H-12), 4.70 (d∼s, 1H, H-1), 3.83 (dd, $J_{1,2}$ = 1.3 Hz, $J_{2,3}$ = 3.1 Hz, 1H, H-2), 3.72-3.67 (m, 3H, H-3, H-6a,b), 3.63-3.57 (m, 3H, H-4, OCH$_2$C$\underline{H}_2$-Ar), 3.49-3.45 (m, 1H, H-5), 3.38-3.32 (m, 10H, Man-OC$\underline{H}_2$CH$_2$O, Man-OCH$_2$C$\underline{H}_2$O, OC$\underline{H}_2$CH$_2$O, OCH$_2$C$\underline{H}_2$O, OC$\underline{H}_2$CH$_2$-Ar) ppm;

^{13}C NMR (125 MHz, D$_2$O, 300 K): δ = 160.8 (C-7), 152.1 (C-13), 146.5 (C-10), 128.9 (C-15, C-17), 124.7 (C-9, C-11), 122.4 (C-14, C-18), 114.6 (C-8, C-12), 99.9 (C-1), 72.7 (C-5), 70.7 (C-3), 70.1 (C-2), 69.8 (C-4), 69.6, 69.5, 68.8, 67.2 (Man-OCH$_2$$\underline{C}H_2O, O\underline{C}H_2CH_2O, OCH_2C\underline{H}_2O, OC\underline{H}_2CH_2$-Ar), 66.6 (OCH$_2$$\underline{C}H_2$-Ar), 66.2 (Man-O$\underline{C}H_2CH_2$O), 60.8 (C-6) ppm;

HR-ESI-MS (*m/z*): [M+H]$^+$ calcd. for $C_{24}H_{32}N_2O_9$, 493.2186, found, 493.2253; [M+Na]$^+$ calcd. for $C_{24}H_{32}N_2O_9$, 515.2006, found, 515.2072;

IR (ATR) ṽ: 3342, 2928, 2873, 1606, 1502, 1448, 1304, 1266, 1141, 1094, 1034, 1055, 836 cm^{-1}.

Heptakis(6-bromo-6-deoxy)cyclomaltoheptaose (60)[130]

The preparative procedure was adapted from *Angew. Chem. Int. Ed. Engl.* **1991**, *30* (1), 78-80:

To a solution of PPh$_3$ (26.1 g, 99.7 mmol, 15 eq) in dry DMF (100 mL) a solution of NBS (17.7 g, 99.7 mmol, 15 eq) also in dry DMF (33 mL) was added dropwise so that the temperature did not exceed 40 °C. Then, predried β-CD (**48**, 7.35 g, 6.48 mmol, 1.0 eq) was added and the reaction mixture was stirred at 80 °C for 36 h and the solution was subsequently reduced to one third of the initial volume. A freshly prepared methanolic NaOMe solution (65.0 mL, 129 mmol) was added and the mixture was stirred for 2 h at room temperature. Overlaying of the solution with MeOH (800 mL) induced the precipitation of a solid, which was filtered off and washed with MeOH. Drying at 30 °C furnished bromide **60** as a brownish solid.

Yield: 9.81 g, 6.23 mmol, 96%.

The obtained spectroscopic data was according to that reported in the literature.[130]

Heptakis(6-hexanoyl)cyclomaltoheptaose (61)[129]

Amphiphilic CD **61** was synthesized according to general procedure A with bromide **60** (1.14 g, 724 µmol) in DMF (6 mL), hexanoic acid (1.17 g, 10.1 mmol), and caesium carbonate (1.64 g, 5.06 mmol) in DMF (6 mL), yielding a white solid.

Yield: 791 mg, 0.434 µmol, 60%.

The obtained spectroscopic data was according to that reported in the literature.[129]

Heptakis(6-dodecanoyl)cyclomaltoheptaose (62)

Amphiphilic CD **62** was synthesized according to general procedure A with bromide **60** (2.00 g, 1.27 mmol) in DMF (10 mL), dodecanoic acid (3.56 g, 17.8 mmol), and caesium carbonate (2.88 g, 8.88 mmol) in DMF (10 mL), yielding a white solid.

Yield: 1.16 g, 482 μmol, 38%;

¹H NMR (500 MHz, DMSO-d_6, 300 K): δ = 6.08 (br s, 14H, 7 OH-2, 7 OH-3), 5.00-4.87 (m, 7H, 7 H-1), 4.34-4.21 (m, 7H, 7 H-6a), 4.09-3.99 (m, 7H, 7 H-6b), 3.80 (m, 7H, 7 H-5), 3.62 (m, 7H, 7 H-3), 3.32 (m, 14H, 7 H-2, 7 H-4), 2.36-2.12 (m, 28H, 7 CH$_2$C$\underline{H}_2$CO, 7 C$\underline{H}_2$CH$_2$CO), 1.46 (m$_c$, 14H, 7 C$\underline{H}_2$CH$_2$CH$_2$CO), 1.22 (m$_c$, 98H, 49 CH$_2$), 0.85 (br t, 21H, 7 CH$_3$) ppm;

¹³C NMR (125 MHz, DMSO-d_6, 300 K): δ = 172.8 (C=O), 102.5 (C-1), 83.2 (C-4), 73.2 (C-3), 72.6 (C-2), 69.6 (C-5), 63.6 (C-6), 33.8 ($\underline{C}$H$_2$CO), 33.5 ($\underline{C}$H$_2$CH$_2$CO), 31.8, 29.5, 29.4, 29.2, 29.1, 29.0 (6 CH$_2$), 24.8 ($\underline{C}$H$_2$CH$_2$CH$_3$), 22.5 ($\underline{C}$H$_2$CH$_3$), 14.3 ($\underline{C}$H$_3$) ppm;

Heptakis(6-tetradecanoyl)cyclomaltoheptaose (63)

Amphiphilic CD **63** was synthesized according to general procedure A with bromide **60** (2.00 g, 1.27 mmol) in DMF (10 mL), dodecanoic acid (4.06 g, 17.8 mmol), and caesium carbonate (2.88 g, 8.88 mmol) in DMF (10 mL), yielding a white solid.

Yield: 285 mg, 109 μmol, 9%;

¹H NMR (500 MHz, DMSO-d_6, 300 K): δ = 6.50 (br s, 14H, 7 OH-2, 7 OH-3), 4.97-4.86 (m, 7H, 7 H-1), 4.27 (m, 7H, 7 H-6a), 4.04 (m, 7H, 7 H-6b), 3.81 (m, 7H, 7 H-5), 3.63 (m, 7H, 7 H-3), 3.33 (m, 14H, 7 H-2, 7 H-4), 2.36-2.10 (m, 28H, 7 CH$_2$C$\underline{H}_2$CO, 7 C$\underline{H}_2$CH$_2$CO), 1.46 (m, 14H, 7 C$\underline{H}_2$CH$_2$CH$_2$CO), 1.24 (m, 126H, 63 CH$_2$), 0.85 (t, $J_{\mathrm{CH_2,CH_3}}$ = 6.8 Hz, 21H, 7 CH$_3$) ppm;

^{13}**C NMR** (125 MHz, DMSO-d_6, 300 K): δ = 176.3 (C=O), 102.5 (C-1), 83.2 (C-4), 73.2 (C-3), 72.6 (C-2), 36.2 (CH$_2$CO), 31.8, 29.5, 29.5, 29.4, 29.2 (5 CH$_2$), 24.8 (CH$_2$CH$_2$CH$_3$), 22.6 (CH$_2$CH$_3$), 14.3 (CH$_3$) ppm;

(*S*)-2-[(*tert*-Butoxycarbonyl)amino]-3-(prop-2-yn-1-yloxy)propanoic acid (69)[131]

The preparative procedure was adapted from *Chem. Sci.* **2012**, *3* (5), 1640-1644:

N-Boc-L-serine (**68**, 500 mg, 2.44 mmol, 1.0 eq) was dissolved in dry DMF (5 mL) and NaH (215 mg, 5.37 mmol, 2.2 eq; 60% suspension in mineral oil) was added portion wise at 0 °C. The reaction mixture was stirred for 30 min at this temperature and propargyl bromide solution (254 µL, 2.68 mmol, 1.1 eq; 80% in toluene) was added. The mixture was stirred for 30 min at 0 °C and after attaining room temperature stirring was continued for 16 h. Then, water (5 mL) was carefully added and the solvent was removed under reduced pressure. The residue was taken up in water and the aqueous phase was extracted four times with Et$_2$O. The aqueous phase was acidified (pH 2-3) with aq. KHSO$_4$ solution (0.5 M) and extracted three times with CH$_2$Cl$_2$. The organic phase was washed three times with aq. KHSO$_4$ solution (pH 2-3), dried over MgSO$_4$, filtered, and the solvent was removed under reduced pressure. The product **69** was obtained as a yellowish oil.

Yield: 572 mg, 2.35 mmol, 96%:

The obtained spectroscopic data was according to that reported in the literature.[131]

(*S*)-2-Amino-3-(prop-2-yn-1-yloxy)propanoic acid hydrochloride (66)[131]

The preparative procedure was adapted from *Chem. Sci.* **2012**, *3* (5), 1640-1644:

N-Boc-*O*-propargyl-L-serine (**69**, 2.62 g, 10.8 mmol) was dissolved EtOAc (5 mL) and aq. HCl solution (7.5 mL, 10 M) was added. The reaction mixture was stirred for 10 min after TLC revealed complete consumption of the starting material. The solvent was removed under

reduced pressure and the remaining solid was washed with CH_2Cl_2 and Et_2O to furnish hydrochloride **66** as a yellowish solid.

Yield: 1.64 g, 9.11 mmol, 84%.

The obtained spectroscopic data was according to that reported in the literature.[131]

2-[2-(2-Chloroethoxy)ethoxy]ethyl 2,3,4,6-tetra-*O*-acetyl α-D-mannopyranoside (71)[134]

The preparative procedure was adapted from *J. Am. Chem. Soc.*, 2009, 131 (6), 2110-2112:

Mannose pentaacetate (**70**, 4.24 g, 10.9 mmol, 1.0 eq) and 2-(2-(2-chloroethoxy)ethoxy)-ethanol (**54**, 4.74 mL, 32.6 mmol, 3.0 eq) were dissolved in dry CH_2Cl_2 (30 mL). Then, BF_3-etherate (5.46 mL, 43.5 mmol, 4.0 eq) was added dropwise at 0 °C and the solution was stirred for 30 min at this temperature. After stirring for 16 h at room temperature, the reaction was quenched by addition of triethylamine (6 mL) and the solution was diluted with CH_2Cl_2. The organic phase was washed three times with water, dried over $MgSO_4$, filtered, and the solvent was removed under reduced pressure. The crude product was purified by flash chromatography (cyclohexane/EtOAc, 1:1), yielding chloride **71** as yellowish syrup.

Yield: 3.41 g, 6.83 mmol, 63%.

The obtained spectroscopic data was according to that reported in the literature.[134]

2-[2-(2-Azidoethoxy)ethoxy]ethyl 2,3,4,6-tetra-*O*-acetyl α-D-mannopyranoside (72)[134a]

The preparative procedure was adapted from *J. Chem. Soc., Perkin Trans. 1* **2001**, 823-831:

NaN_3 (650 mg, 10.0 mmol, 5.0 eq) was added to solution of acetyl-protected mannoside **71** (1.00 g, 2.00 mmol, 1.0 eq) and TBAI (148 mg, 400 µmol, 0.2 eq) in DMF (20 mL). The reaction mixture was stirred at 60 °C for 6 h and after attaining room temperature stirring was continued for 16 h. Water (20 mL) was added and the solution was extracted four times with CH_2Cl_2. The organic phase was dried over $MgSO_4$, filtered, and the solvent was removed under reduced pressure. The residue was purified by flash chromatography (cyclohexane/EtOAc, 1:2), giving azide **72** as a colorless syrup.

Yield: 893 mg, 1.77 mmol, 89%.

The obtained spectroscopic data was according to that reported in the literature.[134a]

2-[2-(2-Azidoethoxy)ethoxy]ethyl α-D-mannopyranoside (65)[134a]

Deprotected mannoside **65** was synthesized according to general procedure C with acetyl-protected carbohydrate **72** (879 mg, 1.74 mmol), NaOMe solution (870 µL, 870 µmol), and methanol (10 mL), giving a colorless syrup.

Yield: 562 mg, 1.67 mmol, 96%;

The obtained spectroscopic data was according to that reported in the literature.[134a]

(S)-2-N-[2-(7-Isopropyl-1-methyl-azulen-4-yl)ethoxycarbonylamido]-3-(prop-2-yn-1-yloxy)propanoic acid (73)

O-Propargyl-L-serine (**66**, 347 mg, 1.93 mmol, 1.0 eq) was dissolved in a mixture of THF and water (1:1, 50 mL) and $NaHCO_3$ was added (648 mg, 7.72 mmol, 4.0 eq). The reaction mixture

was stirred for 15 min at room temperature before carbonate **17** (714 mg, 1.93 mmol, 1.0 eq) was added and stirring was continued for 16 h. The solution was then diluted with a half-satd. aq. NaCl solution and overlaid with EtOAc. The aqueous phase was acidified with aq. HCl solution (2 M) and the phases were separated. The organic phase was subsequently washed twice with brine, dried over Na_2SO_4, filtered, and the solvent was removed under reduced pressure. The crude mixture was purified by flash chromatography ($CHCl_3$/MeOH, 90:1 containing 1% of AcOH), yielding the carboxylic acid **73** as a blue oil.

Yield: 691 mg, 1.74 mmol, 90%;

R$_f$: 0.20 ($CHCl_3$/MeOH, 90:1 containing 1% of AcOH);

¹H NMR (500 MHz, MeOH-d_4, 300 K): δ = 8.19 (d, $J_{6,8}$ = 1.6 Hz, 1H, H-8), 7.63 (d, $J_{2,3}$ = 3.2 Hz, 1H, H-2), 7.47 (dd, $J_{5,6}$ = 10.7 Hz, $J_{6,8}$= 1.7 Hz, 1H, H-6), 7.34 (d, $J_{6,8}$ = 3.8 Hz, 1H, H-3), 7.07 (d, $J_{5,6}$ = 10.7 Hz, 1H, H-5), 4.45 (m$_c$, 2H, OC$\underline{H}_2$CH$_2$-az), 4.38 (dd~t, $J_{OCH,CHN}$ = 4.2 Hz, 1H, OCH$_2$C$\underline{H}$NH), 4.16 (d, $J_{CHO,CH'O}$ = 2.2 Hz, 2H, HC≡CC$\underline{H}_2$O), 3.89 (dd, $J_{OCH,OCH'}$ = 9.6 Hz, $J_{6,8}$= 4.9 Hz, 1H, OC$\underline{H}'$HCHNH), 3.89 (dd, $J_{OCH,OCH'}$ = 9.6 Hz, $J_{6,8}$= 4.9 Hz, 1H, OC$\underline{H}'$HCHNH), 3.78 (dd, $J_{OCH,OCH'}$ = 9.6 Hz, $J_{OCH,CHN}$= 3.5 Hz, 1H, OCH'$\underline{H}$CHNH), 3.47 (m$_c$, 2H, OCH$_2$C$\underline{H}_2$-az), 3.09 (sept, $J_{isopropyl}$ = 6.9 Hz, 1H, az-C$\underline{H}$(CH$_3$)$_2$), 2.84 (dd~t, $J_{HC≡,≡CHO}$ = 2.2 Hz, 1H, $\underline{H}$C≡CCH$_2$O), 2.63 (s, 3H, az-CH$_3$), 1.37 (d, $J_{isopropyl}$ = 6.9 Hz, 6H, az-CH(C$\underline{H}_3$)$_2$) ppm;

¹³C NMR (125 MHz, MeOH-d_4, 300 K): δ = 173.3 ($\underline{C}$O$_2$H), 158.6 (N$\underline{C}$O$_2$), 144.8 (C-7), 141.4 (C-4), 138.9 (C-10), 137.9 (C-2), 137.7 (C-9), 136.0 (C-6), 134.0 (C-8), 126.3 (C-1), 125.9 (C-5), 113.5 (C-3), 80.1 (HC≡$\underline{C}$CH$_2$O), 76.3 (H$\underline{C}$≡CCH$_2$O), 70.4 (O$\underline{C}$H$_2$CHNH), 66.5 (O$\underline{C}$H$_2$CH$_2$-az), 59.2 (HC≡C$\underline{C}$H$_2$O), 55.5 (OCH$_2$$\underline{C}$HNH), 39.4 (az-$\underline{C}$H(CH$_3$)$_2$), 38.6 (OCH$_2$$\underline{C}H_2$-az), 25.1 (az-CH($\underline{C}H_3$)$_2$), 12.9 (az-$\underline{C}H_3$) ppm;

ESI-MS (*m/z*): [M+Na]$^+$ calcd. for $C_{23}H_{27}NO_5$, 420.178, found, 420.171;

IR (ATR) ῦ: 3286, 2959, 1715, 1518, 1464, 1421, 1388, 1334, 1220, 1103, 1054, 1034, 922, 823, 777 cm^{-1}.

(*S*)-1-Adamantylamino-2-*N*-[2-(7-isopropyl-1-methyl-azulen-4-yl)ethoxycarbonyl-amido]-1-oxo-3-(prop-2-yn-1-yloxy)propane (74)

Carboxylic acid **73** (559 mg, 1.41 mmol, 1.5 eq), HBTU (534 mg, 1.41 mmol, 1.5 eq) and HOBt (190 mg, 1.41 mmol, 1.5 eq) were dissolved in dry DMF (25 mL) and DIPEA (479 μL, 2.82 mmol, 3.0 eq) was added. The reaction mixture was stirred for 15 min at room temperature before adamantylamine **67** (142 mg, 939 μmol, 1.0 eq) was added and stirring was continued for 16 h. Then, the solvent was removed under reduced pressure and the residue was purified by flash chromatography (toluene/EtOAc, 15:1→8:1), yielding amide **74** as a blue solid.

Yield: 444 mg, 836 μmol, 89%;

R$_f$: 0.33 (toluene/EtOAc, 9:1);

m.p.: 71 °C;

^{1}H NMR (500 MHz, CDCl$_3$, 300 K): δ = 8.19 (d, $J_{6,8}$ = 1.9 Hz, 1H, H-8), 7.66 (d, $J_{2,3}$ = 3.7 Hz, 1H, H-2), 7.43 (dd, $J_{5,6}$ = 10.7 Hz, $J_{6,8}$= 1.8 Hz, 1H, H-6), 7.33 (d, $J_{6,8}$ = 3.8 Hz, 1H, H-3), 7.02 (d, $J_{5,6}$ = 10.7 Hz, 1H, H-5), 6.02, 5.55 (each br s, each 1H, 2 NH), 4.50 (dd∼t, $_{OCH,CH\text{-}az}$ = 6.9 Hz, 2H, OC$\underline{H}_2$CH$_2$-az), 4.22-4.08 (m, 3H, OCH$_2$C$\underline{H}$NH, HC≡CC$\underline{H}_2$O), 3.85, 3.58 (each m$_c$, each 1H, OC$\underline{H}$′HCHNH, OCH′$\underline{H}$CHNH), 3.47 (dd∼t, $_{OCH,CH\text{-}az}$ = 7.0 Hz, 2H, OCH$_2$C$\underline{H}_2$-az), 3.09 (sept, $J_{isopropyl}$ = 6.9 Hz, 1H, az-C$\underline{H}$(CH$_3$)$_2$), 2.67 (s, 3H, az-CH$_3$), 2.45 (dd∼t, $J_{HC≡,≡CHO}$ = 2.4 Hz, 1H, $\underline{H}$C≡CCH$_2$O), 2.07 (br m$_c$, 3H, CH$_{adamantyl}$), 1.99, 1.68 (each br m$_c$, each 6H, CH$_{2,\,adamantyl}$), 1.37 (d, $J_{isopropyl}$ = 6.9 Hz, 6H, az-CH(C$\underline{H}_3$)$_2$) ppm;

^{13}C NMR (125 MHz, CDCl$_3$, 300 K): δ = 168.4 ($\underline{C}$ONH), 143.6 (C-7), 140.5 (C-4), 137.6 (C-10), 137.1 (C-2), 136.4 (C-9), 135.2 (C-6), 133.6 (C-8), 125.6 (C-1), 124.9 (C-5), 112.6 (C-3), 79.1 (HC≡$\underline{C}$CH$_2$O), 75.3 (H$\underline{C}$≡CCH$_2$O), 69.9 (O$\underline{C}$H$_2$CHNH), 65.7 (O$\underline{C}$H$_2$CH$_2$-az), 58.7 (HC≡C$\underline{C}$H$_2$O), 54.3 (OCH$_2$$\underline{C}$HNH), 52.3 (C$_{quart,\,adamantyl}$), 41.6 (CH$_{2,\,adamantyl}$), 38.4 (az-$\underline{C}$H(CH$_3$)$_2$), 37.8 (OCH$_2$$\underline{C}H_2$-az), 36.4 (CH$_{2,\,adamantyl}$), 29.6 (CH$_{adamantyl}$), 24.9 (az-CH($\underline{C}H_3$)$_2$), 13.0 (az-$\underline{C}H_3$) ppm;

ESI-MS (*m/z*): [M+Na]$^+$ calcd. for C$_{33}$H$_{42}$N$_2$O$_4$, 553.304, found, 553.301;

IR (ATR) $\tilde{υ}$: 3293, 2906, 1660, 1518, 1453, 1359, 1233, 1094, 1051, 922, 824, 778 cm^{-1}.

(*S*)-2-(2-(2-(4-(1-Adamantylamino-2-*N*-(2-(7-isopropyl-1-methyl-azulen-4-yl)ethoxycarbonylamido)-3-methoxy-1-oxopropyl)triazolyl)ethoxy)ethoxy)-ethyl 2,3,4,6-tetra-*O*-acetyl α-D-mannopyranoside (75)

Acetyl-protected mannoside **75** was synthesized according to general procedure B with azide **72** (115 mg, 228 μmol), alkyne **74** (110 mg, 207 μmol), CuSO$_4$·5 H$_2$O (21.7 mg, 86.9 μmol), sodium ascorbate (34.9 mg, 176 μmol), DMF (6 mL), and water (2 mL). The crude product was purified by flash chromatography (CH$_2$Cl$_2$/MeOH, 30:1), giving the product **75** as a blue syrup.

Yield: 106 mg, 102 μmol, 50% (55% based on conversion, 5% starting material reisolated);

R$_f$: 0.26 (CH$_2$Cl$_2$/MeOH, 30:1);

¹H NMR (600 MHz, CDCl$_3$, 300 K): δ = 8.18 (d, $J_{6,8}$ = 1.4 Hz, 1H, H-8), 7.72 (s, 1H, H$_{triazole}$), 7.65 (d, $J_{2,3}$ = 3.5 Hz, 1H, H-2), 7.42 (dd, $J_{5,6}$ = 10.6 Hz, $J_{6,8}$ = 1.3 Hz, 1H, H-6), 7.32 (d, $J_{2,3}$ = 3.6 Hz, 1H, H-3), 7.01 (d, $J_{5,6}$ = 10.6 Hz, 1H, H-5), 6.28, 5.70 (each br s, each 1H, 2 NH), 5.34 (dd, $J_{3',4'}$ = 10.1 Hz, $J_{2',3'}$ = 3.4 Hz, 1H, H-3′), 5.29 (d~t, $J_{3',4'}$ = 10.0 Hz, 1H, H-4′), 5.26-5.25 (m, 1H, H-2′), 4.87 (d, $J_{1',2'}$ = 1.2 Hz, 1H, H-1′), 4.68 (br m$_c$, 2H, triazole-C$\underline{H}_2$O), 4.55 (m$_c$,2H, OCH$_2$C$\underline{H}_2$-triazole), 4.46 (m$_c$, 2H, OC$\underline{H}_2$CH$_2$-az), 4.27 (dd, $J_{6'a,6'b}$ = 12.2 Hz, $J_{5',6'a}$= 5.0 Hz, 1H, H-6′a), 4.17 (m$_c$, 1H, OCH$_2$C$\underline{H}$NH), 4.11 (dd, $J_{6'a,6'b}$ = 12.2 Hz, $J_{5',6'b}$= 2.3 Hz, 1H, H-6′b), 4.04 (ddd, $J_{4',5'}$ = 9.8 Hz, $J_{5',6'a}$ = 5.0 Hz, $J_{5',6'b}$= 2.4 Hz, 1H, H-5′), 3.91-3.85 (m, 3H, OC$\underline{H}_2$CH$_2$-triazole, OC$\underline{H}$′HCHNH), 3.81-3.78 (m, 1H, Man-OC$\underline{H}$′HCH$_2$O), 3.67-3.59 (m, 7H, OC$\underline{H}_2$CH$_2$O, OCH$_2$C$\underline{H}_2$O, Man-OCH′$\underline{H}$CH$_2$O, Man-OCH$_2$C$\underline{H}_2$O), 3.55 (m$_c$, 1H, OCH′$\underline{H}$CHNH), 3.46 (m$_c$, 2H, OCH$_2$C$\underline{H}_2$-az), 3.07 (sept, $J_{isopropyl}$ = 6.9 Hz, 1H, az-C$\underline{H}$(CH$_3$)$_2$), 2.65 (s, 3H, az-CH$_3$), 2.14, 2.09 (each s, each 3H, 2 OAc), 2.05 (br m$_c$, 3H, CH$_{adamantyl}$), 2.03, 1.98 (each s, each 3H, 2 OAc), 1.95, 1.65 (each br m$_c$, each 6H, CH$_{2, adamantyl}$), 1.36 (d, $J_{isopropyl}$ = 6.9 Hz, 6H, az-CH(C$\underline{H}_3$)$_2$) ppm;

¹³C NMR (150.92 MHz, CDCl$_3$, 300 K): δ = 170.8, 170.2, 170.1, 169.8 ($\underline{C}$OCH$_3$), 168.6 ($\underline{C}$ONH), 156.3 (NH$\underline{C}$O$_2$), 144.2 (C$_{quart, triazole}$), 143.6 (C-7), 140.4 (C-4), 137.6 (C-10), 137.0 (C-2), 136.4 (C-9), 135.2 (C-6), 133.6 (C-8), 125.6 (C-1), 124.9 (C-5), 123.9 (C$_{triazole}$), 112.5 (C-3), 97.8 (C-1′), 70.8, 70.7 (O$\underline{C}$H$_2$CH$_2$O, OCH$_2$$\underline{C}H_2$O), 70.4 (O$\underline{C}H_2$CHNH), 70.1 (Man-OCH$_2$$\underline{C}H_2$O), 69.7 (C-2′),

69.6 (O$\underline{C}$H$_2$CH$_2$-triazole), 69.2 (C-3′), 68.6 (C-5), 67.5 (Man-O$\underline{C}$H$_2$CH$_2$O), 66.3 (C-4′), 65.6 (O$\underline{C}$H$_2$CH$_2$-az), 64.5 (triazole-$\underline{C}$H$_2$O), 62.5 (C-6′), 54.2 (OCH$_2$$\underline{C}$HNH), 52.2 (C$_{quart,\ adamantyl}$), 50.4 (OCH$_2$$\underline{C}H_2$-triazole), 41.5 (CH$_{2,\ adamantyl}$), 38.4 (az-$\underline{C}$H(CH$_3$)$_2$), 37.8 (OCH$_2$$\underline{C}H_2$-az), 36.4 (CH$_{2,\ adamantyl}$), 29.5 (CH$_{adamantyl}$), 24.8 (az-CH($\underline{C}H_3$)$_2$), 21.0, 20.9, 20.8 (3 CO$\underline{C}$H$_3$), 13.0 (az-$\underline{C}$H$_3$) ppm;

ESI-MS (*m/z*): [M+Na]$^+$ calcd. for C$_{53}$H$_{73}$N$_5$O$_{16}$, 1058.5, found, 1058.7;

IR (ATR) $\tilde{\upsilon}$: 2907, 1751, 1676, 1510, 1367, 1218, 1088, 1047, 978, 921, 787 cm^{-1}.

(*S*)-2-(2-(2-(4-(1-Adamantylamino-2-*N*-(2-(7-isopropyl-1-methyl-azulen-4-yl)ethoxy-carbonylamido)-3-methoxy-1-oxopropyl)triazolyl)ethoxy)ethoxy)ethyl α-ᴅ-mannopyranoside (64)
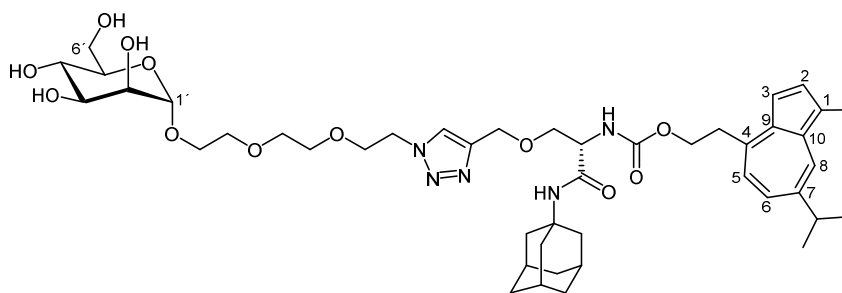
Deprotected mannoside **64** was synthesized according to general procedure C with acetyl-protected carbohydrate **75** (75.2 mg, 72.6 µmol), NaOMe solution (50.0 µL, 50.0 µmol), and methanol (1 mL), giving a blue amorphous solid.

Yield: 55.6 mg, 64.1 µmol, 88%;

R*f*: 0.23 (EtOAc/MeOH, 5:1);

¹H NMR (600 MHz, MeOH-*d₄*, 300 K): δ = 8.18 (d~s, 1H, H-8), 7.98 (s, 1H, H$_{triazole}$), 7.62 (d, *J*$_{2,3}$ = 3.4 Hz, 1H, H-2), 7.46 (dd~d, *J*$_{5,6}$ = 10.5 Hz, 1H, H-6), 7.32 (d~s, 1H, H-3), 7.06 (d, *J*$_{5,6}$ = 10.6 Hz, 1H, H-5), 4.79 (d~s, 1H, H-1′), 4.60 (br m$_c$, 2H, triazole-C$\underline{H}$$_2$O), 4.55 (m$_c$, 2H, OCH$_2C\underline{H}$$_2$-triazole), 4.45 (m$_c$, 2H, OC$\underline{H}$$_2CH_2$-az), 4.22 (m$_c$, 1H, OCH$_2C\underline{H}$NH), 3.86-3.78 (m, 5H, H-2′, H-6′a, Man-OC$\underline{H}$′HCH$_2$O, OC$\underline{H}$$_2CH_2$-triazole), 3.75-3.56 (m, 13H, H-3′, H-4′, H-5′, H-6′b, Man-OCH′$\underline{H}$CH$_2$O, Man-OCH$_2$C$\underline{H}$$_2O, OC\underline{H}$$_2CH_2O, OCH_2C\underline{H}$$_2O, OC\underline{H}$$_2$CHNH), 3.46 (m$_c$, 2H, OCH$_2C\underline{H}$$_2$-az), 3.08 (sept, *J*$_{isopropyl}$ = 6.8 Hz, 1H, az-C$\underline{H}$(CH$_3$)$_2$), 2.62 (s, 3H, az-CH$_3$), 2.02 (br m$_c$, 3H, CH$_{adamantyl}$), 1.96, 1.68 (each br m$_c$, each 6H, CH$_{2,\ adamantyl}$), 1.36 (d, *J*$_{isopropyl}$ = 6.9 Hz, 6H, az-CH(C$\underline{H}$$_3$)$_2$) ppm;

¹³C NMR (150.92 MHz, CDCl$_3$, 300 K): δ = 171.2 ($\underline{C}$ONH), 158.3 (NH$\underline{C}$O$_2$), 145.4 (C$_{quart,\ triazole}$), 144.8 (C-7), 141.4 (C-4), 139.0 (C-10), 137.9 (C-2), 137.7 (C-9), 136.0 (C-6), 134.0 (C-8), 126.4 (C$_{triazole}$), 125.8 (C-5), 113.5 (C-3), 101.7 (C-1′), 74.6 (C-3), 72.6 (C-5), 72.1 (C-2), 71.6, 71.5,

71.4, 71.3 (OCH$_2$CH$_2$O, OCH$_2$CH$_2$O, Man-OCH$_2$CH$_2$O, OCH$_2$CHNH), 70.4 (OCH$_2$CH$_2$-triazole), 68.6 (C-4), 67.7 (Man-OCH$_2$CH$_2$O), 66.6 (OCH$_2$CH$_2$-az), 65.0 (triazole-CH$_2$O), 63.0 (C-6′), 56.6 (OCH$_2$CHNH), 53.1 (C$_{quart, adamantyl}$), 51.4 (OCH$_2$CH$_2$-triazole), 42.2 (CH$_{2, adamantyl}$), 39.4 (az-CH(CH$_3$)$_2$), 38.5 (OCH$_2$CH$_2$-az), 37.4 (CH$_{2, adamantyl}$), 30.9 (CH$_{adamantyl}$), 25.1 (az-CH(CH$_3$)$_2$), 12.9 (az-CH$_3$) ppm;

HR-ESI-MS (*m/z*): [M+H]$^+$ calcd. for C$_{45}$H$_{65}$N$_5$O$_{12}$, 868.4708, found, 868.4742;

IR (ATR) ṽ: 3338, 2909, 1663, 1528, 1454, 1359, 1255, 1240, 1056, 814 cm^{-1}.

N-Boc-4-nitrosobenzylamine[137] (78)
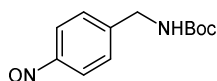
The preparative procedure was adapted from *J. Org. Chem.* **2005**, *70* (6), 2350-2352:

A solution of Oxone® (6.33 g 10.3 mmol, 1.5 eq) in water (60 mL) was added to a solution of Boc-protected 4-aminobenzylamine **76** (1.53 g, 6.88 mmol, 1.0 eq) in CH$_2$Cl$_2$ (60 mL) and the reaction mixture was stirred for 16 h at room temperature. After phase separation, the aqueous phase was extracted three times with CH$_2$Cl$_2$. The organic phase was washed first with aq. HCl solution (1 M), then with brine, dried over MgSO$_4$, filtered, and the solvent was removed under reduced pressure. A crude mixture of the nitroso compound **78** and the corresponding nitro compound was obtained as a green solid.

Yield: 975 mg, 3.30 mmol, 48% (determined by ^{1}H NMR);

The obtained spectroscopic data was according to that reported in the literature.[137]

N-Boc-(*E*)-*p*-(*p*′-methoxyphenylazo)benzylamine (81)
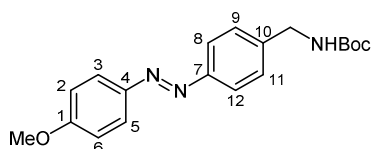
Crude nitroso compound **78** (975 mg) and *p*-anisidine (**79**, 406 mg, 1.0 eq) were dissolved in DMSO (18 mL) and glacial AcOH (18 mL) was added. The reaction mixture was stirred for 16 h at room temperature and subsequently water was added. The precipitated solid was collected

by filtration and washed with water. Purification by flash chromatography (cyclohexane/EtOAc, 4:1) gave azobenzene derivative **81** as an orange solid.

Yield: 929 mg, 2.72 mmol, 82%;

R$_f$: 0.44 (CH$_2$Cl$_2$);

m.p.: 117 °C;

^{1}H NMR (500 MHz, CDCl$_3$, 300 K): δ = 7.91 (m$_c$, 2H, H-3, H-5), 7.84 (m$_c$, 2H, H-8, H-12), 7.41 (d, $J_{8,9}$ = 8.4 Hz, 2H, H-9, H-11), 7.01 (m$_c$, 2H, H-2, H-6), 4.90 (br s, 1H, N<u>H</u>Boc), 4.39 (d, $J_{CH,NH}$ = 5.3 Hz, 2H, C<u>H$_2$</u>NHBoc), 3.89 (s, 3H, OCH$_3$), 1.48 (s, 9H, NHC(O)OC(C<u>H$_3$</u>)$_3$) ppm;

^{13}C NMR (125 MHz, CDCl$_3$, 300 K): δ = 162.2 (C=O), 156.0 (C-1), 152.2 (C-7), 147.2 (C-4), 141.5 (C-10), 128.2 (C-9, C-11), 124.9 (C-3, C-5), 123.0 (C-8, C-12), 114.4 (C-2, C-6), 55.7 (OCH$_3$), 44.6 (<u>C</u>H$_2$NHBoc), 28.6 (NHC(O)OC(<u>C</u>H$_3$)$_3$) ppm;

HR-EI-MS (*m/z*): [M]$^+$ calcd. for C$_{19}$H$_{23}$N$_3$O$_3$, 341.1739, found, 341.1749;

IR (ATR) ũ: 3367, 2982, 1681, 1602, 1524, 1501, 1395, 1293, 1247, 1163, 1143, 1104, 1025, 863, 838 cm^{-1}.

(*E*)-*p*-(*p*´-Methoxyphenylazo)benzylammonium trifluoroacetate (83)
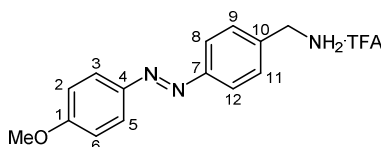
Azobenzene derivative **81** (924 mg, 2.71 mmol) was dissolved in CH$_2$Cl$_2$ (30 mL) and TFA (5 mL) was added. The reaction mixture was stirred for 2 h at room temperature and the solvent was removed under reduced pressure. The residue was taken up in MeOH and was codistilled with toluene, giving TFA salt **83** as an orange solid.

Yield: 964 mg, 2.71 mmol, quant.;

m.p.: 219 °C;

^{1}H NMR (500 MHz, MeOH-d_4, 300 K): δ = 7.92 (m$_c$, 4H, H-3, H-5, H-8, H-12), 7.61 (m$_c$, 2H, H-9, H-11), 7.08 (m$_c$, 2H, H-2, H-6), 4.85 (br s, 3H, NH$_3^+$), 4.20 (br s, C<u>H$_2$</u>NH$_3^+$), 3.90 (s, 3H, OCH$_3$) ppm;

¹³C NMR (125 MHz, CDCl₃, 300 K): δ = 164.2 (C-1), 154.4 (C-7), 148.2 (C-4), 136.5 (C-10), 130.9 (C-9, C-11), 126.0 (C-3, C-5), 124.1 (C-8, C-12), 115.5 (C-2, C-6), 56.2 (OCH₃), 44.0 ($\underline{C}$H₂NH₃⁺) ppm;

λ$_{max}$ (ε): 349 nm (21705 L mol⁻¹ cm⁻¹);

HR-EI-MS (*m/z*): [M]⁺ calcd. for C₁₄H₁₅N₃O, 241.1215, found, 241.1150;

IR (ATR) ṽ: 2933, 2844, 2638, 1664, 1599, 1580, 1498, 1411, 1255, 1203, 1176, 1126, 1109, 1035, 985, 840, 800 cm⁻¹.

_N_-Boc-(_E_)-_p_-(phenylazo)benzylamine (80)
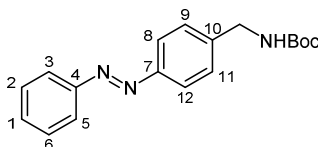
Acetic acid (50 mL) was added to a solution of 4-[*N*-Boc-aminomethyl]aniline **76** (2.86 g, 12.9 mmol, 1.0 eq) and nitrosobenzene **77** (1.38 g, 12.9 mmol, 1.0 eq) in DMSO (50 mL). After the reaction mixture was stirred for 16 h at room temperature, water (200 mL) was added and the precipitated solid was collected by filtration. The crude product was recrystallized from a mixture of water and MeOH (4:1), giving the azobenzene derivative **80** as an orange solid.

Yield: 3.05 g, 9.73 mmol, 75%;

R$_f$: 0.38 (CH₂Cl₂);

m.p.: 119 °C;

¹H NMR (500 MHz, CDCl₃, 300 K): δ = 8.14 (m$_c$, 1H, H-1), 7.93-7.90 (m, 2H, H-8, H-12), 7.90-7.86 (m, 2H, H-3, H-5), 7.55-7.39 (m, 4H, H-2, H-6, H-9, H-11), 4.94 (m$_c$, 1H, NH), 4.40 (d, $J_{CH,NH}$ = 4.6 Hz, 2H, C$\underline{H}$₂NHBoc), 1.48 (s, 9H, NHC(O)OC(C$\underline{H}$₃)₃) ppm;

¹³C NMR (125 MHz, CDCl₃, 300 K): δ = 156.1 (C=O), 152.8 (C-4), 152.1 (C-7), 142.2 (C-10), 131.1 (C-1), 129.2 (C-2, C-6), 128.2 (C-9, C-11), 123.3 (C-8, C-12), 123.0 (C-3, C-5), 79.9 (NHC(O)O$\underline{C}$(CH₃)₃), 44.5 ($\underline{C}$H₂NHBoc), 28.6 (NHC(O)OC($\underline{C}$H₃)₃) ppm;

EI-MS (*m/z*): [M]⁺ calcd. for C₁₈H₂₁N₃O₂, 311.16, found, 311.12.

IR (ATR) ṽ: 3321, 2980, 2927, 1683, 1523, 1366, 1285, 1245, 1155, 1135, 930, 846, 764 cm⁻¹.

(*E*)-*p*-(Phenylazo)benzylammonium trifluoroacetate (82)
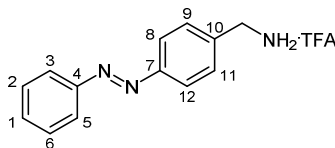
Azobenzene derivative **80** (233 mg, 748 μmol) was dissolved in CH_2Cl_2 (9 mL) and TFA (1 mL) was added. The reaction mixture was stirred for 30 min at room temperature and the solvent was removed under reduced pressure. The residue was taken up in MeOH and was codistilled with toluene, giving TFA salt **82** as an orange solid.

Yield: 243 mg, 747 μmol, quant.;

m.p.: 173 °C;

¹H NMR (500 MHz, DMSO-d_6, 300 K): δ = 8.37 (br s, 2H, NH$_2$), 8.30 (m$_c$, 1H, H-1), 7.96-7.93 (m, 2H, H-8, H-12), 7.93-7.88 (m, 2H, H-3, H-5), 7.68 (m$_c$, 2H, H-9, H-11), 7.64-7.56 (m, 2H, H-2, H-6), 4.16 (s, 2H, C$\underline{H}_2$NH$_3^+$) ppm;

¹³C NMR (125 MHz, DMSO-d_6, 300 K): δ = 151.9 (C-4), 151.8 (C-7), 137.4 (C-10), 131.8 (C-1), 130.0 (C-2, C-6), 129.5 (C-9, C-11), 122.7 (C-8, C-12), 122.6 (C-3, C-5), 41.9 (CH$_2$NH$_3^+$) ppm;

λ$_{max}$ (ε): 320 nm (23892 L mol^{-1} cm^{-1});

EI-MS (*m/z*): [M]$^+$ calcd. for $C_{13}H_{13}N_3$, 211.11, found, 211.09.

IR (ATR) ṽ: 3005, 2771, 2622, 1662, 1503, 1210, 1173, 1128, 1102, 998, 899, 840, 801 cm^{-1}.

(*E*)-*p*-(Phenylazo)benzylammonium hydrochloride (19)
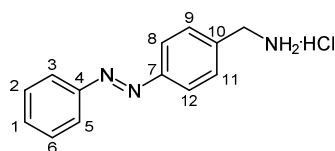
Azobenzene derivative **80** (175 mg, 562 μmol) was dissolved in CH_2Cl_2 (10 mL) and conc. aq. HCl solution (2 mL) was added. The reaction mixture was stirred for 4 h at room temperature and the solvent was removed under reduced pressure, giving hydrochloride salt **19** as an orange solid.

Yield: 139 mg, 561 μmol, quant.;

m.p.: 236-240 °C;

¹H NMR (600 MHz, DMSO-d_6, 300 K): δ = 8.58 (NH_3^+), 7.93-7.90 (m, 4H, H-3, H-5, H-8, H-12), 7.73 (m_c, 2H, H-9, H-11), 7.63-7.59 (m, 3H, H-1, H-2, H-6), 4.13 ($C\underline{H}_2NH_3^+$) ppm;

¹³C NMR (150.92 MHz, CDCl$_3$, 300 K): δ = 151.9 (C-4), 151.7 (C-7), 137.5 (C-10), 131.8 (C-1), 130.1 (C-9, C-11), 129.5 (C-2, C-6), 122.6 (C-3, C-5, C-8, C-12), 41.8 ($\underline{C}H_2NH_3^+$) ppm;

HR-EI-MS (*m/z*): [M]$^+$ calcd. for $C_{13}H_{13}N_3$, 211.1109, found, 211.1118;

IR (ATR) ṽ: 3276, 2873, 1592, 1522, 1486, 1442, 1384, 1214, 1154, 1074, 976, 851, 773 cm^{-1}.

p-Hydroxyphenyl 2,3,4,6-tetra-*O*-acetyl α-D-mannopyranoside (87)
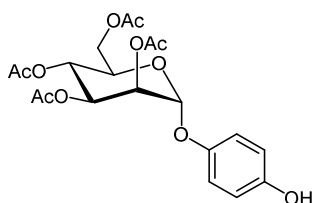
Mannose pentaacetate (**70**, 1.02 g, 2.62 mmol, 1.0 eq) and hydroquinone (**86**, 1.16 g, 10.5 mmol, 4.0 eq) were dissolved in a mixture of dry CH$_2$Cl$_2$ (80 mL) and dry acetonitrile (30 mL). Then, BF$_3$·etherate (610 µL, 4.97 mmol, 1.9 eq) was added dropwise at 0 °C and the mixture was stirred for 48 h at room temperature. After dilution with CH$_2$Cl$_2$, the organic phase was washed with satd. aq. NaHCO$_3$ solution and water. The organic phase was then dried over MgSO$_4$, filtered and the solvent was removed under reduced pressure. The crude product was then purified by flash chromatography (2:1→1:2), yielding mannoside **87** as a colorless syrup.

Yield: 822 mg, 1.87 mmol, 71%;

R$_f$: 0.27 (cyclohexane/EtOAc, 2:1);

$[\alpha]_D^{20}$ = 67.8 (c = 0.7, CH$_2$Cl$_2$);

¹H NMR (500 MHz, CDCl$_3$, 300 K): δ = 6.95 (m, 2H, Ar-H), 6.75 (m, 2H, Ar-H), 5.54 (dd, $J_{2,3}$ = 10.0 Hz, $J_{3,4}$ = 3.5 Hz, 1H, H-3), 5.42 (dd, $J_{1,2}$ = 1.7 Hz, $J_{2,3}$ = 3.5 Hz, 1H, H-2), 5.38 (d, $J_{1,2}$ = 1.8 Hz, 1H, H-1), 5.35 (dd~t, $J_{4,5}$ = 10.0 Hz, $J_{3,4}$ = 10.0 Hz, 1H, H-4), 4.27 (dd, $J_{6a,6b}$ = 12.0 Hz, $J_{5,6a}$ = 5.2 Hz, 1H, H-6a), 4.14 (ddd, $J_{4,5}$ = 9.9 Hz, $J_{5,6a}$ = 5.3 Hz, $J_{5,6b}$ = 2.4 Hz, 1H, H-5), 4.10 (dd, $J_{6a,6b}$ = 12.0 Hz, $J_{5,6b}$ = 2.4 Hz, 1H, H-6b), 2.19, 2.06, 2.05, 2.03 (each s, each 3H, 4 OAc) ppm;

¹³C NMR (125 MHz, CDCl₃, 300 K): δ = 170.8, 170.3, 170.2, 170.0 (4 C=O), 151.7, 149.8 (2 Ar-C$_{quart}$), 118.0, 116.2 (2 Ar-C), 96.8 (C-1), 69.7 (C-2), 69.2 (C-5), 69.1 (C-3), 66.2 (C-4), 62.4 (C-6), 21.6, 21.0, 20.8 (3 CO$\underline{C}$H₃) ppm;

ESI-MS (*m/z*): [M+Na]⁺ calcd. for C₂₀H₂₄O₁₁, 463.12, found, 463.08.

IR (ATR) ṽ: 3448, 2960, 1742, 1509, 1368, 1203, 1125, 1034, 979, 832, 808, 756 cm⁻¹.

p-(Prop-2-yn-1-yloxy)phenyl 2,3,4,6-tetra-*O*-acetyl α-D-mannopyranoside (88)
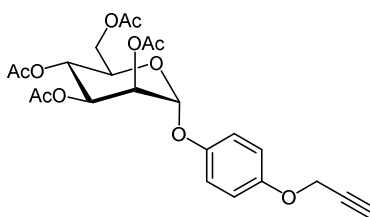
Potassium carbonate (189 mg, 1.37 mmol, 1.5 eq) was added to a solution of mannoside **87** (400 mg, 910 μmol, 1.0 eq) in DMF (20 mL). The reaction mixture was stirred for 30 min at room temperature and propargyl bromide solution (100 μL, 1.06 mmol, 1.2 eq; 80% in toluene) was added. The mixture was stirred at 100 °C for 12 h and subsequently for 24 h at room temperature. The solvent was removed under reduced pressure and the crude product was purified by flash chromatography (cyclohexane/EtOAc, 2:1), giving alkyne **88** as a white solid.

Yield: 284 mg, 594 μmol, 65%;

R$_f$: 0.26 (cyclohexane/EtOAc, 2:1);

m.p.: 63 °C;

$[\alpha]_D^{20}$ = 60.1 (c = 0.5, CH₂Cl₂);

¹H NMR (500 MHz, CDCl₃, 300 K): δ = 7.05-7.00 (m, 2H, Ar-H), 6.94-6.88 (m, 2H, Ar-H), 5.54 (dd, $J_{2,3}$ = 3.4 Hz, $J_{3,4}$ = 10.0 Hz, 1H, H-3), 5.43 (dd, $J_{1,2}$ = 1.9 Hz, $J_{2,3}$ = 3.4 Hz, 1H, H-2), 5.42 (d, $J_{1,2}$ = 1.9 Hz, 1H, H-1), 5.35 (dd∼t, $J_{4,5}$ = 10.0 Hz, $J_{3,4}$ = 10.0 Hz, 1H, H-4), 4.65 (d, $J_{OCH_2,C≡CH}$ = 2.4 Hz, 2H, OC$\underline{H}$₂C≡CH), 4.27 (dd, $J_{6a,6b}$ = 11.9 Hz, $J_{5,6a}$ = 5.2 Hz, 1H, H-6a), 4.15-4.09 (m, 2H, H-5, H-6b), 2.50 (t, $J_{OCH_2,C≡CH}$ = 2.5 Hz, 1H, OCH₂C≡C$\underline{H}$), 2.19, 2.05, 2.04, 2.03 (each s, each 3H, 4 OAc) ppm;

¹³C NMR (125 MHz, CDCl₃, 300 K): δ = 170.7, 170.1, 170.1, 169.9 (4 C=O), 153.5, 150.5 (2 Ar-C$_{quart}$), 117.9, 116.1 (2 Ar-C), 96.7 (C-1), 78.7 (OCH₂$\underline{C}$≡CH), 75.7 (OCH₂C≡$\underline{C}$H), 69.6 (C-2), 69.2 (C-5), 69.1 (C-3), 66.2 (C-4), 62.4 (C-6), 56.5 (O$\underline{C}$H₂C≡CH), 21.2, 21.0, 20.8 (3 CO$\underline{C}$H₃) ppm;

ESI-MS (*m/z*): [M+Na]$^+$ calcd. for $C_{23}H_{26}O_{11}$, 501.1, found, 501.5.

IR (ATR) ṽ: 3274, 2957, 1739, 1508, 1367, 1211, 1125, 1027, 974, 912, 831, 807 cm^{-1}.

p-(Prop-2-yn-1-yloxy)phenyl α-ᴅ-mannopyranoside (89)
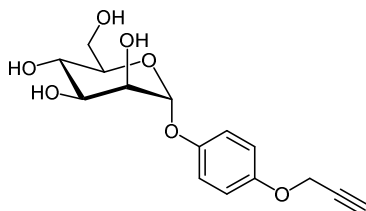
Deprotected mannoside **89** was synthesized according to general procedure C with acetyl-protected carbohydrate **88** (152 mg, 318 μmol), NaOMe solution (100 μL, 100 μmol) and methanol (10 mL), giving a white solid.

Yield: 80.2 mg, 258 μmol, 81%;

R$_f$: 0.15 (CH$_2$Cl$_2$/MeOH, 9:1);

$[\alpha]_D^{20}$ = 65.2 (c = 0.3, MeOH);

¹H NMR (500 MHz, MeOH-d_4, 300 K): δ = 7.09-7.04 (m, 2H, Ar-H), 6.96-6.90 (m, 2H, Ar-H), 5.37 (d, $J_{1,2}$ = 1.4 Hz, 1H, H-1), 4.68 (d, $J_{OCH_2,C\equiv CH}$ = 2.1 Hz, 2H, OC$\underline{H}_2$C≡CH), 4.00 (dd, $J_{1,2}$ = 1.8 Hz, $J_{2,3}$ = 3.3 Hz, 1H, H-2), 3.89 (dd, $J_{2,3}$ = 3.4 Hz, $J_{3,4}$ = 9.4 Hz, 1H, H-3), 3.79 (dd, $J_{6a,6b}$ = 11.9 Hz, $J_{5,6a}$ = 2.4 Hz, 1H, H-6a), 3.76-3.70 (m, 2H, H-4, H-6b), 3.66 (ddd, $J_{4,5}$ = 9.7 Hz, $J_{5,6b}$ = 5.3 Hz, $J_{5,6a}$ = 2.3 Hz, 1H, H-5), 2.92 (t, $J_{OCH_2,C\equiv CH}$ = 2.4 Hz, 1H, OCH$_2$C≡C$\underline{H}$) ppm;

¹³C NMR (125 MHz, MeOH-d_4, 300 K): δ = 154.2, 152.6 (2 Ar-C$_{quart}$), 119.1, 117.0 (2 Ar-C), 101.1 (C-1), 80.0 (OCH$_2\underline{C}$≡CH), 76.6 (OCH$_2$C≡$\underline{C}$H), 75.3 (C-5), 72.4 (C-3), 72.1 (C-2), 68.4 (C-4), 62.7 (C-6), 57.2 (O$\underline{C}$H$_2$C≡CH) ppm;

ESI-MS (*m/z*): [M+Na]$^+$ calcd. for $C_{15}H_{18}O_7$, 333.1, found, 333.4.

IR (ATR) ṽ: 3558, 3413, 3274, 2940, 2889, 1739, 1506, 1367, 1213, 1124, 1012, 806 cm^{-1}.

Mono(6^A-(4-((α-D-mannopyranosyl)methyloxy)triazolyl))cyclomaltoheptaose (85)
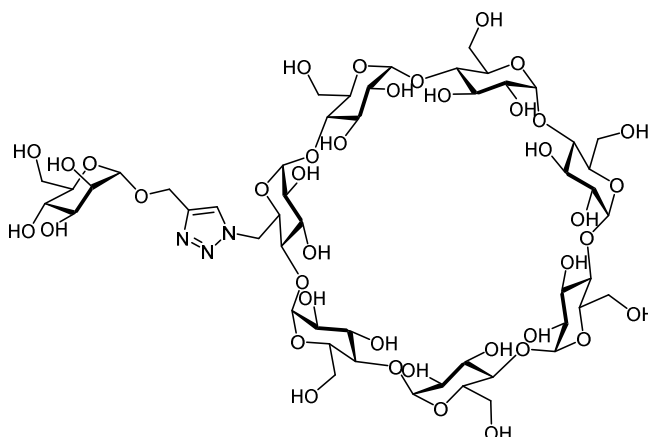
CD conjugate **85** was synthesized according to general procedure B with azide **50** (292 mg, 251 µmol), alkyne **84** (54.8 mg, 251 µmol), CuSO$_4$ · 5 H$_2$O (26.5 mg, 106 µmol), sodium ascorbate (42.3 mg, 214 µmol), DMF (7 mL), and water (2 mL). The crude product was purified by GPC with DMF as the eluent, giving the product **85** as a white solid.

Yield: 318 mg, 231 µmol, 92%;

R$_f$: 0.37 (^{i}PrOH/H$_2$O/EtOAc/NH$_4$OH (conc.), 5:3:1:1);

$[\alpha]_D^{20}$ = +128.9 (c = 0.4, H$_2$O);

m.p.: decomposition at 165 °C;

^{1}H NMR (600 MHz, DMSO-d_6, 300 K): δ = 8.02 (s, 1H, H$_{triazole}$), 5.94-5.50 (m, 17H, 7 OH-2$_{CD}$, 7 OH-3$_{CD}$, OH-2$_{Man}$, OH-3$_{Man}$, OH-4$_{Man}$), 5.05 (d, $J_{1,2}$ = 3.4 Hz, 1H, H-1$^A_{CD}$), 4.92-4.38 (m, 15H, 6 H-1$_{CD}$, 6 OH-6$_{CD}$, 2 H-6$^A_{CD}$, H-1$_{Man}$), 4.24 (dd~t, $J_{6,OH}$ = 5.7 Hz, 1H, OH-6$_{Man}$), 3.99 (dd~t, $J_{4,5}$ = 8.7 Hz, 1H, H-4$_{Man}$), 3.76-3.20 (m, 47H, 7 H-2$_{CD}$, 7 H-3$_{CD}$, 7 H-4$_{CD}$, 7 H-5$_{CD}$, 12 H-6$_{CD}$, H-2$_{Man}$, H-3$_{Man}$, H-5$_{Man}$, 2 H-6$_{Man}$, OC$\underline{H}_2$-triazole, overlap with HDO) ppm;

^{13}C NMR (150.92 MHz, DMSO-d_6, 300 K): δ = 143.4 (C-4$_{triazole}$), 124.9 (C-3$_{triazole}$), 102.0 (C-1$_{CD}$), 99.0 (C-1$_{Man}$), 81.6 (C-4$_{CD}$), 74.1, 70.9, 70.2 (C-2$_{Man}$, C-3$_{Man}$, C-5$_{Man}$) 73.07, 72.4, 72,1 (C-2$_{CD}$, C-3$_{CD}$, C-5$_{CD}$), 67.0 (C-4$_{Man}$), 61.3, 59.9 (C-6$_{Man}$, C-6$_{CD}$), 58.7 (OC$\underline{H}_2$-triazole) 50.2 (C-6$^A_{CD}$) ppm;

MALDI-MS (*m/z*): [M+Na]$^+$ calcd. for C$_{51}$H$_{83}$N$_3$O$_{40}$, 1400.445, found, 1401.159;

IR (ATR) ṽ: 3306, 2938, 1654, 1366, 1249, 1153, 1078, 1019, 999, 948, 846 cm^{-1}.

Mono(6^A-(4-(4-(α-D-mannopyranosyloxo)methoxyphenyl)triazolyl))-cyclomaltoheptaose (90)
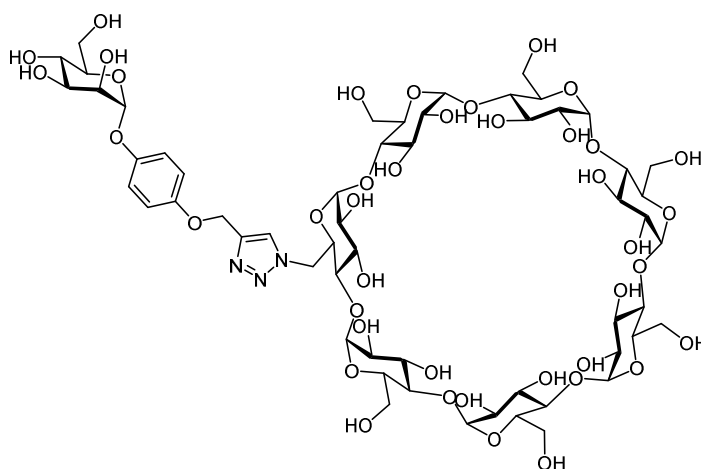
CD conjugate **90** was synthesized according to general procedure B with azide **50** (1.25 g, 1.08 mmol), alkyne **89** (334 mg, 1.08 mmol), $CuSO_4 \cdot 5\,H_2O$ (113 mg, 454 µmol), sodium ascorbate (182 mg, 918 µmol), DMF (24 mL), and water (8 mL). The crude product was purified by RP chromatography (ACN/ddH$_2$O, cf. Appendix), giving the product **90** as a white solid.

Yield: 1.23 g, 837 µmol, 78%;

R$_f$: 0.43 (^{i}PrOH/H$_2$O/EtOAc/NH$_4$OH (conc.), 5:3:1:1);

$[\alpha]_D^{20}$ = +139.4 (c = 1.5, H$_2$O);

m.p.: decomposition at 280 °C;

^{1}H NMR (500 MHz, DMSO-d_6, 300 K): δ = 8.13 (s, 1H, H$_{triazole}$), 7.03 (m$_c$, 2H, Ar-H), 6.95 (m$_c$, 2H, Ar-H), 5.87 (d, $J_{OH,CH}$ = 6.6 Hz, 1H, OH-4$_{Man}$), 5.77-5.63 (m, 14H, 7 OH-2$_{CD}$, 7 OH-3$_{CD}$), 5.22 (d, $J_{1,2}$ = 1.7 Hz, 1H, H-1$_{Man}$), 5.03 (m$_c$, 3H, H-1$^A_{CD}$, OC$\underline{H}_2$-triazole), 4.94 (d, $J_{OH,CH}$ = 4.4 Hz, 1H, OH-2$_{Man}$), 4.90 (m$_c$, 1H, H-6a$^A_{CD}$), 4.85-4.77 (m, 7H, 6 H-1$_{CD}$), 4.69 (d, $J_{OH,CH}$ = 6.1 Hz, 1H, OH-3$_{Man}$), 4.59 (dd, $J_{6a,6b}$ = 14.5 Hz, $J_{5,6a}$ = 8.4 Hz, 1H, H-6b$^A_{CD}$), 4.52-4.43 (m, 6H, OH-6$_{CD}$), 4.28 (m$_c$, 1H, OH-6$_{Man}$), 3.99 (m$_c$, 1H, H-5$^A_{CD}$), 3.81 (m$_c$, 1H, H-2$_{Man}$), 3.76-3.24 (m, 42H, H-2$^A_{CD}$, 6 H-2$_{CD}$, H-3$^A_{CD}$, 6 H-3$_{CD}$, H-4$^A_{CD}$, 6 H-4$_{CD}$, 6 H-5$_{CD}$, 12 H-6$_{CD}$, H-3$_{Man}$, H-4$_{Man}$, H-5$_{Man}$, overlap with HDO), 3.14-3.10 (m, 1H, H-6a$_{Man}$), 2.92-2.89 (m, 1H, H-6b$_{Man}$) ppm; **^{13}C NMR** (125 MHz, DMSO-d_6, 300 K): δ = 153.4, 150.7 (2 Ar-C$_{quart}$), 142.7 (C$_{quart, triazole}$), 125.4 (C$_{triazole}$), 118.3, 115.5 (2 Ar-C), 102.2, 102.1, 102.0, 101.9, 101.3 (C-1$^A_{CD}$, C-1$_{CD}$), 99.9 (C-1$_{Man}$), 83.5, 82.1, 81.6, 81.5, 81.4, 81.0 (C-3$_{Man}$, C-3$^A_{CD}$, C-3$_{CD}$), 74.8, 73.2, 73.1, 73.0, 72.9, 72.7, 72.5, 72.5, 72.4, 72.3, 72.3, 72.2, 72.1,

71.8, 70.7 (C-2$^{A}_{CD}$, C-2$_{CD}$, C-4$^{A}_{CD}$, C-4$_{CD}$, C-5$_{CD}$, C-5$_{Man}$), 70.2 (C-2$_{Man}$), 70.0 (C-5$^{A}_{CD}$), 66.8 (C-4$^{A}_{Man}$), 61.4 (O$\underline{C}$H$_2$-triazole), 61.1, 60.2, 60.0, 59.9, 59.0 (C-6$_{CD}$), 50.4 (C-6$^{A}_{CD}$) ppm;

HR-ESI-MS (*m/z*): [M+H]$^+$ calcd. for C$_{57}$H$_{87}$N$_3$O$_{41}$, 1470.4893, found, 1470.4878;

IR (ATR) ṽ: 3306, 2938, 1504, 1334, 1203, 1152, 1079, 1024, 1002, 946, 832 cm^{-1}.

Mono(6^{A}-amino-6^{A}-deoxy)cyclomaltoheptaose (91)[139]
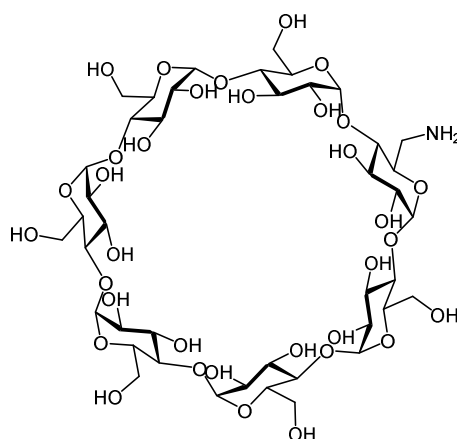
The preparative procedure was adapted from *J. Chromatogr. A* **2005**, *1094* (1–2), 187-191:

PPh$_3$ (196 mg, 748 μmol, 1.1 eq) was added to a solution of azido-β-CD **50** (789 mg, 680 μmol, 1.0 eq) in DMF (10 mL). The reaction mixture was stirred for 2 h at room temperature and water (1 mL) was added subsequently. The mixture was then stirred at 90 °C for 3 h and after cooling to room temperature was poured onto acetone. The precipitated solid was collected by filtration, washed with acetone, and dried at 60 °C, yielding amino-β-CD **91** as a white solid.

Yield: 725 mg, 639 μmol, 94%;

The obtained spectroscopic data was according to that reported in the literature.[140]

Mono(6ᴬ-*N′*-(3′,6′-dihydroxy-3*H*-spiro[2-benzofuran-1,9′-xanthen]-3-one-5-yl)thioureido-6ᴬ-deoxy)cyclomaltoheptaose (93)
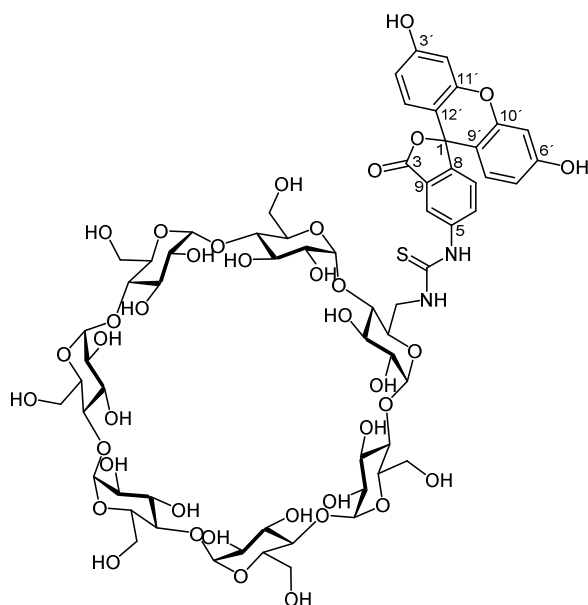
Amino-β-CD **91** (100 mg, 88.2 μmol, 1.0 eq) and fluorescein isothiocyanate isomer I (**92**, 37.8 mg, 97.0 μmol, 1.1 eq) were dissolved in dry DMF (20 mL). Then, DIPEA (15.0 μL, 88.2 μmol, 1.0 eq) was added and the mixture was stirred for 16 h at room temperature. The solution was poured onto Et₂O and the precipitated solid was collected by filtration, washed thoroughly with Et₂O, and dried at 60 °C. The fluorescein-tagged CD **93** was obtained as an orange solid.

Yield: 86.4 mg, 56.7 μmol, 64%;

R$_f$: 0.60 (*i*PrOH/H₂O/EtOAc/NH₄OH (conc.), 5:3:1:1);

$[\alpha]_D^{20}$ = +94.1 (c = 1.0, DMSO);

¹H NMR (500 MHz, DMSO-*d₆*, 300 K): δ = 10.0 (br s, 1H, Ar-OH), 8.31 (d∼s, 1H, H-4), 7.94 (br s, 1H, NH), 7.78 (d, *J*$_{6,7}$ = 8.1 Hz, 1H, H-6), 7.15 (d, *J*$_{6,7}$ = 8.3 Hz, 1H, H-7), 6.65-6.62 (m, 4H, H-1′, H-4′, H-5′, H-8′), 6.54 (m$_c$, 2H, H-2′, H-7′), 5.89-5.66 (m, 14H, 7 OH-2, 7 OH-3$_{CD}$), 4.89-4.82 (m, 7H, 7 H-1$_{CD}$), 4.55-4.37 (m, 6H, 6 OH-6$_{CD}$), 4.16 (m$_c$, 1H, H-6ᴬa$_{CD}$), 3.82-3.24 (m, 41H, 7 H-2$_{CD}$, 7 H-3$_{CD}$, 7 H-4$_{CD}$, 7 H-5$_{CD}$, H-6ᴬb$_{CD}$, 6 H-6a,b$_{CD}$, overlap with HDO) ppm;

¹³C NMR (125 MHz, DMSO-*d₆*, 300 K): δ = 180.6 (C=S), 168.6 (C=O), 152.4 (C-10′, C-11′), 141.3 (C-8), 129.2 (C-1′, C-8′), 128.4 (C-6), 124.5 (C-7), 117.1 (C-4), 113.7 (C-2′, C-7′), 110.1 (C-9′, C-12′), 102.5, 102.3, 102.1, 102.0, 101.8, 101.7 (C-4′, C-5′, C-1ᴬ$_{CD}$, C-1$_{CD}$), 83.8 (C-1), 81.8, 81.5, 81.2 (C-3ᴬ$_{CD}$, C-3$_{CD}$), 73.1, 73.0, 72.8, 72.5, 72.4, 72.3, 72.1, 72.0, 69.7, 69.6, 69.5, 68.5 (C-2ᴬ$_{CD}$, C-2$_{CD}$, C-4ᴬ$_{CD}$, C-4$_{CD}$, C-5ᴬ$_{CD}$, C-5$_{CD}$), 59.9, 59.7 (C-6$_{CD}$), 44.8 (C-6ᴬ$_{CD}$) ppm;

HR-ESI-MS (*m/z*): [M+H]$^+$ calcd. for $C_{63}H_{82}N_2O_{39}S$, 1523.4294, found, 1523.4298;

IR (ATR) ũ: 3305, 2939, 1577, 1460, 1317, 1209, 1153, 1109, 1078, 1024, 946, 916, 847 cm^{-1}.

7.4 Photoirradiation Experiments

Photoirradiation experiments were performed by A. Müller (for azobenzene derivative **82**) and myself (for azobenzene derivative **83**).

E/*Z* ratios were determined by irradiating a sample of the respective azobenzene derivative and subsequent measurement by ^{1}H NMR spectroscopy. Therefore, an NMR tube containing the azobenzene sample (≈10 mg dissolved in 500 μL MeOH-*d$_6$*) was set up at a distance of approx. 5 cm to the LED and was irradiated at 365 nm for 15 min when the photostationary state (PSS) was reached. Afterwards, the sample was immediately measured by ^{1}H NMR spectroscopy in order to prevent back-isomerization. The respective PSS was calculated by integration of an isolated proton signal (OC$\underline{H}_3$ or C$\underline{H}_2$NH$_3^+$) of the corresponding azobenzene derivative.

Kinetics of the thermal *Z*→*E* relaxation were determined by ^{1}H NMR spectroscopy. For this, ^{1}H NMR spectra were recorded in regular intervals of 3-4 h over a period of 5-6 d. The half-life was determined by integration of isolated *Z* and *E* isomer proton signals (OC$\underline{H}_3$ or C$\underline{H}_2$NH$_3^+$). Both the decrease of the *Z* isomer integral and the increase of the *E* isomer integral were plotted and the data was fitted by a first order exponential decay. The half-life $\tau_{1/2}$ was calculated by the formula: $\tau_{1/2}$ = ln 2/k.

For UV/Vis spectroscopy, a UV cuvette containing a sample of the respective azobenzene derivative was set up at a distance of approx. 5 cm to the LED and was irradiated at 365 nm for 15 min. Afterwards, UV/Vis spectra (cf. Appendix) were immediately recorded, revealing the formation of the respective *Z* isomer by an increase of the n-π* transition absorbance and a decrease of the π-π* transition absorbance. Extinction coefficients (ε) were calculated through linear regression of absorbance maxima deduced from UV/Vis spectra measured at different concentrations (5 μM, 10 μM, 20 μM, 40 μM, 60 μM and 80 μM).

Table 7.1: Characterization of the *E* and *Z* isomers of azobenzene derivatives **82** and **83**.

Azobenzene derivative	*E/Z* (PSS)[a]	λ_{max} (*E* and *Z*) [nm]	half-life, $\tau_{1/2}$ [h]
82	58:42	320 320, 440	680
83	3:97	349 311, 438	146

[a] Determined by the integration ratio of OCH_3 or $CH_2NH_3^+$ moieties in the ¹H NMR spectra.

7.5   Bacterial Adhesion Assays

7.5.1   Media and Buffer Solutions

LB medium: tryptone (10.0 g), sodium chloride (10.0 g) and yeast extract (5.00 g) were dissolved in distilled deionized water (1.00 L) and after autoclavation chloramphenicol (50.0 mg) and ampicillin (100 mg) were added.

PBS buffer solution (pH 7.2): sodium chloride (8.00 g), potassium chloride (200 mg), sodium hydrogen phosphate dihydrate (1.44 g) and potassium dihydrogen phosphate (200 mg) were dissolved in distilled deionized water (1.00 L).

PBST buffer solution (pH 7.2): PBS buffer + Tween® 20 (0.05% v/v).

Carbonate buffer solution (pH 9.6): sodium carbonate (1.59 g) and sodium hydrogen carbonate (2.52 g) were dissolved in distilled deionized water (1.00 L).

MES buffer (0.5 M, pH 6.3): 2-(*N*-Morpholino)ethanesulfonic acid (9.76 g) were dissolved in distilled deionized water (1.00 L) and the pH value was adjusted to 6.3 with sodium carbonate solution (2.5 M).

Reagent solution for activation of magnetic PEG beads: EDC (32 mg) and NHS (64 mg) were dissolved in MES buffer (1 mL).

Adjustment of pH values: The buffer pH values were adjusted with aqueous 0.1 M HCl or 0.1 M NaOH solution

7.5.2 Cultivation of Bacteria

GFP-expressing *E. coli* bacteria (strain pPKL1162)[145] were cultured from a frozen stock in LB medium and incubated overnight at 37 °C. After centrifugation, the bacteria pellet was washed twice with PBS buffer (2.00 mL) and then resuspended in PBS buffer. Finally, the suspension was adjusted to OD_{600} = 0.4 (2 mg/mL) with PBS.

7.5.3 Adhesion-inhibition Assay with GFP-expressing *E. coli*

Black 96-well microtiter plates (Nunc™, MaxiSorp™) were incubated with a solution of mannan from *Saccharomyces cerevisiae* (1.2 mg/mL in carbonate buffer, 120 μL/well) and desiccated overnight at 37 °C and 100 rpm. The plates were washed three times with PBST (150 μL/well) and subsequently blocked by incubation with a PVA solution (1% in PBS, 120 μL/well) for 4 h at 4 °C. The plates were then washed twice with PBST (150 μL/well) and once with PBS (150 μL/well). Serial dilutions (1:1) of the respective inhibitor in PBS were prepared on the plates (100 μL/well; start concentrations are indicated at the corresponding inhibition curves). The bacterial suspension (OD_{600} = 0.4, 50 μL/well) was then added and the plates were incubated for 1 h at 37 °C and 100 rpm. Subsequently, the plates were washed twice with PBS (150 μL), the wells were filled with PBS (100 μL/well), and fluorescence (485 nm/535 nm) was measured.[146] Each inhibitor was tested at least in triplicate and with the standard inhibitor MeMan on the same plate.

The percentage of inhibition was calculated:

$$Inhibition\ (\%) = \frac{I_0 - I}{I_0} \cdot 100$$

where I_0 = intensity of fluorescence without inhibitor; I = intensity of fluorescence with inhibitor.

7.5.4 Covalent Functionalization of Polystyrene Microtiter Plates

Black 96-well microtiter plates (Nunc Immobilizer™ Amino) were incubated with solutions of the respective amino functionalized compound in carbonate buffer (100 μL/well; concentrations are indicated at the corresponding binding curves) overnight at room temperature and 100 rpm. The plates were washed three times with PBST (150 μL/well) and subsequently blocked by incubation with an ethanolamine solution (10 mM in carbonate buffer, 120 μL/well) for 2 h at room temperature and 100 rpm. Finally, the microtiter plates were washed twice with PBST (150 μL/well) and once with PBS (150 μL/well).[146]

7.5.5   Non-covalent Functionalization of Polystyrene Microtiter Plates

Transparent 96-well microtiter plates (Nunc-Immuno™ MicroWell™ MaxiSorp™) were incubated with a solution of the respective amphiphilic CD (5 μM in ddH$_2$O, diluted from stock solution containing 1% DMSO, 100 μL/well) overnight at room temperature. The plates were washed twice with PBS (200 μL/well) and blocked by incubation with a BSA solution (1% m/v in PBS, 150 μL/well) for 1 h at 37 °C. Finally, the microtiter plates were washed twice with PBS (200 μL/well).

7.5.6   Binding Assay with GFP-expressing *E. coli* and Cyclodextrin Inclusion Complexes on Polystyrene Microtiter Plates

Covalently functionalized microtiter plates were prepared according to 7.5.4 either by incubation with an azobenzene solution of static concentration or by preparation of serial dilutions (1:1, concentrations are indicated at the corresponding binding curves). Then, solutions of the respective CD conjugate (100 μL/well, static concentration or serially diluted, concentrations are indicated at the corresponding binding curves) were added and the plates were incubated for 1 h at 37 °C and 100 rpm. After washing once with PBS (150 μL/well), one half of the plates was covered while the other half was irradiated with 365 nm for 15 min. Subsequently, the plates were washed once with PBS (150 μL/well), the bacterial suspension (OD$_{600}$ = 0.4, 100 μL/well) was added and the plates were incubated for 1 h at 37 °C and 100 rpm. Finally, the plates were washed three times with PBS (150 μL/well), PBS was added to the wells (100 μL/well) and fluorescence (485 nm/535 nm) was measured.

On each plate *p*APMan (10 mM in static concentration or serially diluted) was covalently immobilized as a reference.

7.5.7   Binding Assay with Magnetic PEG Beads

Assays with magnetic PEG beads were performed by A. Müller and myself.

Magnetic PEG beads (2x 450 μL, micromod, PEG-COOH coating micromer®-M) were incubated with a freshly-prepared activation reagent solution (112.5 μL) for 16 h at room temperature and 600 rpm. After washing twice with PBS (1 mL) by using a magnetic rack, the two portions were combined in an Eppendorf tube®, the supernatant was removed, and the beads were resuspended in PBS (600 μL).

Taken from this stock suspension, the activated beads (100 µL) were then incubated with azobenzene derivatives **82** and **83**, respectively, (15 mM in carbonate buffer containing 10% of DMSO and 1% of TEA, 1 mL) for 4 h at room temperature and 600 rpm. After washing twice with PBS (1 mL), the beads were blocked by incubation with an ethanolamine solution (10 mM in carbonate buffer, 1 mL) for 1 h at room temperature and 600 rpm. Then, the beads were washed twice with PBS (1 mL) and resuspended in PBS (1 mL).

The azobenzene functionalized beads (50 µL) were incubated with CD conjugate **90** (8 mM in PBS, 100 µL) for 2 h at room temperature and 600 rpm. After washing twice with PBS (100 µL), the beads were resuspended in PBS (50 µL), transferred to a small plastic bowl and PBS (450 µL) was added. One portion of the beads was irradiated for 10 min with UV light (365 nm) and agitated at 600 rpm while the other portion was agitated and kept in the dark. Subsequently, the beads were transferred to an Eppendorf tube®, washed with PBS (400 µL), and resuspended in PBS (400 µL). A bacterial suspension (OD_{600} = 0.6, 100 µL) was added and the beads were incubated for 30 min at room temperature and 600 rpm. After washing with PBS (500 µL) and transfer to a new Eppendorf tube®, the beads were taken up in PBS (100 µL), transferred to a black 96-well microtiter plate (Nunc™, MaxiSorp™), and fluorescence (485 nm/535 nm) was measured.

Each type of azobenzene functionalized beads (azobenzene **82** or **83**) was tested in duplicate and unfunctionalized beads provided the blank fluorescence value.

7.5.8 Enzyme Activity Test (for ELLA)

This assay as well as the one described in 7.5.9 was performed at the CSIC – University of Seville under supervision of Jose Manuel García Fernández.

Transparent 96-well microtiter plates (Nunc-Immuno™ MicroWell™ MaxiSorp™) were incubated with a solution of mannan from *Saccharomyces cerevisiae* (10 µg/mL in PBS containing 0.1 mM of Ca^{2+} and 0.1 mM of Mn^{2+}, 100 µL/well) overnight at room temperature. The plates were subsequently washed three times with PBST (200 µL/well) and blocked by incubation with a BSA solution (1% m/v in PBS, 150 µL/well) for 1 h at 37 °C. After washing three times with PBST (200 µL/well), the wells were filled with serial dilutions of Con A-HRP (10^{-1}-10^{-5} mg/mL in PBS, 100 µL/well) and incubated for 1 h at 37 °C. The plates were again washed three times with PBST (200 µl/well) and a solution of ABTS (0.25 mg/mL in citrate-phosphate buffer with 0.015% H_2O_2, 50 µL/well) was added, resulting in a color reaction. After 20 min, the reaction was stopped by addition of H_2SO_4 (1 M, 50 µL/well) and the

absorbance at 415 nm was measured. The concentration of Con A-HRP which gave absorbance values between 0.8 and 1.0 was used for surface binding assays.[147]

7.5.9 Enzyme-linked Lectin Assay (ELLA) with Cyclodextrin Inclusion Complexes

Non-covalently functionalized microtiter plates were prepared according to 7.5.5. Then, serial dilutions (1:1) of the respective guest molecules were prepared on the plates (start concentration: 40 µM) and the plates were incubated for 1 h at 37 °C. After washing twice with PBS (200 µL/well), a Con A-HRP solution (concentration determined by enzyme activity test) was added, the microtiter plates were incubated for 1 h at 37 °C, and subsequently washed twice with PBS (200 µL/well). Then, a solution of ABTS (0.25 mg/mL in citrate-phosphate buffer with 0.015% H_2O_2, 50 µL/well) was added, the reaction was stopped after 20 min by addition of H_2SO_4 (1 M, 50 µL/well) and the absorbance at 415 nm was measured.

7.5.10 Phenol-Sulfuric Acid Assay

Covalently functionalized microtiter plates (transparent 96-well Nunc Immobilizer™ Amino) were prepared according to 7.5.4 by incubation with solutions of the respective amino functionalized compound (10 mM in carbonate buffer). Serial dilutions (1:1) of azido-β-CD **50** (start concentration: 5 mM in PBS) and mannoside **52** (start concentration: 10 mM in PBS) were prepared in a separate area on the same plates and subsequently desiccated overnight at 37 °C. Then, every well was incubated with a phenol solution (5% in ddH_2O, 25 µL/well) and conc. sulfuric acid (125 µL/well) for 30 min at room temperature and 100 rpm, followed by determination of the absorbance at 490 nm.[148]

References and Notes

1.   Voet, D.; Voet, J. G., *Biochemistry*. Wiley: 2004.

2.   Ball, D. W.; Hill, J. W.; Scott, R. J., *Chemistry: General, Organic, and Biological v. 1.0*. Creative Commons: 2011.

3.   Sharon, N.; Lis, H., *Science* **1989**, *246* (4927), 227-34.

4.   Sharon, N.; Lis, H., *Sci. Am.* **1993**, *268* (1), 82-9.

5.   Ofek, I.; Hasty, D. L.; Sharon, N., *FEMS Immunol. Med. Microbiol.* **2003**, *38* (3), 181-191.

6.   Chappell, D.; Jacob, M.; Hofmann-Kiefer, K.; Rehm, M.; Welsch, U.; Conzen, P.; Becker, B. F., *Cardiovasc. Res.* **2009**, *83* (2), 388-396.

7.   Gorelik, E.; Galili, U.; Raz, A., *Cancer Metastasis Rev.* **2001**, *20* (3-4), 245-77.

8.   Stanley, P.; Schachter, H.; Taniguchi, N., N-Glycans. In *Essentials of Glycobiology*, 2nd ed.; Varki, A.; Cummings, R. D.; Esko, J. D., Eds. Cold Spring Harbor Laboratory Press: Cold Spring Harbor (NY), 2009.

9.   (a) Tabak, L. A., *Annu. Rev. Physiol.* **1995**, *57*, 547-64; (b) Brockhausen, I., *Biochem. Soc. Trans.* **2003**, *31* (2), 318-25.

10.   Merrill, A. H., Jr., *Chem. Rev.* **2011**, *111* (10), 6387-422.

11.   Minko, T., *Adv. Drug. Deliv. Rev.* **2004**, *56* (4), 491-509.

12.   (a) Bouckaert, J.; Berglund, J.; Schembri, M.; De Genst, E.; Cools, L.; Wuhrer, M.; Hung, C.-S.; Pinkner, J.; Slättegård, R.; Zavialov, A.; Choudhury, D.; Langermann, S.; Hultgren, S. J.; Wyns, L.; Klemm, P.; Oscarson, S.; Knight, S. D.; De Greve, H., *Mol. Microbiol.* **2005**, *55* (2), 441-455; (b) Rabinovich, G. A.; Toscano, M. A.; Jackson, S. S.; Vasta, G. R., *Curr. Opin. Struct. Biol.* **2007**, *17* (5), 513-520.

13.   Stillmark, H. Ueber Ricin, ein giftiges Ferment aus den Samen von Ricinus comm. L. und einigen anderen Euphorbiaceen. Dorpat, 1888.

14.   Sumner, J. B.; Howell, S. F., *J. Bacteriol.* **1936**, *32* (2), 227-37.

15.   Sharon, N.; Lis, H., *Glycobiology* **2004**, *14* (11), 53R-62R.

16.   Hartmann, M.; Lindhorst, T. K., *Eur. J. Org. Chem.* **2011**, *2011* (20-21), 3583-3609.

17.   Firon, N.; Ofek, I.; Sharon, N., *Carbohydr. Res.* **1983**, *120*, 235-249.

18.   (a) Ofek, I.; Mirelman, D.; Sharon, N., *Nature* **1977**, *265* (5595), 623-625; (b) Ofek, I.; Beachey, E. H., *Infect. Immun.* **1978**, *22* (1), 247-254.

19.   Vetsch, M.; Puorger, C.; Spirig, T.; Grauschopf, U.; Weber-Ban, E. U.; Glockshuber, R., *Nature* **2004**, *431* (7006), 329-333.

20.   Waksman, G.; Hultgren, S. J., *Nat. Rev. Micro.* **2009**, *7* (11), 765-774.

21.   Choudhury, D.; Thompson, A.; Stojanoff, V.; Langermann, S.; Pinkner, J.; Hultgren, S. J.; Knight, S. D., *Science* **1999**, *285* (5430), 1061-1066.

22.   Hung, C.-S.; Bouckaert, J.; Hung, D.; Pinkner, J.; Widberg, C.; DeFusco, A.; Auguste, C. G.; Strouse, R.; Langermann, S.; Waksman, G.; Hultgren, S. J., *Mol. Microbiol.* **2002**, *44* (4), 903-915.

23.   Firon, N.; Ashkenazi, S.; Mirelman, D.; Ofek, I.; Sharon, N., *Infect. Immun.* **1987**, *55* (2), 472-476.

24. Lindhorst, T. K., CHAPTER 1 Small Molecule Ligands for Bacterial Lectins: Letters of an Antiadhesive Glycopolymer Code. In *Glycopolymer Code: Synthesis of Glycopolymers and their Applications*, The Royal Society of Chemistry: 2015; pp 1-16.

25. Nicotra, F.; Cipolla, L.; Peri, F.; La Ferla, B.; Redaelli, C., *Adv. Carbohydr. Chem. Biochem.* **2007**, *61*, 353-98.

26. (a) Camarero, J. A.; Kwon, Y.; Coleman, M. A., *J. Am. Chem. Soc.* **2004**, *126* (45), 14730-14731; (b) Kent, S. B. H., *Chem. Soc. Rev.* **2009**, *38* (2), 338-351; (c) Weissenborn, M. J.; Castangia, R.; Wehner, J. W.; Sardzik, R.; Lindhorst, T. K.; Flitsch, S. L., *Chem. Commun.* **2012**, *48* (37), 4444-4446.

27. Saxon, E.; Bertozzi, C. R., *Science* **2000**, *287* (5460), 2007-2010.

28. Dondoni, A.; Marra, A., *Chem. Soc. Rev.* **2012**, *41* (2), 573-586.

29. (a) Houseman, B. T.; Mrksich, M., *Chemistry & Biology* **2002**, *9* (4), 443-454; (b) Blackman, M. L.; Royzen, M.; Fox, J. M., *J. Am. Chem. Soc.* **2008**, *130* (41), 13518-13519; (c) Beckmann, H. S. G.; Niederwieser, A.; Wiessler, M.; Wittmann, V., *Chem. Eur. J.* **2012**, *18* (21), 6548-6554.

30. (a) Kolb, H. C.; Finn, M. G.; Sharpless, K. B., *Angew. Chem. Int. Ed.* **2001**, *40* (11), 2004-2021; (b) Rostovtsev, V. V.; Green, L. G.; Fokin, V. V.; Sharpless, K. B., *Angew. Chem.* **2002**, *114* (14), 2708-2711; (c) Tornoe, C. W.; Christensen, C.; Meldal, M., *J. Org. Chem.* **2002**, *67* (9), 3057-64; (d) Meldal, M.; Tornøe, C. W., *Chem. Rev.* **2008**, *108* (8), 2952-3015.

31. Huisgen, R., *Proc. Chem. Soc. London* **1961**, *357* (October), 357-396.

32. (a) Lee, Y. C.; Lee, R. T., *Acc. Chem. Res.* **1995**, *28* (8), 321-327; (b) Mammen, M.; Choi, S.-K.; Whitesides, G. M., *Angew. Chem.* **1998**, *110* (20), 2908-2953.

33. Lundquist, J. J.; Toone, E. J., *Chem. Rev.* **2002**, *102* (2), 555-578.

34. (a) Weber, T.; Chandrasekaran, V.; Stamer, I.; Thygesen, M. B.; Terfort, A.; Lindhorst, T. K., *Angew. Chem. Int. Ed.* **2014**, *53* (52), 14583-14586; (b) Mockl, L.; Muller, A.; Brauchle, C.; Lindhorst, T. K., *Chem. Commun.* **2015**.

35. Hartley, G. S., *Nature* **1937**, *140*, 281.

36. (a) Suginome, H., In *CRC Handbook of Organic Photochemistry and Photobiology*, Horspool, W. M.; Song, P.-S., Eds. CRC Press: Boca Raton, 1995; pp 824–840; (b) Brieke, C.; Rohrbach, F.; Gottschalk, A.; Mayer, G.; Heckel, A., *Angew. Chem. Int. Ed.* **2012**, *51* (34), 8446-8476.

37. Russew, M.-M.; Hecht, S., *Adv. Mater.* **2010**, *22* (31), 3348-3360.

38. García-Amorós, J.; Velasco, D., *Beilstein J. Org. Chem.* **2012**, *8*, 1003-1017.

39. (a) Amadori, M., *Atti reale Accad. Naz. dei Lincei* **1925**, *6* (2), 337; (b) Amadori, M., *Atti reale Accad. Naz. dei Lincei* **1929**, *6* (9), 68; (c) Amadori, M., *Atti reale Accad. Naz. dei Lincei* **1929**, *6* (9), 226; (d) Amadori, M., *Atti reale Accad. Naz. dei Lincei* **1931**, *6* (13), 72.

40. Kuhn, R.; Dansi, A., *Chem. Ber.* **1936**, *69* (7), 1745-1754.

41. Kuhn, R.; Weygand, F., *Chem. Ber.* **1937**, *70* (4), 769-772.

42. (a) Heyns, K.; Beilfuß, W., *Chem. Ber.* **1973**, *106* (8), 2680-2692; (b) Stanìk, J.; Èerny, M.; Kocourek, J.; Pacák, J., Heyns Rearrangement. In *The Monosaccharides*, Publishing House of the Czechoslovak Academy of Science: Prague, 1963; p 458.

43. (a) Maillard, L. C., *C. R. Acad. Sci., Ser. II* **1912**, *154*; (b) Maillard, L. C., *C. R. Acad. Sci., Ser. II* **1912**, *155*; (c) Ledl, F.; Schleicher, E., *Angew. Chem.* **1990**, *102* (6), 597-626.

44. van den Ouweland, G. A. M.; Peer, H. G.; Tjan, S. B., Occurrence of Amadori and Heyns Rearrangement Products in Processed Foods and Their Role in Flavor Formation. In *Flavor of Foods and Beverages*, Inglett, G. C. E., Ed. Academic Press: 1978; pp 131-143.

45. (a) Mauron, J., *Prog. Food Nutr. Sci.* **1981**, *5* (1-6), 5-35; (b) Mottram, D. S.; Wedzicha, B. L.; Dodson, A. T., *Nature* **2002**, *419* (6906), 448-449; (c) Stadler, R. H.; Blank, I.; Varga, N.; Robert, F.; Hau, J.; Guy, P. A.; Robert, M.-C.; Riediker, S., *Nature* **2002**, *419* (6906), 449-450.

46. Kuhn, R.; Krüger, G.; Seeliger, A., *Liebigs Ann. Chem.* **1959**, *628* (1), 240-255.

47. (a) Montgomery, E. M.; Hudson, C. S., *J. Am. Chem. Soc.* **1930**, *52* (5), 2101-2106; (b) Bots, J. P. L., *Recl. Trav. Chim. Pays-Bas* **1957**, *76* (7), 515-518.

48. (a) Paulsen, H., *Liebigs Ann. Chem.* **1965**, *683* (1), 187-198; (b) Paulsen, H.; Todt, K., *Adv. Carbohydr. Chem.* **1968**, *23*, 115-232.

49. Stütz, A. E., Ed. *Iminosugars as Glycosidase Inhibitors*. Wiley-VCH: Weinheim, 1999.

50. Wrodnigg, T.; Eder, B., The Amadori and Heyns Rearrangements: Landmarks in the History of Carbohydrate Chemistry or Unrecognized Synthetic Opportunities? In *Glycoscience*, Stütz, A., Ed. Springer Berlin Heidelberg: 2001; Vol. 215, pp 115-152.

51. (a) Wrodnigg, T. M.; Stütz, A. E.; Withers, S. G., *Tetrahedron Lett.* **1997**, *38* (31), 5463-5466; (b) Wrodnigg, T. M.; Gaderbauer, W.; Greimel, P.; Häusler, H.; Sprenger, F. K.; Stütz, A. E.; Virgona, C.; Withers, S. G., *J. Carbohydr. Chem.* **2000**, *19* (8), 975-990.

52. Legler, G.; Korth, A.; Berger, A.; Ekhart, C.; Gradnig, G.; Stütz, A. E., *Carbohydr. Res.* **1993**, *250* (1), 67-77.

53. Dondoni, A.; Marra, A., *Chem. Rev.* **2000**, *100* (12), 4395-4422.

54. Lin, Z.; Zheng, J., *Appl. Microbiol. Biotechnol.* **2010**, *86* (6), 1613-9.

55. Financial support by the DFG in the frame of an ERA-Chemistry grant is gratefully acknowledged.

56. Hojnik, C. Unpublished Work. Graz, 2016.

57. Aumüller, I. B.; Lindhorst, T. K., *Eur. J. Org. Chem.* **2006**, 1103-1108.

58. Wuts, P. G. M.; Greene, T. W., Protection for the Amino Group. In *Greene's Protective Groups in Organic Synthesis*, John Wiley & Sons, Inc.: 2006; pp 696-926.

59. Aumüller, I. B.; Lindhorst, T. K., *J. Carbohydr. Chem.* **2009**, *28* (6), 330-347.

60. Timmer, M. S. M.; Stocker, B. L.; Northcote, P. T.; Burkett, B. A., *Tetrahedron Lett.* **2009**, *50* (51), 7199-7204.

61. Aumüller, I. B. Azulen-unterstützte Substanzreinigung - eine Strategie für die parallele Ligandsynthese. Dissertation, Kiel, 2002.

62. (a) Gallas, K.; Pototschnig, G.; Adanitsch, F.; Stütz, A. E.; Wrodnigg, T. M., *Beilstein J. Org. Chem.* **2012**, *8*, 1619-1629; (b) Gloe, T.-E.; Stamer, I.; Hojnik, C.; Wrodnigg, T. M.; Lindhorst, T. K., *Beilstein J. Org. Chem.* **2015**, *11*, 1096-1104.

63. Wrodnigg, T. M.; Kartusch, C.; Illaszewicz, C., *Carbohydr. Res.* **2008**, *343* (12), 2057-2066.

64. Roy, R.; Shiao, T. C., *Chem. Soc. Rev.* **2015**, *44* (12), 3924-3941.

65. Meutermans, W.; Le, G. T.; Becker, B., *ChemMedChem* **2006**, *1* (11), 1164-1194.

66.   (a) Dubber, M.; Lindhorst, T. K., *Carbohydr. Res.* **1998**, *310* (1–2), 35-41; (b) Dubber, M.; Sperling, O.; Lindhorst, T. K., *Org. Biomol. Chem.* **2006**, *4* (21), 3901-3912; (c) Lindhorst, T. K.; Dubber, M., *Carbohydr. Res.* **2015**, *403*, 90-97.

67.   Dubber, M.; Lindhorst, T. K., *Org. Lett.* **2001**, *3* (25), 4019-4022.

68.   Thomas, B.; Fiore, M.; Bossu, I.; Dumy, P.; Renaudet, O., *Beilstein J. Org. Chem.* **2012**, *8*, 421-427.

69.   Ortega-Muñoz, M.; Perez-Balderas, F.; Morales-Sanfrutos, J.; Hernandez-Mateo, F.; Isac-García, J.; Santoyo-Gonzalez, F., *Eur. J. Org. Chem.* **2009**, *2009* (15), 2454-2473.

70.   Solomon, D.; Kitov, P. I.; Paszkiewicz, E.; Grant, G. A.; Sadowska, J. M.; Bundle, D. R., *Org. Lett.* **2005**, *7* (20), 4369-4372.

71.   Wang, C.; Sanders, B.; Baker, D. C., *Can. J. Chem.* **2011**, *89* (8), 959-963.

72.   Horlacher, T.; Seeberger, P. H., *Chem. Soc. Rev.* **2008**, *37* (7), 1414-1422.

73.   Dubber, M.; Lindhorst, T. K., *J. Org. Chem.* **2000**, *65* (17), 5275-5281.

74.   Köhn, M.; Benito, J. M.; Ortiz Mellet, C.; Lindhorst, T. K.; García Fernández, J. M., *ChemBioChem* **2004**, *5* (6), 771-777.

75.   Kulkarni, A. A.; Weiss, A. A.; Iyer, S. S., *Anal. Chem.* **2010**, *82* (17), 7430-7435.

76.   Fagan, V.; Toth, I.; Simerska, P., *Beilstein J. Org. Chem.* **2014**, *10*, 1741-1748.

77.   (a) Natarajan, A.; Du, W.; Xiong, C.-Y.; DeNardo, G. L.; DeNardo, S. J.; Gervay-Hague, J., *Chem. Commun.* **2007**, 695-697; (b) Norberg, O.; Deng, L.; Yan, M.; Ramström, O., *Bioconjugate Chem.* **2009**, *20* (12), 2364-2370.

78.   Sperling, O.; Dubber, M.; Lindhorst, T. K., *Carbohydr. Res.* **2007**, *342* (5), 696-703.

79.   Lindhorst, T.; Kieburg, C.; Krallmann-Wenzel, U., *Glycoconjugate J.* **1998**, *15* (6), 605-613.

80.   (a) Baussanne, I.; Benito, J. M.; Ortiz Mellet, C.; García Fernández, J. M.; Defaye, J., *ChemBioChem* **2001**, *2* (10), 777-783; (b) Ortega-Caballero, F.; Giménez-Martínez, J. J.; García-Fuentes, L.; Ortiz-Salmerón, E.; Santoyo-González, F.; Vargas-Berenguel, A., *J. Org. Chem.* **2001**, *66* (23), 7786-7795; (c) Vargas-Berenguel, A.; Ortega-Caballero, F.; Santoyo-González, F.; García-López, J. J.; Giménez-Martínez, J. J.; García-Fuentes, L.; Ortiz-Salmerón, E., *Chem. Eur. J.* **2002**, *8* (4), 812-827.

81.   Crini, G., *Chem. Rev.* **2014**, *114* (21), 10940-10975.

82.   (a) Villiers, A., *Bull. Soc. Chim. Paris* **1891**, *45*, 468; (b) Villiers, A., *C. R. Acad. Sci.* **1891**, *CXII*, 435.

83.   Maquenne, L.; Roux, E., *Ann. Chim. Phys.* **1906**, *9*, 179.

84.   (a) Villiers, A., *Bull. Soc. Chim. Paris* **1891**, *46*, 470; (b) Villiers, A., *C. R. Acad. Sci.* **1891**, *CXII*, 536.

85.   Schardinger, F., *Zeitschr. f. Untersuchung d. Nahr.-u. Genußmittel* **1903**, *6* (19), 865-880.

86.   Schardinger, F., *Wien. Klin. Wochenschr.* **1903**, *16*, 468.

87.   Schardinger, F., *Zentralbl. Bakteriol., Parasitenkd., Infektionskrankh. Hyg., Abt. 2* **1911**, *29*, 188.

88.   Schardinger, F., *Wien. Klin. Wochenschr.* **1904**, *17*, 207.

89.   Brock, T. D., *Robert Koch: A Life in Medicine and Bacteriology*. ASM Press: 1988.

90.   Freudenberg, K.; Blomqvist, G.; Ewald, L.; Soff, K., *Chem. Ber.* **1936**, *69* (6), 1258-1266.

91.   Freudenberg, K.; Jacobi, R., *Liebigs Ann. Chem.* **1935**, *518* (1), 102-108.

92.   French, D.; Rundle, R. E., *J. Am. Chem. Soc.* **1942**, *64* (7), 1651-1653.

93.   French, D.; Knapp, D. W.; Pazur, J. H., *J. Am. Chem. Soc.* **1950**, *72* (11), 5150-5152.

94. (a) Freudenberg, K., *Chem. Ber.* **1943**, *76* (8), A71-A96; (b) Freudenberg, K.; Cramer, F., *Z. Naturforsch. B* **1948**, *3*, 464.

95. Cramer, F., *Angew. Chem.* **1952**, *64* (16), 437-447.

96. (a) Cramer, F.; Henglein, F. M., *Angew. Chem.* **1956**, *68* (20), 649; (b) Cramer, F.; Henglein, F. M., *Chem. Ber.* **1957**, *90* (11), 2572-2575.

97. Lüttringhaus, A.; Cramer, F.; Prinzbach, H.; Henglein, F. M., *Liebigs Ann. Chem.* **1958**, *613* (1), 185-198.

98. Freudenberg, K. D.; Cramer, F. D.; Plieninger, H. D. Verfahren zur Herstellung von Einschlussverbindungen physiologisch wirksamer organischer Verbindungen. DE895769 (C), 1953.

99. French, D., The Schardinger Dextrins. In *Adv. Carbohydr. Chem.*, Melville, L. W.; Tipson, R. S., Eds. Academic Press: 1957; Vol. 12, pp 189-260.

100. (a) Lach, J. L.; Cohen, J., *J. Pharm. Sci.* **1963**, *52* (2), 137-142; (b) Lach, J. L.; Chin, T.-F., *J. Pharm. Sci.* **1964**, *53* (1), 69-73.

101. Tang, W.; Ng, S.-C.; Sun, D., Eds. *Modified Cyclodextrins for Chiral Separation*. Springer: Berlin Heidelberg, 2013.

102. Cramer, F., *Chem. Ber.* **1953**, *86* (12), 1576-1581.

103. (a) Komiyama, M.; Bender, M. L., *Proc. Natl. Acad. Sci. USA* **1976**, *73* (9), 2969-2972; (b) Komiyama, M.; Bender, M. L., *Bioorg. Chem.* **1977**, *6* (3), 323-328; (c) Bender, M.; Komiyama, M., *Cyclodextrin Chemistry*. Springer: Berlin Heidelberg, 1978; Vol. 6.

104. Gao, S.; Wang, L., *Huanjing Kexue Jinzhan* **1998**, *6*, 80-86.

105. Rajewski, R. A.; Stella, V. J., *J. Pharm. Sci.* **1996**, *85* (11), 1142-1169.

106. Del Valle, E. M. M., *Process Biochem.* **2004**, *39* (9), 1033-1046.

107. Hedges, A. R., *Chem. Rev.* **1998**, *98* (5), 2035-2044.

108. Woo, R. A. M.; Trinh, T.; Cobb, D. S.; Schneiderman, E.; Wolff, A. M.; Rosenbalm, E. L.; Ward, T. E.; Chung, A. H.; Reece, S. Uncomplexed cyclodextrin compositions for odor control. US5942217 A, 1999.

109. Prasad, N.; Reichart, G.; Strauss, D. Flavor delivery system. EP 1084625, 1999.

110. (a) Ferris, D. P.; Zhao, Y.-L.; Khashab, N. M.; Khatib, H. A.; Stoddart, J. F.; Zink, J. I., *J. Am. Chem. Soc.* **2009**, *131* (5), 1686-1688; (b) Harada, A.; Takashima, Y.; Nakahata, M., *Acc. Chem. Res.* **2014**, *47* (7), 2128-2140; (c) Shi, W.; Deng, J.; Qin, H.; Wang, D.; Zhao, C., *J. Membr. Sci.* **2014**, *455*, 357-367.

111. Hu, Y.; Tabor, R. F.; Wilkinson, B. L., *Org. Biomol. Chem.* **2015**, *13* (8), 2216-2225.

112. Samanta, A.; Stuart, M. C. A.; Ravoo, B. J., *J. Am. Chem. Soc.* **2012**, *134* (48), 19909-19914.

113. Inoue, Y.; Kuad, P.; Okumura, Y.; Takashima, Y.; Yamaguchi, H.; Harada, A., *J. Am. Chem. Soc.* **2007**, *129* (20), 6396-6397.

114. Thoms, V. Cyclodextrin-Einschlussverbindungen: Synthese und Anwendung. Bachelor thesis, Kiel, 2013.

115. Jaeschke, S. O. Photoschaltbare Azobenzolderivate als Liganden für Cyclodextrine. Bachelor thesis, Kiel, 2014.

116. (a) Michalke, A.; Janshoff, A.; Steinem, C.; Henke, C.; Sieber, M.; Galla, H.-J., *Anal. Chem.* **1999**, *71* (13), 2528-2533; (b) Onclin, S.; Mulder, A.; Huskens, J.; Ravoo, B. J.; Reinhoudt, D. N., *Langmuir* **2004**, *20* (13), 5460-5466; (c) Städe, L. W.; Nielsen, T. T.; Duroux, L.; Hinge, M.; Shimizu, K.; Gurevich, L.; Kristensen, P. K.; Wingren, C.; Larsen, K. L., *ACS Applied Materials & Interfaces* **2015**, *7* (7), 4160-4168.

117. Tsujihara, K.; Kurita, H.; Kawazu, M., *Bull. Chem. Soc. Jpn.* **1977**, *50* (6), 1567-1571.

118. Staab, H. A.; Wendel, K., *Chem. Ber.* **1960**, *93* (12), 2902-2915.

119. (a) Petter, R. C.; Salek, J. S.; Sikorski, C. T.; Kumaravel, G.; Lin, F. T., *J. Am. Chem. Soc.* **1990**, *112* (10), 3860-3868; (b) Byun, H.-S.; Zhong, N.; Bittman, R., *Org. Synth.* **2000**, *77*, 225.

120. Chernyak, A. Y.; Sharma, G. V. M.; Kononov, L. O.; Krishna, P. R.; Levinsky, A. B.; Kochetkov, N. K.; Rama Rao, A. V., *Carbohydr. Res.* **1992**, *223* (0), 303-309.

121. Chandrasekaran, V.; Kolbe, K.; Beiroth, F.; Lindhorst, T. K., *Beilstein J. Org. Chem.* **2013**, *9*, 223-233.

122. Jung, K.-H.; Hoch, M.; Schmidt, R. R., *Liebigs Ann. Chem.* **1989**, *1989* (11), 1099-1106.

123. Zemplén, G.; Pacsu, E., *Chem. Ber.* **1929**, *62* (6), 1613-1614.

124. Saha, A. K.; Brewer, C. F., *Carbohydr. Res.* **1994**, *254*, 157-167.

125. Grabosch, C.; Kolbe, K.; Lindhorst, T. K., *ChemBioChem* **2012**, *13* (13), 1874-1879.

126. Cristiano, A.; Lim, C. W.; Rozkiewicz, D. I.; Reinhoudt, D. N.; Ravoo, B. J., *Langmuir* **2007**, *23* (17), 8944-8949.

127. (a) Park, I.-K.; von Recum, H. A.; Jiang, S.; Pun, S. H., *Mol Ther* **2006**, *13* (S1), S67-S67; (b) Koopmans, C.; Ritter, H., *Macromolecules* **2008**, *41* (20), 7418-7422; (c) Holzinger, M.; Bouffier, L.; Villalonga, R.; Cosnier, S., *Biosens. Bioelectron.* **2009**, *24* (5), 1128-1134.

128. I am grateful to Jose Manuel García Fernández and Juan Manuel Benito Hernández for support during the short term scientific mission at the CSIC – University of Seville. Financial support by the COST program in the frame of a grant for the short term scientific mission is gratefully acknowledged.

129. Memişoğlu, E.; Bochot, A.; Şen, M.; Charon, D.; Duchêne, D.; Hıncal, A. A., *J. Pharm. Sci.* **2002**, *91* (5), 1214-1224.

130. Gadelle, A.; Defaye, J., *Angew. Chem. Int. Ed. Engl.* **1991**, *30* (1), 78-80.

131. Dupuis, S. N.; Robertson, A. W.; Veinot, T.; Monro, S. M. A.; Douglas, S. E.; Syvitski, R. T.; Goralski, K. B.; McFarland, S. A.; Jakeman, D. L., *Chem. Sci.* **2012**, *3* (5), 1640-1644.

132. Szurmai, Z.; Szabo, L.; Liptak, A., *Acta Chim. Hung.* **1989**, *126* (2), 259-269.

133. Bonner, W. A., *J. Am. Chem. Soc.* **1958**, *80* (13), 3372-3379.

134. (a) Lindhorst, T. K.; Kotter, S.; Krallmann-Wenzel, U.; Ehlers, S., *J. Chem. Soc., Perkin Trans. 1* **2001**, 823-831; (b) Kikkeri, R.; Lepenies, B.; Adibekian, A.; Laurino, P.; Seeberger, P. H., *J. Am. Chem. Soc.* **2009**, *131* (6), 2110-2112.

135. Voskuhl, J.; Sankaran, S.; Jonkheijm, P., *Chem. Commun.* **2014**, *50* (96), 15144-15147.

136. Mills, C., *J. Chem. Soc., Trans.* **1895**, *67*, 925-933.

137. Priewisch, B.; Rück-Braun, K., *J. Org. Chem.* **2005**, *70* (6), 2350-2352.

138. Poláková, M.; Beláňová, M.; Mikušová, K.; Lattová, E.; Perreault, H., *Bioconjugate Chem.* **2011**, *22* (2), 289-298.

139. Hadjoudis, E.; Kondilis, P.; Mavridis, I.; Tsoucaris, G., Environmental Effects on Molecular Properties of Organic Compounds. Part III. Cyclodextrins with a Schiff Base Moiety. In *Proc. Int. Symp. Cyclodextrins, 4th*, Huber, O.; Szejtli, J., Eds. Springer Netherlands: 1988; Vol. 5, pp 119-123.

140. Tang, W.; Muderawan, I. W.; Ng, S. C.; Chan, H. S. O., *J. Chromatogr. A* **2005**, *1094* (1–2), 187-191.

141. Yousif, E.; Haddad, R., *SpringerPlus* **2013**, *2*, 398.

142. Bléger, D.; Hecht, S., *Angew. Chem. Int. Ed.* **2015**, *54* (39), 11338-11349.

143. Behra, M.; Azzouz, N.; Schmidt, S.; Volodkin, D. V.; Mosca, S.; Chanana, M.; Seeberger, P. H.; Hartmann, L., *Biomacromolecules* **2013**, *14* (6), 1927-1935.

144. Jayamohan, H.; Gale, B.; Minson, B.; Lambert, C.; Gordon, N.; Sant, H., *Sensors* **2015**, *15* (5), 12034.

145. (a) Reisner, A.; Haagensen, J. A. J.; Schembri, M. A.; Zechner, E. L.; Molin, S., *Mol. Microbiol.* **2003**, *48* (4), 933-946; (b) The *E. coli* strain pPKL1162 was constructed in the Klemm group where the plasmid pPKL174 was introduced into the *E. coli* strain SAR18; pPKL174 contains the *fim* gene cluster required for expression of type 1 fimbriae whereas SAR18 from the Reisner group contains the GFP gene in its genome controlled by a constitutive promoter.

146. Hartmann, M.; Horst, A. K.; Klemm, P.; Lindhorst, T. K., *Chem. Commun.* **2010**, *46* (2), 330-332.

147. Benito, J. M.; Gómez-García, M.; Ortiz Mellet, C.; Baussanne, I.; Defaye, J.; García Fernández, J. M., *J. Am. Chem. Soc.* **2004**, *126* (33), 10355-10363.

148. Saha, S. K.; Brewer, C. F., *Carbohydr. Res.* **1994**, *254*, 157-67.

Appendix

UV/Vis Spectra of Selected Compounds
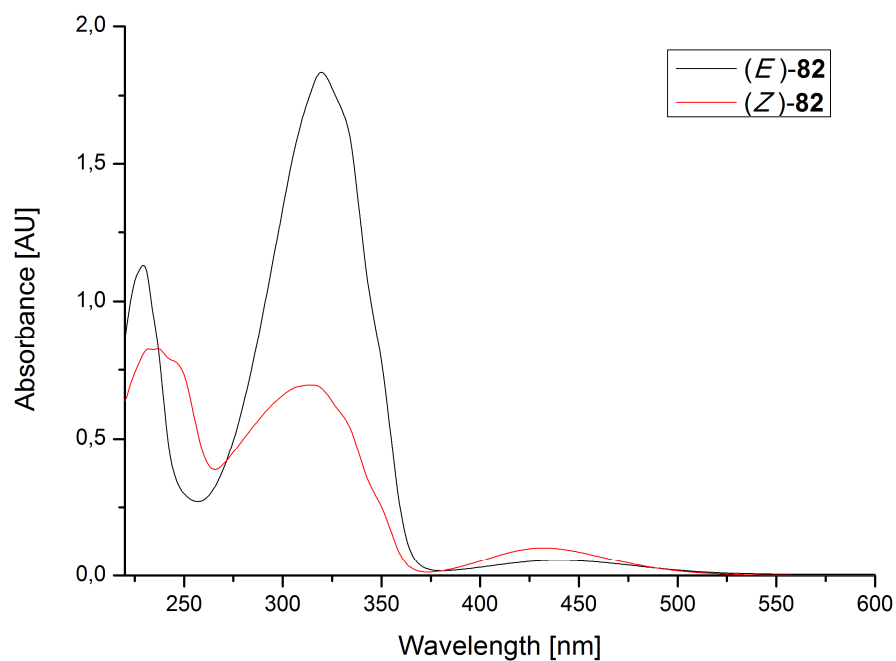
Figure A1: UV/Vis spectrum of azobenzene derivative **82**.
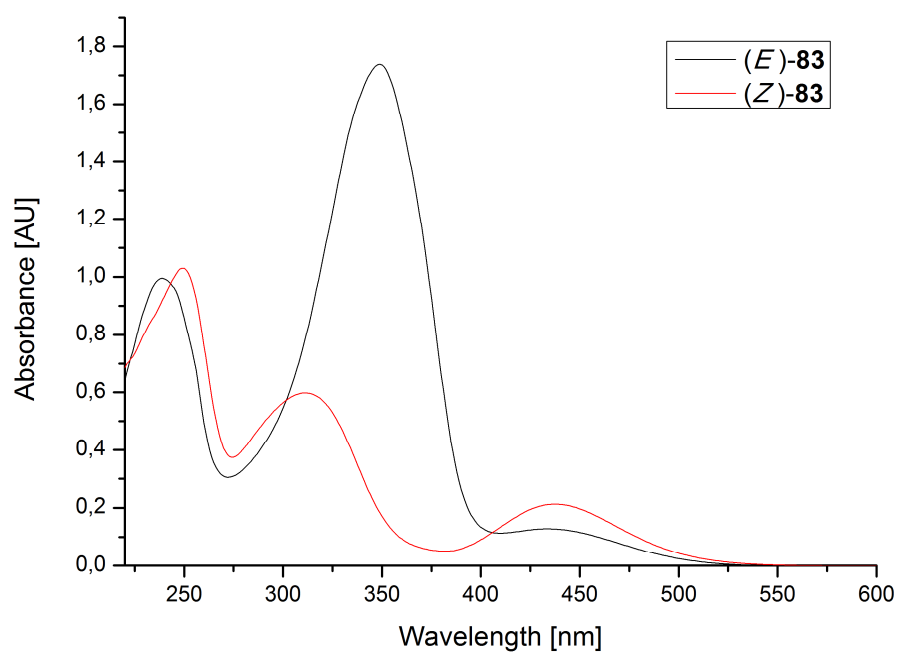
Figure A2: UV/Vis spectrum of azobenzene derivative **83**.
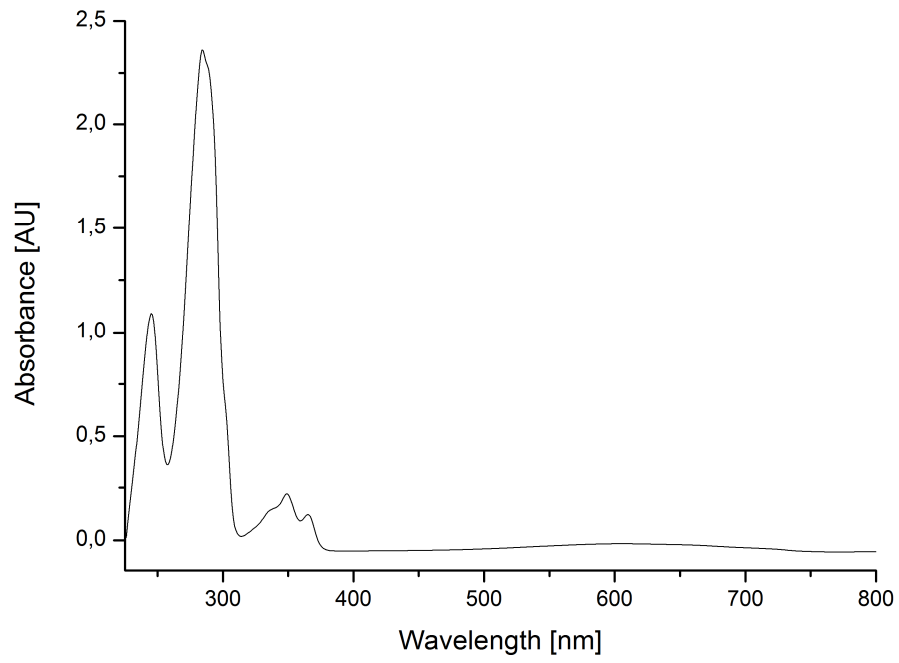
Figure A3: UV/Vis spectrum of Amadori product **21**.
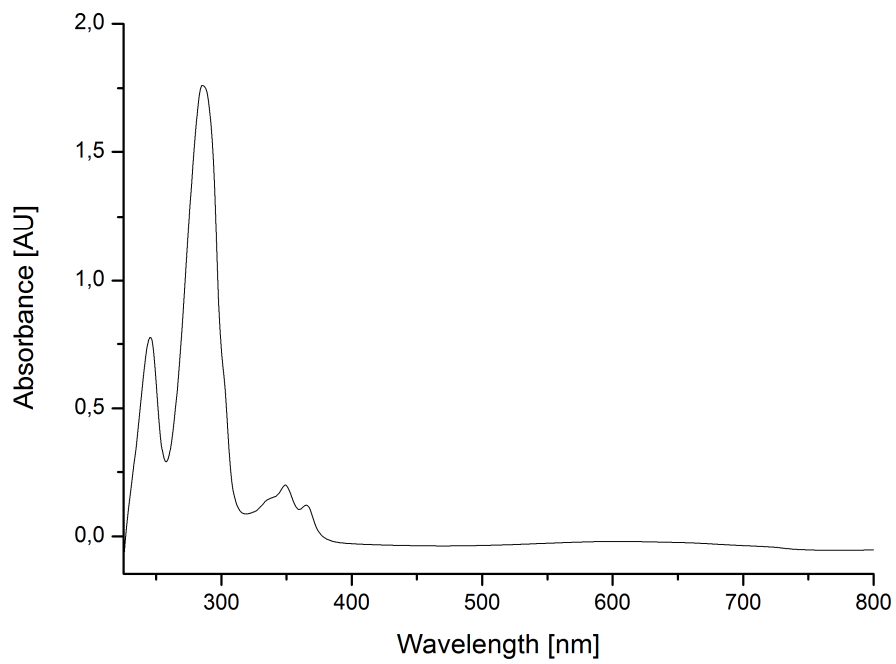
Figure A4: UV/Vis spectrum of Amadori product **24**.

Chromatograms of Selected Compounds
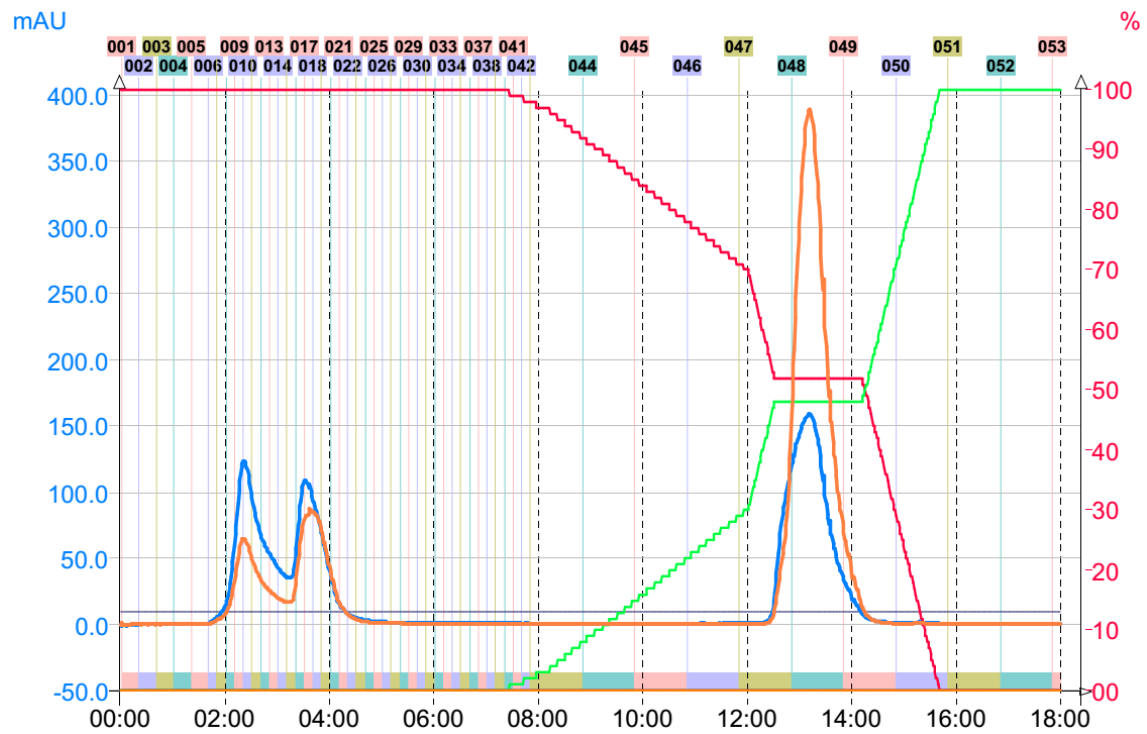
Figure A5: Chromatogram of the RP purification of CD conjugate **90**. Left y-axis: absorbance [mAU], right y-axis: amount of ACN in percent; x-axis: time [min]. R_t = 13.12 min.
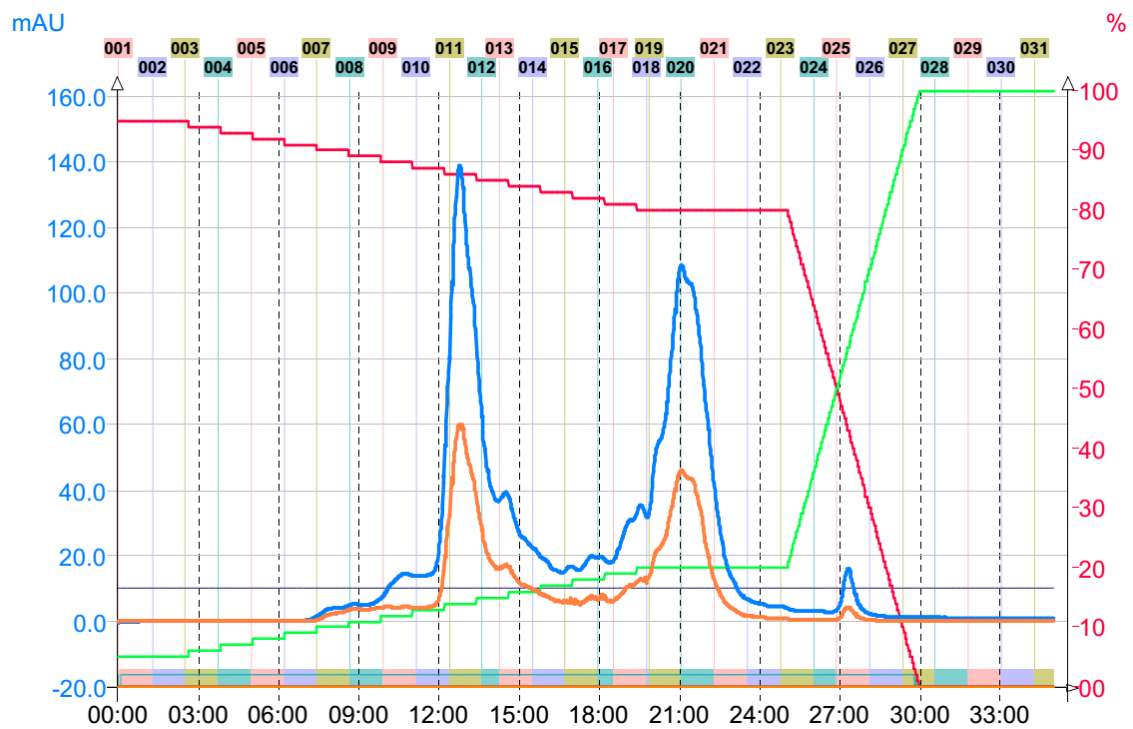
Figure A6: Chromatogram of the RP purification of glycocluster **47**. Left y-axis: absorbance [mAU], right y-axis: amount of ACN in percent; x-axis: time [min]. R_t = 12.46 min

Abbreviations

9-BBN	9-borabicyclo[3.3.1]nonane
ABTS	2,2´-azino-bis(3-ethylbenzo-thiazoline-6-sulphonic acid
ACN	acetonitrile
Asn	asparagine
Asp	aspartic acid
Boc	*tert*-butyloxycarbonyl
br	broad signal
BSA	bovine serum albumin
CD	cyclodextrin
Con A	concanavalin A
CRD	carbohydrate recognition domain
CSP	chromophore-supported purification
CuAAC	copper(I)-catalyzed azide alkyne cycloaddition
d	doublet
DIPEA	*N,N*-diisopropylethylamine
DMF	*N,N*-dimethylformamide
DMSO	dimethyl sulfoxide
DSC	*N,N´*-disuccinimidyl carbonate
E. coli	*Escherichia coli*
EDC	1-ethyl-3-(3-dimethylaminopropyl)carbodiimide
EE	ethyl acetate
EI	electron ionization
ELLA	enzyme-linked lectin assay
ER	endoplasmic reticulum
ESI	electrospray ionization
Gal	galactose
GalNAc	*N*-acetylgalactosamine
GC	gas chromatography
GFP	green fluorescent protein
GlcNAc	*N*-acetylglucosamine
Gln	glutamine
HBTU	2-(1H-benzotriazol-1-yl)-1,1,3,3-tetramethyluronium hexafluorophosphate
HMEC	human mammary epithelial cells
HOBt	hydroxybenzotriazole
HPLC	high performance liquid chromatography

HR	high resolution, high-resolution
HRP	horseradish peroxidase
IC_{50}	half maximal inhibitory concentration
IR	infrared
LDA	lithium diisopropylamide
LED	light-emitting diode
m	multiplet
m.p.	melting point
MALDI	matrix-assisted laser desorption ionization
Man	mannose
m-CPBA	*m*-chloroperoxybenzoic acid
MeMan	methyl α-D-mannoside
MS	mass spectrometry
NBS	*N*-bromosuccinimide
Neu5Ac	*N*-acetylneuraminic acid
NHS	*N*-hydroxyl succinimide
NMR	nuclear magnetic resonance spectroscopy
OD	optical density
OEG	oligo ethylene glycol
PBS	phosphate buffered saline
PBST	phosphate buffered saline with Tween®
PEG	polyethylene glycol
pH	potentia Hydrogenii
Phe	phenylalanine
PMDTA	*N,N,N′,N′′,N′′*-pentamethyldiethylenetriamine
PNA	peanut agglutinin
*p*NPMan	*p*-nitrophenyl α-D-mannoside
PSS	photostationary state
PVA	polyvinyl alcohol
q	quartet
R_f	retardation factor
RIP	relative inhibitory potency
RIT	relative inhibition titre
ROESY	rotating-frame nuclear Overhauser effect correlation spectroscopy
RP	reverse phase
rt	room temperature
s	singlet

SAM	self assembled monolayer
SD	standard deviation
Ser	serine
t	triplet
TBABr	tetra-*n*-butylammonium bromide
TBAI	tetra-*n*-butylammonium iodide
TEA	triethylamine
TEM	transmission electron microscopy
TFA	trifluoroacetic acid
THF	tetrahydrofuran
Thr	threonine
TLC	thin layer chromatography
Tyr	tyrosine
UV	ultraviolet
Y	tyrosine

Lists of Figures, Schemes, and Tables

Schemes

b) propargyl bromide, K_2CO_3, KI, MeCN, 70 °C, 16 h, 65%; c) NaOMe, MeOH, rt, 16 h, 81%; d) $CuSO_4 \cdot 5 \, H_2O$, sodium ascorbate, DMF/H_2O (3:1), rt, 16 h, 78%. 115

Scheme 5.10: Synthesis of fluorescein-tagged CD derivative **93**. a) 1. PPh$_3$, DMF, rt, 2 h; 2. H_2O, 90 °C, 2 h, 91%; b) DIPEA, DMF, rt, 16 h, 64%. 115

Tables

Acknowledgements

Curriculum Vitae

Personal Details

Date and place of birth: 16.09.1985 in Bad Oldesloe

Academic Career

since 07/2012   **PhD thesis** under supervision of Prof. Dr. Thisbe K. Lindhorst at the Otto Diels Institute of Organic Chemistry of the Christiana Albertina University of Kiel

10/2009 – 05/2012   **Master studies** (M.Sc.) in chemistry at the University of Hamburg

- Focus: Organic chemistry and analytical methods
- Title of master thesis: „Design and Synthesis of Inhibitors of the Myelin-Associated Glycoprotein"

10/2006 – 09/2009   **Bachelor studies** (B.Sc.) in chemistry at the University of Hamburg

- Title of bachelor thesis: „Diastereoselective Synthesis of Pronucleotides"

School Education

07/1996 – 07/2006   **Abitur** at the Theodor-Mommsen-Schule (TMS) in Bad Oldesloe